ACADEMIA OPEROSORUM · MDCXCIII
SLOVENSKA AKADEMIJA ZNANOSTI IN UMETNOSTI
SLOVENIAN ACADEMY OF SCIENCES AND ARTS

FOLIA BIOLOGICA ET GEOLOGICA

63/2 · 2022

FOLIA BIOLOGICA ET GEOLOGICA

Ex: Razprave razreda za naravoslovne vede
Dissertationes classis IV (Historia naturalis)

63/2
2022

SLOVENSKA AKADEMIJA ZNANOSTI IN UMETNOSTI
ACADEMIA SCIENTIARUM ET ARTIUM SLOVENICA
Razred za naravoslovne vede – Classis IV: Historia naturalis

LJUBLJANA 2022

FOLIA BIOLOGICA ET GEOLOGICA **ISSN 1855-7996**

Sprejeto na seji razreda za naravoslovne vede SAZU dne 9. septembra 2021 in na seji predsedstva SAZU 22. februarja 2022.

Naslov Uredništva / *Editorial Office Address*
FOLIA BIOLOGICA ET GEOLOGICA
SAZU
Novi trg 3, SI-1000 Ljubljana, Slovenia
Faks / Fax: +386 (0)1 4253 423, E-pošta / E-mail: sazu@sazu.si; www.sazu.si

Avtorji v celoti odgovarjajo za vsebino in jezik prispevkov.
The autors are responsible for the content and for the language of their contributions.

Revija izhaja dvakrat do štirikrat letno / *The Journal is published two to four times annually*

Zamenjava / *Exchange*
Biblioteka SAZU, Novi trg 3, SI-1000 Ljubljana, Slovenia
Faks / Fax: +386 (0)1 4253 462, E-pošta / E-mail: sazu-biblioteka@zrc-sazu.si

FOLIA BIOLOGICA ET GEOLOGICA (Ex *Razprave IV. razreda SAZU*) je vključena v / *is included into*: Index to Scientific & Technical Proceedings (ISTP, Philadelphia) / Index to Social Sciences & Humanities Proceedings (ISSHP, Philadelphia) / *GeoRef Serials / BIOSIS Zoological Record / Internationale Bibliographie des Zeitschriften (IBZ) / Redakcion Homo / Colorado State University Libraries / CABI (Wallingford, Oxfordshire).*

FOLIA BIOLOGICA ET GEOLOGICA (Ex *Razprave IV. razreda SAZU*) izhaja s finančno pomočjo / *is published with the financial support* Javne agencije za raziskovalno dejavnost RS / *Slovenian Research Agency*.

Naslovnica: Spodnjejurski kremenasti apnenci formacije "Passée Jaspeuse", Budvanska cona, Uvala Pećin, Čanj, Črna gora.
Cover photo: Lower Jurassic siliceous limestone, "Passée Jaspeuse" formation, Budva Zone, Uvala Pećin, Čanj, Montenegro.

Folia biologica et geologica • Volume / Letnik **63** • Number / Številka **2** • **2022**

VSEBINA
CONTENTS

InterRad XVI, Ljubljana 2022

16th international conference on fossil and living radiolaria

Excursion Guide

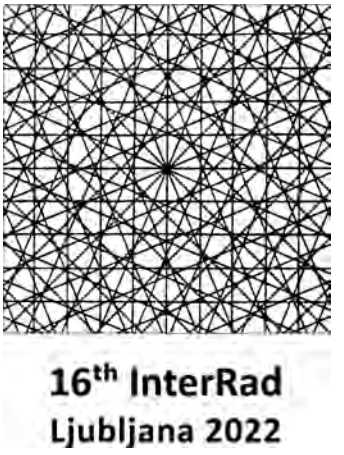

V tem zvezku objavljene razprave bodo služile kot dodatne informacije za udeležence ekskurzij v okviru mednarodne konference InterRad XVI, Ljubljana, 8–20 september 2022.

Here published papers will serve as supporting information for the participants of field trips in the frame of the international conference InterRad XVI, Ljubljana, September 8–20, 2022.

MESOZOIC TECTONOSTRATIGRAPHY OF THE EASTERN ALPS (NORTHERN CALCAREOUS ALPS, AUSTRIA): A RADIOLARIAN PERSPECTIVE

MEZOZOJSKA TEKTONOSTRATIGRAFIJA VZHODNIH ALP (SEVERNE APNENIŠKE ALPE, AVSTRIJA): RADIOLARIJSKA PERSPEKTIVA

Hans-Jürgen GAWLICK[1], Sigrid †MISSONI[1], Hisashi SUZUKI[2], Špela GORIČAN[3,4] & Luis O´DOGHERTY[5]

http://dx.doi.org/10.3986/fbg0096

ABSTRACT

Mesozoic tectonostratigraphy of the Eastern Alps (Northern Calcareous Alps, Austria): a radiolarian perspective

The topic of the field trip is the Mesozoic geodynamic evolution in the Western Tethys realm well recorded in deep-water settings, especially in the radiolarian-bearing sedimentary rocks and radiolarites in the Eastern Alps (Northern Calcareous Alps). The well preserved Mesozoic sedimentary successions deposited in the Northern Calcareous Alps reflect two different Wilson cycles with its mountain building processes:

Evolution of the Neo-Tethys Ocean to the south/southeast: The Middle Triassic oceanic break-up (Late Anisian) was followed by the Middle Triassic to Middle Jurassic passive margin evolution and later by Middle to early Late Jurassic thrusting related to ophiolite obduction and subsequent latest Jurassic to Early Cretaceous mountain uplift of the Neo-Tethys orogen to the south of the todays Northern Calcareous Alps.

Evolution of the Alpine Atlantic Ocean (named Penninic Ocean in the Eastern Alps) to the north/northwest: The Late Early to Middle Jurassic oceanic break-up was followed by the Middle Jurassic to Late Cretaceous passive margin evolution and Late Cretaceous to Palaeogene subduction of the Penninic realm, Palaeogene collision and subsequent Neogene mountain uplift with its gravitational collapse (Lateral Tectonic Extrusion) of the Alpine orogen s.str.

For another orogenesis in the "Mid-Cretaceous" (Aptian-Cenomanian), i.e. between these two well recognizable

IZVLEČEK

Mezozojska tektonostratigrafija Vzhodnih Alp (Severne Apneniške Alpe, Avstrija): radiolarijska perspektiva

Ekskurzija je posvečena mezozojski geodinamični evoluciji zahodne Tetide. Ta je dobro zabeležena v globokomorskih okoljih, še posebej v radiolaritih in drugih radiolarijskih sedimentnih kamninah v Vzhodnih Alpah, katerih del so Severne Apneniške Alpe. Dobro ohranjena mezozojska sedimentna zaporedja v Severnih Apneniških Alpah odražajo dva različna Wilsonova cikla z gorotvornimi procesi.

Prvi cikel se nanaša na razvoj oceana Neotetida na jugu do jugovzhodu. Oceanskemu razpadu v srednjem triasu (zgornjem aniziju) je sledil razvoj pasivnega roba do srednje jure in pozneje, v srednji in zgornji juri, narivanje, povezano z obdukcijo ofiolitov. Na koncu jure in v spodnji kredi se je dvigal Neotetidin orogen, lociran južno od današnjih Severnih Apneniških Alp.

Drugi cikel je povezan z razvojem oceana Alpski Atlantik (imenovanega Peninski ocean v Vzhodnih Alpah) na severu do severozahodu. Oceanskemu razpadu proti koncu spodnje jure in v srednji juri je sledil razvoj pasivnega roba od srednje jure do zgornje krede in subdukcija Peninika v zgornji kredi in paleogenu. Sledila je kolizija v paleogenu, v neogenu pa nadaljnje dviganje orogena z gravitacijskim kolapsom (lateralnim tektonskim iztiskanjem) Alpskega orogena *sensu stricto*.

Obstajajo še dokazi za orogenezo v "srednji kredi" (aptij-cenomanij) med tema dvema dobro prepoznavnima Wilsonovima cikloma, vendar geodinamično ozadje te orogene-

[1] Montanuniversitaet Leoben, Department of Applied Geosciences and Geophysics, Petroleum Geology, Peter-Tunner Strasse 5, 8700 Leoben, Austria, gawlick@unileoben.ac.at

[2] Otani University, Koyama-Kamifusa-cho, Kita-ku, Kyoto 603-8143, Japan, hsuzuki@res.otani.ac.jp

[3] ZRC SAZU, Paleontološki inštitut Ivana Rakovca, Novi trg 2, SI-1000 Ljubljana, Slovenia, spela.gorican@zrc-sazu.si

[4] Podiplomska šola ZRC SAZU, Novi trg 2, SI-1000 Ljubljana, Slovenia.

[5] Instituto Universitario de Investigación Marina (INMAR), Facultad de Ciencias del Mar, Universidad de Cádiz, 11510 Puerto Real, Spain, luis.odogherty@uca.es

Wilson cycles, the geodynamic background has not been well explored or explained yet. This "Mid-Cretaceous" orogenesis draws a veil over the older Mesozoic plate configuration and has generated controversial discussion about the geodynamic evolution and palaeogeography in Triassic to Early Cretaceous times. However, this orogenesis is not connected to the Neo-Tethys or the Alpine Atlantic Wilson cycle.

The field trip will focus on Triassic to Early Cretaceous deep-water, radiolarian-bearing sedimentary rocks deposited during the geodynamic history of the Neo-Tethys in different basins: rift-basins, shelf areas to continental slope, oceanic domains, and trench-like foreland basins. Special emphasis will be on the Jurassic to Early Cretaceous history, i.e. the geodynamic evolution before the "Mid-Cretaceous" tectonic motions and the influence of the evolution of two oceanic domains on the depositional environment above a drowned Triassic shelf (Apulian or wider Adria plate) between the Neo-Tethys Ocean to the south/southeast and the Alpine Atlantic Ocean to the north/northwest.

The geodynamically triggered interplay between carbonate production, siliciclastic/volcanic input and deposition of siliceous rocks/radiolarites in combination with the asynchrony of basin formation frequently allows the calibration of radiolarians with e.g., ammonoids, conodonts, calpionellids and other organisms. Following the Middle Triassic (Late Anisian) Neo-Tethys oceanic break-up and the demise of shallow-water carbonate production, deposition of Middle Triassic (Late Anisian to Ladinian) radiolarian-bearing, mainly carbonate deep-water sediments is widespread all over the shelf. Deposition of radiolarites in the Eastern Alps is limited to the outer shelf/continental slope and the Neo-Tethys oceanic domain to the south/southeast. Widespread shallow-water carbonate production started again in the latest Middle Triassic (Late Ladinian) and lasted until the end of the Triassic, interrupted only by short-lasting siliciclastic intervals ("Mid-Carnian" turnover, Lunz event). In the Late Triassic huge carbonate platforms were formed. Deposition of Late Triassic open-marine and radiolarian-bearing sediments is therefore limited mainly to the outer shelf region and radiolarites were deposited only on the Neo-Tethys ocean floor.

In Jurassic times, after the demise/drowning of the Late Triassic carbonate platform, calcareous siliceous sediments were again deposited widely. Rifting in the Alpine Atlantic realm to the north/northwest started in the Early Jurassic with oceanic break-up occurring from the Early/Middle Jurassic boundary onwards. The opening of the Alpine Atlantic to the north/northwest and, contemporaneously, the onset of convergence in the Neo-Tethys to the south/southeast worked in concert with radiolarite deposition culminating in the Middle Jurassic. Radiolarites were deposited practically all over the drowned continent except the areas of the Adriatic Carbonate Platform. Obduction of Neo-Tethys derived ophiolites since the Middle Jurassic led to the formation of a thin-skinned orogen with the formation of trench-like foreland basins in front of the advancing ophiolites. In these basins sedimentary mélanges with a radiolaritic-argillaceous matrix were deposited until the early Late Jurassic. Kimmeridgian-Tithonian shallow-water carbonate production on upper surfaces of the nappes restricted radiolarite

ze še ni dobro raziskano ali pojasnjeno. "Srednjekredna" orogeneza zakriva starejšo mezozojsko konfiguracijo plošč, kar je vzrok za kontroverzno razpravo o geodinamičnem razvoju in paleogeografiji od triasa do spodnje krede. Ta orogeneza ni bila povezana z Wilsonovim ciklom Neotetide ali Alpskega Atlantika.

Fokus ekskurzije je na radiolarijskih globokomorskih sedimentnih zaporedjih na robu Neotetide od triasa do spodnje krede. Zaporedja so bila odložena v različnih okoljih: v riftnih bazenih, na šelfu in kontinentalnem pobočju, v oceanu in v predgornih bazenih. Poseben poudarek bo na evoluciji v juri in spodnji kredi oziroma na geodinamičnem razvoju pred "srednjekrednimi" tektonskimi premiki. Poudarjen bo vpliv razvoja dveh oceanov na sedimentacijsko okolje, ki se je diferenciralo, ko se je potopil triasni šelf (Apulijska ali širša Jadranska plošča) med Neotetido na jugu/jugovzhodu in poznejšim Alpskim Atlantikom na severu/severozahodu.

Geodinamična evolucija in medsebojni vplivi med produkcijo karbonatov, siliciklastičnim ali vulkanskim vnosom in odlaganjem kremenični sedimentov/radiolaritov v kombinaciji z asinhronim oblikovanjem bazenov omogočajo, da se v določenih obdobjih radiolariji pojavljajo skupaj z drugimi organizmi, npr. amonoidi, konodonti in kalpionelidami. Po razpadu Neotetide v srednjem triasu (zgornjem aniziju) in prenehanju produkcije karbonatov v plitvi vodi so bili po celotnem šelfu razširjeni srednjetriasni (zgornjeanizijski do ladinijski) radiolarijski, predvsem karbonatni globokomorski sedimenti. Odlaganje radiolaritov je bilo v Vzhodnih Alpah omejeno na zunanji šelf in kontinentalno pobočje ter na oceansko območje Neotetide na jugu/jugovzhodu. Razširjena produkcija karbonatov v plitvi vodi se je ponovno vzpostavila na koncu srednjega triasa (v zgornjem ladiniju) in je trajala do konca triasa. Prekinjena je bila le s kratkotrajnimi siliciklastičnimi intervali (»srednjekarnijski« obrat, dogodek Lunz). V zgornjem triasu so nastale obsežne karbonatne platforme. Odlaganje zgornjetriasnih globokomorskih sedimentov in sedimentov, ki vsebujejo radiolarije, je bilo torej omejeno predvsem na območja zunanjega šelfa, radiolariti pa so se odlagali zgolj na oceanskem dnu Neotetide.

V juri, po potopitvi zgornjetriasne karbonatne platforme, so se s kremenico bogati karbonatni sedimenti ponovno odlagali na širšem območju. V spodnji juri se je začel tudi rifting na severu/severozahodu, ki je na meji med spodnjo in srednjo juro privedel do oceanizacije Alpskega Atlantika. Odpiranje Alpskega Atlantika na severu/severozahodu in sočasni začetek konvergence v Neotetidi na jugu/jugovzhodu sta hkrati delovala na poglabljanje bazenov na kontinentalnem robu, tako da je odlaganje radiolaritov v srednji juri doseglo višek. Radiolariti so se odlagali tako rekoč po celotnem potopljenem območju razen na Jadranski karbonatni platformi. Obdukcija ofiolitov z območja Neotitide od srednje jure dalje je privedla do oblikovanja tankoslojnega orogena in nastanka jarkom podobnih predgornih bazenov pred napredujočimi ofioliti. V teh bazenih so se do začetka zgornje jure odlagali melanži z radiolaritno-glinastim vezivom. V kimmeridgiju in tithoniju se je na novo nastalih pokrovih vzpostavila plitvovodna karbonatna produkcija, radiolariti pa so ostali omejeni na preostale globokovodne bazene. Zaradi dvigovanja orogena od zgornje jure (od titho-

deposition to remaining deep-water basins. In the frame of mountain uplift from the latest Jurassic (Tithonian) onwards the palaeotopography becomes overprinted by unroofing. Remaining deep-water foreland basins were successively filled in the Early Cretaceous by the erosional products of the uplifted Middle-Late Jurassic Neotethyan orogen.

During this field trip in one of the most classical areas of the world, the central Northern Calcareous Alps with its world-wide known touristic highlights, we will visit locations documenting the interplay between siliciclastic input, volcanic activity, carbonate production, various tectonic motions and deposition of radiolarian-bearing siliceous rocks to radiolarites.

Key words: Western Tethys realm, Triassic, Jurassic, Radiolarites, Palaeogeography

nija) naprej in posledično erozije se je paleotopografija popolnoma spremenila. Preostali globokomorski predgorni bazeni so bili v spodnji kredi drug za drugim zapolnjeni z materialom, erodiranim z dvignjenega srednje do zgornjejurskega orogena Neotetide.

Ekskurzija je speljana po enem najbolj klasičnih območij sveta, osrednjih Severnih Apneniških Alpah, s svetovno znanimi turističnimi znamenitostmi. Obiskali bomo lokacije s sedimentnimi zaporedji, iz katerih lahko razberemo medsebojno povezanost med vnosom siliciklastitov, vulkansko dejavnostjo, produkcijo karbonatov, različnimi tektonskimi dogajanji ter odlaganjem radiolaritov in drugih kremeničnih kamnin z radiolariji.

Ključne besede: Zahodna Tetida, trias, jura, radiolariti, paleogeografija

1 INTRODUCTION

Triassic–Jurassic/Early Cretaceous siliceous sedimentary rocks and radiolarites play a crucial role for palaeogeographic and geodynamic reconstructions of the Western Tethyan realm and occur widespread in the different orogenic belts around the Mediterranean. Their deposition is related to two oceanic realms, the Tethyan and the Atlantic oceanic systems and the continental realm in between (wider Adria since Jurassic times with the Eastern Alps as part of it, the field trip area: Figure 1).

In the eastern Mediterranean mountain ranges (Eastern and Southern Alps, Western Carpathians, units in the Pannonian realm, Dinarides, Albanides, Hellenides) the deposition of Triassic–Jurassic/Early

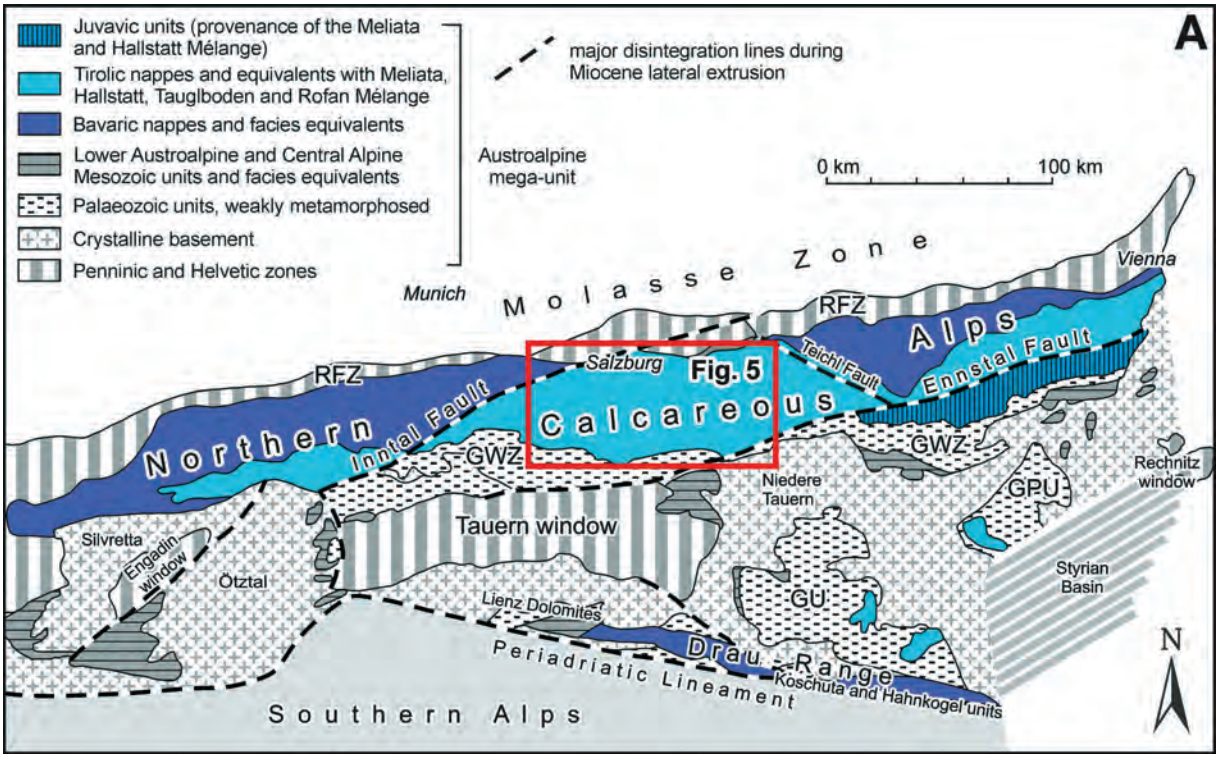

Figure 1: Tectonic sketch map of the Eastern Alps and field trip area (marked by the red box) in the central Northern Calcareous Alps (compare Figure 5; after Tollmann 1977; Frisch & Gawlick 2003; modified). GPU Graz Palaeozoic unit; GU Gurktal unit; GWZ Greywacke Zone; RFZ Rhenodanubian Flysch Zone.

Cretaceous siliceous sedimentary rocks and radiolarites is characteristic for specific stratigraphic levels (Figure 2). Related to specific events they were deposited widespread in open shelf areas, not only in the oceanic domains but also in deep-water foreland basins (Late Jurassic to Early Cretaceous). We discuss these radiolarite events on basis of the sedimentary evolution and tectonostratigraphy of the Northern Calcareous Alps as part of the Eastern Alps (Figs. 3, 4).

Herein follows a brief summary of the most important tectonostratigraphic and other events and its effect on the sedimentological record and biological response for Triassic to Early Cretaceous times. For a more detailed explanation interested readers are referred to the publication of Gawlick & Missoni (2019) with references therein.

Rifting in the Neo-Tethys Ocean (= Meliata-Hallstatt, Maliac, Dinaride, Pindos/Mirdita, Vardar oceans) began in the Late Permian, the oceanic break-up followed in the Middle Triassic (Late Anisian) and intra-oceanic convergence started around the Early/Middle Jurassic boundary followed by ophiolite obduction and formation of an orogen during Middle-Late Jurassic (Bajocian to Oxfordian) times (see Gawlick & Missoni 2019 for a recent overview, and references therein). Rifting in the Alpine Atlantic (= Magura/Vah, Penninic, Piemont, Ligurian oceans) started shortly after the Triassic/Jurassic-boundary in the Middle/Late Hettangian, followed by continental break-up in the late Early Jurassic (Toarcian), and closure started in the Late Cretaceous.

Triassic sedimentation in the eastern Mediterranean mountain ranges was triggered by the evolution of the Neo-Tethys, whereas in Jurassic to Early Cretaceous times sedimentation was controlled by both the evolution of the Neo-Tethys and the Alpine Atlantic. Whereas in the Eastern and Southern Alps, the Western Carpathians and units in the Pannonian realm, the Alpine Atlantic has a direct influence on the depositional record, this influence is minor in the Dinarides-Albanides-Hellenides because these areas are shielded by the Adriatic Platform (Vlahović et al. 2005). Jurassic to Early Cretaceous sedimentation was therefore controlled by the opening of the Alpine Atlantic Ocean to the north/northwest (break-up in the Toarcian: Ratschbacher et al. 2004), the partial closure of the Neo-Tethys Ocean to the south/southeast from the Early/Middle Jurassic boundary onwards, the Middle Jurassic to Early Cretaceous mountain building process related to Middle to early Late Jurassic ophiolite obduction, and latest Jurassic to Early Cretaceous mountain uplift and unroofing (Missoni & Gawlick 2011a; Gawlick & Missoni 2019; Gawlick et al. 2020a and references therein). Whereas the more southern orogenic belts (Dinarides, Albanides, Hellenides) were little affected by the Atlantic related rifting in Jurassic times, the Eastern and Southern Alps, Western Carpathians and some units in the Pannonian were affected by both events: closure of the Neo-Tethys to the east/southeast and opening of the Alpine Atlantic to the north/northwest.

Radiolarites were deposited on the Neo-Tethys passive margin and as sedimentary cover of the Neo-Tethys oceanic crust, beginning in the Late Anisian (Gawlick et al. 2008; Ozsvárt et al. 2012). Radiolarites are the typical sedimentary rocks deposited (often accompanied with volcanics) in Late Anisian to Ladinian times in the Dinaride-Hellenide mountain chain (for a recent review, see Gawlick et al. 2012a). In contrast, radiolarites are only rarely reported from the Triassic sedimentary shelf successions of the Alpine–Carpathian mountain belt. In this domain radiolarian-rich cherty limestones were mainly deposited (Figure 3) and often the radiolarians are recrystallized and/or not well preserved. The oldest widespread deposited radiolarites related to the Neo-Tethys Ocean were formed in Late Anisian to early Late Ladinian times, in both the Neo-Tethys ocean and in the (distal) passive margin setting, where the water depth did not exceed a few hundred metres.

The peak event of radiolarite deposition was in the Late Anisian (Illyrian), a period characterized by intense volcanism, restricted carbonate production and a relative high sea-level. The second more short-lasting radiolarite event followed the demise of the Late Ladinian - Early Carnian shallow-water platform cycle (Wetterstein Carbonate Platform) in the Middle Carnian (upper Julian), but was restricted to not filled intra-platform basins formed between the Wetterstein Carbonate Platform pattern before they became filled by siliciclastics (e.g. Eastern and Southern Alps, Western Carpathians) (Figure 3). This is in contrast to the southern orogenic belts (e.g. Hellenides, Albanides, Dinarides) where deposition of siliciclastic sedimentary rocks is restricted to the northern Outer Dinarides. Radiolarites and/or siliceous claystones were deposited in the oceanic domain, but were sparse in the distal margin. Mid-Carnian radiolarites or radiolarian-rich cherty limestones therefore occur more rarely, but also in in the Dinarides.

The peak of this radiolarite event predates the "Mid Carnian Pluvial Event" (Ogg 2015 and references therein) and can be related to a sea-level lowstand (Göstling Formation in the Northern Calcareous Alps with rich radiolarian faunas – Kozur & Mostler 1981). The Late Carnian to Norian is characterized by carbonate platform formation elsewhere in the West-

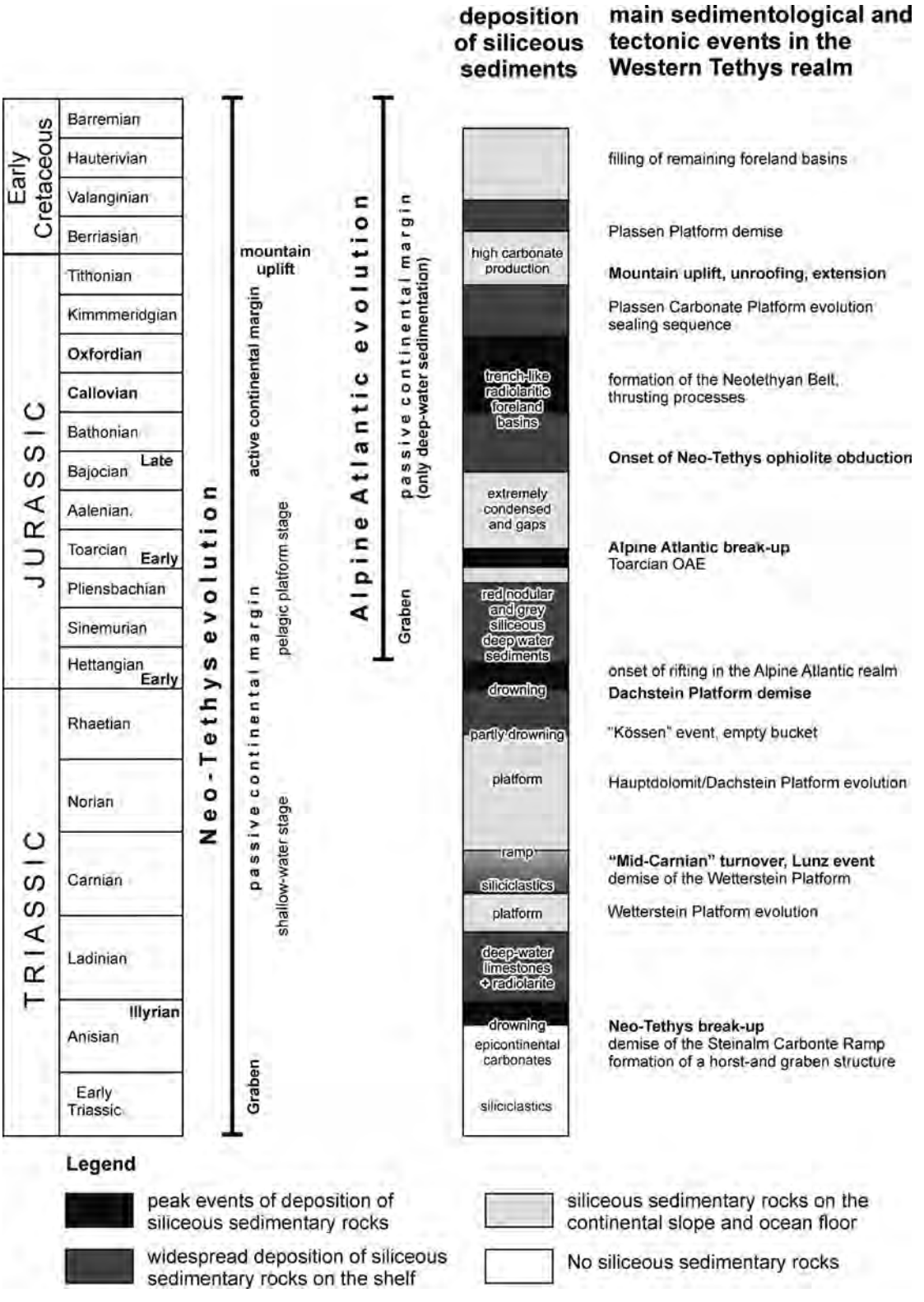

Figure 2: Triassic to Early Cretaceous geological time scale and frequency of radiolarite deposition related to different events in the sedimentary record of the Western Tethyan realm. During the peak event times spans siliceous sedimentary rocks and radiolarites were deposited not only in the oceanic domains. They were formed widespread also on the shelf areas in relatively shallow-water depths (maximum 200–300 m) and in deep-water foreland basins.

ern Tethys realm (Hauptdolomit/Dachstein Carbonate Platform) (Figure 3). In the northern orogenic belt the Rhaetian siliciclastic "Kössen event" decreased the carbonate production in certain areas and in deepened lagoons siliceous marls were deposited (Figure 3). In addition, in the Rhaetian in some areas of the distal Neo-Tethys passive margin radiolarian-rich sediments were deposited related to the partial drowning of the Late Triassic platform due to the increase of siliciclastics and the formation of deep lagoonal areas (e.g. Kössen Basin in the Eastern and Southern Alps, Western Carpathians).

The final drowning of the Late Triassic platform around the Triassic/Jurassic boundary is widespread followed by radiolarite deposition or radiolarian-rich siliceous marly limestones in the earliest Jurassic distal

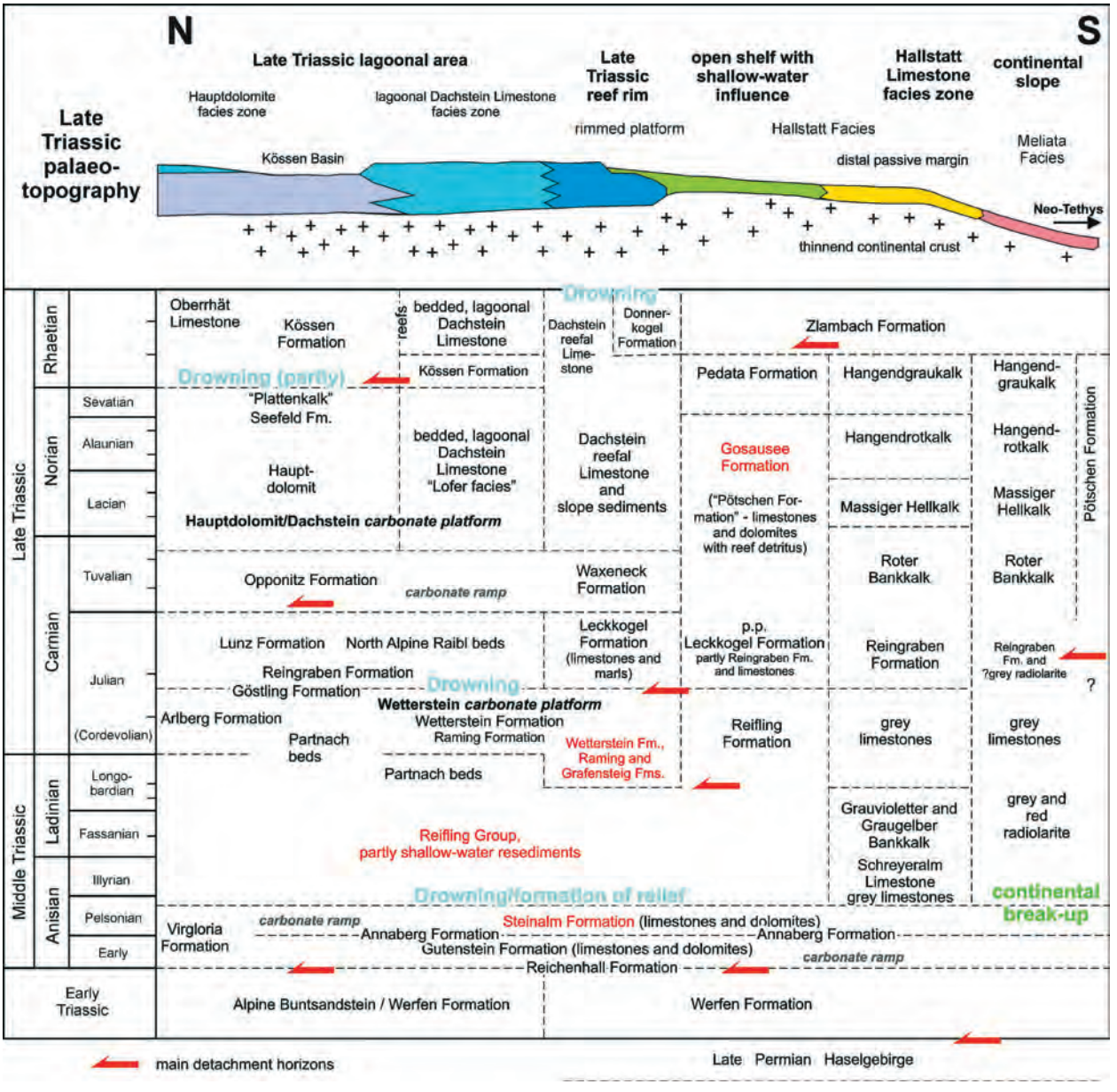

Figure 3: Simplified lithostratigraphic table of Triassic Formations in the central Northern Calcareous Alps with some important tectonostratigraphic events (added after Gawlick & Missoni 2019) and latest Triassic palaeotopography with indication of the different facies zones. Some important detachment horizons are indicated (Missoni & Gawlick 2011a, b) because of their importance during Middle to early Late Jurassic nappe stacking and disintegration of the sequence in the course of the northward propagating ophiolite obduction and formation of trench-like foreland basins in front of the advancing nappes filled with sedimentary mélanges (Figure 4). North-South after present directions. Formations indicated in red will be visited during the field trip.

passive margin setting and in former deep lagoon areas (sea-level lowstand to sea-level rise). In the deep lagoon grey cherty limestones, rich in radiolarians and spicules, were deposited (Figure 4). The Toarcian black shale event, with deposition of radiolarian-rich sediments, is contemporaneous with the eruption of two large igneous provinces (Karoo and Ferrar) and the break-up of the Alpine Atlantic (Neumeister et al. 2015 and references therein), which was contemporaneous with the onset of intra-oceanic subduction in

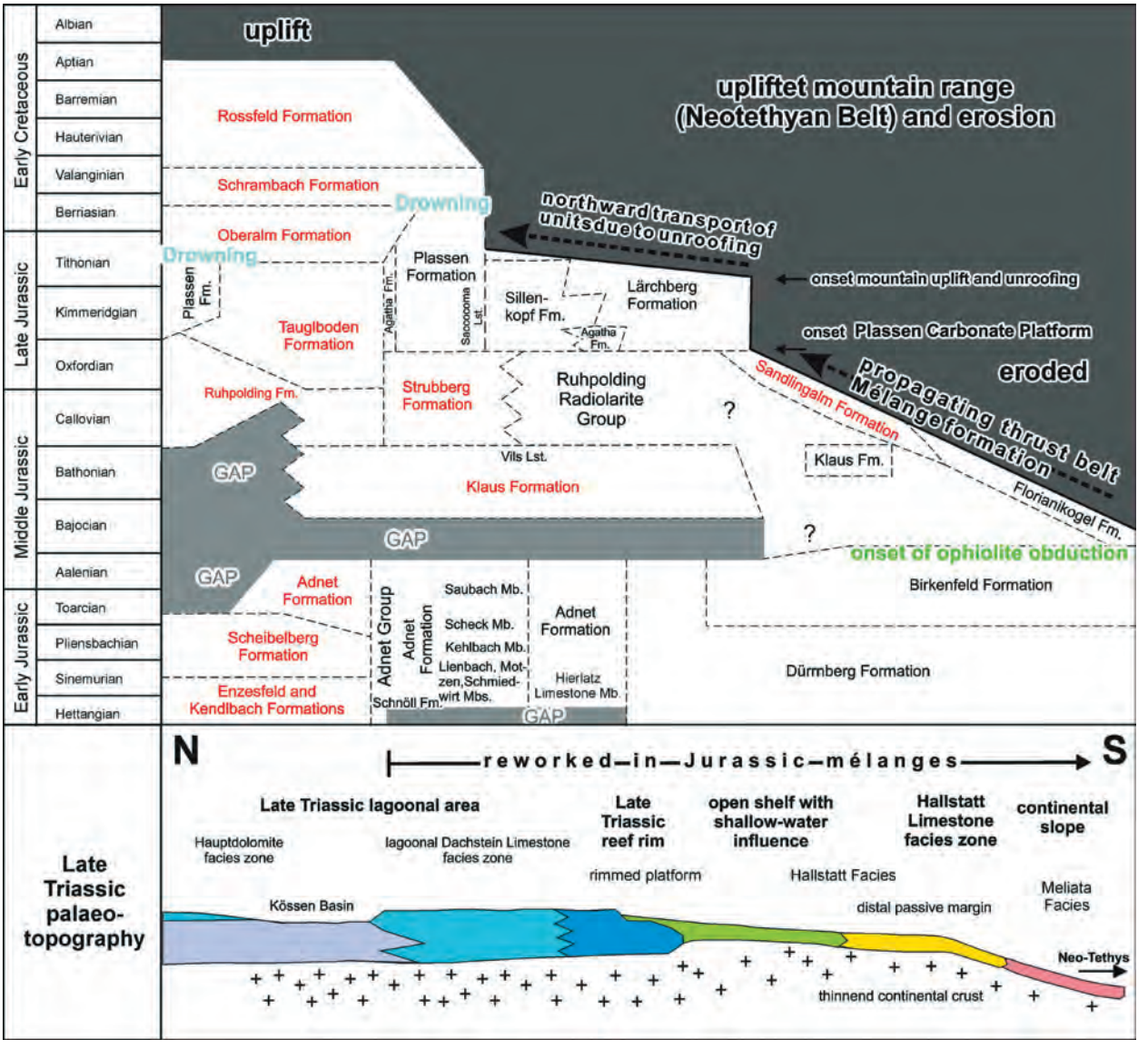

Figure 4: Simplified lithostratigraphic table of Jurassic to Early Cretaceous formations in the central Northern Calcareous Alps (after Gawlick & Missoni 2019) and latest Triassic palaeotopography with indication of the different facies zones. After the drowning of the Late Triassic Hauptdolomite/Dachstein Carbonate Platform, deposition in Early to early Middle Jurassic times followed the latest Triassic palaeotopography. In the Middle Jurassic the situation changed due to the onset of north-directed ophiolite obduction. In Middle to early Late Jurassic times the former outer passive margin became imbricated. In front of the northward propagating thrust belt deep-water trench-like foreland basins were formed and filled with the erosional products from the advancing nappe stack (= sedimentary mélange formation). During a period of relative tectonic quiescence, the Plassen Carbonate Platform sealed the older tectonic structures before mountain uplift and unroofing started in the Tithonian. This resulted in the stepwise destruction of the Plassen Carbonate Platform, which became either uplifted and eroded or drowned. During the Early Cretaceous the erosional products of the uplifted orogen filled the remaining deep-water foreland basins. Of the different Bathonian to Oxfordian trench-like basins and the Early Cretaceous foreland basins, we will visit resediments from the whole Triassic to Middle Jurassic outer continental margin and the Neo-Tethys Ocean. Formations indicated in red will be visited during our field trip.

the Neo-Tethys Ocean (Karamata 2006) and therefore easily recognized (sea-level highstand). Strong Middle Jurassic rifting in the Alpine Atlantic and onset of ophiolite obduction in the Neo-Tethys resulted in the Bathonian-Oxfordian radiolarite event with the peak in the Callovian-Oxfordian (Figure 2). On the Neo-Tethys-side new trench-like basins began filling with argillaceous-radiolaritic carbonate-clastic sedimentary mélanges from Bathonian times onwards (Figure 4). These radiolarites were deposited in a relative deep-water setting. From the latest Oxfordian/Kimmeridgian onwards a new carbonate platform pattern was formed on top of the obducted ophiolites and the rising nappe fronts (Figure 4). Therefore, on the Neo-Tethys-side intense carbonate production hampered widespread radiolarite deposition from the Kimmeridgian onwards. In the underfilled foreland basins between these platforms siliceous limestones with radiolarians were deposited, whereas more to the Alpine Atlantic-side radiolarites were still formed. In the Tithonian, the uplift and unroofing of the Neotethyan Belt (Missoni & Gawlick 2011a) started with intense erosion and the foreland basins received more and more resediments from the northward gliding units due to unroofing. In the earliest Cretaceous the transport of erosional products to the north was shielded by the still existing Late Jurassic to earliest Cretaceous carbonate platform pattern (Plassen Carbonate Platform). In addition, the now blooming calcareous nannoplankton in deep-water settings produced micritic limestones in rock forming quantities and siliceous marly limestones were deposited. From the Middle/Late Berriasian onwards, after the final drowning of the Plassen Carbonate Platform, more and more siliciclastic material became transported to the north.

In the underfilled foreland basins, intercalated mass transport deposits in the prograding delta fronts during sea-level lowstands contain the whole reworked Middle-Late Triassic radiolarite sequence from the obducted Neo-Tethys ophiolites and all materials from the ophiolitic mélange (Krische et al. 2014). Northward of these underfilled foreland basins in direction to the outer southern passive continental margin of the Alpine Atlantic Ocean, siliceous marls were deposited widespread.

2 THE FIELD TRIP

During the field trip in the Salzburg and Berchtesgaden Calcareous Alps and Salzkammergut (Figure 5), we will visit almost the entire Triassic to Early Cretaceous sedimentary history (Figures 3, 4), excepting the Early Triassic, with special emphasis on siliceous sedimentary rocks and radiolarites. In the Clessinsperre section we will observe the evolution from an Early to Middle Anisian shallow-marine ramp (Gutenstein to Steinalm Formations) to Late Anisian – Ladinian deep-water siliceous limestones (Reifling Formation) followed by the onset of the latest Ladinian to earliest Carnian Wetterstein Carbonate Platform (Figure 3). At Mt. Mehlstein (optional) we will visit radiolarian-bearing siliceous dolomites to limestones of the Gosausee Formation (Figure 3). The section Mörtlbach will provide an Early Jurassic (Hettangian) to Late Jurassic (Oxfordian) succession (Kendlbach/Enzesfeld Formations to Tauglboden Formation: Figure 4). In the area of the Mischenirwiese and at the footwall of Mt. Sandling we will see the Sandlingalm Basin fill (Bathonian to Oxfordian). Around Mt. Hochkranz or in the Lammer valley we will visit the Lammer Basin fill (Callovian to Oxfordian) and in the Tauglboden valley and the Fludergraben area we will visit the whole Tauglboden Basin fill (Oxfordian to Tithonian). The Leube quarry will provide insights in the latest Jurassic to Barremian sedimentary evolution.

2.1 Triassic

Clessinsperre near Saalfelden – Middle Triassic

Further reading: Gawlick et al. (2021) and references therein. For radiolarians see Kozur & Mostler (1981)

The Clessinsperre section (Pia 1924), located on the southern rim of the Steinernes Meer Mts. northeast of the town Saalfelden (Figure 5), represents the type locality of the Steinalm Formation (Pia 1930). At the section Clessinsperre (Öfenbachgraben) a continuous succession from the early Anisian Gutenstein Formation, deposited under restricted conditions, to the Late Ladinian – Early Carnian Wetterstein Carbonate Platform is exposed (Figure 6).

The section in the Öfenbachgraben starts with dark-grey decimeter-bedded Gutenstein Limestone directly followed by the light- to medium-grey thick-bedded Steinalm Limestone. Microfacies characteristics change from dark-grey micritic limestones (Gutenstein Formation) very poor in organisms to microbial-dominated medium to light-grey limestones, indicating a still restricted environment. Other organisms are very rare in this part of the roughly 70 meter-thick Steinalm Limestone succession. More open-marine conditions are only observed in the upper part, and the

algae and foraminifera-bearing horizon is restricted to the uppermost part of the Steinalm Limestone (Pia 1912, 1930; Wagner 1970; Ott, in Tollmann 1976), about one meter below the base of the deepening sequence (Figure 6). The algae are moderately preserved and the assemblage is dominated by *Oligoporella* species.

The highest part of the "Steinalm Formation" consists of shallow-water material with some millimeter-thick deep-water intercalations, i.e. this part of the Steinalm Limestone indicates that the decrease in carbonate production was not abrupt. These deep-water intercalations contain filaments, ostracod shells and a few recrystallized radiolarians. To attribute this part of the succession to the Steinalm Formation or the Reifling Formation is a matter for discussion. Due to the appearance of deep-water organisms it should rather be the base of the Reifling Formation, but the overall lithology fits better to the Steinalm Formation. The thin open-marine intercalations are hard to detect and mostly invisible in outcrops. In fact, it is a transitional part in the section from the shallow-water Steinalm Formation s. str. to the deep-water Reifling Formation s. str., not described to date due to the lack of appropriate sections or simply overlooked. The drowning sequence s. str., i.e. the demise of the shallow-water Steinalm Carbonate Ramp is here represented by decimeter-bedded grey siliceous limestones, i.e. the Reifling Formation (Tollmann 1976 for details), here Late Pelsonian in age (Gawlick et al. 2021). However, in the first (Late Pelsonian) beds shallow-water debris is still common. Above the Early Illyrian ammonoid-rich horizon (Broili 1927; Schnetzer 1934; Assereto 1971) siliceous radiolaria-filament wackestones predominate. Beside conodonts (Gawlick et al. 2021 and references therein), new species of well-preserved radiolarian faunas were described by Kozur & Mostler (1981).

The age of the Reifling Formation is Late Anisian to Late Ladinian, dated by conodonts. In the Illyrian and Late Ladinian intercalations of volcanic ashes are characteristic. Upsection of these volcanic ash layers,

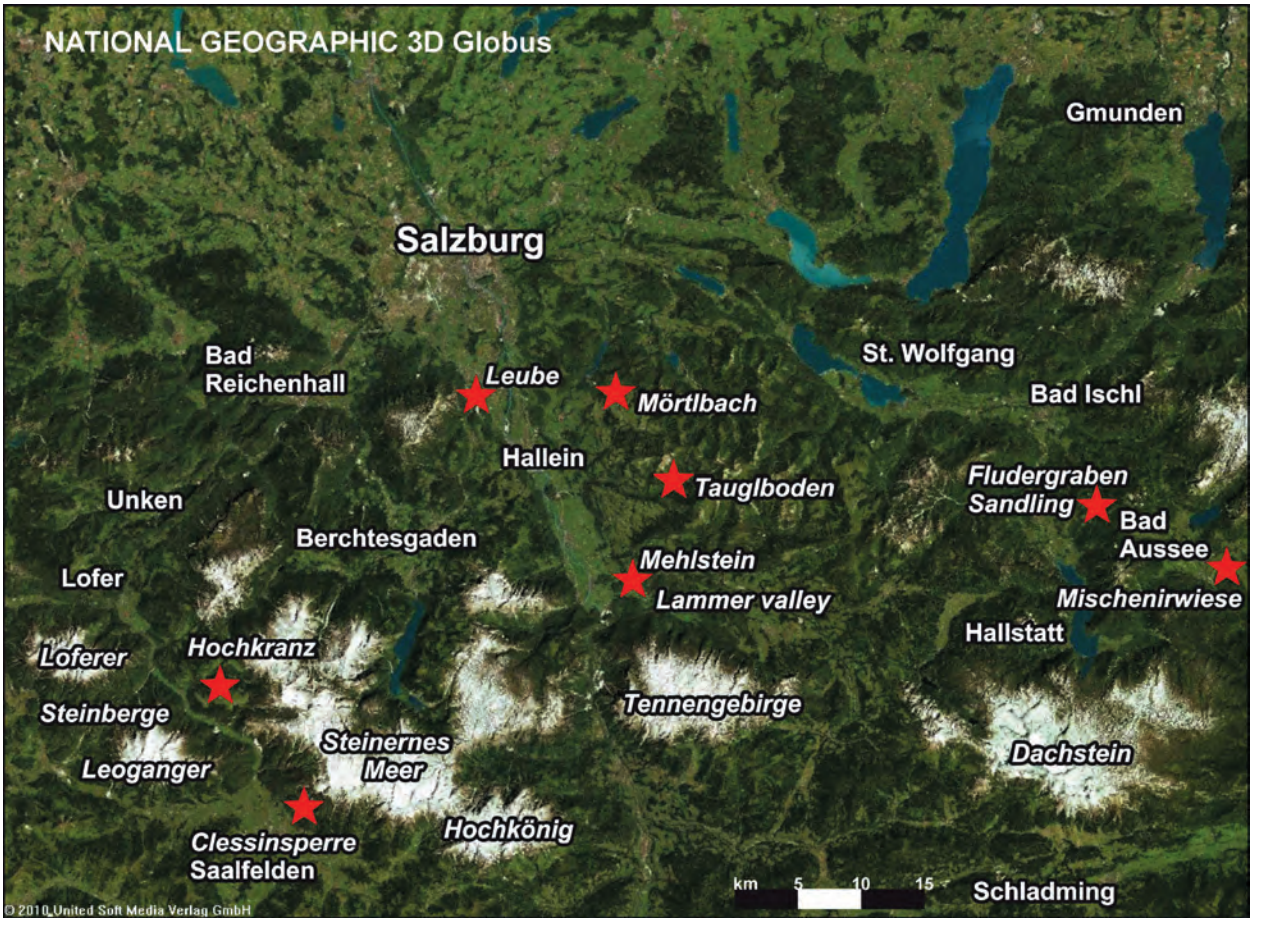

Figure 5: Satellite image of the central Northern Calcareous Alps (compare Figure 1) with the planned localities (red stars), which will be visited during this field trip in the Salzkammergut area, the Salzburg and Berchtesgaden Calcareous Alps.

the first shallow-water resediments of the prograding Wetterstein Carbonate Platform occur; further upsection we will see the dolomitized Wetterstein Carbonate Platform (Late Ladinian to Early Carnian). Due to intense dolomitization, the typical microfacies of the Wetterstein Carbonate Platform are fore-reef carbonates, but subsequent reefal and back-reefal carbonates topped by lagoonal carbonates are barely visible. Dolomitization of the Wetterstein Carbonate Platform is a widespread phenomenon, especially in the Tirolic Nappe of the Northern Calcareous Alps.

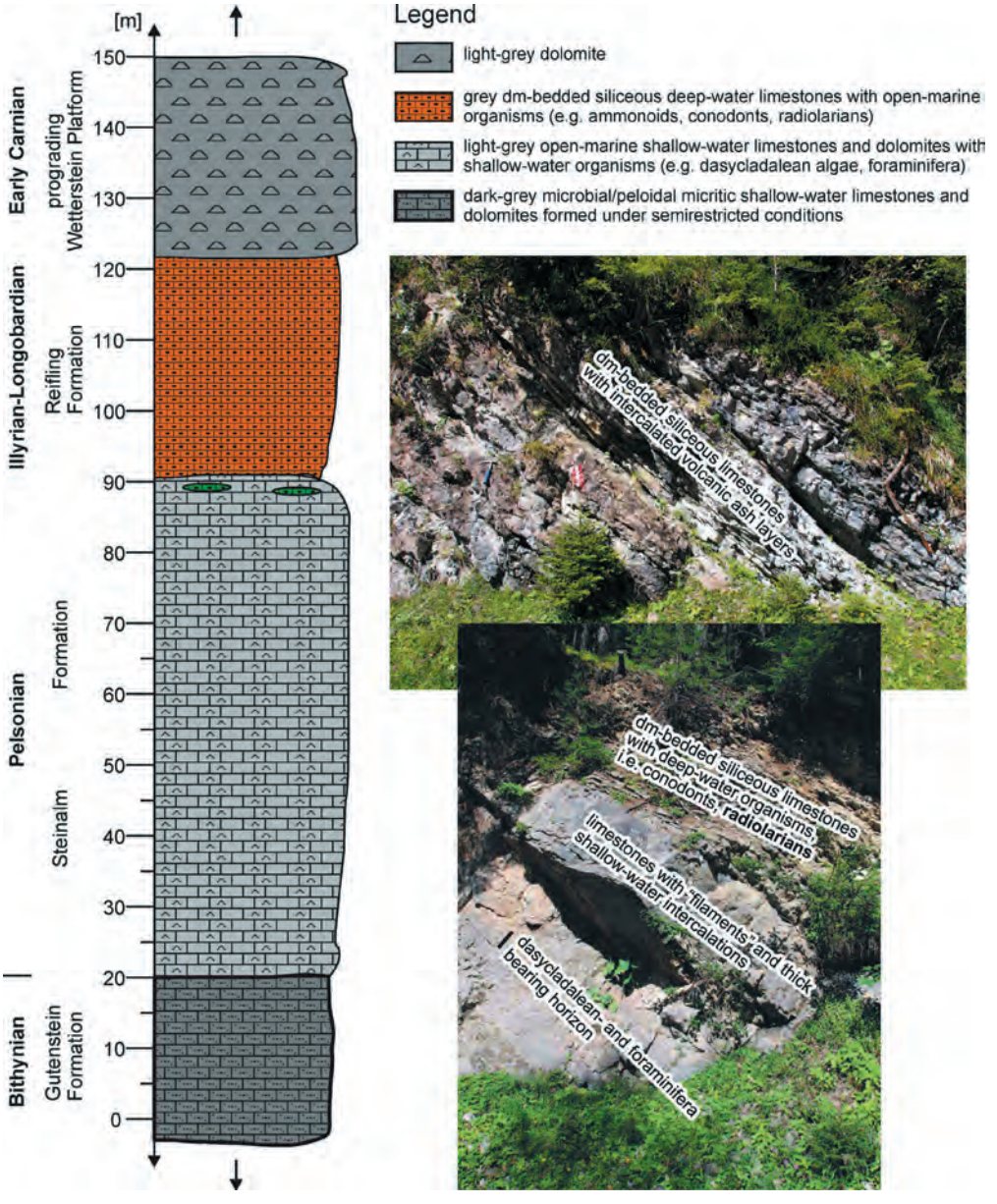

Figure 6: Clessinsperre section north of the town Saalfelden with different formations/ages, modified after Gawlick et al. (2021). In this section the shallow-marine Steinalm Limestone directly overlies the Gutenstein Formation without intercalated deeper-water limestones (Annaberg Formation). The lower photo shows the drowning unconformity: thick-bedded to massive Steinalm Limestone overlain by the grey siliceous decimeter-bedded deep-water limestones of the Reifling Formation. The topmost Steinalm Limestone consists of a mixture of shallow-water material and deeper-water organisms; thin-shelled bivalves (filaments) and crinoids indicate a rapid deepening in the Late Pelsonian. The upper part shows the Middle-Late Illyrian decimeter-bedded deep-water siliceous limestones of the Reifling Formation with intercalated volcanic ash layers (bentonites). This part contains in some layers a relatively rich radiolarian fauna, as described by Kozur & Mostler (1981).

Mehlstein – Late Triassic (optional)

The Upper Triassic (Tuvalian to Middle Norian) sedimentary sequence of Mt. Mehlstein is an allochthonous block in the Callovian-Oxfordian sedimentary Hallstatt Mélange in the Lammer valley (Gawlick 1996, 2004). The sedimentary succession consists of grey cherty limestones and siliceous basinal dolomites (Figure 7). The grey bedded limestones with chert nodules and chert layers contain only recrystallized radiolarians, whereas the Norian siliceous and in parts organic rich basinal dolomites contain relatively well preserved pyritized radiolarians beside conodonts (Gawlick & Dumitrica, in preparation). The provenance area of Mt. Mehlstein is the reef-near facies belt (Figure 3), which became imbricated since the Callovian. The thickness of the decimeter-bedded grey cherty limestones is in comparison with the meter-bedded to massive siliceous dolomites relatively low. Dolomite formation is interrupted only during the Late Carnian transgressive cycle and the late Lacian regressive cycle. Dolomite formation ended in the Late Alaunian contemporaneous with the culmination of the late Middle/Late Norian tectonic motions.

2.2 Jurassic

In the Alpine-Carpathian domain the sedimentation pattern diachronously changed from carbonate to siliceous deposition in the Middle Jurassic (Schlager & Schöllnberger 1974). Also the tectonic regime changed. A characteristic new feature was the formation of trench-like radiolaritic basins with up to 2000 metres of sediment infill in their south-eastern oceanward parts, characterized by rapid subsidence due to tectonic load. In contrast, their north-western continentward edges were characterized by uplift and condensed sedimentation or erosion. The derivation of the resedimented components differs. In the south-eastern basin group, the material was shed either from the Triassic to Early Jurassic distal, hemipelagic to pelagic continental margin (Hallstatt and Meliata Zones) or from the Zlambach facies and the Dachstein reef rim zone. In contrast, in the north-western basin group the material was derived from the Triassic to Middle Jurassic lagoonal area (Dachstein and Hauptdolomit facies zones) (Figs. 4, 5).

Each reconstruction of the Jurassic tectonic movements depends on detailed studies on components and

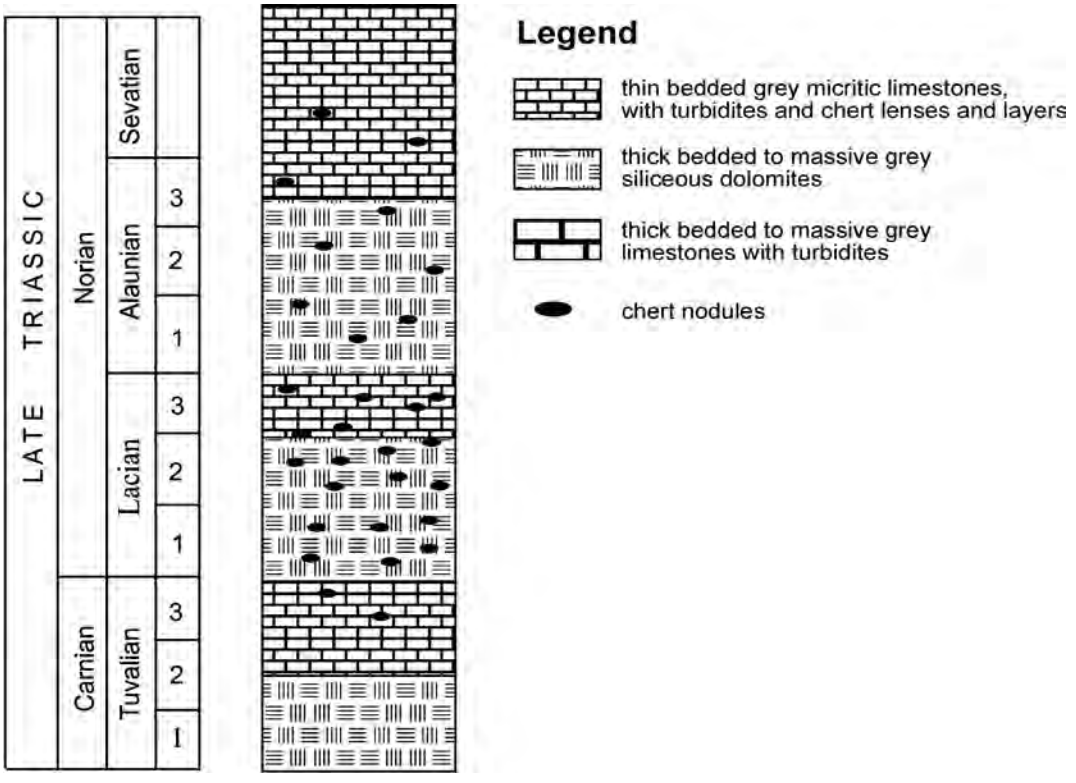

Figure 7: Generalized Late Triassic sedimentary succession of Mt. Mehlstein in the village Unter Scheffau, modified and complemented after Gawlick (1998). The Norian siliceous bituminous basinal dolomites contain in certain levels relatively well preserved pyritized radiolarians.

stratigraphy of the siliceous matrix sediments. The following different carbonate-clastic, radiolaritic sequences with characteristic Middle to Late Jurassic sedimentation in the Northern Calcareous Alps can be distinguished at the moment (from south to north, except the Sillenkopf Basin which represents a remnant radiolaritic basin between the Lärchberg and the Plassen Carbonate Platform):

Florianikogel Basin with the Florianikogel Formation (Figure 5): Its ?Bajocian to Callovian matrix contains material from the Hallstatt Salzberg and Meliata facies zones (Mandl & Odrejičková 1991, 1993; Kozur & Mostler 1992) as well as volcanogenic greywacke layers as erosional products derived from the Neo-Tethys oceanic crust (Neubauer et al. 2007). This basin fill is similar to the Meliata Formation in the sense of Kozur & Mock (1985) in the Western Carpathians (Kozur & Mock 1997; Mock et al. 1998; Gawlick & Missoni 2019).

Sandlingalm Basin group with the Sandlingalm Formation (Gawlick et al. 2007a; Gawlick & Missoni 2019 and references therein): These ?Bajocian/Bathonian to Late Oxfordian basins contain only material from the Hallstatt Salzberg facies zone and limestones of the Meliata Zone (Pötschen Formation without shallow-water material).

Lammer Basin with the Strubberg Formation (Gawlick & Missoni 2019 and references therein): This Early Callovian to Middle Oxfordian basin contains mainly material from the Zlambach facies zone and the Dachstein Limestone reefs (Gawlick 1996; Missoni & Gawlick 2011a).

Tauglboden Basin with the Tauglboden Formation: In this Early Oxfordian to Tithonian basin (Huckriede 1971; Gawlick et al. 2009a) the first phase of resedimentation started in the Early Oxfordian (Gawlick et al. 2007a) with material derived from the lagoonal Dachstein Limestone facies zone and ended around the Middle/Late Oxfordian boundary. Following a period of tectonic quiescence and low sediment supply in latest Oxfordian to Early Tithonian the second phase of intense resedimentation had its climax in Late Tithonian and was accompanied by an overall extensional regime (Missoni & Gawlick 2011a, b). The change from older Triassic to Middle Jurassic clasts in the first phase to clasts of Late Jurassic reefal sediments in the second phase is characteristic (Steiger 1981; Gawlick et al. 2005).

Rofan Basin with the Rofan Breccia: Resedimentation started in the Late Oxfordian (Gawlick et al. 2009a) with material derived from the Hauptdolomit facies zone (Figs. 5, 6; Wächter 1987) and prevailed until the Oxfordian/Kimmeridgian boundary or Early Kimmeridgian. By that time the sedimentation changed to mostly carbonate detritus, derived from a carbonate platform to the south (Wolfgangsee Carbonate Platform - Gawlick et al. 2007b).

Sillenkopf Basin: Another type of basin represents the Kimmeridgian to ?Tithonian Sillenkopf Basin with the Sillenkopf Formation and components of mixed palaeogeographic origin (Missoni et al. 2001). The spectra of clasts in the Sillenkopf Formation prove the following provenance areas: A) The accreted Hallstatt units and an overlying Late Jurassic shallow-water carbonate platform, B) a deeply eroded hinterland further south (probably a part of the crystalline basement of the Northern Calcareous Alps), and C) an ophiolite nappe pile probably carrying an island arc (Missoni & Kuhlemann 2001; Gawlick et al. 2015), similar to the obducted ophiolites which acted as source for radiolaritic-ophiolitic mélanges in the Dinaridic/Albanide realm.

The radiolarite basins A to E were formed in sequence, propagating from a south-east to north-west direction (= from the Meliata to the Hauptdolomit facies zone), in the time span from the Bajocian to the Oxfordian/Kimmeridgian boundary. Basins A and C were accreted and overthrusted, basin B only partly. Basins D, E, F, and partly B existed in Kimmeridgian to early Early Tithonian time as remnant basins in between newly formed shallow-water carbonate platform areas of the Plassen Carbonate Platform sensu lato, which was formed since the Late Oxfordian (Auer et al. 2009).

During this field trip through the central Northern Calcareous Alps (Figure 2) we will study, as one topic, deep-water basin fills with its underlying and overlying sedimentary successions: Sandlingalm Basin fill, Lammer Basin fill, Tauglboden Basin fill.

The onset and drowning/demise of carbonate platforms (Plassen Carbonate Platform sensu lato) on top of the nappe stack and their progradation over the radiolarite basins and the remaining starved deep-water basins between the platforms is not a topic of this field trip.

Sandlingalm Basin

This basin fill contains blocks up to kilometre-size, derived exclusively from the Hallstatt Salzberg facies zone (various coloured Hallstatt Limestone sequence) and – in rare cases – mixed with components from the Meliata facies zone (including cherty Pötschen Limestone without reefal detritus) in a radiolaritic or radiolaritic-argillaceous matrix. The sedimentary succes-

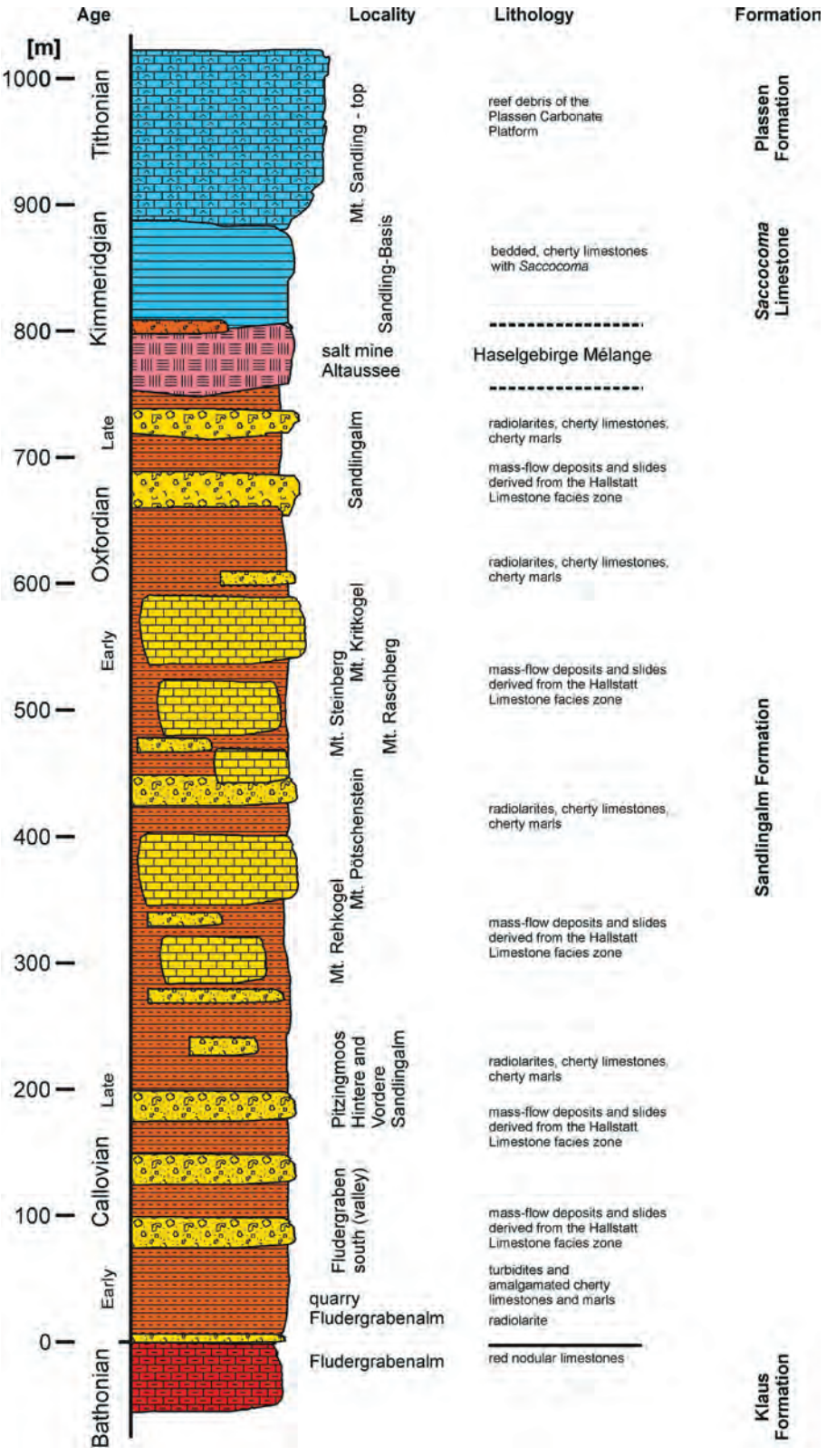

Figure 8: Schematic section of the Sandlingalm Basin fill in the area around Mount Sandling: Fludergrabenalm – Fludergraben – Pitzingmoos – Mt. Rehkogel – Sandlingalm – Mount Sandling. During the field trip we will visit nearly the whole basin fill starting at the Fludergrabenalm. Slightly modified after Gawlick et al. (2007a).

sion of the Sandlingalm Basin is composed of various slide masses. Resedimentation of Hallstatt blocks in this basin started in the Late Bathonian and ended in the Middle Oxfordian.

Following the emplacement of the Haselgebirge Mélange around the Oxfordian/Kimmeridgian (Missoni & Gawlick 2011a), deposition of grey siliceous deep-water limestones began in basinal areas as part of the Plassen Carbonate Platform (compare Gawlick et al. 2010 for the field trip area). Aside from the early Plassen Carbonate Platform sensu lato, these basinal limestones, were deposited on top of slide masses sealing the chaotic basin fill whereas on top of the nappe fronts carbonate platforms were established.

We will visit the type-area of this basin in the central Salzkammergut area north of the small towns Altaussee and Bad Mitterndorf.

Most samples from the Sandlingalm Basin contain rich, well-preserved radiolarian assemblages.

Mt. Sandling area

Further reading: Suzuki & Gawlick (2003), Gawlick et al. (2007a, 2010, 2012), Gawlick & Missoni (2019) and references therein, Suzuki & Gawlick (2020).

In the Sandlingalm area we will visit two different basin fills: The proximal Tauglboden Basin fill and the Sandlingalm Basin fill (see below).

In the Mount Sandling area the Sandlingalm Basin is situated directly south of the Tauglboden Basin (see below). The tectonic contact is a sharp strike-slip fault. The sedimentary succession of the Sandlingalm Basin fill (Figure 8) starts with red nodular limestones of the Early Jurassic Adnet and the Middle Jurassic Klaus Formation (*Bositra* Limestone), whose upper part is siliceous with a well preserved radiolarian fauna. Upsection are red radiolarites which turn rapidly to green-grey radiolarites with intercalated carbonate turbidites (Figure 9) followed by the first mass transport deposits with dm-sized-blocks. The provenance area of the different limestone and siliceous marl components is the distal shelf area, i.e. the Hallstatt Limestone facies zone and the continental slope (Meliata facies zone). The Lower Jurassic cm- to dm-sized components correspond to the Lower Jurassic Dürrnberg Formation, which we plan to visit in the Teltschengraben area (see below). Upsection in the basin fill Lower Jurassic components decrease and older components started to be redeposited. In addition, the component size of the redeposited Hallstatt sequence increases and the basin fill reflects a coarsening-upward cycle, as typical for foreland basin fills and advancing nappes.

Figure 9: Radiolarite quarry west of the Fludergrabenalm. Slump deposits of reddish radiolarite are intercalated in dark-grey dm-bedded radiolarites, which are in parts laminated. Fine-grained turbidites consist of open-marine limestones from the open-marine distal shelf (Hallstatt Limestone facies).

Mischenirwiese and Teltschengraben (optional)

Further reading: O´Dogherty et al. (2008, 2017) and references therein.

In the area around Bad Mitterndorf, a Sandlingalm Basin filled with several mass transport deposits consisting of reworked material from the outer shelf (Hallstatt Limestone facies) and km-sized slide blocks is preserved. The component spectrum differs slightly from that in the type area around Mount Sandling indicating that the Sandlingalm Basin fills are in fact a series of imbricated trench-like basins fills in front of the advancing nappe pile. In all Sandlingalm Basin fill areas the components derive from the Triassic to Early Jurassic outer shelf, i.e. the various coloured Hallstatt Limestone facies zone.

In the Teltschengraben a slide of uppermost Lower Pliensbachian (*Gigi fustis – Lantus sixi* Radiolarian Zone of Carter et al. 2010) cherty marls and cherty limestones is embedded in Callovian radiolarites. The wacke- to packstones are in parts rich in crinoids and frequently contain recrystallized radiolarians; well-preserved radiolarians also occur in a few layers. The detection of this slide is important because it is one of the few Pliensbachian siliceous sedimentary sequences with a well preserved radiolarian fauna in the whole Western Tethyan Realm (compare Cifer et al. 2020). Some new taxa could be described from this succession. The outcrop is situated in a steep valley and is therefore optional (further reading O´Dogherty et al. 2008).

The Mischenirwiese section (Figure 10) northwest of Bad Mitterndorf (for details see O´Dogherty et al. 2017) consists of a slightly folded but complete Late Bajocian/Bathonian to Oxfordian-?Kimmeridgian radiolarite succession. This nearly 100 m thick radiolarite succession represents the distal part of the Sandlingalm Basin where intercalated mass transport deposits and big slides are missing. The isolated, highly diverse and well-preserved radiolarian assemblages have been used by O´Dogherty et al. (2017) for a detailed taxonomic study. Two new families, 6 new genera, and 2 species were described from the Mischenirwiese section.

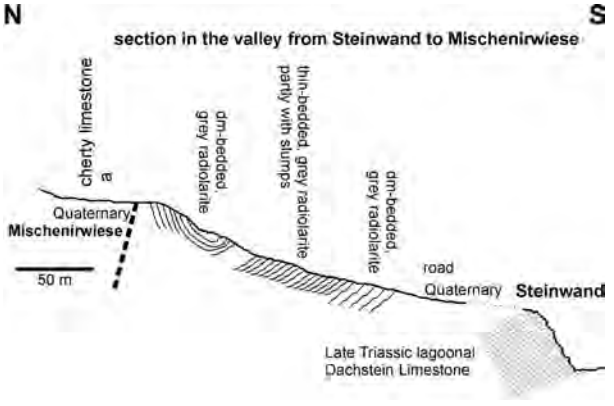

Figure 10: Mischenirwiese section: cross-section in the small valley from the Steinwand to the Mischenirwiese. Modified after O´Dogherty et al. (2017).

Lammer Basin

The palaeogeographic position of this Callovian-Oxfordian basin fill was in the former lagoonal area of the Late Triassic Dachstein Carbonate Platform, i.e., it took a middle shelf position. The basin fill is characterized mainly by reworked material from the Dachstein reef facies belt and the reef-near open-marine grey Hallstatt facies/Gosausee Limestone facies. Two different reworked successions can be reconstructed: (I) A Middle to Late Triassic open-marine succession with re-sedimented material from the reef rim, and (II) a Middle to Late Triassic open-marine to shallow-water sequence from the reef rim facies zone. Material from the upper continental slope or the Hallstatt Limestone facies zone occur re-mobilized and transported in a piggy-back manner together with its substratum (Gawlick & Missoni 2015), a km-sized slide block from the open shelf area showing shallow-water influence. The matrix consists of dark-grey to black siliceous limestones to radiolarites, argillaceous siliceous marls, and manganese-enriched shales to carbonates. The Haselgebirge Mélange (Late Permian evaporites - Tollmann 1976) with the Hallstatt Limestone mélange was thrust over the basin fill around the Oxfordian/Kimmeridgian boundary. The subsequent Kimmeridgian to Early Cretaceous foreland basin sedimentation sealed the older structures and basin geometries (Missoni & Gawlick 2011a).

Depending on the field trip route we will visit the Lammer Basin fill either in the type area or in the area of Mount Hochkranz.

The preservation of the radiolarians in the Lammer Basin is moderate to poor. Only few samples contain moderate to well-preserved radiolarian assemblages. In most cases the radiolarians are completely recrystallized.

Lammer valley

Further reading: Gawlick (1996), Gawlick & Suzuki (1999), Gawlick et al. (2012) and references therein, Gawlick & Missoni (2015).

The type area of the Lammer Basin fill is situated in the western Lammer valley between Golling to the west and Abtenau to the east (details in Gawlick, 1996). In this area the complete, coarsening- upward basin fill of nearly 2000 m thickness is preserved, The slides in the higher part of the basin fill are km-sized blocks from the Late Triassic Dachstein reef belt. We will visit the lower to middle part of the basin fill in detail. Above the Upper Triassic (Rhaetian) lagoonal Dachstein Limestone, the Lower Jurassic sequence is composed of grey cherty limestones (Hettangian to Pliensbachian), followed by Upper Pliensbachian to Lower Toarcian mass transport deposits consisting of reworked Adnet Limestones and subsequent Middle Jurassic *Bositra* Limestones after a gap. In the Callovian, limestone deposition changed to deposition of siliceous sedimentary rocks: radiolarites (first reddish, later grey to black), siliceous limestones, and argillaceous-siliceous marls. First mass transport deposits appear in the argillaceous-siliceous marls in the latest Callovian below a manganese carbonate level that was formed around the Callovian/Oxfordian boundary. Upsection, i.e. in the Early to Middle Oxfordian, the amount of intercalated mass transport deposits and the reworked component size increases. In this part of the basin fill the reworked material was derived exclusively from the open shelf area adjacent to the reef rim. Upsection follow km-sized blocks with complete Carnian to Rhaetian sedimentary successions from this facies belt. These blocks carry, in a piggy-back manner,

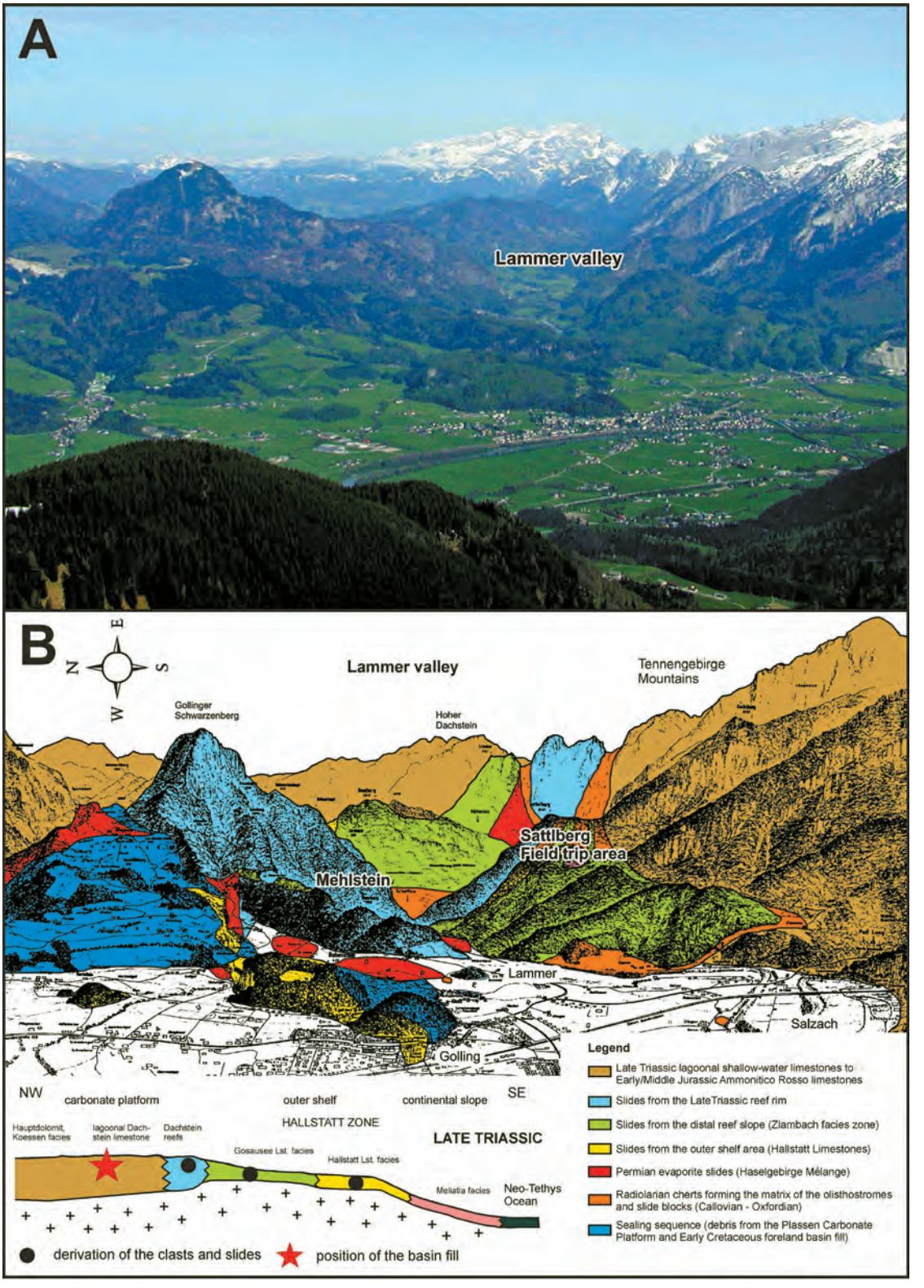

Figure 11: A: Photo from the west showing the type area of the Lammer Basin fill, and B: Geological interpretation (modified after Gawlick et al. 2012 and Gawlick & Missoni 2015). The basin fill with a coarsening-upward trend consists exclusively of allochthonous material of different age and provenance from the outer shelf area of the northwestern Neo-Tethys passive continental margin.

material from the outer shelf transitional to the continental slope, i.e. the Meliata facies zone. Characteristic for this reworked sedimentary succession are Middle Triassic (Upper Anisian to Ladinian) radiolarites (Gawlick & Missoni 2015). Later huge slides from the Late Triassic reef belt were transported into the Lammer Basin. In addition, Hallstatt Limestone blocks with complete Upper Anisian to Upper Norian sedimentary successions and Upper Permian evaporites appear in the northwestern part of the Lammer Basin fill.

Moderately preserved radiolarian assemblages occur throughout the whole siliceous sedimentary succession, i.e. in the matrix of the different mass transport deposits and slides (Gawlick & Suzuki 1999). The entire basin fill is sealed by a relatively flat lying Kimmeridgian to Aptian sedimentary sequence (Figure 11).

Hochkranz (optional)

In the area of Mount Hochkranz, west of St. Martin in the Saalach valley, a fill similar to that of the Lammer Basin type area (Lammer valley) is preserved. The basin fill in the area around Mount Hochkranz is in direct continuation to the west of the Lammer valley and can be traced all along the way from the Lammer valley to the Mount Hochkranz area (Missoni & Gawlick 2011a, b). Whereas in the Lammer valley the most proximal part of the basin fill is preserved, in the Mount Hochkranz area a more distal part of the basin fill is preserved. Also the component spectrum is slightly different. Outer shelf components are missing as well as components from the more basin ward depositional realm of the reef rim.

The relatively thick radiolarite succession (various coloured radiolarites) below the first mass transport deposits consists of grey to dark-grey radiolarites and siliceous limestones with moderately preserved radiolarian faunas. Slump deposits and sediment creeping is a characteristic sedimentological feature for this radiolaritic sequence. After deposition of the manganese-rich horizon the first mass transport deposits are intercalated in a siliceous-radiolaritic matrix. The component spectrum reflects a reworked Late Triassic sedimentary sequence from the Dachstein reef rim facies zone. The basin fill shows a coarsening-upward trend and is sealed by the limestones of the prograding Kimmeridgian-Tithonian Plassen Carbonate Platform (Mount Hochkranz).

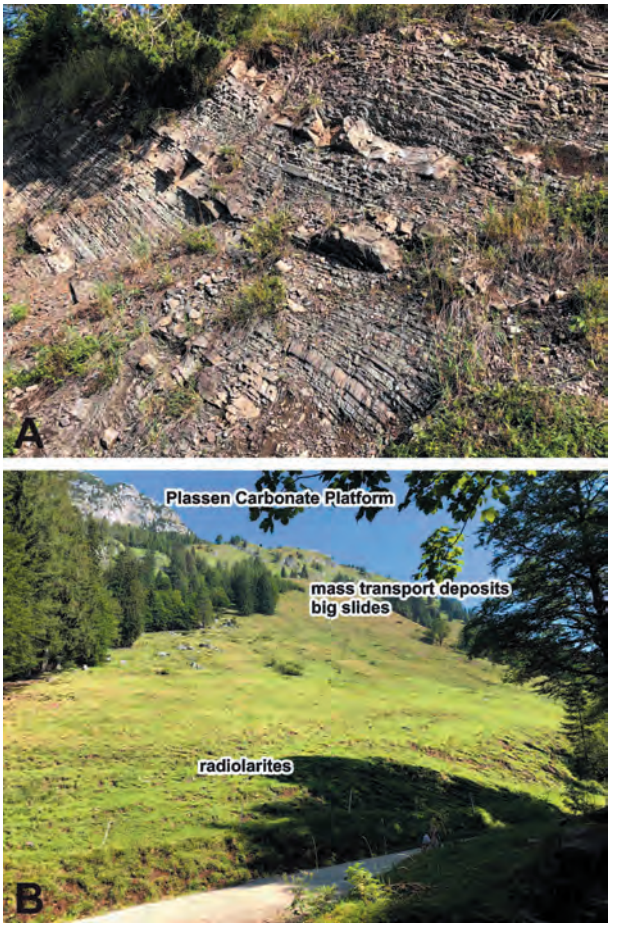

Figure 12: 12 A: Callovian rhythmic radiolarite sequence from the deeper part of the Lammer Basin fill in the area of Mount Hochkranz. With grey laminated radiolarite beds. 12 B: Field view of the coarsening upward cycle of the distal Lammer Basin Fill topped by shallow-water limestone of the Plassen Carbonate Platform (Mount Hochkranz).

Tauglboden Basin

Fludergraben/Knerzenalm area

The sedimentary succession starts with Rhaetian lagoonal Dachstein Limestone with megalodonts. Below the drowning sequence corals in situ are preserved. Drowning of the Dachstein Platform is characterized by the change from shallow-water lagoonal limestones to condensed red nodular limestones with crinoids, ammonoids and foraminifera (Adnet Formation). Red nodular limestone formation continued until the Middle/Late Jurassic boundary. In the Middle Jurassic this red nodular limestone is characterized by hardground formation (Klaus Formation). Directly above, deposition of red radiolarites began, These soon turned to

grey to black radiolarites indicating a change in the basin geometry. Slump deposits are a characteristic feature of this basal part of the basin fill. Some metres upsection, the first turbidites and mass transport deposits occur in the sedimentary succession. The component spectrum in these mass transport deposits reflects the Upper Triassic to Middle Jurassic sedimentary succession of the lagoonal Dachstein Limestone facies belt. Note that instead of a complete Lower Jurassic red nodular Adnet Limestone succession, grey cherty limestones begin to appear indicating a Lower Jurassic basinal sequence south of the Tauglboden Basin, which is not preserved anymore. In total the Tauglboden Basin (Figure 13) fill reflects a coarsening-upward cycle.

The base of the Fludergraben section (Figure 14) is important for the calibration of radiolarian faunas with ammonoids. Suzuki & Gawlick (2020) studied the radiolarian faunas from the lowermost part of the radiolarite succession and discussed the biostratigraphic ranges of several species and proposed some promising marker species for the Oxfordian.

In the area north of Mount Sandling, the proximal Tauglboden Basin fill is preserved. The thickness is nearly 900 m.

The preservation of radiolarians in the Tauglboden Basin is moderate to poor. Only a few samples contain moderate to well-preserved radiolarian assemblages. In most cases the radiolarians are completely recrystallized. The best radiolarian assemblages appear in the proximal Tauglboden Basin.

Tauglboden

Further reading: Schlager & Schlager (1969, 1973), Diersche (1980), Gawlick et al. (1999, 2009, 2012).

In the Tauglboden area west of the small town Kuchl in the Salzach valley we will visit the central part of the Tauglboden Basin fill (Figure 15). This basin is located in the Late Triassic Hauptdolomit facies belt. In the Tauglboden valley a complete Lower Jurassic to Upper Jurassic sedimentary sequence is preserved with radiolarite deposition beginning in the Early Oxfordian (Huckriede 1971). Red bedded radiolarites 5-10 cm-thick formed first. Next, radiolarite-beds changed to grey due to the change in the basin geometry upsection, and some laminated radiolarites were deposited with intercalated turbidites and mass transport deposits. In addition, some volcanic ash layers, mostly at the base of the mass transport deposits, are intercalated in the succession. Both the change in the colour of the radiolarites and the occurrence of first reworked material indicates the change in the depositional environment from an open and fully oxygenated basin floor to the geometry of a deep trench-like foreland basin. The sedimentology of the Tauglboden sequence and especially the sedimentological features of the different mass transport deposits and breccias were studied in detail by Schlager & Schlager (1969, 1973) and in a more regional context by Diersche (1980).

Detailed component analysis and age dating of the radiolaritic matrix was carried out by Gawlick et al. (1999) and later by Gawlick et al. (2012). The component spectrum reflects a complete Upper Triassic to Middle Jurassic sedimentary sequence from the facies zone of the open lagoon of the Dachstein Carbonate Platform, i.e. Norian Dachstein Limestone, Lower Rhaetian Kössen marls, Rhaetian Dachstein Limestone, lower Lower Jurassic Scheibelberg Formation, upper Lower Jurassic Adnet Formation, *Bositra* Limestone (Klaus Formation) and Callovian radiolarites. This component spectrum contrasts with that of the Lammer Basin fill to the south. In addition, resedimentation in the Tauglboden Basin started later as in the Lammer Basin. This clearly indicates the propagation of the nappe stack to the north.

The first part of the basin fill is characterized by a coarsening-upward trend: the intercalated mass transport deposits in the argillaceous-radiolaritic matrix increase in thickness and also the component size increases. More and more slump deposits occur in the sequence. According to radiolarian ages, the base of the Tauglboden Formation and the top of the coarsening cycle are the same age, i.e. Early to Middle Oxfordian. Upsection follows a series of dark grey dm-bedded radiolarites to cherty limestones without turbidites or mass transport deposits. Slump deposits are also missing. Higher up again mass transport deposits and dm-thick volcanic ash layers appear. This part of the sequence is early Tithonian in age based on radiolarian assemblages and forms the base of a fining-upward cycle ending in the Berriasian. The latest Oxfordian to earliest Tithonian represents a condensed part of the sequence with relative tectonic quiescence, i.e. a starved basin. In the early Tithonian a new cycle in the basin fill began. Whereas the Oxfordian part of the basin fill reflects a compressional regime expressed in a coarsening-upward cycle, the Tithonian part of the basin fill reflects an extensional regime with accompanied intense explosive volcanism, and is expressed in a fining-upward cycle. This extension is related to mountain uplift and unroofing (Missoni & Gawlick 2011a, b) of the Neotethyan orogenic belt, as known in the Dinarides (Gawlick et al. 2020 and references therein).

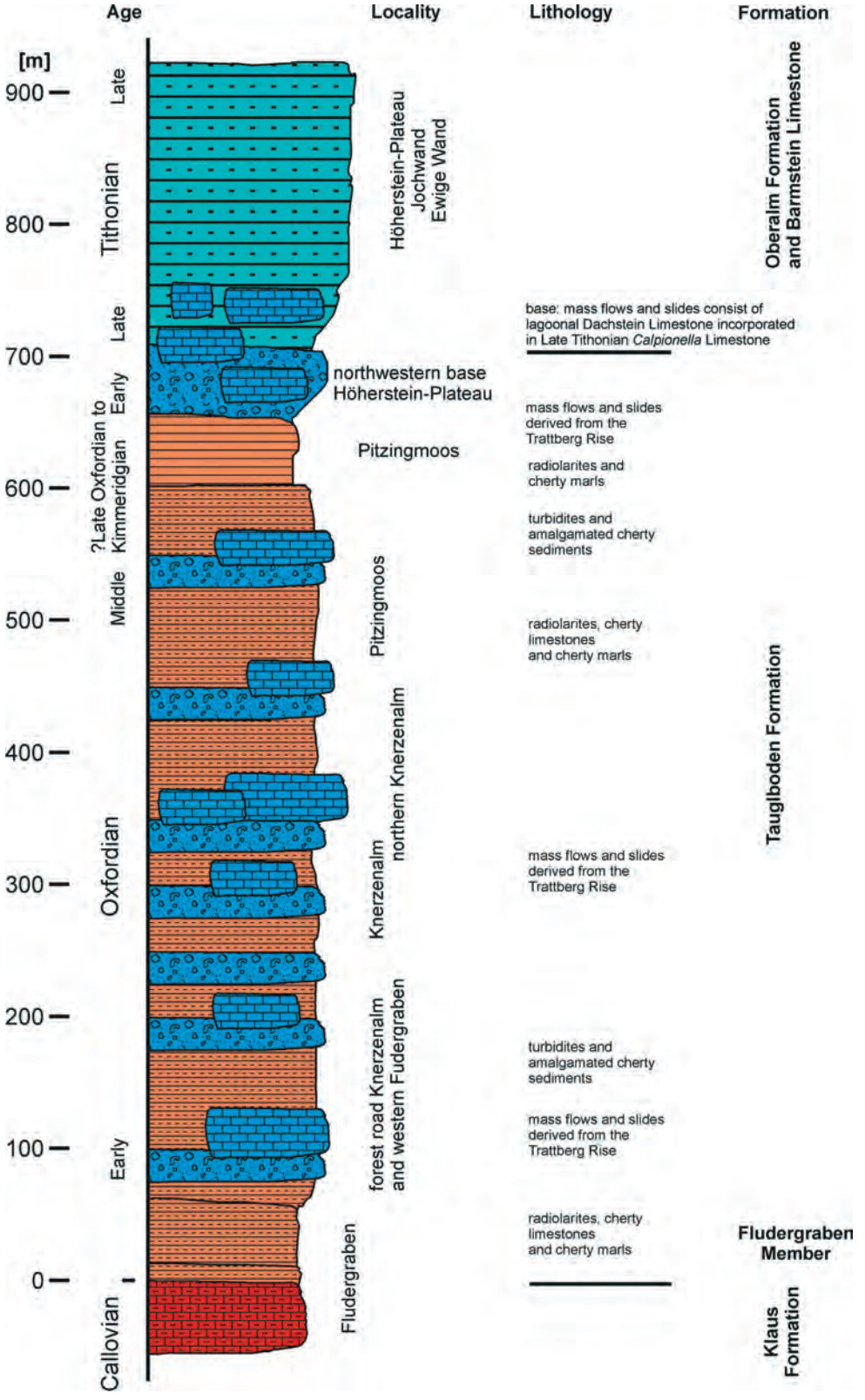

Figure 13: Schematic section of the Tauglboden Basin fill in the area north of Mount Sandling: Fludergraben – Knerzenalm – Höherstein. During the field trip we will visit nearly the whole basin fill starting in the Fludergraben. Slightly modified after Gawlick et al. (2012).

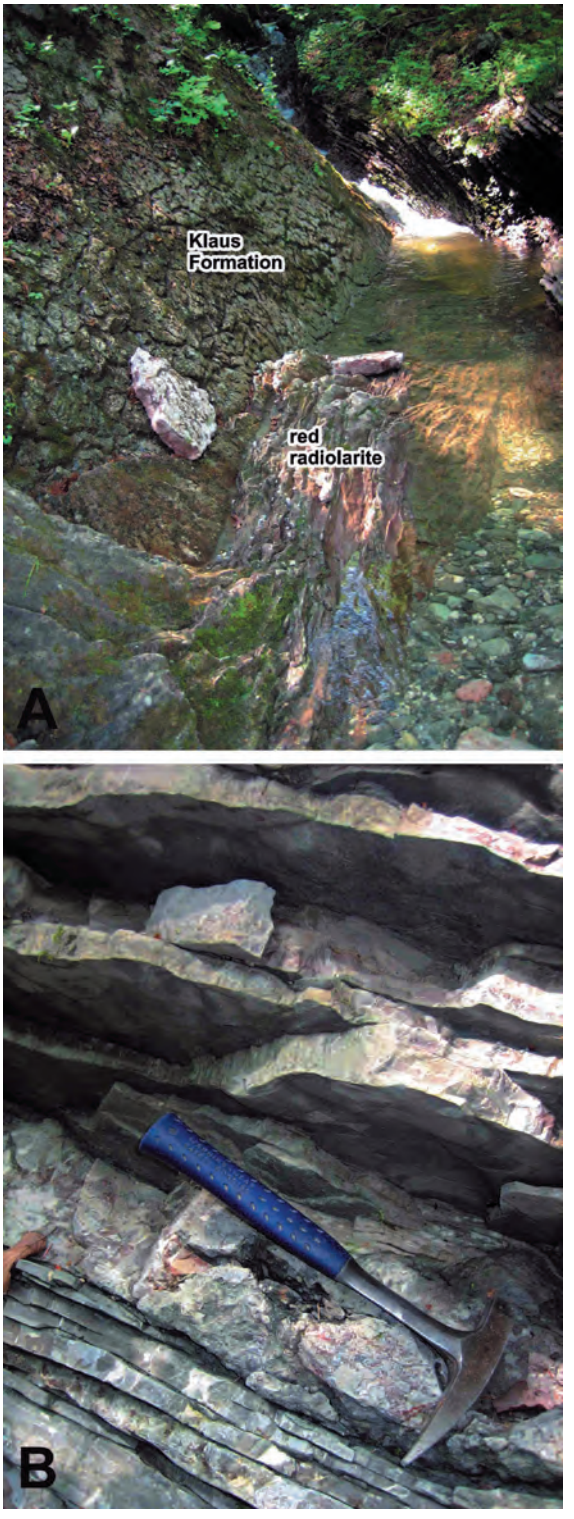

Figure 14: Fludergraben section. A: Red nodular limestones with ammonoids from the Callovian/Oxfordian boundary overlain by thin-bedded Oxfordian red radiolarite. B) Thin bedded grey radiolarite with intercalated mass transport deposit from the lower part of the Tauglboden Basin fill in the Fludergraben valley.

The component spectrum of the Early Tithonian part of the basin is similar to that of the Oxfordian part of the basin fill, but in contrast, Jurassic components are rare and Dachstein Limestone and Kössen Formation components dominate. Also during the Tithonian, radiolarites become more and more carbonate and preservation of radiolarians is very poor. Higher in the section (in the latest Tithonian) the first shallow-water components from the prograding Plassen Carbonate Platform appear in the mass transport deposits.

Mörtlbach valley

Further reading: Diersche (1980), Gawlick et al. (2012).

In the Mörtlbach valley section, i.e. along the parking place on the road to Krispl, a complete uppermost Triassic to Oxfordian sedimentary sequence is exposed (Figure 16). The section starts with Rhaetian Dachstein Limestone transitional to the Kössen Basin overlain by grey cherty limestones of the Scheibelberg Formation, 6-8 m in thickness. These grey cherty limestones with spicules and rare recrystallized radiolarians are overlain by reworked red nodular limestones of the Adnet Formation, forming a series of mass transport deposits. This part of the section is late Pliensbachian to early Toarcian in age. Upsection follows a thin layer of marly limestones of Aalenian age, rich in *Bositra* shells. After a gap, expressed by a ferromanganese horizon, deposition of a 1 m thick Callovian black thick-bedded to massive radiolarite started. Upsection the colour of the radiolarite changed to red. This 15 m thick part of the section consists of dm-bedded red massive radiolarites with claystone intercalations and is Late Callovian to Early/Middle Oxfordian in age. Only in a few beds the preservation of the radiolarians is good. In most beds the radiolarians are recrystallized and poorly preserved. Up-section in the Early-Middle Oxfordian the red radiolarite passed into grey radiolarites and cherty limestones. These siliceous sedimentary rocks are laminated and indicate a change in the basin geometry. In addition, few volcanic ash layers and fine-grained turbidites are intercalated in the succession but the clasts are too small to determine their stratigraphic age. Upsection the clasts become coarser and consist mainly of Upper Triassic lagoonal Dachstein Limestone and rare Jurassic components. The component spectrum is identical to that of the Tauglboden valley to the south.

The thickness of this part of the sequence does not exceed 10-20 m (details in Diersche, 1980), and

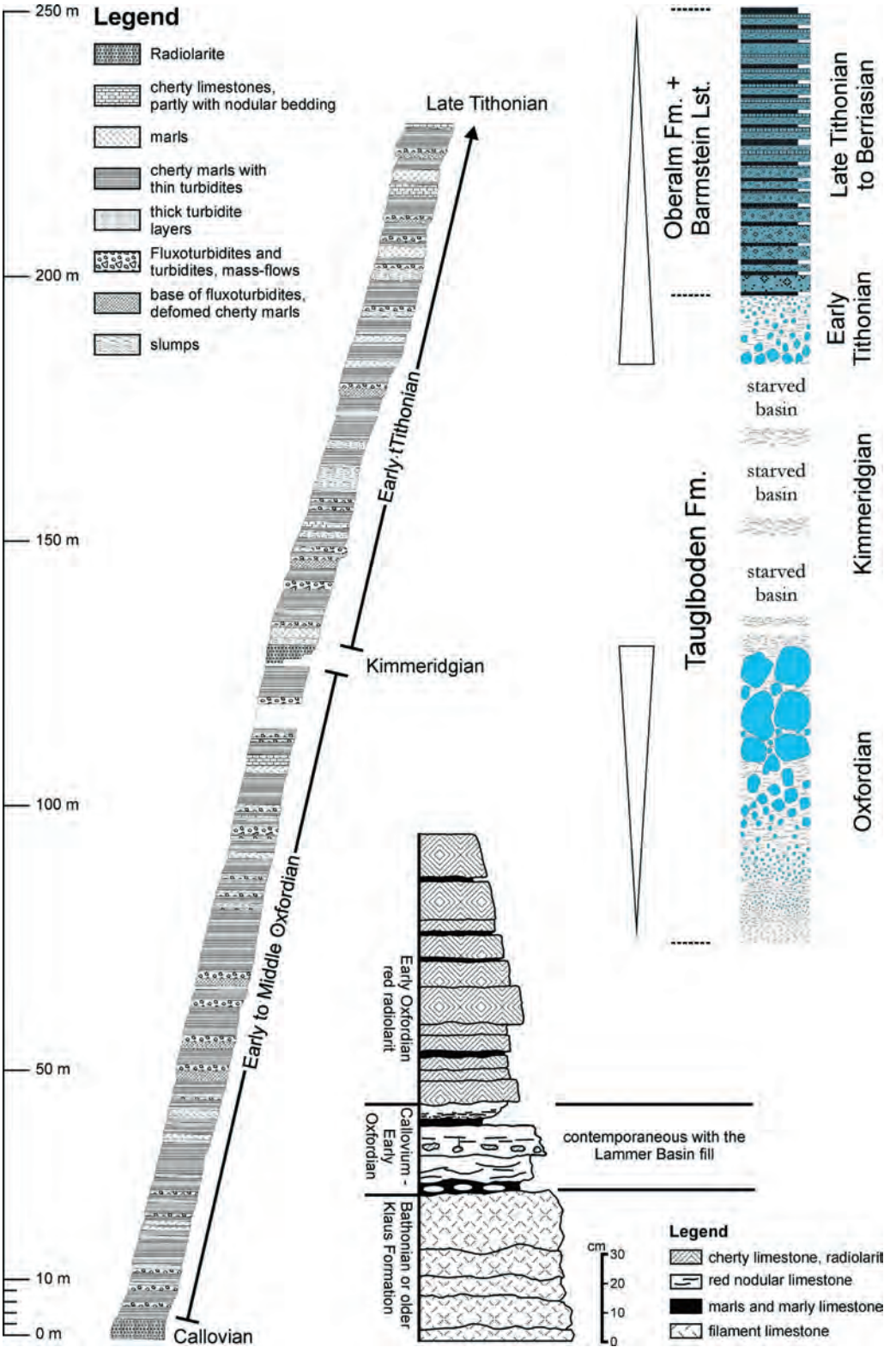

Figure 15: "Idealized section" of the Tauglboden Formation in the type-area (see Schlager & Schlager 1973 for details). Redrawn after unpublished data of M. and W. Schlager, printed with permission of W. Schlager (Amsterdam) in Gawlick (2000). Ages of the different parts of the section according to Huckriede (1971), Gawlick et al. (1999, 2012) and unpublished data. Basal part of the section according to Huckriede (1971), from Gawlick et al. (2012), modified. Sedimentological trends after Missoni & Gawlick (2011a).

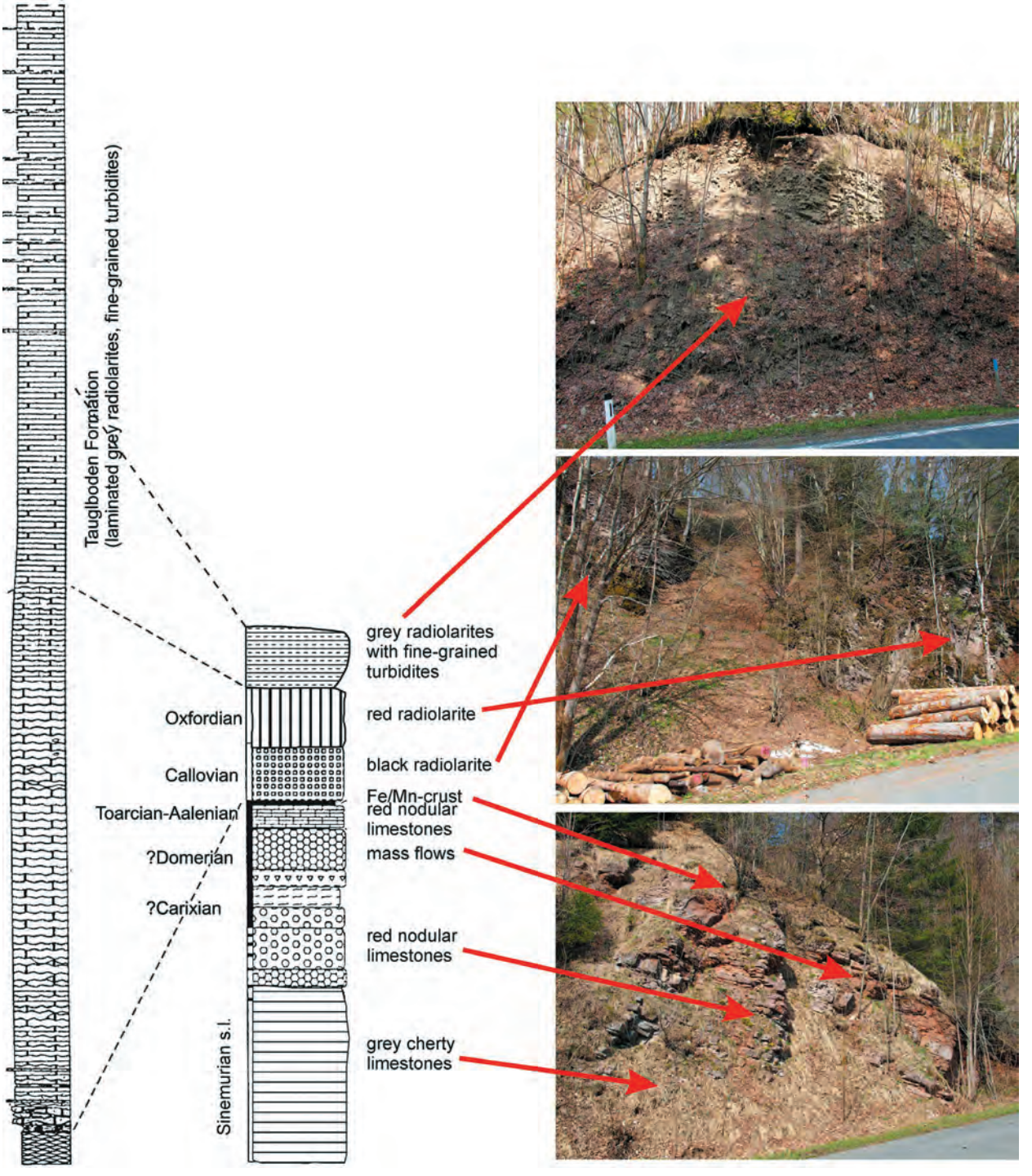

Figure 16: Sedimentary succession along the parking place on the road to Krispl. Right section with photographs after Böhm (1992), modified and completed for the Callovian-Oxfordian part of the section. Left section from Diersche (1980). Modified after Gawlick et al. (2012).

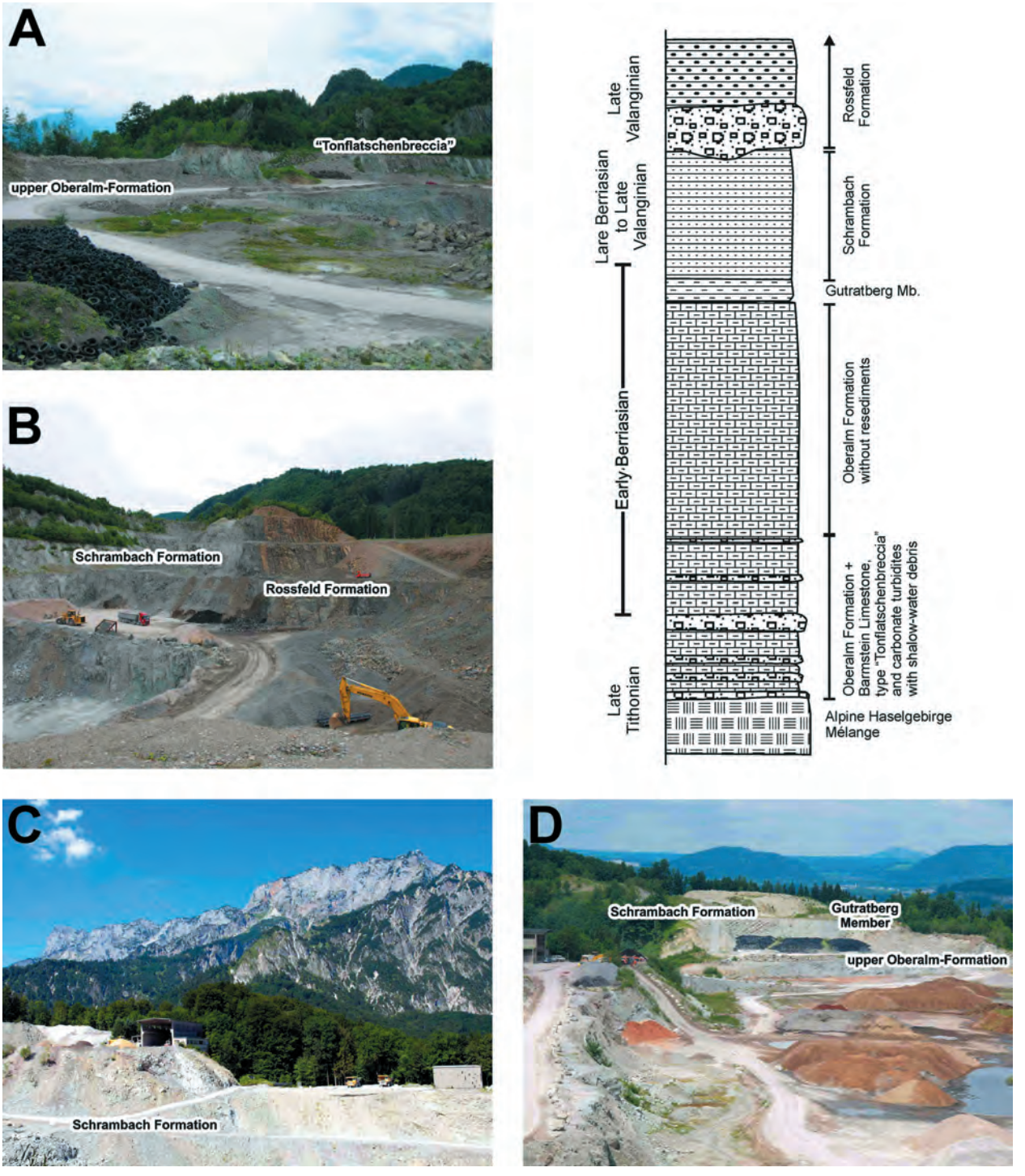

Figure 17: Different views of the Leube quarry and formations that will be visited. Due to the fact of ongoing exploitation in the quarry the outcrop situation and available parts of the succession may change. A: Northwestern part of the quarry with the Lower Berriasian part of the succession. B: Northern part of the quarry with the Lower Berriasian upper Oberalm Formation, the Middle Berriasian Gutratberg Member of the Oberalm Formation, and the Upper Berriasian Schrambach Formation. C: Eastern side of the quarry with the part of the succession studied in detail for magnetostratigraphy, gamma ray spectrometry, AMS studies, and geochemical analysis (Grabowski et al. 2016, 2017a, b). D: Southern part of the quarry with the transition from the Schrambach Formation to the Rossfeld Formation.

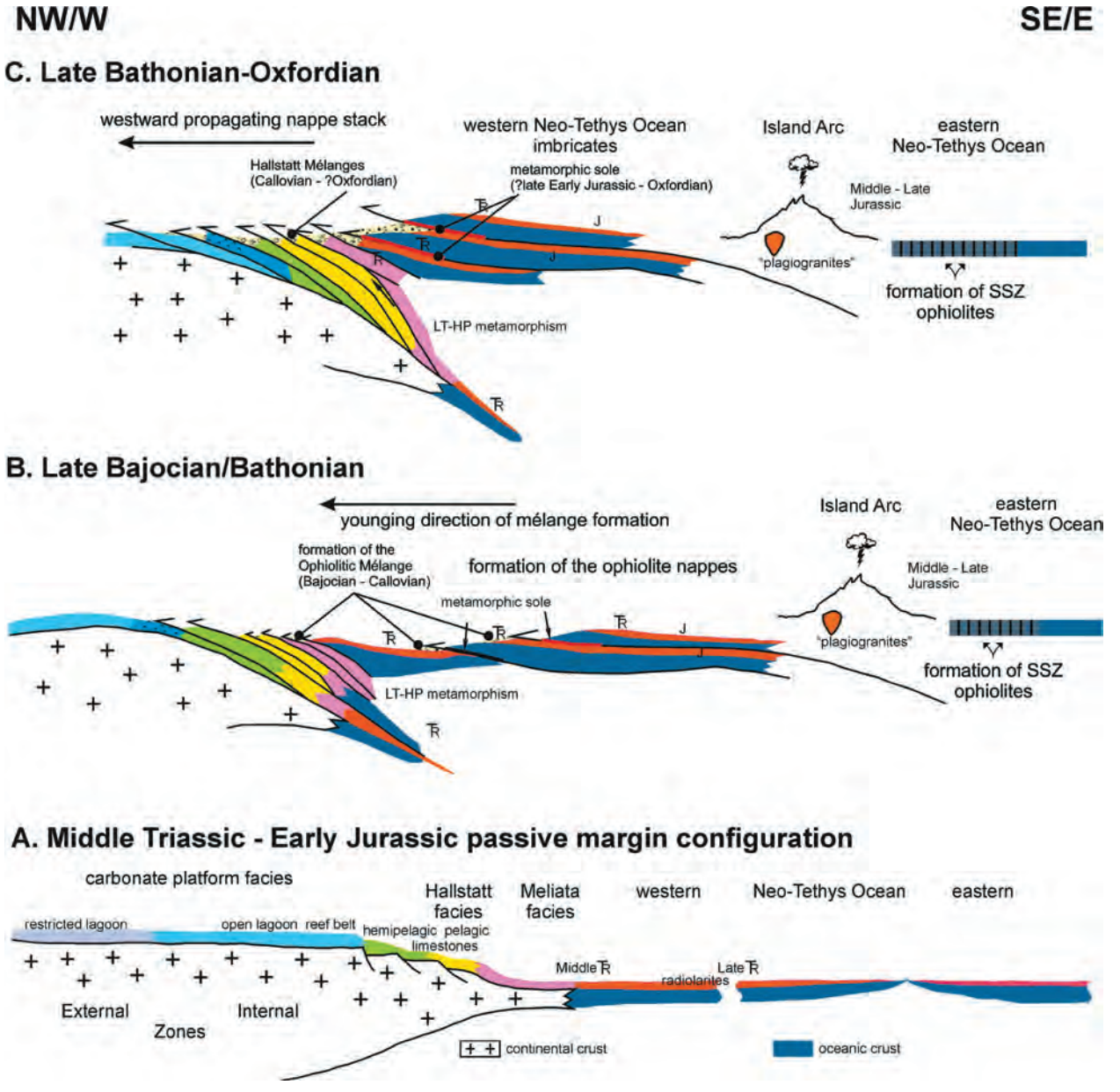

Figure 18: Triassic–Jurassic geodynamic evolution of the western Neo-Tethys margin after Gawlick & Missoni (2019) with a few modifications. A: Middle Triassic to Early Jurassic passive margin configuration. For details of the stratigraphic evolution, see Figure 3 and Figure 4. Continental break-up and generation of Neo-Tethys oceanic crust started around the Middle/Late Anisian boundary. B: Onset of ophiolite obduction started in the Bajocian and the formation of ophiolitic mélanges in the oceanic realm since the Early/Middle Jurassic boundary. From Bajocian time the ophiolitic mélanges in sub-ophiolite positions contain reworked blocks from the continental slope (Meliata facies zone). Concerning the position and formation of the plagiogranites see Michail et al. (2016). C: Late Middle Jurassic to early Late Jurassic propagating ophiolite obduction and imbrication of the former Neo-Tethys passive margin, resulting in the formation of a thin-skinned orogen. Trench-like basin and sedimentary mélanges formed in front of the propagating nappe stack. Some of the southern basin groups became sheared off and transported in northwest-/west-ward directions. The deeper parts of the imbricate stack of the outer shelf underwent low temperature – high pressure (LT-HP) metamorphism.

the thickness of the intercalated turbidites is only 10-20 cm. This section was formed on the northern slope of the Tauglboden Basin and represents a very distal part.

Leube quarry

Further reading: Krische et al. (2013, 2014, 2018) and references therein, Bujtor et al. (2013).

In the Leube quarry south of Salzburg (near to the villages Gartenau and St. Leonhard) we will visit the uppermost Jurassic to Lower Cretaceous sedimentary rocks. Here in several tectonic slices, separated by Miocene strike-slip faults, sedimentary successions from the higher Oberalm Formation including the Barmstein Limestone to the Roßfeld Formation are well preserved (Figure 17).

A detailed description of the section, the history of investigations in the quarry and a description/definition of the formations is given by Krische et al. (2018). New studies since 2018 (Hirschhuber et al. 2019; Hirschhuber 2020) result in a more detailed subdivision of the different tectonic slices in the quarry.

The Leube quarry provides one of the best preserved and exposed uppermost Jurassic to Early Cretaceous sedimentary successions in the central Northern Calcareous Alps. New calpionellid data, in combination with ammonite, microfacies and lithology analyses, form the basis for a detailed, revised biostratigraphy of this time interval (Krische et al. 2013) that gave rise to further very detailed investigations. Additionally, the investigation of hemipelagic basinal sedimentary sequences is very important for a better understanding of the Late Jurassic to Early Cretaceous evolution of the central Northern Calcareous Alps and also allows new insights into the development of the Late Jurassic to Early Cretaceous shallow-water carbonate platform at the southern rim of the basin (Plassen Carbonate Platform sensu stricto). The remarkably rich Late Berriasian ammonite fauna (Bujtor et al., 2013) reveals strong biogeographic connections toward the Tethyan faunas along the northern margin of the Tethys; many are reported for the first time from Austria.

The results achieved in the Leube quarry contribute to an improvement of the palaeogeographical and geodynamical model of the Northern Calcareous Alps for this time span. For this field trip, published results are combined with the recently obtained and still unpublished ones, which are here presented for the first time.

2.3 Geodynamic history

Further reading: Frisch & Gawlick (2003), Missoni & Gawlick (2011a, b), Gawlick et al. (2012), Gawlick & Missoni (2019) and references therein.

The Middle-Late Jurassic mountain building process in the Western Tethyan realm was triggered by west- to northwestward-directed ophiolite obduction onto the wider Adriatic shelf. This southeastern to eastern Adriatic shelf was the former passive continental margin of the Neo-Tethys, which started to open in the Middle Triassic. Its western parts closed from around the Early/Middle Jurassic boundary with the onset of east-dipping intra-oceanic subduction. Ongoing contraction led to ophiolite obduction onto the former continental margin since the Bajocian. Trench-like basins formed concomitantly within the evolving thin-skinned orogen in a lower plate situation. Deep-water basins formed in sequence with the northwest-/westward propagating nappe fronts, which served as source areas of the basin fills. Basin deposition was characterized by coarsening-upward cycles, i.e. sedimentary mélanges as synorogenic sediments. The basin fills became sheared successively by ongoing contractional tectonics with features of typical mélanges. Analyses of ancient Neo-Tethys mélanges along the Eastern Mediterranean mountain ranges allow both, a facies reconstruction of the outer western passive margin of the Neo-Tethys and conclusions on the processes and timing of Jurassic orogenesis. Comparisons of mélanges identical in age and component spectrum in all eastern Mediterranean mountain belts confirm a single Neo-Tethys Ocean model in the Western Tethyan realm, instead of multi-ocean and multi-continent scenarios.

ACKNOWLEDGEMENTS

This paper was written in the frame of the IGCP 710 "Eastern Tethys meets Western Tethys" and is dedicated to Sigrid Missoni. English corrections of Elizabeth Carter are gratefully acknowledged.

REFERENCES

Assereto, R., 1971: *Die* Binodosus*-Zone. Ein Jahrhundert wissenschaftlicher Gegensätze*. Sitzber Österr. Akad. Wiss. Wien math.-naturwiss. Kl. Abt. I 179: 25–53.

Auer, M., Gawlick, H.-J., Suzuki, H. & Schlagintweit, F., 2009: *Spatial and temporal development of siliceous basin and shallow-water carbonate sedimentation in Oxfordian Northern Calcareous Alps*. Facies 55: 63–87.

Böhm, F., 1992: *Mikrofazies und Ablagerungsmilieu des Lias und Dogger der Nordöstlichen Kalkalpen*. Erlanger Geologische Abhandlungen 121: 55–217.

Broili, F., 1927: *Eine Muschelkalkfauna aus der Nähe von Saalfelden*. Sitzber Bayr. Akad. Wiss. math.-natw. Kl. 1927: 229–242.

Bujtor, L., Krische, O. & Gawlick, H.-J., 2013: *Late Berriasian ammonite assemblage and biostratigraphy of the Leube quarry near Salzburg (Northern Calcareous Alps, Austria).* Neues Jahrbuch für Geologie und Paläontologie, Abhandlungen 267: 273–295.

Carter, E.S., Goričan, Š., Guex, J., O'Dogherty, L., De Wever, P., Dumitrica, P., Hori, R.S., Matsuoka, A. & Whalen, P.A., 2010: *Global radiolarian zonation for the Pliensbachian, Toarcian and Aalenian.* Palaeogeography, Palaeoclimatology, Palaeoecology 297, 401–419.

Cifer, T., Goričan, Š., Gawlick, H.-J. & Auer, M., 2020: *Pliensbachian, Early Jurassic radiolarians from Mount Rettenstein in the Northern Calcareous Alps, Austria*. Acta Palaeontologica Polonica 65: 167–207.

Diersche, V., 1980: *Die Radiolarite des Oberjura im Mittelabschnitt der Nördlichen Kalkalpen*. Geotektonische Forschungen 58: 1–217.

Frisch, W. & Gawlick, H.-J., 2003: *The nappe structure of the central Northern Calcareous Alps and its disintegration during Miocene tectonic extrusion – a contribution to understanding the orogenic evolution of the Eastern Alps.* International Journal of Earth Sciences 92 (5): 712–727.

Gawlick, H.-J., 1996: *Die früh-oberjurassischen Brekzien der Stubbergschichten im Lammertal – Analyse und tektonische Bedeutung (Nördliche Kalkalpen, Österreich).* Mitteilungen Gesellschaft Geologie Bergbaustudenten Österreichs 39/40: 119–186.

Gawlick, H.-J., 1998: *Obertriassische Brekzienbildung und Schollengleitung im Zlambachfaziesraum (Pötschenschichten) – Stratigraphie, Paläogeographie und diagenetische Überprägung des Lammeregg-Schollenkomplexes (Nördliche Kalkalpen, Salzburg).* Jb. Geol. B.-A. 141 (2): 147–165.

Gawlick, H.-J., 2004: *Die Gollinger Hallstätter Schollenregion – neue Daten zur stratigraphischen, faziellen und tektonischen Entwicklung.* Geo. Alp. 1: 11–36.

Gawlick, H.-J., 2000: *Die Radiolaritbecken in den Nördlichen Kalkalpen (hoher Mittel-Jura, Ober-Jura)*. Mitteilungen Gesellschaft Geologie- Bergbaustudenten Österreich 44: 97–156.

Gawlick, H.-J. & Missoni, S., 2015: *Middle Triassic radiolarite pebbles in the Middle Jurassic Hallstatt Mélange of the Eastern Alps: implications for Triassic–Jurassic geodynamic and palaeogeographic reconstructions of the western Tethyan realm*. Facies 61:13, 19 pages, DOI 10.1007/s10347-015-0439-3

Gawlick, H.-J. & Missoni, S., 2019: *Middle-Late Jurassic sedimentary mélange formation related to ophiolite obduction in the Alpine-Carpathian-Dinaridic Mountain Range*. Gondwana Research 74: 144–172. DOI: 10.1016/j.gr.2019.03.003

Gawlick, H.-J. & Suzuki, H., 1999: *Zur stratigraphischen Stellung der Strubbergschichten in den Nördlichen Kalkalpen (Callovium – Oxfordium).* Neues Jahrbuch Geologie Paläontologie, Abhandlungen 211: 233–262.

Gawlick, H.-J., Suzuki, H., Vortisch, W. & Wegerer, E., 1999: Zur stratigraphischen Stellung der Tauglbodenschichten an der Typlokalität in der Osterhorngruppe (Nördliche Kalkalpen, Ober-Oxfordium – Unter-Tithonium). Mitteilungen Gesellschaft Geologie- Bergbaustudenten Österreich, 42: 1–20.

Gawlick, H.-J., Schlagintweit, F. & Missoni, S., 2005: *Die Barmsteinkalke der Typlokalität nordwestlich Hallein (hohes Tithonium bis tieferes Berriasium; Salzburger Kalkalpen) Sedimentologie, Mikrofazies, Stratigraphie und Mikropaläontologie: neue Aspekte zur Interpretation der Entwicklungsgeschichte der Ober-Jura-Karbonatplattform und der tektonischen Interpretation der Hallstätter Zone von Hallein–Bad Dürrnberg.* Neues Jahrbuch Geologie Paläontologie, Abhandlungen 236: 351–421.

Gawlick, H.-J., Schlagintweit, F. & Suzuki, H., 2007a: *Die Ober-Jura bis Unter-Kreide Schichtfolge des Gebietes Sandling-Höherstein (Salzkammergut, Österreich) – Implikationen zur Rekonstruktion des Block-Puzzles der zentralen Nördlichen Kalkalpen, der Gliederung der karbonatklastischen Radiolaritflyschbecken und der Entwicklung der Plassen-Karbonatplattform*. Neues Jahrbuch Geologie Paläontologie, Abhandlungen 243 (1): 1–70.

Gawlick, H.-J., Schlagintweit, F. & Missoni, S., 2007b: *Das Ober-Jura Seichtwasser-Karbonat-Vorkommen der Drei Brüder am Wolfgangsee (Salzkammergut, Österreich): das westlichste Vorkommen der Wolfgangsee-Karbonatplattform südlich der Brunnwinkl-Schwelle am Nordrand des Tauglboden-Beckens.* Journal of Alpine Geology (Mitteilungen Gesellschaft Geologie- Bergbaustudenten Österreich) 48: 83–100.

Gawlick, H.-J., Frisch, W., Hoxha, L., Dumitrică, P., Krystyn, L., Lein, R., Missoni, S. & Schlagintweit, F., 2008: *Mirdita Zone ophiolites and associated sediments in Albania reveal Neotethys Ocean origin.* Int. Journ. Earth. Sci. 97, 865–881.

Gawlick, H.-J., Missoni, S., Schlagintweit, F., Suzuki, H., Frisch, W., Krystyn, L., Blau, J. & Lein, R., 2009: *Jurassic Tectonostratigraphy of the Austroalpine domain*. Journal of Alpine Geology, 50: 1–152.

Gawlick, H.-J., Missoni, S., Schlagintweit, F. & Suzuki, H., 2010: *Tiefwasser Beckengenese und Initiierung einer Karbonatplattform im Jura des Salzkammergutes (Nördliche Kalkalpen, Österreich).* Journal of Alpine Geology 53: 63–136.

Gawlick, H.-J., Missoni, S., Schlagintweit, F. & Suzuki, H., 2012: *Jurassic active continental margin deep-water basin and carbonate platform formation in the north-western Tethyan realm (Austria, Germany).* Journal of Alpine Geology 54: 189–292.

Gawlick, H.-J., Aubrecht, R., Schlagintweit, F., Missoni, S. & Plašienka, D., 2015: *Ophiolitic detritus in Kimmeridgian resedimented limestones and its provenance from an eroded obducted ophiolitic nappe stack south of the Northern Calcareous Alps (Austria).* Geologica Carpathica 66: 473–487.

Gawlick, H.-J., Sudar, M., Missoni, S., Aubrecht, R., Schlagintweit, F., Jovanović, D. & Mikuš, T., 2020: *Formation of a Late Jurassic carbonate platform on top of the obducted Dinaridic ophiolites deduced from the analysis of carbonate pebbles and ophiolitic detritus in southwestern Serbia.* International Journal of Earth Sciences 109: 2023–2048.

Gawlick, H.-J., Lein, R. & Bucur, I.I., 2021: *Precursor extension to final Neo-Tethys break-up: Flooding events and their significance for the correlation of shallow-water and deep-marine organisms (Anisian, Eastern Alps, Austria).* International Journal of Earth Sciences 110: 419–446.

Grabowski, J., Gawlick, H.-J., Iwanczuk, J., Krische, O., Rehakova, D. & Wojcik, K., 2016: *Tithonian-Berriasian magnetostratigraphy in the Northern Calcareous Alps (Leube quarry, Northern Calcareous Alps, Austria) – first results.* In: Michalik, J. & Fekete, K. (Eds.): XIIth Jurassica Conference, Field Trip Guide and Abstract Book, 91–92, Earth Science Institute, Slovak Academy of Science, Bratislava.

Grabowski, J., Gawlick, H.-J., Hirschhuber, H.-J., Iwanczuk, J., Krische, O., Rehakova, D., Ziolkowski, P., Teodorski, A. & Vršič, A., 2017a: *Tithonian–Berriasian magnetic stratigraphy, gamma ray spectrometry, AMS studies, and geochemical analyses in the Northern Calcareous Alps (Leube quarry, Salzburg area, Austria) – first results.* Jurassica XIII: Jurassic Geology of Tatra Mts., Abstracts and Field Trip guidebook, 34–35, Koscielisko, Polish Geological Institute.

Grabowski, J., Gawlick, H.-J., Hirschhuber, H.-J., Iwanczuk, J., Krische, O., Rehakova, D., Ziotkowski, P., Teodorski, A. & Vršič, A., 2017b: *Primary magnetization in the Berriasian of the Northern Calcareous Alps (Salzburg area).* In: Šarić, K., Prelević, D., Sudar, M. & Cvetković, V., (Eds.): Émile Argand Conference – 13th Workshop on Alpine Geological Studies, September 7th–18th 2017, Zlatibor Mts. (Serbia), p. 37, University of Belgrade, Faculty of Mining and Geology, Beograd.

Hirschhuber, H.J., Gawlick, H.-J. & Maier, G., 2019: *The J/K-boundary section in the Leube quarry (Northern Calcareous Alps): sedimentology, stratigraphy, microfacies combined with geochemical proxies.* - In: Fekete, K., Michalik, J. & Reháková, D. (Eds.): XIVth Jurassica Conference & Workshop of the ICS Berriasian Group, 120–121, Earth Science Institute, Slovak Academy of Sciences & Faculty of Natural Sciences, Comenius University, Bratislava.

Hirschhuber, H.J., 2020: *The Jurassic/Cretaceous boundary section in the Leube quarry (Northern Calcareous Alps, Salzburg): Sedimentology, microfacies and calpionellid biostratigraphy combined with geochemical proxies.* BSc thesis Montanuniversitaet Leoben, 1–26, Leoben.

Huckriede, R., 1971: *Rhyncholithen-Anreicherung (Oxfordium) an der Basis des Älteren Radiolarits der Salzburger Kalkalpen*. Geologica et Palaeontologica 5: 131–147.

Karamata, S., 2006: *The geological development of the Balkan Peninsula related to the approach, collision and compression of Gondwanan and Eurasian units*. In: Robertson A.H.F. & Mountrakis, D. (Eds.): *Tectonic Development of the Eastern Mediterranean Region.* Geological Society London Special Publication 260: 155–178.

Kozur, H. & Mock, R., 1985: *Erster Nachweis von Jura in der Meliata-Einheit der südlichen Westkarpaten*. Geologisch-Paläontologische Mitteilungen Innsbruck 13 (10): 223–238.

Kozur, H. & Mock, R., 1997: *New paleogeographic and tectonic interpretations in the Slovakian Carpathians and their implications for correlations with the Eastern Alps and other parts of the Western Tethys. Part II: Inner Western Carpathians*. Mineralia Slovaca 29: 164–209.

Kozur, H. & Mostler, H., 1981: *Beiträge zur Erforschung der mesozoischen Radiolarien. Teil IV: Thalassospaeracea Haeckel, 1862, Hexastylacea Haeckel, 1882 emend. Petruševskaja, 1979, Sponguracea Haeckel, 1862 emend., und weitere triassische Lithocycliacea, Trematodiscacea, Actinommacea und Nassellaria*. Geologisch-Paläontologische Mitteilungen Innsbruck, Sonderband: 1–208.

Kozur, H. & Mostler, H., 1992: *Erster paläontologischer Nachweis von Meliaticum und Süd-Rudabanyaicum in den Nördlichen Kalkalpen (Österreich) und ihre Beziehungen zu den Abfolgen in den Westkarpaten*. Geologisch-Paläontologische Mitteilungen Innsbruck 18: 87–129.

Krische, O., Bujtor, L. & Gawlick, H.-J., 2013: *Calpionellid and ammonite biostratigraphy of uppermost Jurassic to Lower Cretaceous sedimentary rocks from the Leube quarry (Northern Calcareous Alps, Salzburg, Austria)*. Austrian Journal of Earth Sciences 101: 26–45.

Krische, O., Goričan, Š. & Gawlick, H.-J. 2014: *Erosion of a Jurassic ophiolitic nappe-stack as indicated by exotic components in the Lower Cretaceous Rossfeld Formation of the Northern Calcareous Alps (Austria)*. Geologica Carpathica 65: 3–24.

Krische, O., Grabowski, J., Bujtor, L. & Gawlick, H.-J., 2018: *Latest Jurassic to Early Cretaceous evolution in the central Northern Calcarous Alps*. Berichte der Geologischen Bundesanstalt 126: 223–258.

Mandl, G.W. & Ondrejičková, A., 1991: *Über eine triadische Tiefwasserfazies (Radiolarite, Tonschiefer) in den Nördlichen Kalkalpen – ein Vorbericht*. Jahrbuch der Geologischen Bundesanstalt 134: 309–318.

Mandl, G.W. & Ondrejičková, A., 1993: *Radiolarien und Conodonten aus dem Meliatikum im Ostabschitt der Nördlichen Kalkalpen (Österreich)*. Jahrbuch der Geologischen Bundesanstalt 136: 841–871.

Michail, M., Pipera, K., Koroneos, A., Kilias, A. & Ntaflos, T., 2016: *New perspectives on the origin and emplacement of the Late Jurassic Fanos granite, associated with an intra-oceanic subduction within the Neotethyan Axios-Vardar Ocean*. International Journal Earth Sciences 105: 1965–1983.

Missoni, S. & Gawlick, H.-J., 2011a: *Evidence for Jurassic subduction from the Northern Calcareous Alps (Berchtesgaden; Austroalpine, Germany)*. International Journal of Earth Sciences 100 (7), 1605–1631.

Missoni, S. & Gawlick, H.-J., 2011b: *Jurassic mountain building and Mesozoic-Cenozoic geodynamic evolution of the Northern Calcareous Alps as proven in the Berchtesgaden Alps (Germany)*. Facies 57: 137–186.

Missoni, S., Schlagintweit, F., Suzuki, H. & Gawlick, H.-J., 2001: *Die oberjurassische Karbonatplattformentwicklung im Bereich der Berchtesgadener Kalkalpen (Deutschland) - eine Rekonstruktion auf der Basis von Untersuchungen polymikter Brekzienkörper in pelagischen Kieselsedimenten (Sillenkopf-Formation)*. Zentralblatt Geologie Paläontologie, Teil 1, 2000: 117–143.

Missoni, S. & Kuhlemann, A., 2001: *Geröllpetrographie und Diagenese des karbonatklastischen Radiolaritflysches der Sillenkopf-Formation (Kimmeridgium) in den südlichen Berchtesgadener Alpen*. Schriftenreihe der deutschen geologischen Gesellschaft 13: 71, Hannover.

Mock, R., Sýkora, M., Aubrecht, R., Ožvoldová, L., Kronome, B., Reichwalder, R.P. & Jablonský, J., 1998: *Petrology and stratigraphy of the Meliaticum near the Meliata and Jaklovce villages, Slovakia*. Slovak Geological Magazine 4: 223–260.

Neubauer, F., Friedl, G., Genser, J., Handler, R., Mader, D. & Schneider, D., 2007: *Origin and tectonic evolution of the Eastern Alps deduced from dating of detrital white mica: a review*. Austrian Journal Earth Sciences, 100: 8–23.

Neumeister, S., Gratzer, R., Algeo, T.J., Bechtel, A., Gawlick, H.-J., Newton, R.J. & Sachsenhofer, R.F., 2015: *Oceanic response to Pliensbachian and Toarcian magmatic events: Implications from an organic-rich basinal succession in the NW Tethys*. Global and Planetary Change 126: 62–83.

O´Dogherty, L. & Gawlick, H.-J., 2008: *Pliensbachian Radiolaria in Teltschengraben (Northern Calcareous Alps, Austria): a keystone in reconstructing the Early Jurassic evolution of the Tethys*. Stratigraphy 5 (1): 63–81.

O´Dogherty, L., Goričan, Š. & Gawlick, H.-J., 2017: *Middle and Late Jurassic radiolarians from the Neotethys suture in the Eastern Alps*. Journal of Paleontology 91: 25–72.

Ogg, J.G., 2015: *The Mysterious Mid-Carnian "Wet Intermezzo" Global event*. Journal of Earth Science 26, 181–191.

Ozsvárt, P. & Kovács, S., 2012: *Revised Middle and Late Triassic radiolarian ages for ophiolite mélanges: implications for the geodynamic evolution of the northern part of the early Mesozoic Neotethyan subbasins.* Bulletin de la Société géologique de France 183: 273–286.

Pia, J., 1912: *Neue Studien über die triadischen Siphoneae Verticillatae.* Beitraege zur Paläontologie Österreich-Ungarn XXV: 25–81, Plate I–VIII.

Pia, J., 1924: *Geologische Skizze der Südwestecke des Steinernen Meeres bei Saalfelden.* Sitzber. Österr. Akad. Wiss., math.-natw. Klasse Abt. 1, 132: 35–79.

Pia, J., 1930. *Grundbegriffe der Stratigraphie mit ausführlicher Anwendung auf die europäische Mitteltrias.* Deuticke, Wien, 252 pp.

Ratschbacher, L., Dingeldey, C., Miller, C., Hacker, B.R. & McWilliams, M.O., 2004: *Formation, subduction, and ex-humation of Penninic oceanic crust in the Eastern Alps: time constraints from $^{40}Ar/^{39}Ar$ geochronology.* Tectonophysics 394: 155–170.

Schlager, M. & Schlager, W., 1969: *Über die Sedimentationsbedingungen der jurassischen Tauglbodenschichten (Osterhorngruppe, Salzburg).* Anzeiger der Österreichischen Akademie der Wissenschaften. Mathematisch-naturwissenschaftlichen Klasse, 106: 178–183.

Schlager, W. & Schlager, M., 1973: *Clastic sediments associated with radiolarites (Tauglbodenschichten, Upper Jurassic, Eastern Alps).* Sedimentology 20: 65–89.

Schlager, W. & Schöllnberger, W., 1974: *Das Prinzip stratigraphischer Wenden in der Schichtfolge der Nördlichen Kalkalpen*. Mitteilungen der geolologischen Gesellschaft Wien 66/67: 165–193.

Schnetzer, R., 1934: *Die Muschelkalkfauna des Öfenbachgrabens bei Saalfelden*. Palaeontographica 81: 1–160, 8 Pls.

Steiger, T., 1981: *Kalkturbidite im Oberjura der Nördlichen Kalkalpen (Barmsteinkalke, Salzburg, Österreich)*. Facies 4: 215–348.

Suzuki, H. & Gawlick, H.-J., 2003: *Die jurassischen Radiolarienzonen der Nördlichen Kalkalpen*. In: Weidinger, J.T., Lobitzer, H. & Spitzbart, I. (Eds.): *Beiträge zur Geologie des Salzkammerguts*. Gmundner Geo-Studien 2: 115–122, Gmunden.

Suzuki, H. & Gawlick, H.-J., 2020: *Early Oxfordian radiolarians from the ammonite-bearing Fludergraben section (Northern Calcareous Alps, Austria).* Bulletin of the Geological Survey of Japan 71 (4): 38 pp.

Tollmann, A., 1976: *Analyse des klassischen nordalpinen Mesozoikums*. Deuticke, Wien, 580 pp.

Tollmann, A., 1977: *Geologie von Österreich, Band 1: Die Zentralalpen*. Deuticke, Wien, 766 pp.

Vlahović I., Tišljar J., Velić I. & Matičec D., 2005: *Evolution of the Adriatic Carbonate Platform: Paleogeography, main events and depositional dynamics*. Palaeogeography, Palaeoclimatology, Palaeoecology 220: 333–360.

Wächter, J., 1987: *Jurassische Massflow- und Internbreccien und ihr sedimentär-tektonisches Umfeld im mittleren Abschnitt der Nördlichen Kalkalpen*. Bochumer geologische geotechnische Arbeiten 27: 1–239.

Wagner, L., 1970: *Die Entwicklung der Mitteltrias in den östlichen Kalkvoralpen im Raum zwischen Enns und Wiener Becken*. Unpubl. PhD thesis, University of Vienna, 202 pp.

SLOVENE CLASSICAL KARST: KRAS PLATEAU AND THE RECHARGE AREA OF LJUBLJANICA RIVER

KLASIČNI KRAS: PLANOTA KRAS IN KRAŠKO ZALEDJE IZVIROV LJUBLJANICE

Franci GABROVŠEK[1*], Andrej MIHEVC[1], Cyril MAYAUD[1], Matej BLATNIK[1] & Blaž KOGOVŠEK[1]

http://dx.doi.org/10.3986/fbg0097

ABSTRACT

Slovene Classical karst: Kras Plateau and the Recharge Area of Ljubljanica River

The area of the Classical Karst is roughly defined by a triangle with Ljubljana, Trieste and Rijeka as its vertices. This is the area where the first scientific studies of karst phenomena were conducted. Two sub-regions that particularly attracted researchers are presented. Kras/Carso plateau with the Škocjan caves and the underground course of the Reka river. The groundwater flow of Reka-Timavo is characterised by high recharge variability of allogenic inflow of Reka River and flow restrictions in the upper part of subterranean flow, which control regional backfloodings observed in cave systems. The recharge area of Ljubljanica Springs is known for a cascading series of poljes in intermediate cave systems. The area has been in focus of hydrological studies for over a century, but many phenomena have been resolved in the last decade based on results of continuous autonomous monitoring in the last decade.

Key words: Classical Karst, Kras, Škocjanske Jame, Reka-Timavo system, Ljubljanica Recharge Area, Polje.

IZVLEČEK

Klasični kras: planota Kras in kraško zaledje izvirov Ljubljanice

Območje Klasičnega krasa v grobem objema trikotnik z Ljubljano, Reko in Trstom v ogliščih. Tu se je začelo znanstveno proučevanje krasa. Dve kraški območji sta tu še posebej pritegnili pozornost raziskovalcev. Prvo je planota Kras s Škocjanskimi jamami in podzemnim tokom Reke med Škocjanskimi jamami in izviri Timave. Ta tok močno zaznamuje velika spremenljivost dotoka reke Reke in lokalne zožitve v vodonosniku, ki povzročajo regionalno poplavljanje, kot ga beležimo v jamah. Drugo je območje kraške Ljubljanice z značilnim nizom dinarskih kraških polj in jamskih sistemov, ki polja hidrološko povezujejo. Območje je že več kot stoletje predmet številnih raziskav, zvezno spremljanje parametrov toka v kraških jamah v zadnjih desetih letih, pa je omogočilo nova spoznanja o lastnostih in mehanizmih pretakanja vode v celotnem sistemu.

Ključne besede: Klasični kras, Kras, Škocjanske jame, podzemni tok reke Reke, kraško zaledje izvirov Ljubljanice, polje.

[1] ZRC SAZU, Karst Research Institute, Titov trg 2, SI-6230 Postojna, Slovenia.

* E-mail address of corresponding author: franci.gabrovsek@zrc-sazu.si

KRAS PLATEAU AND ŠKOCJAN CAVES

Kras Plateau

The Kras/Carso is a low, 40 km long and up to 13 km wide, NW–SE-trending limestone plateau in Slovenia and Italy, stretching between Trieste Bay, the northernmost part of the Adriatic Sea, Vipava valley in north-east, and Friuli-Venezia Giulia lowlands and river Soča in north-west (Figure 1).

The name for the area comes from genetic word *kras*; in Slovene it means rocky surface The term gave the name to the whole plateau Kras. From this toponym the international term – karst – for such type of landscape is derived. The name and some other terms from the area like *dolina*, *polje*, and *ponor* have also entered to international scientific terminology from here.

Climate is sub-Mediterranean with warm dry summers and most of the precipitation in autumn and spring. Cold winters, with NE wind "burja" (bora = borealis) show strong influence of the continent. Average yearly precipitation on Kras varies from 1,400 to 1,650 mm, and average yearly evapotranspiration from 700 to 750 mm. Because of different land use, pasturing, in past centuries, the Kras was bare, with rocky and grassy surface. In the last decades the bushes and trees are overgrowing the landscape.

The main part of the plateau is essentially levelled, inclined slightly towards the north-west, with numerous dolines, caves and other karst features. Over 3500 caves are known on the plateau. In seven of them we can reach over 30 km of passages of the underground Reka which flows between 200 and 300 m below the surface. There is a belt of slightly higher relief in the central part of the plateau, formed by conical hills like Grmada (324 m.a.s.l.), and dissected by large depressions. The higher relief divides the Kras into two separated levelled surfaces. In the north-western part, the plateau descends to below 50 m.a.s.l. on the edge of the Friuli Plain; on its south-eastern edge altitudes are about 500 m.a.s.l. There is about 300 m of accessible vadose zone with caves formed at all altitudes from the surface to the sea level and below it.

No superficial streams occur on the Kras surface, because all rainwater immediately infiltrates to carbonate rocks. There are two dry valleys crossing the plateau and some NW–SE-trending belts of lower relief which are result of young tectonics.

The age of the karst of Kras plateau can be defined as the time when the karst rocks were uplifted out of the sea. For the most of Dinaric karst in Slovenia this occurred after the Eocene, since after that there is no

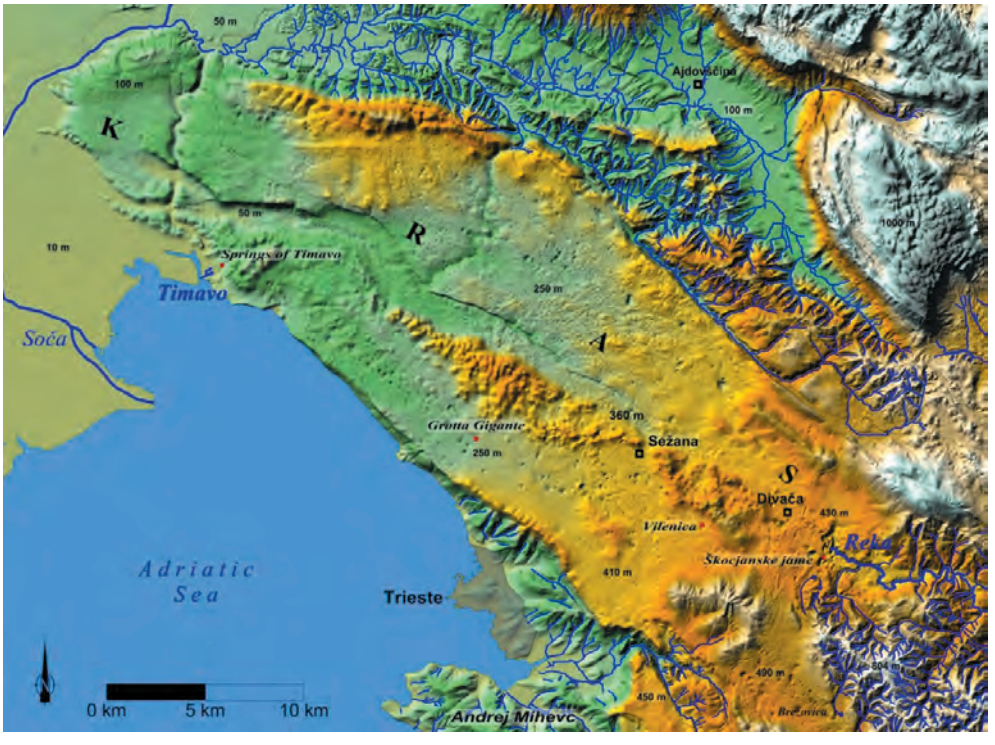

Figure 1: Digital elevation model of the Kras Plateau.

evidence of younger marine sediments. As soon as the carbonate rocks were exposed, we can expect that the karst was formed, but there are no remnants of karst features from that time. Most likely denudation has already destroyed them.

The oldest features in the karst relief are unroofed caves. They were caves that were formed by sinking rivers, bringing allogenic sediments to caves in Kras. At the end of the morphogenetic phase all these caves were filled with fluvial sediments. This indicates the diminishing of the gradient in the whole area. Diminishing of the gradient, which ended with planation could mean tectonic phase, which ended at about 6 Ma ago. After that a new tectonic phase started. Three areas faced uplift and tilting for several hundred meters. The uplift was stronger in the SE part of the area. Karst denudation was evenly lowering the surface, so the surface remained well preserved, dissected on central parts of karst with dolines, which represent few percents of total area only. The even denudation exposed former old caves to the surface. Some of them are filled with sediments, some sediments were washed away or were never filled.

Geological and hydrogeological settings of the Kras Plateau

Figure 2 presents a simplified geological situation. The plateau is made up of a succession of Cretaceous to Lower Paleogene carbonates deposited on the Adriatic–Dinaric Carbonate Platform (Buser et al. 1968; Jurkovšek et al. 2016). The geological structure of the broader area is a result of the collision between the Apulian and Eurasian lithospheric plates. The Kras Plateau is an anticlinorium, which structurally belongs to the External Dinaric Imbricated Belt, a part of the thrust system of the External Dinarides, which furthermore underthrusts below the Southern Alps. Underthrusting also resulted in an en-echelon formation of strike slip faults. Several fault systems cross the area, typically along the so-called Dinaric SE–NW and cross-Dinaric direction. The most recent structural description of the area can be found in Placer (2008, 2015). Some faults have been identified to affect the groundwater flow (Šebela 2009; Žvab Rožič et al. 2015) The carbonates are surrounded by flysch, which provides the input of allogenic water on the SE, while at the same time prevents outflow along the SW boundary. This way, the main flow is forced to follow the Dinaric (SE–NW) direction. Along the NW coast of the Trieste Bay, the topographical elevation of the limestone flysch contact is low enough to permit outflow through numerous karst springs. Among these, the Timavo Springs, with an average discharge of almost 30 m^3/s are the most important.

The Reka River is the main allogenic input to the system; ~41 % of its catchment is karstic and ~54 % is underlain by flysch. It flows ~50 km on the impermeable

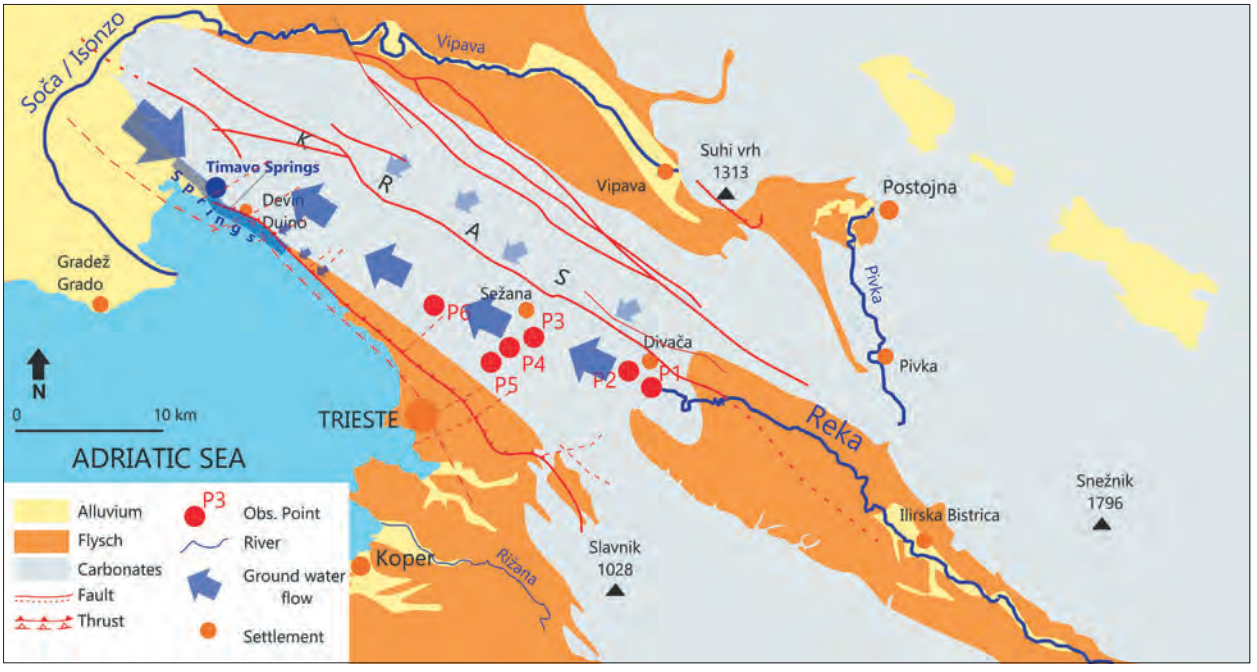

Figure 2: A simplified geology of the area with main lithological units and structural elements. P1–P6 mark the position of the caves with active groundwater flow. Blue arrows indicate the general groundwater flow direction towards the springs.

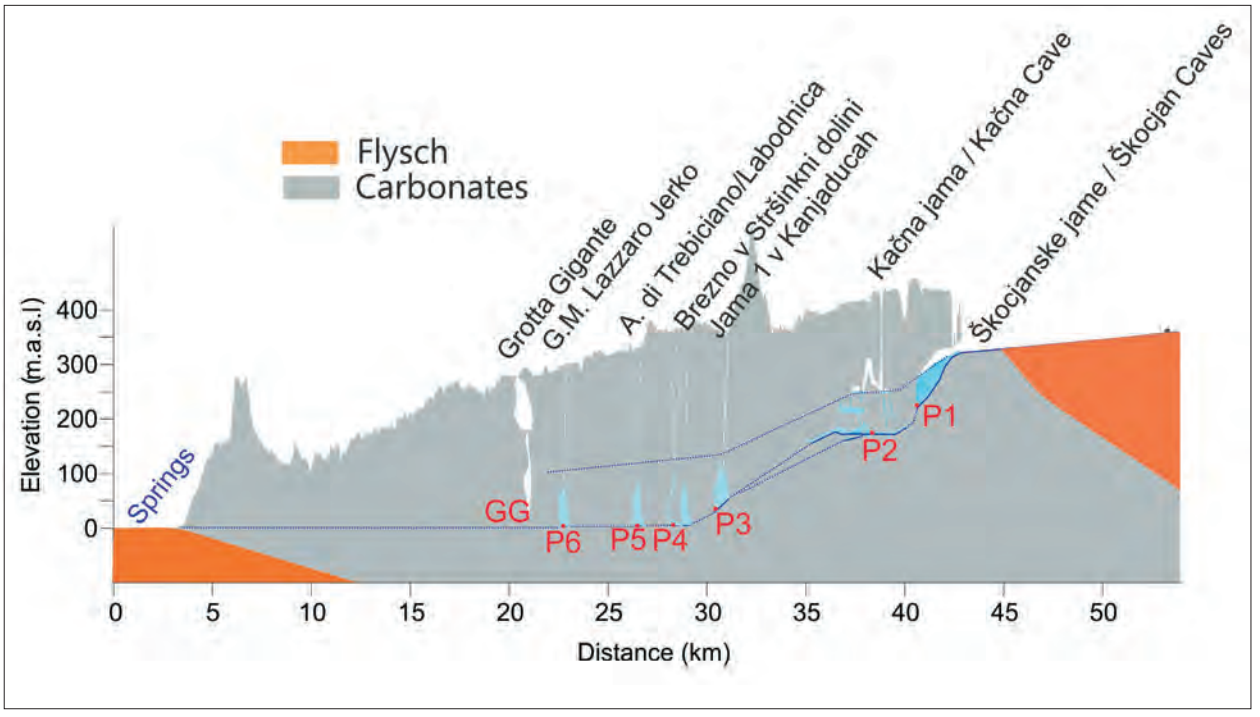

Figure 3: An idealised cross-section of the Kras Plateau between the Škocjan Caves and the springs along the NW coast of Trieste Bay. The dotted blue lines denote the position of the base flow and extreme floods. P1 to P6 indicate the positions of the observation points used in this work. Vadose parts are filled white, while phreatic and epiphreatic parts are filled by light blue. Higher base flow line between P2 and P3 denotes flow along the partially known overflow channels in this segment.

flysch rocks, continues for another 7 km as a surface flow on a limestone terrain, sinks at the Škocjan Caves and contributes to the springs in the Trieste Bay (Figs. 1 & 2). The straight-line distance between the Škocjan Caves and the Timavo Springs is ~33 km. The average discharge of the Reka River in the period 2007–2013 was 7.1 m^3/s, while the long-term average (1952–2013) is about 8 m^3/s. The ratio between the highest and the lowest flow rate is ~1700, with the maximum measured discharge 305 m^3/s, and the minimum 0.18 m^3/s. It should be noted, that the Reka River makes an important contribution to the Timavo Springs during high flow, however, during mean and base flow, most of the spring water originates from the Soča alluvium in the NW (Doctor 2008) and from diffuse infiltration from rainwater (Civita et al. 1995). In other words, the Soča River provides the base flow while the Reka River and diffuse infiltration from the surface contribute the variability of the Timavo and other springs.

Yearly precipitation in the mountainous catchment of the Reka River can reach > 2000 mm. These areas form an important orographic barrier where extreme precipitation events (e.g., 250 mm in 12 hours) have been recorded.

The epiphreatic flow of the Reka–Timavo system

Figure 3 shows an idealised cross-section through the Kras Plateau. Several caves have been explored that cross vertically the entire vadose zone and reach the epiphreatic level with the Reka River flow. In caves P1-P6, long term monitoring of water level, temperature and electric conductivity have been monitored with autonomous instruments. The Reka starts its underground flow at Škocjanske Caves (P1 in Figs. 2 & 3), where flow is more or less uninterrupted and follows the channels of extreme dimensions until the available cross-section drops by three orders of magnitude at Martel's chamber. Škocjan Caves end with a sump, not yet explored. About 800 m NW Reka reappears in Kačna Jama (P2 in Figs 2 & 3). The cave is >20 km long and 280 m deep. The lower epiphreatic level is dominated by the flow of the Reka River, which mostly flows in an open channel during low to medium hydrological conditions, when water leaves the cave through the terminal sump at 156 m a.s.l. The base level sump has limited flow capacity, as soon as the recharge surpasses 15 m^3/s, it is diverted to the sequence of large overflow galleries. More than 2 km of

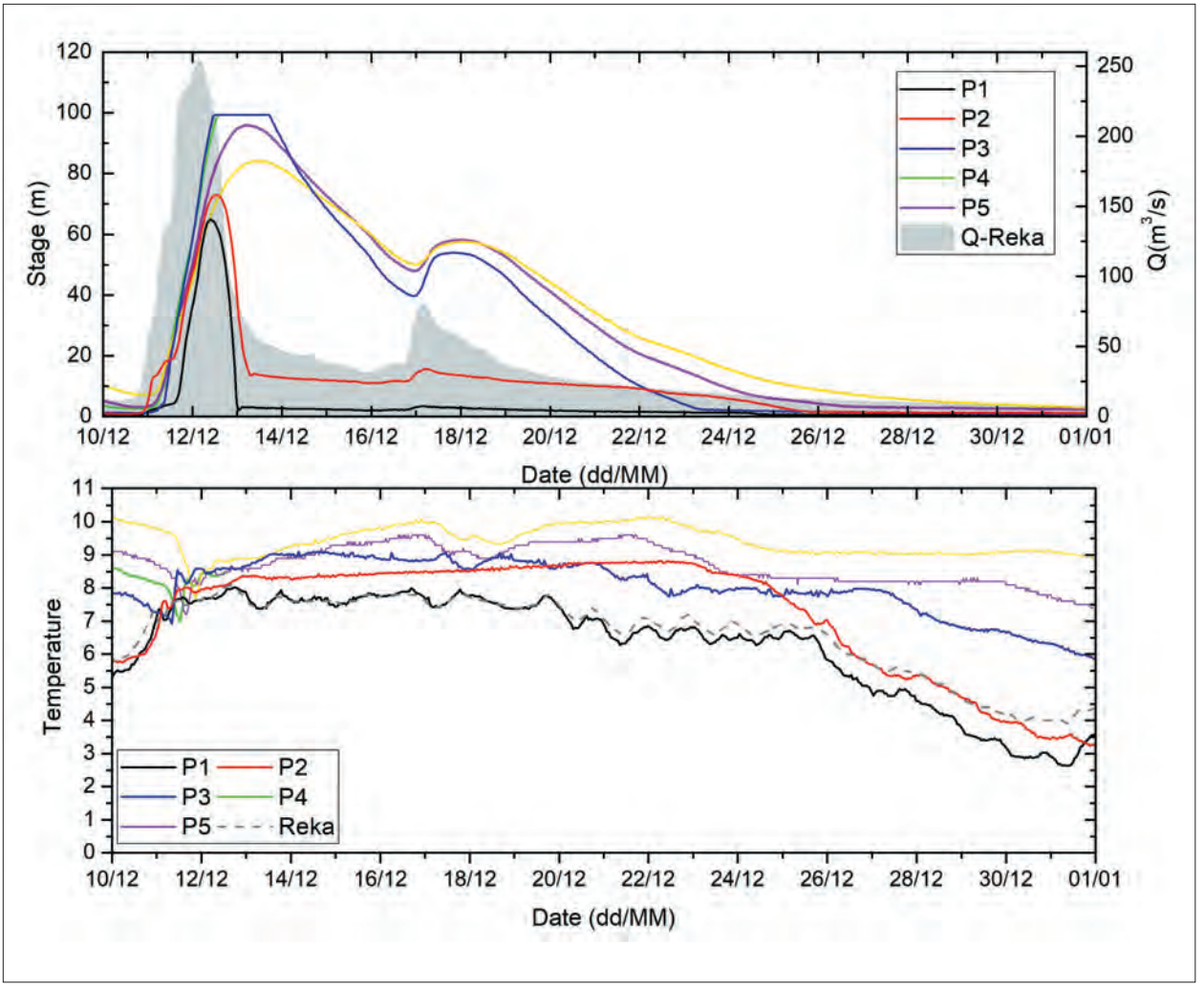

Figure 4: Level and temperature hydrographs recorded in caves of the Reka-Timavo system during major flood in December 2008.

the overflow channels, interrupted by perched sumps, have been explored. The underground flow can be observed in several other caves (observed caves are P3 to P6), where typically a series of rather narrow shafts lead to large chamber or passage with groundwater flow.

Characteristics of flood propagation through the Reka-Timavo system

Details on monitoring, interpretation and modelling can be found in Gabrovšek et al. (2018). Here we outline just some conclusion of their work:

Floods in Škocjan Caves (P1) and Kačna Jama (P2) are controlled by local restrictions. During large events, back-flooding of Škocjan Caves and Kačna Jama are caused by the same restriction.

The base outflow sump in Kačna Jama drains water effectively until the discharge is below 15 m^3/s. When this is surpassed, the flow is diverted along higher positioned overflow galleries. This can drain efficiently flow rates up to 130–150 m^3/s. At higher discharge the levels in Kačna Jama and Škocjan Caves rise very fast with increasing flow. The rate of the level rise can reach 10 m/h.

Analysis of temperature hydrographs showed that a large amount of perched water is stored in the galleries between P2 and P3 between successive floods.

The level in the lower part of the system P3–P6 reacts very simultaneously, indicating uniform variations of water level in this part of the system.

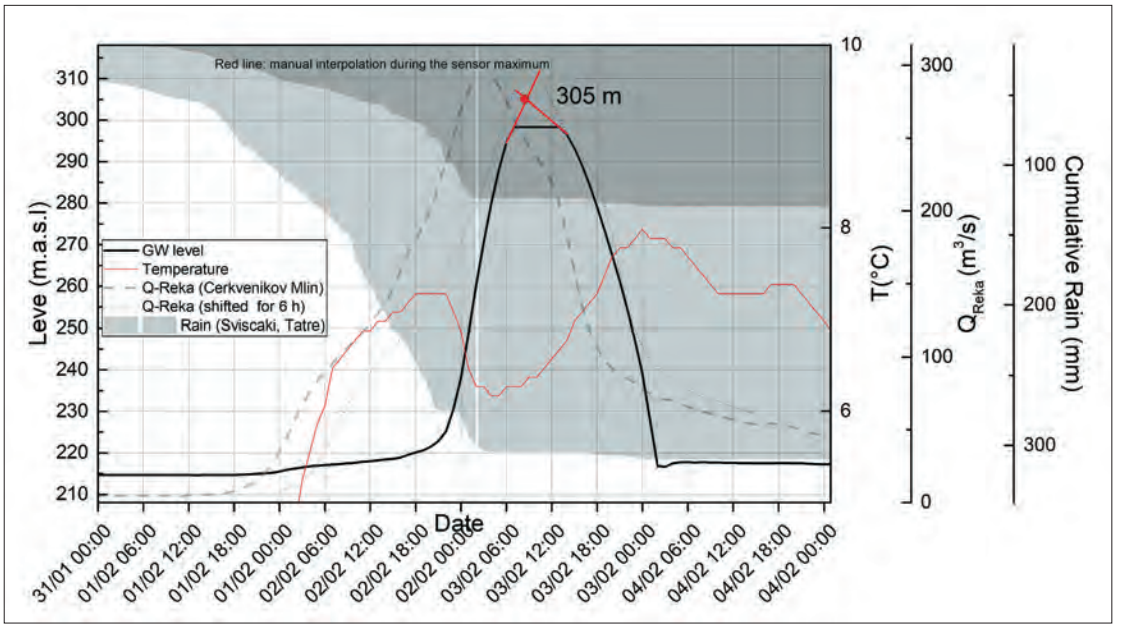

Figure 5: The flood event of 2019: Cumulative rain at two stations, discharge of Reka and level and temperature in Martel's chamber. Dotted grey line shows discharge shifted for six hours, an estimated travel time from gaging station to Martel's chamber.

Figure 6: The water rose for over 90 m during flood in February 2019. The flood caused severe damage in infrastructure and deposited a thick layer of mud. Lower right: a satellite picture of Timavo springs region on February 5th (Photos: Borut Lozej, Škocjan Caves Regional Park, ESA Sentinel). Below: rough cross-sectional schematic view of water level during the 2019 flood.

The flood event in February 2019

Between January 27th and February 4th 2019 over 300 mm (almost 200 mm in the most intensive 30 h period) of rain fell in the mountainous region of Mt. Snežnik and about 150 mm in the area of Škocjan. The discharge of Reka at the gaging station Cerkvenikov Mlin peaked at 300 m^3/s. During the event the water in Škocjan Caves rose with rates up to 10 m/h and reached the level of 305 m a.s.l. in Martel's chamber and about 307.5 m a.s.l. in Šumeča Jama (Figs. 5 & 6) . The flood was largest in the last 50 years. High water caused severe damage to infrastructure and deposited a considerable amount of mud; at some places the thickness of fresh deposits was above 50 cm (Figure 6).

Geophysical and geodetic response to floods

Continuous recording gravity stations were installed above the Škocjan Caves and inside Grotta Gigante in 2018 (Pivetta et al. 2021). The Škocjan Caves serve as a test site because the cave geometry and the hydraulic system here are well known. Gravitational response of 2019 flood was clearly recorded and the records are currently being analysed. Furthermore, high overpressure (up to 10^6 Pa) may form in conduits during flood propagation. This could result in measurable terrain uplift as discussed in recent paper by Braitenberg et al. (2019).

A brief speleological review of Škocjanske jame

Škocjanske Jame (Škocjan Caves) are 5.8 km long cave (Figure 7) formed by the river Reka that enters the cave at an altitude of 314 m a.s.l., flows towards Martelova Dvorana (Martel's Chamber) at 214 m a.s.l. and to terminal sump at 190 m a.s.l. (i.e. 124 m lower). At low water levels the Reka sinks before it enters the cave. Floods usually reach up to 30 m. The largest known flood in the 19th century raised the water table level by 132 m. The largest chambers are Martelova Dvorana, with a volume of 2.6 x 10^6 m^3, and Šumeča Jama with

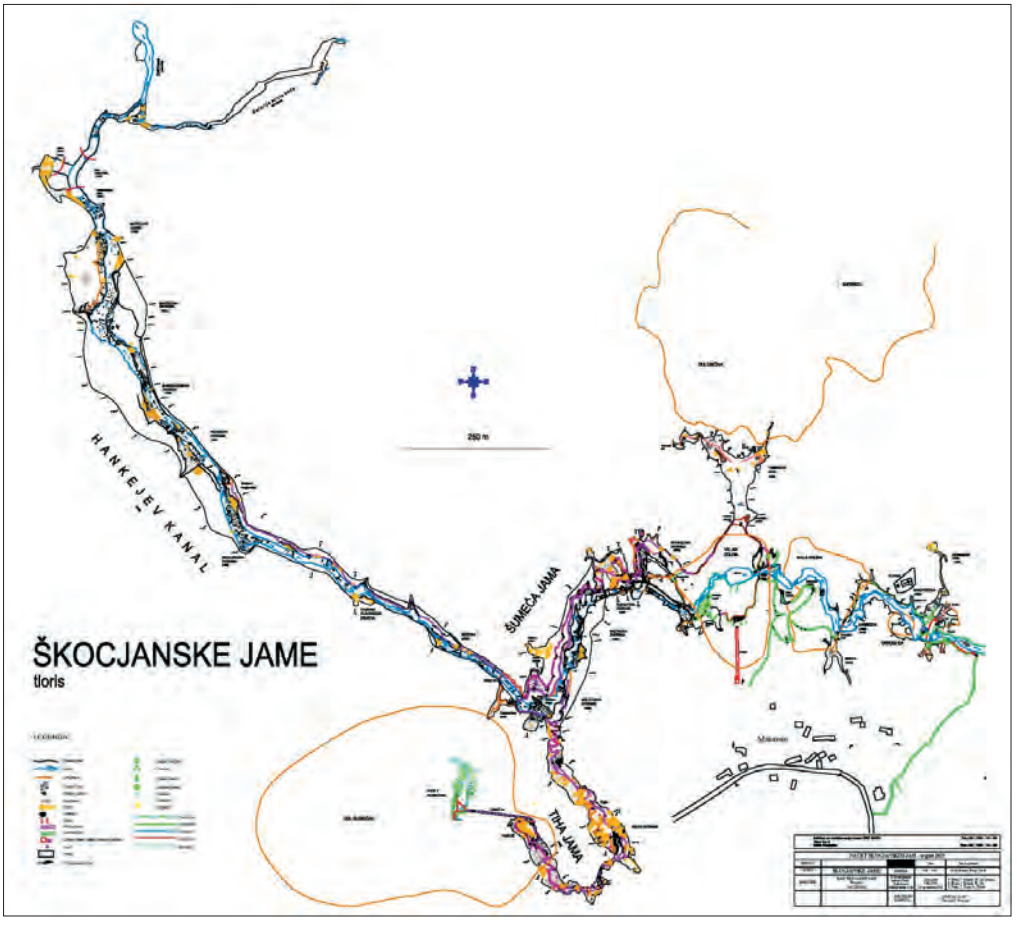

Figure 7: Map of Škocjanske Jame (Cave Register 2019).

0.87×10^6 m^3 (Mihevc 2001). Some of the big chambers have been transformed into collapse dolines like Velika and Mala dolina. Škocjanske Jame are developed on a contact area of Cretaceous thick-bedded rudist limestone and Paleocene thin-bedded dark limestone (Šebela 2009). The passages were initially formed in phreatic conditions along tectonized bedding-planes, and later modified by paragenesis or gravitational entrenchments and collapses.

Exploration and tourism in Škocjanske Jame

The first paths in the cave area were made in 1823, but construction of paths for exploration and for the visitors started in 1884. Cave exploration was done by cavers of DÖAV (Littoral section of Austrian Alpine Club) from Trieste. The most important explorers were Anton Hanke and Joseph Marinitsch. In 1891 they had already reached the final sump in the cave.

In 2019 a new connecting surface and Martel's chamber was explored. In the cave two large passages were found that offer promising leads along the high flood pathways. In 2018 and 2019 a complete lidar scan of the caves was made.

Because of the caves' extraordinary significance for the world's natural heritage, the Škocjanske Jame were included in UNESCO's World Heritage List in 1986. The Republic of Slovenia pledged to ensure the protection of the Škocjanske Jame area and therefore adopted the Škocjanske Jame Regional Park Act.

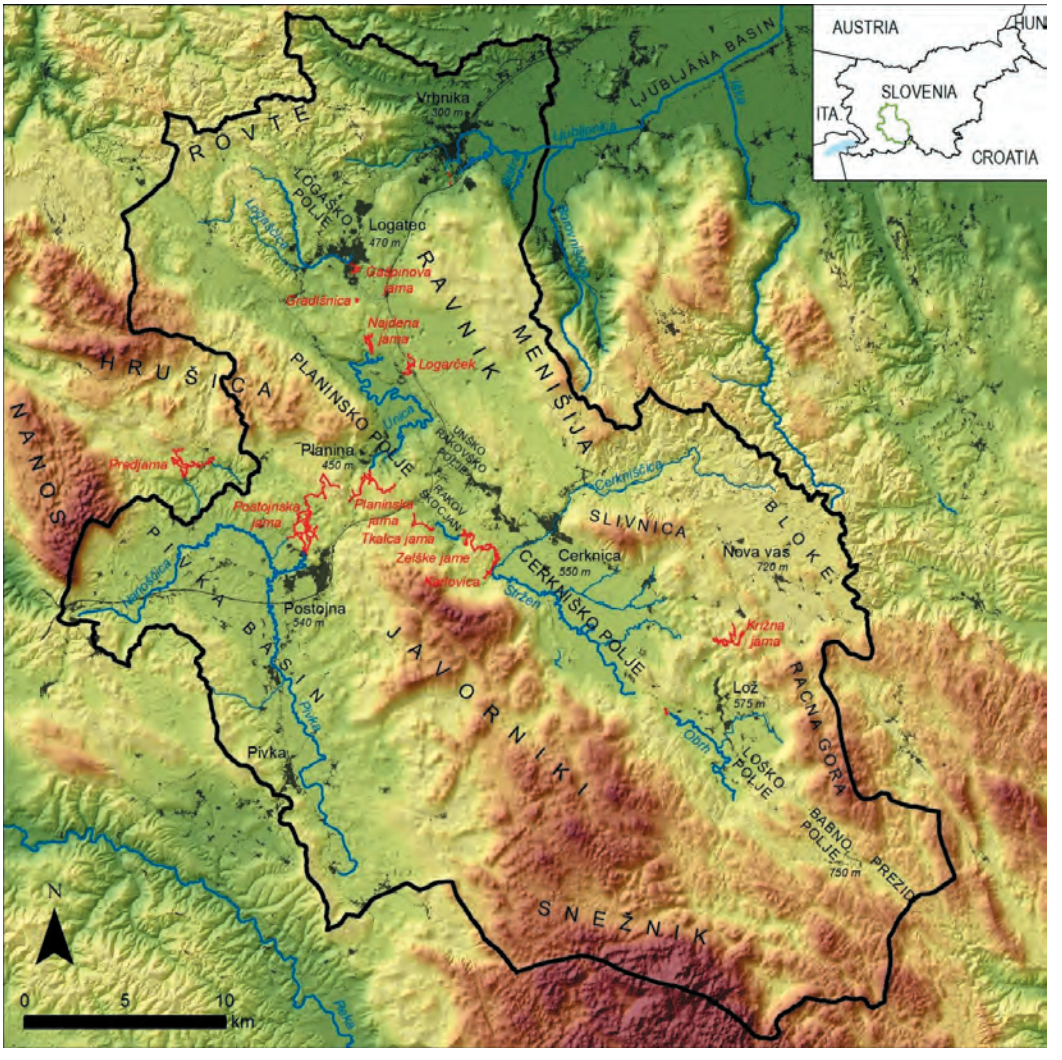

Figure 8: Thel Ljubljanica River recharge area with high karstic plateaus, karst poljes and surface rivers. The main caves are shown with red lines.

THE LJUBLJANICA RIVER RECHARGE AREA

The central part of the Slovenian Dinaric Karst drains to the springs of the Ljubljanica River, located on the southern edge of the Ljubljana Basin (Figure 8). Although the area is about 26 km of straight-line distance close to the Adriatic Sea, intense tectonic activity has triggered drainage into the Sava-Danube river basin, which flows to the Black Sea. The estimated total size of the Ljubljanica recharge area is almost 1800 km^2, of which about 1100 km^2 are karstified. The karst catchment area was delineated during an extensive tracing campaign in the 1970s (Gospodarič & Habič 1976).

The karst rocks are mostly of Mesozoic age. They are generally micritic, locally oolitic limestones and predominantly late-diagenetic dolomites. They formed on the Dinaric platform under conditions of continuous sedimentation that allowed high rock purity, gen-

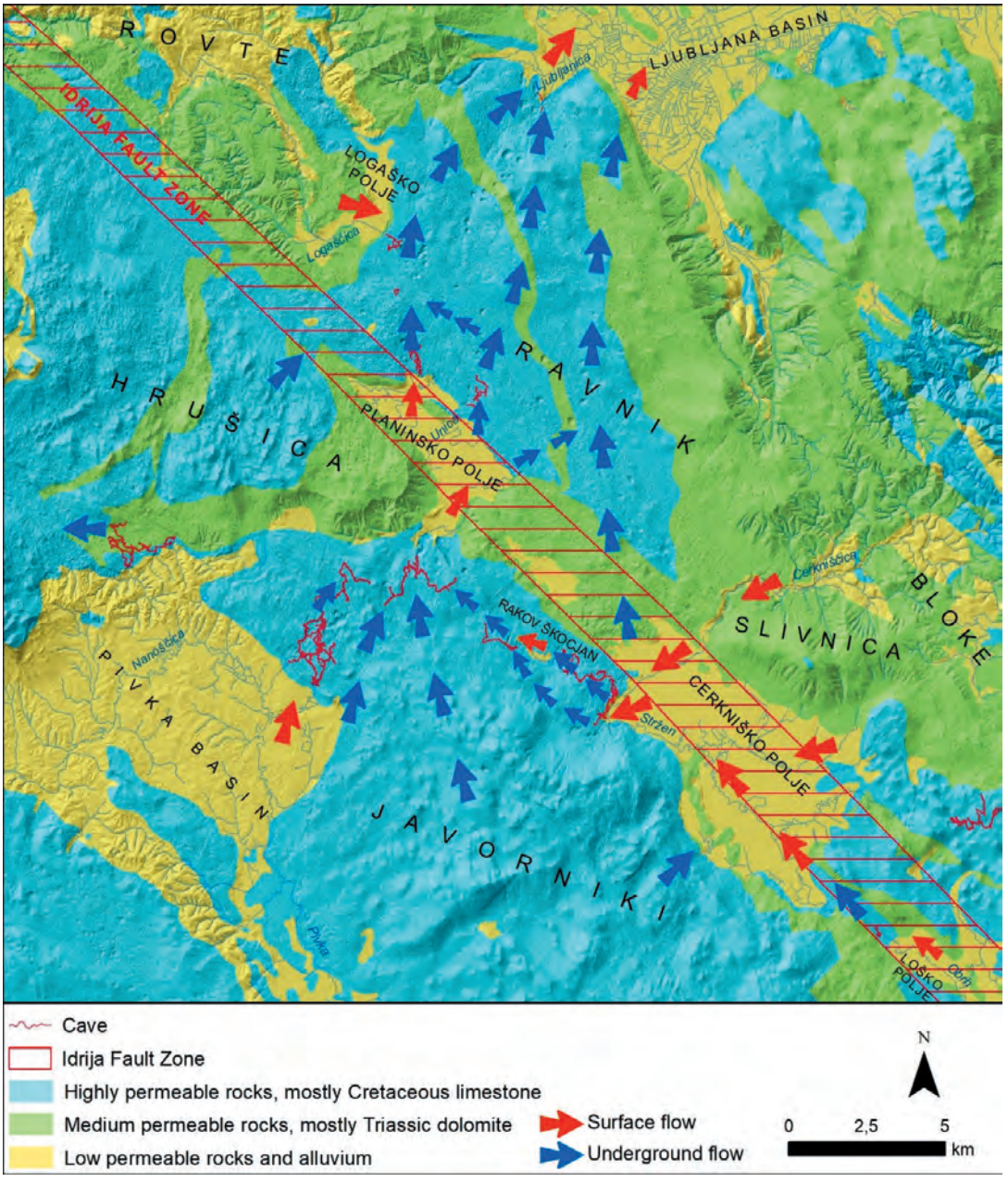

Figure 9: Hydrogeological map of the Ljubljanica recharge area (adapted from Krivic et al. 1976).

erally with less than 5%, locally even only 0.1%, insoluble residues. The total thickness of the carbonate sequence is almost 7 km.

Structurally, the entire Ljubljanica catchment belongs to the Adriatic Plate. The area consists of several nappes that were overthrust during the peak of the Alpine orogeny in the Oligocene in a NE to SW direction (Placer 2008; Placer et al. 2010). A later change in the direction of plate movement led to the formation of the Idrija Fault Zone, a dextral strike-slip fault that crosses the area in the direction of NW-SE (Figure 9) (Vrabec 1994). The Idrija Fault Zone largely determines the direction of regional flow (Figure 9). In general, the steepest hydraulic gradient is oriented northwards, from the Notranjska region towards the Ljubljana Basin, which represents a regional base level. However, the fault zone acts as a barrier to groundwater flow and forces the water to surface in the poljes. At the same time, it diverts the flow in the Dinaric direction (SE-NW) (Šušteršič 2006).

Several poljes have developed along the Idrija Fault Zone (Gams 1965, 1978; Šušteršič 1996). These large flat-bottomed depressions are regularly flooded and are often the only areas where water appears at the surface. The formation of poljes is preconditioned by tectonics, in this case by the structures within the Idrija strike slip fault, but the forming mechanism is the corrosional planation at the groundwater level.

In general, the water follows the SE-NW direction with surface flow on the poljes and groundwater flow in-between (Figure 10). Additional water enters the flow system at numerous springs draining the areas of the Snežnik and Javorniki mountains in the south of the Idrija Fault Zone. Several sinking rivers draining dolomite or flysch areas also contribute to this system (Gams 2004). The altitude of the poljes drops from about 750 m to 450 m (Figure 10). The streams that flow through them have different names: Trbuhovica, Obrh, Stržen, Rak, Pivka and Unica. Apart from a relatively small amount of water flowing directly from Cerkniško

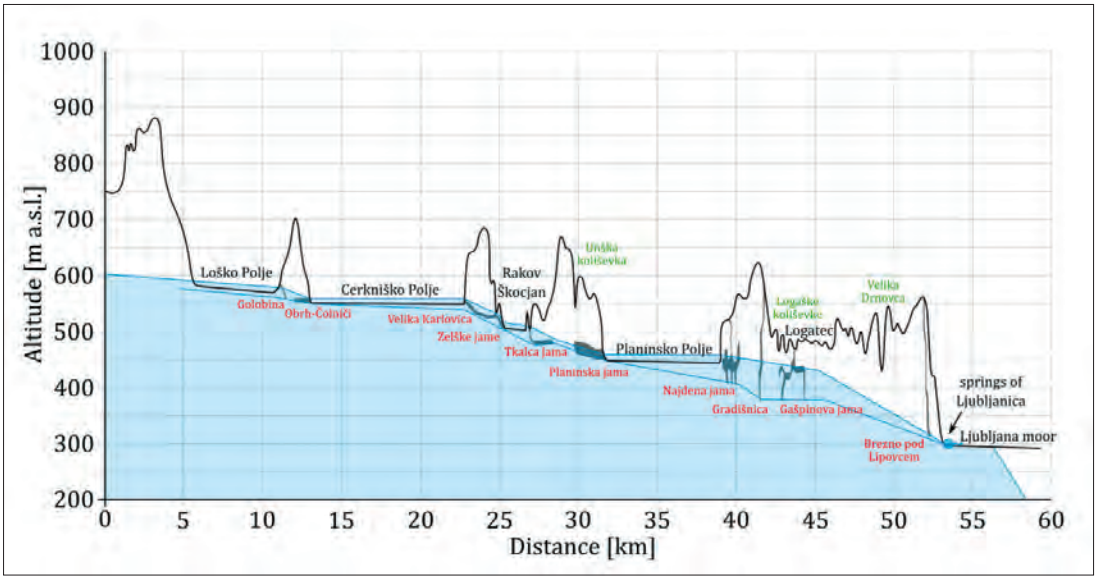

Figure 10: Cross section of Ljubljanica River recharge area following an initially SE-NW trend along the Idrija Fault Zone between Loško and Planinsko Polje, and turning N from Planinsko Polje toward the Ljubljanica springs near Vrhnika. The major caves are indicated in red, large collapse dolines in green.

Polje to the springs of Ljubljanica, most of the water comes to the surface along the southern edge of Planinsko Polje. Along its eastern and northern edges, the water sinks back underground and flows northwards to several large and many small springs aligned along the southern edge of the Ljubljana Basin, which is connected to the gradual tectonic subsidence of the area (Krivic et al. 1976; Gams 2004). The average annual discharge of the Ljubljanica springs is 38.6 m^3. An additional amount of water drains from the low- to medium-permeable Rovte plateau and contributes to the Ljubjanica springs by sinking into the ponors of Logaško Polje (Mihevc et al. 2010).

There are over 1600 known caves in the recharge area of the Ljubljanica River (Cave Register 2019). Most of them are accessible fragments of a fossil un-

Figure 11: (a) Flooded Cerkniško Jezero (Spring 2013) (Photo: C. Mayaud). (b) Ponors of Rešeta during low flow conditions (Summer 2017) (Photo: M. Blatnik).

derground drainage system (Habič 1973; Gospodarič 1981; Šušteršič 1999, 2002). The average cave length is 48 m and the depth 18 m. However, the largest cave systems are water-active and sum a total of about 80 km of epiphreatic channels.

Cerkniško Polje

Cerkniško Polje is the largest karst polje in Slovenia (Gams 1978, 2004). It is often called Cerkniško Jezero (Lake of Cerknica) because of its regular floods (Figure 11a). When full, the intermittent lake covers up to 26 km^2 out of 38 km^2 of the polje's total area. The bottom of the lake is at an altitude of 550 m. Its intermittency has attracted many scholars since the beginning of the New age including the polihistorian Valvasor, who published his famous study of the Cerkniško Jezero in 1689 (Shaw & Čuk 2015). The main part of the polje is underlained by Upper Triassic dolomite at its N, E and SE borders. The areas to the W and NW, on the other hand, are mainly underlain by Cretaceous limestone (Figure 9).

The polje is regularly flooded for several months, mostly in autumn, winter and spring (Kovačič & Ravbar 2010). On average, about ten days a year the water is above the level of 550.3 m, which corresponds to a flooded area of 21.84 km^2 (Ravbar et al. 2021). The main in-

flows into the polje come from a series of karst springs called Žerovniščica, Šteberščica and Stržen, located on its eastern and southern borders. The springs on the SW side (e.g. Suhadolca, Vranja jama) contribute substantial amount of water during floods. In addition, an important allogenic component comes from the Cerkniščica River, which drains a dolomitic area of about 44 km^2 in the east (Gams 2004). Finally, several estavelles (e.g., Vodonos) also contribute to the inflow into the polje.

In addition to the estavelles, several ponor zones located in the inner part of the polje drain a certain amount of water directly to the springs of Ljubljanica (Krivic et al. 1976) (Figure 11b), while the main ponors are aligned along the W side of the polje, with Velika and Mala Karlovica being the most prominent. Both caves extend for over 8.5 km between Cerkniško Polje and the Rakov Škocjan karst valley. So far, only a small section between Velika Karlovica and Zelške Jame (located in Rakov Škocjan) is unexplored as an important collapse zone is located there. Recent studies have shown that at low to medium water levels (Gabrovšek et al. 2010; Ravbar et al. 2012; Kogovšek 2022), a large part of the water sinking into the ponor of Mala Karlovica reaches the Kotliči springs in the middle of Rakov Škocjan and a smaller part reaches Zelške Jame, which would be the most logical direction.

In the last centuries, several attempts were made to change the hydrological behaviour of the polje, but none was completed or successful. In the 1960s, a plan to transform the Cerkniško Jezero into a permanent

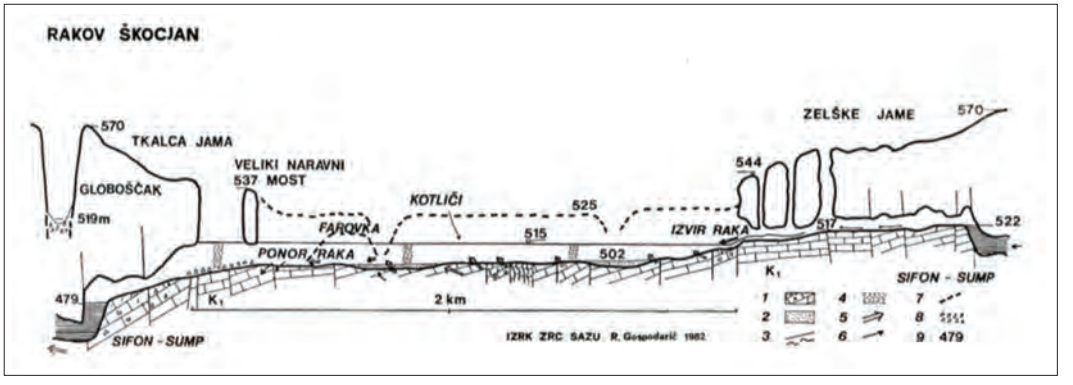

Figure 12: Cross-section of the Rakov Škocjan karst valley between the Rak spring at Zelške Jame and the terminal ponor in Tkalca Jama. Legend: 1. rocky bottom; 2. alluvia; 3. fault zone; 4. flood level in 1982; 5. karst spring: 6. water flow directions; 7. terraces; 8. boulder rocks; 9. altitude.

Figure 13: Rakov Škocjan karst valley. a) The arch of Mali Naravni Most. b) Kotliči spring at the beginning of a hydrological event (Photos: M. Blatnik).

lake was initiated. The entrances to the caves Velika and Mala Karlovica were closed with concrete walls and a 30 m tunnel was built to connect Karlovica to the surface. However, it had a minor impact on water retention during dry periods (Shaw & Čuk 2015).

Rakov Škocjan karst window

Between Cerkniško and Planinsko Polje, the water surfaces in an about 1.5 km long and 200 m wide karst valley (karst window) Rakov Škocjan (Figure 12). On the upstream side (SE) the water emerges as the Rak River from the cave Zelške Jame. Zelške Jame is about 5 km long. The breakdown below the collapse doline of Velika Šujca prevents cavers to connect the cave to Karlovica cave system, which drains water from Cerkniško Polje. The entrance area of Zelške Jame is a fragmented system of channels and collapse dolines. The most prominent feature is Mali Naravni Most (Small Natural Bridge; Figure 13a), where an impressive narrow arch, which was part of the former cave ceiling, crosses the collapse doline (Gams 2004).

Downstream, the valley widens and several springs (Figure 13b) located along the SW side of the valley (e.g. Kotliči, Prunkovec) form perennial or intermittent tributaries of the Rak River. The valley narrows an impressive natural bridge called Veliki Naravni Most (Big Natural Bridge; Figure 14). The rocky arch is made of thick-bedded and anticline-folded Lower Cretaceous limestone.

Figure 14: a) Flooded Rakov Škocjan Karst Valley in October 2020, b) Veliki Naravni Most (Big Natural Bridge) during dry period in summer; and c) during high water event in winter (Photos: M. Blatnik; RI-SI-LifeWatch)

After Veliki Naravni Most, the channel opens into a 150 m long canyon that ends at the entrance to Tkalca Jama, an almost 3 km long cave that drains the water towards Planinsko Polje. The connections of the Rak with the water from Cerkniško Polje and with the Unica springs at Planinsko Polje have been proven by several tracer tests under different hydrological conditions (Gabrovšek et al. 2010; Ravbar et al. 2012). A narrow passage in Tkalca Jama acts as a flow constriction that causes regular floodings of Rakov Škocjan. The floods can reach a height of 19 m above the cave entrance (located at 496 m a.s.l.), bringing large part of the Rakov Škocjan under water (Drole 2015; Figure 14a). Before World War 1, Rakov Škocjan was a private park owned by the Windischgrätz family, while between the First and Second World Wars the Italians used it as a military site. Since 1949 Rakov Škocjan has been a Landscape Park open to the public.

Planinsko Polje and Planinska Jama

Planinsko Polje is one of the finest examples of an overflow structural polje (Gams 1978; Šušteršič 1996). The springs located on the southern side recharge the Unica River that sinks in two major outflow zones located along the eastern and northern borders of polje (Figure 15). The polje surface is slightly undulating and about 10 km^2 large, with a bottom elevation between 444.5 m and 450 m a.s.l (Blatnik et al. 2017). Apart

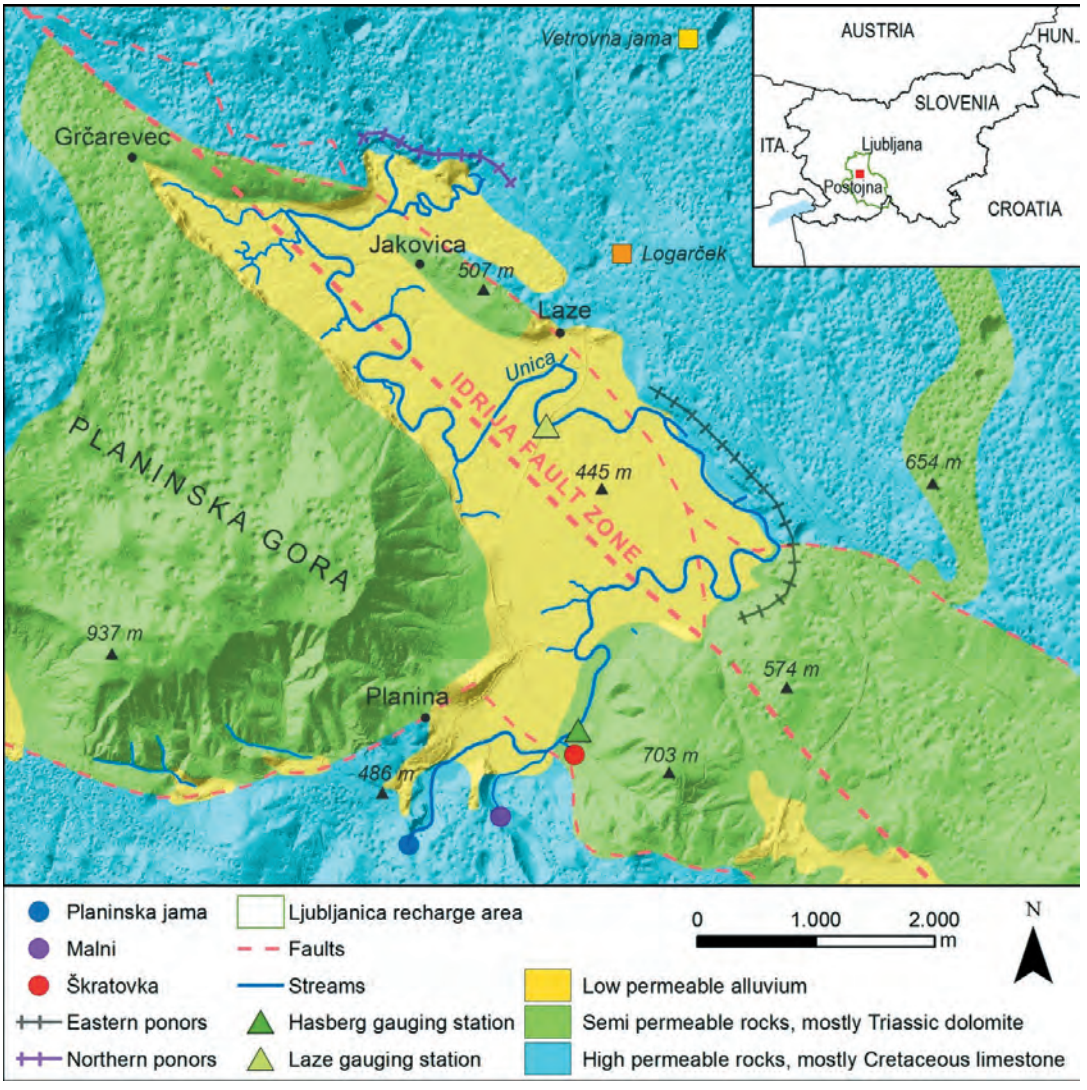

Figure 15: Planinsko Polje and its surrounding area with the position of caves, springs, ponor zones and main gauging stations. The upper right insert shows the regional position of the area in Slovenia.

from the wetlands close to the Unica, the polje is used for field crops and grass. Three settlements are located on the elevated slopes around Planinsko Polje, which is surrounded by forested karst plains at elevations between 520 m and 600 m a.s.l. and by mountains reaching up to 1000 m a.s.l. after.

Planinsko Polje has formed along the Idrija Fault Zone. Its southern and western borders mostly consist of Upper Triassic Main Dolomite, while its two main springs are located within a band of Cretaceous limestone in the south. The average thickness of the alluvium cover is about 4 m (Breznik 1961; Ravnik 1976). The polje bedrock base is dominantly Upper Triassic Main Dolomite, whereas its eastern and northern sides include most of the ponors and are composed of highly karstified Cretaceous limestone (Čar 1982).

Besides Planinska Jama, the most important recharge input is the spring of Malni (Malenščica River, Q_{min} = 1.1 m^3/s, Q_{mean} = 6.7 m^3/s, Q_{max} = 9.9 m^3/s; Frantar 2008), which receives water from Rakov Škocjan and the Javorniki mountains. The Malni spring is used as a water supply for more than 20,000 inhabitants (Petrič 2010). The Unica River flows rather uninterrupted over the polje's surface for the first 7 km. Along its course in proximity to the eastern border, it loses water along a 2 km long reach due to the presence

Figure 16: Two of the many ponors draining Planinsko Polje. Left: Velike Loke located at the eastern border. Right: So-called Putick's Well (Putickova štirna) located at the terminal outflow zone at the northern border (Photos: M. Blatnik).

of several groups of ponors and zones of intense leakage. The water sinks into well-expressed ponors, along lines of diffuse discharge into fractures and small dissolutional openings, as well as into small blind valleys entrenched into the sediment (Figure 16). A recent study carried out by Blatnik et al. (2017) revealed new details on the location and capacity of the eastern ponor zone, with a total outflow capacity of about 18 m^3/s and individual outflow ranging between 1.0 and 5.6 m^3/s at each group of ponors. After 2 km of flow along the eastern border, the river crosses the polje and follows the western border. Then the Unica turns northeast towards the second ponor zone that are distributed along the polje northern border. The capacity of northern group of ponors was estimated between 40 and 60 m^3/s (Šušteršič 2002).

Similar to Cerkniško Polje, Planinsko Polje can be flooded up to several times per year (Kovačič & Ravbar 2010). The period with the greatest probability that an extreme flood occurs is the cold part of the year, tied to the mid-autumn rainfall peak, winter rains and snowmelting. Although historical data are difficult to compare to current regular measurements, several extreme floods have been recorded in the past such as in 1801, in 1851/52; when the water level presumably reached an elevation between 456 and 458 m a.s.l.; and in 1923 when water level reached 453.4 m a.s.l. (Gams 1980). In February 2014, the floods reached altitude of 453.2 m a.s.l. and 72 million cube meters of water were stored in the polje (Frantar & Ulaga 2015). The lake extended over 10.3 km^2 and more than fourty houses and other facilities have been flooded (Mihevc 2014).

During the period between 1954 and 2014, high waters on the polje occurred on average 37.9 days per year (Ravbar et al. 2021). The longest periods the polje has been overflown were recorded in 1960 (altogether 137 days) and in 2014 (altogether 126 days). An event of high waters lasts on average for ten days, but can also be as long as 78 days such as the flood that occurred in autumn and winter 2000/01 (Ravbar et al. 2021). To prevent extreme flooding in Planinsko Polje, different measures have been undertaken in the beginning of 20th century (Putick 1889). They consisted to increase the outflow capacity of the ponors zone by mean of different constructions to prevent their plugging by flotsam (Figure 16).

In a recently published work, Mayaud et al. (2019) listed and tested the parameters that could potentially control flooding in poljes. If the method is applied on Planinsko Polje and focus on the high flood event of February 2014, the role of ponor zones can be emphasized. Due to the sudden arrival of an important quantity of melted water carrying a lot of flotsam, all the ponors were plugged. This can explain the high amplitude and long duration of the flood. This result is confirmed when comparing this flood with the high flood of November 2014. Despite a much higher amount of precipitation released within a similar time span, the maximum stage in the polje that was three meters lower than the flood of February 2014. The only explanation is that all ponor zones have been cleaned in between (Mayaud et al. 2019).

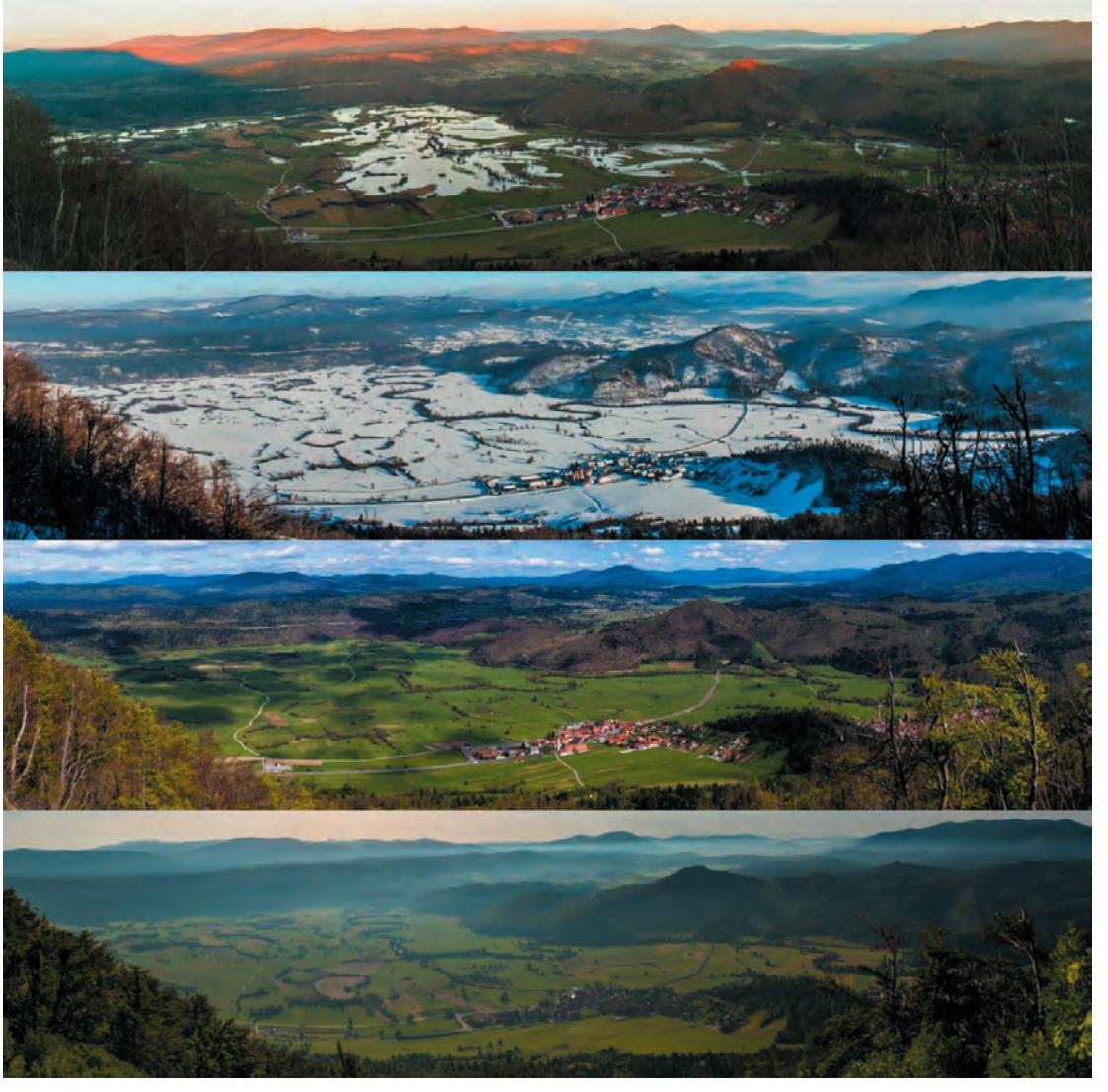

Figure 17: Planinsko Polje in different hydrological situations (Photos: M. Blatnik).

Planinska Jama (Planina Cave) is a large spring cave located on the southern edge of Planinsko Polje (Figs. 18 & 19). The cave is about 6.6 km long and consists mostly of large active river passages with cross-sections larger than 100 m^2.

The cave entrance is in Upper Cretaceous limestones and dolomites. The entrance part and the Rak Branch are developed in Lower Cretaceous bedded limestones, limestones with chert and limestone breccia. The Pivka Branch and the Rudolfov Rov (passage south of the Rak Branch), on the other hand, are formed in Upper Cretaceous massive limestone and breccia with Caprinidae and Chondrodontae (Habič 1984). Both parts of the cave end with siphons that have been dived but do not yet have a connection to the upstream systems. However, the recent dives in the final siphon of the Pivka Branch give justified hope that a connection to the Postojnska jama cave system could be established in the near future.

The cave is known to be the confluence of two important regional rivers (Figs 18, 19): the Pivka River, which drains a large allogenic catchment through the

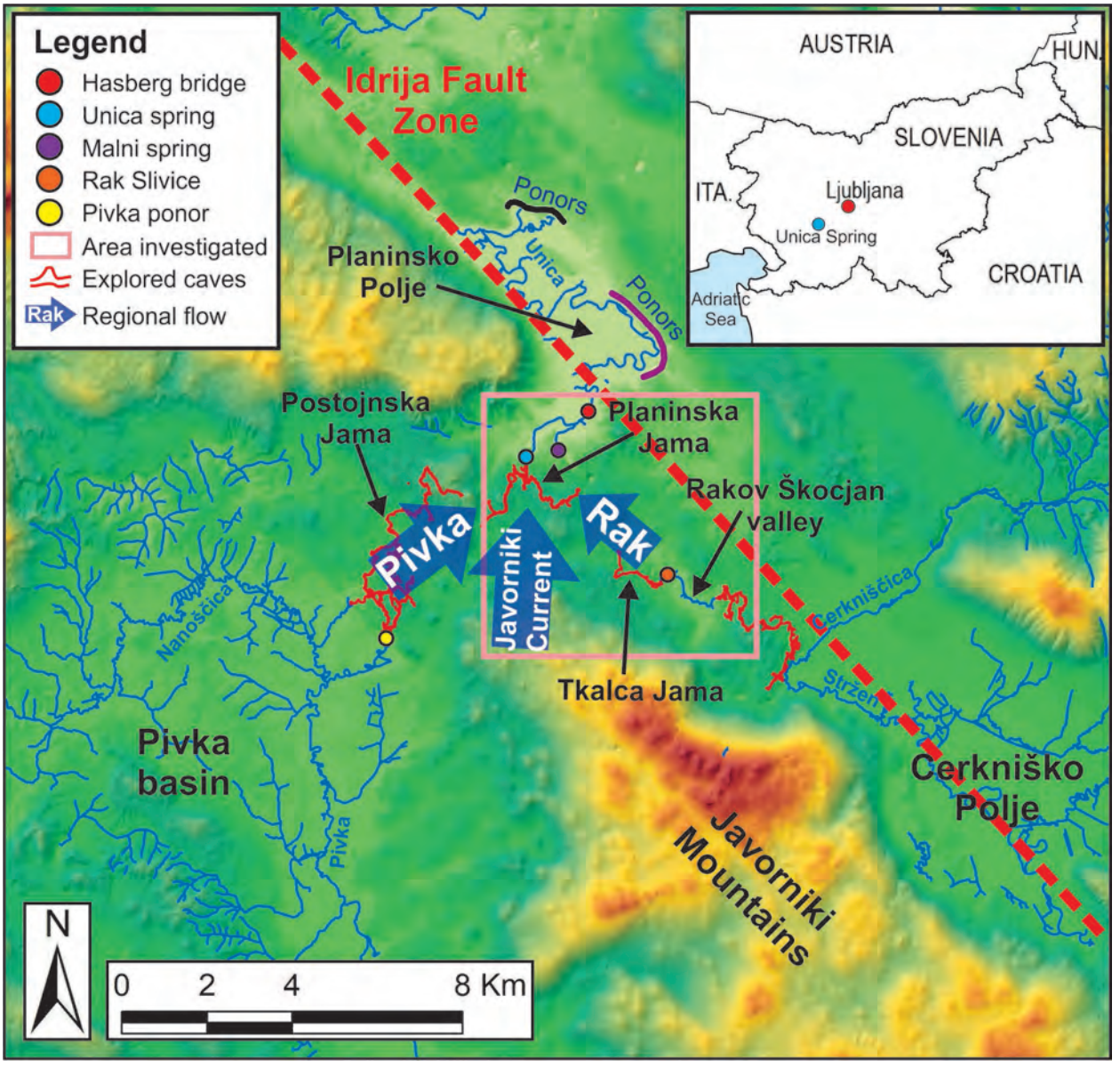

Figure 18: Map of the Unica catchment with explored cave systems, main springs and ponors, and assumed flow directions. The pink frame delineates approximately the area that is further investigated. Inset: location of the Unica Spring in Slovenia.

Postojnska Jama (Gabrovšek et al. 2010; Kaufmann et al. 2016; Kogovšek 2022) and reaches the confluence with the cave via the Pivka Branch, and the Rak River, which carries water from Rakov Škocjan and Cerkniško Polje via the Rak Branch. Finally, a large amount of water also flows into the Rak Branch via the siphon of the Javornik Current, which is located below the Mysterious Lake (Figure 21) (Kaufmann et al. 2020). The water exits the cave under the common name Unica River with a discharge between 0.2 and 90 m^3/s (Kogovšek 2022).

The different parts of the aquifer that feed the Unica spring show considerable differences in water contribution (Savnik 1960, Kogovšek 2022). During high water conditions, there is a groundwater divide in the Javorniki Mountains. The water discharges through the western, eastern and northern edges of the massif. Then the nearby Malni Spring (Figure 18), which is mainly fed by the autogenic Javorniki water and allogenic water from the Rakov Škocjan reaches a maximum discharge of 9-10 m^3/s (Kogovšek 1999; Kovačič 2010, 2011). As the spring is damped, the Rak Branch is activated and acts

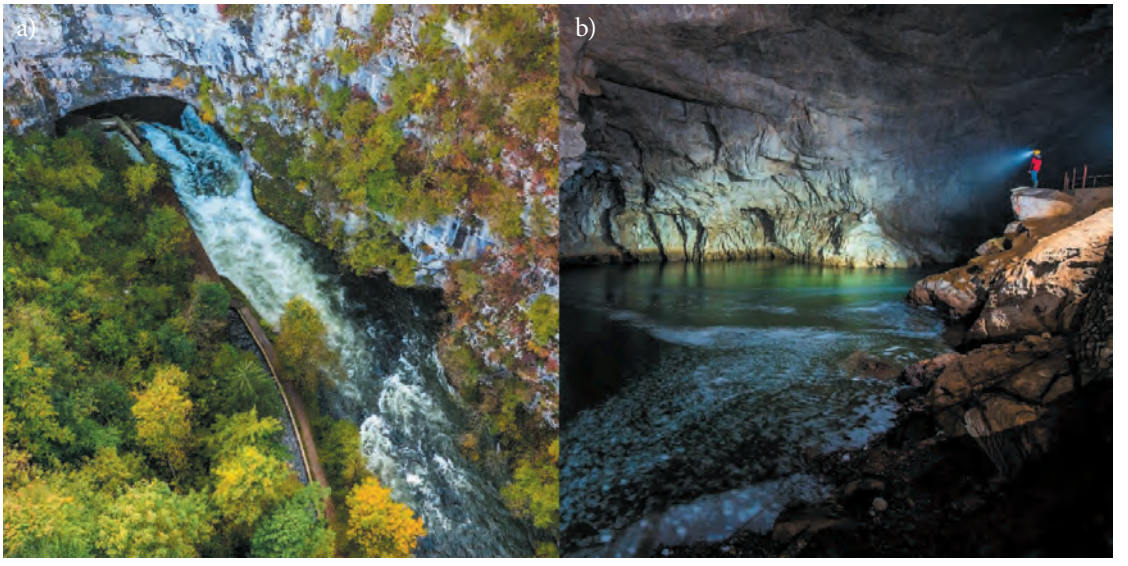

Figure 19: Planinska Jama. a) Cave entrance. b) Confluence of the Pivka and Rak Branches (Photos: M. Blatnik; RI-SI-EPOS).

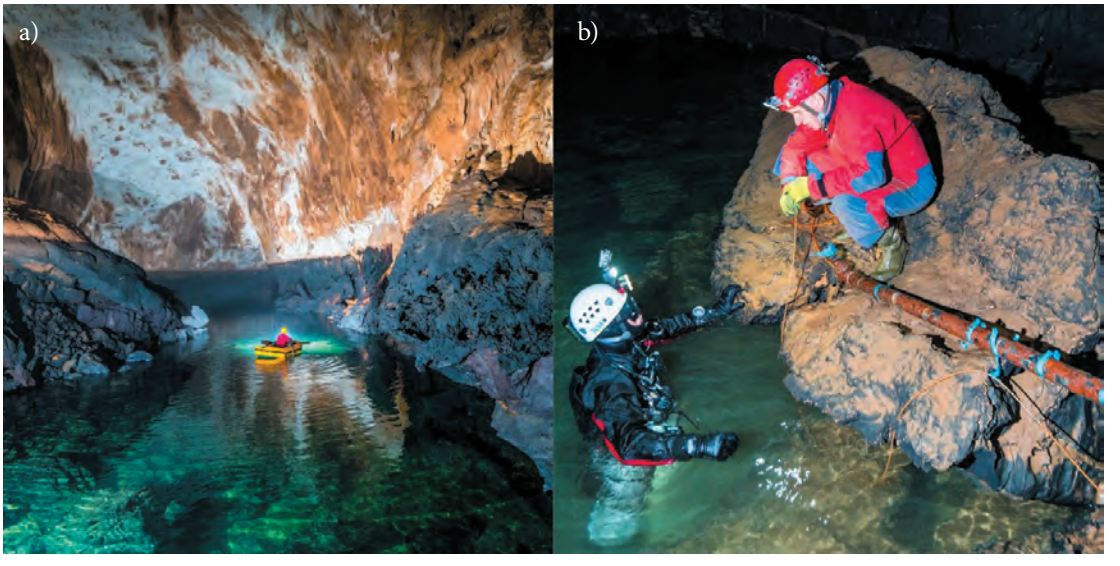

Figure 20: Planinska Jama. a) example of typical large cave passage in the Rak Branch. b) recent diving exploration in the Mysterious Lake and Javornik Current (Photos: M. Blatnik).

as an overflow, while the Unica spring also receives water from the Pivka Branch. At low-flow, after the Cerkniško Jezero is drained, the outflow is solely directed towards the Malenščica spring, while the Unica spring is fed exclusively by the Pivka Branch (Kaufmann et al. 2020, Kogovšek 2022). The inversion of the flow direction between the Mysterious Lake and the Malenščica spring was numerically simulated with a pipe flow model (Kaufmann et al. 2020).

There are also differences in flow velocities between low and high flow conditions (Petrič et al. 2018). In general, the apparent dominant flow velocities in the karst aquifer are five times higher during high water (between 20 and 25 m/h) than during low water conditions (~ 4 m/h). In the well-developed conduit networks of Karlovica-Zelške Jame, Tkalca-Planinska Jama and Postojnska-Planinska Jama, flow velocities were up to fifty or even ninety times higher during high water (between 170 and 1000 m/h) compared to the velocities observed during low water (~ 4-23 m/h) (Petrič et al. 2018).

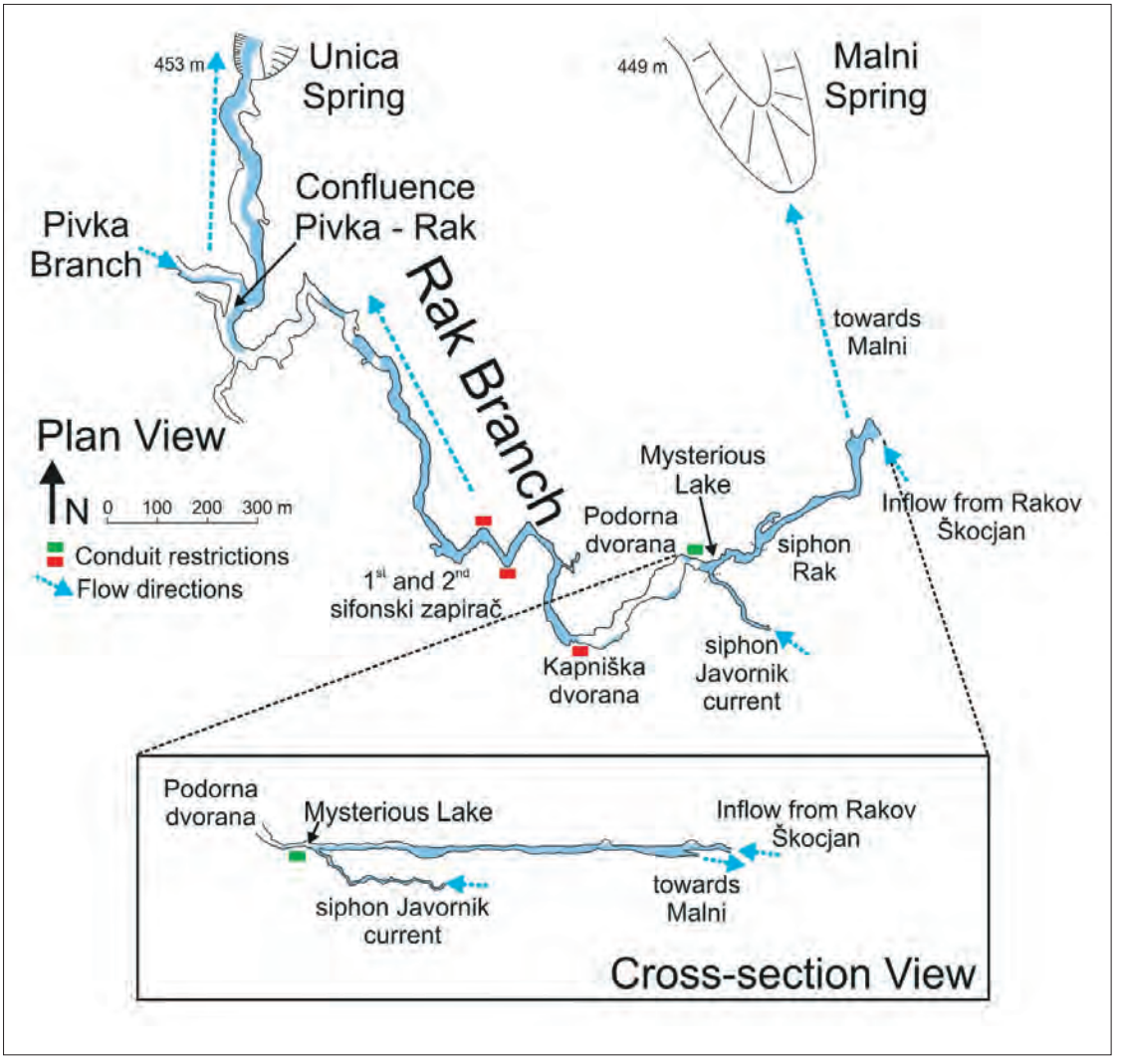

Figure 21: Detailed view of the Rak Branch of Planinska Jama and cross-section of its terminal siphon in the Mysterious Lake (Gams 2004; Kaufmann et al. 2020).

Groundwater flow between Planinsko Polje and Ljubljanica Springs

Water level and temperature have been monitored in all active caves between Planinsko Polje and Ljubljana basin in years from 2006 to 2009 and from 2015 on (Turk 2010; Gabrovšek & Turk 2010; Blatnik et al.

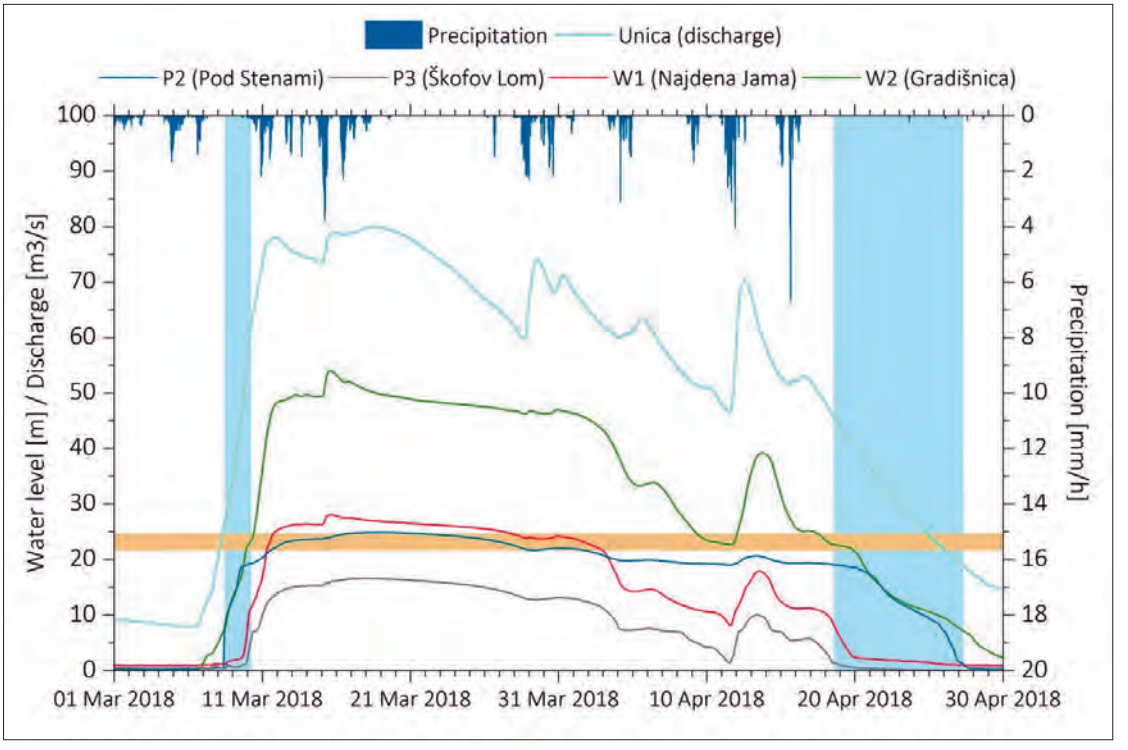

Figure 22: Water level dynamic in selected caves between Planinsko Polje and Ljubljanica springs during high water event in March and April 2018. Blue areas denote different response of water level change, orange area denotes temporal slower increase(decrease of water level in cave Gradišnica.

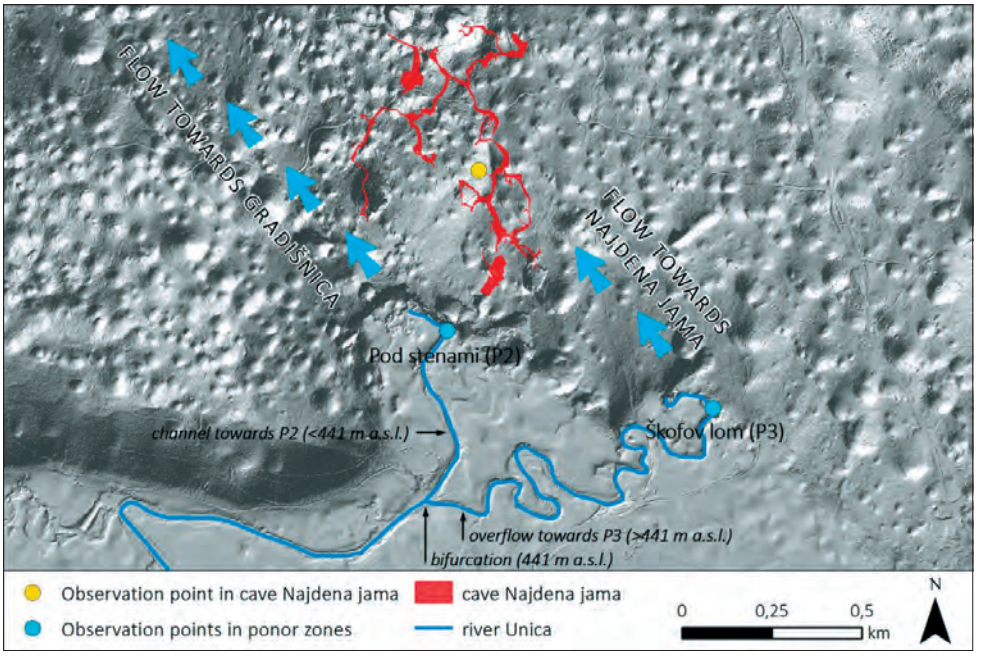

Figure 23: Assumed grondwater flow directions between the northern ponors (Pod Stenami and Škofov Lom) and Najdena Jama and Gradišnica.

2019). Data loggers are installed in 7 caves (Logarček, Vetrovna Jama, Najdena Jama, Gradišnica, Gašpinova Jama, Brezno pod Lipovcem, Veliko Brezno v Grudnovi Dolini) and three ponors on the rim of Planinsko Polje (Velike Loke, Pod Stenami, Škofov Lom). Figure 22 presents the recorded dynamics of underground water in March and April 2018.

Water level measurements showed complex dynamics in water level variations (up to 60 m, Figure 22) and different rate of changes of groundwater level (from several hours during increase to several weeks during decrease). The duration of the high water event is dependent on the duration of flooding of Planinsko Polje (Figure 22). During all high water events there is different response in water level increase. When the discharge of the Unica River is increasing, water reaches different ponor zones at different time (in Planinsko Polje first eastern, then northern ponors), resulting in different response in downstream located caves (Figs. 22 & 23). This dynamic explains late response in cave Najdena Jama in comparison to nearby located ponor zone Pod Stenami. There, the water bypasses cave Najdena jama, which is recharged through more apparent ponor zone Škofov Lom (Figure 23). Water level hydrographs also shows in-

Figure 24: Main chamber of the cave Gradišnica during low water conditions. Dark colour on the rock wall indicates the position of high water level (Photo: M. Blatnik).

flection points, presenting temporal slower increase/decrease of the water level. This dynamic indicate presence of overflow passages at certain levels. Temperature and EC hydrographs have been interpreted for the travel time estimation between successive observation points.

The Springs of Ljubljanica River

The water of the Ljubljanica karst catchment emerges at number of springs located near Vrhnika, at the rim of the Ljubljana Basin. The line of spring generally follows the contact of Jurassic limestone and Quarternary sediments underlain by Triassic dolomite (Celarc et al. 2013) (Figure 25). Most important springs are aligned along the gradually retreating pocket valleys of Močilnik and Retovje. The springs at Močilnik ($Q_{av} \approx$ 6–7 m^3/s) feed Mala (=small) Ljubljanica and springs at Retovje ($Q_{av} \approx$ 16 m^3/s) feed Velika (= big) Ljubljanica, the main tributaries related to karst springs of the Ljubljanica River. Easterly, another tributary Ljubija ($Q_{av} \approx$ 6–7 m^3/s) is also fed by several springs. The eastern-

most set of springs at Bistra are already positioned in Triassic dolomites and add on average 7 m^3/s to the last true karstic tributary of Ljubljanica. Mean annual discharge of the Ljubljanica karst springs is about 24 m^3/s (Gospodarič & Habič 1976).

Temperature monitoring at springs have shown, that major springs show similar temperature dynamics, however, easternmost spring at Bistra differs quite substantially from the others (Figure 26). The temperature lag is higher and the hydrograph lacks short-time disturbances. This indicates longer retention time (Blatnik et al. 2019). Water tracing in in 1970s also revealed, that the direct flow from the Cerkniško Polje, mostly goes to the Bistra springs (Gospodarič & Habič 1976).

Collapse dolines in the hinterland of the ljubljanica springs

Collapse dolines are large closed depressions formed by subsidence and/or partial collapses of cave ceilings. Large collapse dolines form in the crushed/fractured zones above the main groundwater flow, where dissolutional yield is high due to high (rock surface)/ (water volume) ratio (Gabrovšek & Stepišnik 2011).

Between Logatec and Vrhnika several large collapse dolines formed along the main drainage pathways of underground Ljubljanica River (Celarc et al. 2013). Table 1 lists the bottom elevations, and dimensions of the largest. Estimated volume of the biggest of them (Velika Drnovica) is around 1.6 million m^3.

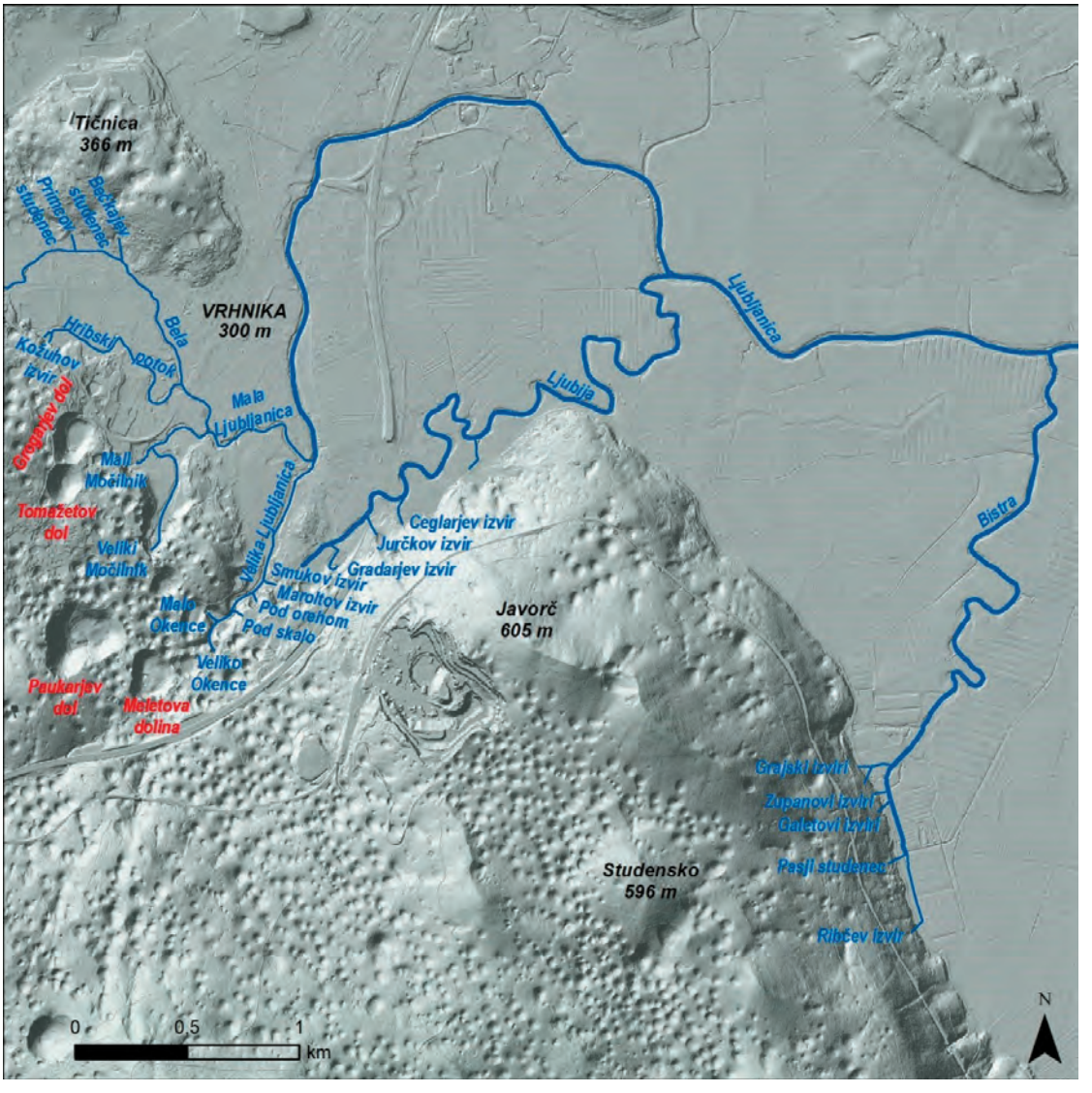

Figure 25: Location of collapse dolines and Ljubljanica springs near Vrhnika.

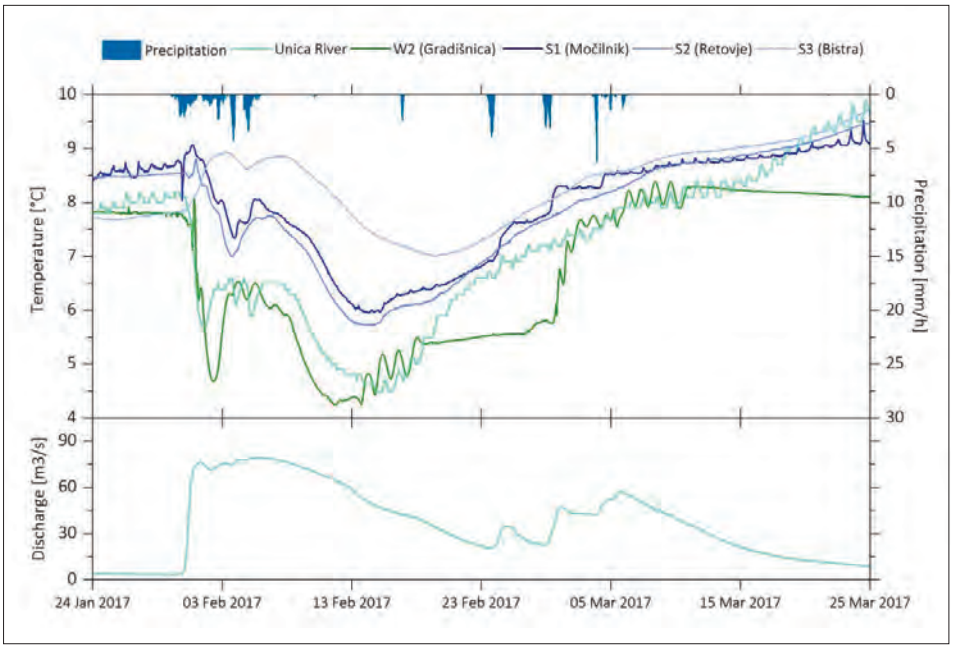

Figure 26: Temperature hydrographs at springs of Ljubljanica compared to the cave Gradišnica and Unica River.

Tab. 1: Some characteristics of collapse dolines along the main pathways of Ljubljanica River.

Name	Bottom elevation (m)	Radius (m)	Average depth (m)
Velika Drnovica	409.0	157	106
Velika Jama	424.0	143	66
Mala Drnovica	520.0	101	60
Stranski dolec	457.0	90	69
Masletova Koliševka	435.0	89	70
Srednja Lovrinova Koliševka	443.0	96	57

Seven collapse dolines are located in the immediate hinterland of the main Ljubljanica spring (Tab. 2, Figure 25). The bottoms are relatively levelled and covered with over 30 m thick loamy sediment. The elevation of the bottoms of all these dolines are within 10 m of each other. Flooding has been observed in Grogarjev Dol. The estimated volume of Paukarjev dol is about 1 million m^3 (Gabrovšek & Stepišnik 2011).

Tab. 2: Some characteristics of collapse dolines located in the near hinterland of the Ljubljanica springs.

Name	Bottom elevation (m)	Radius (m)	Average depth (m)
Paukarjev Dol	297.3	125	55
Meletova Dolina	297.7	84	33
Grogarjev Dol	294.0	80	35
Tomažetov Dol	304.4	66	35
Babni Dol	295.0	58	27
Susmanov Dol	298.9	50	18
Nagodetov Dol	300.8	38	18

ACKNOWLEDGMENT

The authors acknowledge the project "L7-2630 Characterisation of karst aquifers on regional and local scales: the recharge area of the Malni water source«, financially supported by the Slovenian Research Agency.

REFERENCES

Blatnik, M., Frantar, P., Kosec, D. & F. Gabrovšek, 2017: *Measurements of the outflow along the eastern border of Planinsko Polje, Slovenia*. Acta Carsologica 46 (1): 83–93.

Blatnik, M., Mayaud, C. & F. Gabrovšek, 2019: *Groundwater dynamics between Planinsko Polje and springs of the Ljubljanica River, Slovenia.* Acta Carsologica 48 (2): 199–226.

Braitenberg, C., Pivetta, T., Barbolla, D. F., Gabrovšek, F., Devoti, R. & I. Nagy, 2019: *Terrain uplift due to natural hydrologic overpressure in karstic conduits*. Scientific Reports: 3934

Breznik, M., 1961: *Akumulacija na Cerkniškem in Planinskem polju*. Geologija 7: 119–149.

Buser, S., Pavlovec, R. & M. Pleničar, 1968: *Osnovna geološka karta SFRJ, list Gorica,* 1 : 100 000. Zvezni geološki zavod Beograd, Beograd.

Cave Register, 2019: *Cave Register of the Karst Research Institute ZRC SAZU and Speleological Association of Slovenia*. Postojna, Ljubljana.

Celarc, B., Jež, J., Novak, M. & L. Gale, 2013: *Geološka karta Ljubljanskega barja 1:25,000*. Geološki zavod Slovenije, Ljubljana.

Civita, M., Cucchi, F., Eusebio, A., Garavoglia, S., Maranzana, F. & B. Vigna, 1995: *The Timavo hydrogeologic system: an important reservoir of supplementary water resources to be reclaimed and protected*. Acta Carsologica 24: 169–186.

Čar, J., 1981: *Geološka zgradba požiralnega obrobja Planinskega polja*. Acta Carsologica10: 75–106.

Doctor, D. H., 2008: *Hydrologic connections and dynamics of water movement in the Classical karst (Kras) aquifer: Evidence from frequent chemical and stable isotope sampling.* Acta Carsologica 37: 101–123.

Drole, F., 2015: *Rakov Škocjan in Planinsko polje 2014*. Proteus 76 (6): 275–281.

Frantar, P. (Ed.), 2008: *Water balance of Slovenia 1971–200*0. Ministrstvo za okolje in prostor, Agencija Republike Slovenije za okolje, pp. 119, Ljubljana.

Frantar, P. & F. Ulaga, 2015: *Visoke vode Planinskega polja leta 2014*. Ujma, 29: 66–73.

Gabrovšek, F. & J. Turk, 2010: *Observations of stage and temperature dynamics in the epiphreatic caves within the catchment area of the Ljubljanica river*. Geologia Croatica 63 (2): 187–193.

Gabrovšek, F. & U. Stepišnik, 2011: *On the formation of collapse dolines: a modelling perspective*. Geomorphology 134 (1-2): 23–31.

Gabrovšek, F., Kogovšek, J., Kovačič, G., Petrič, M., Ravbar, N. & J., Turk, 2010: *Recent results of tracer tests in the catchment of the Unica River (SN Slovenia).* Acta Carsologica 39 (1): 27–38.

Gabrovšek, F., Peric, B. & G. Kaufmann, 2018: *Hydraulics of epiphreatic flow of a karst aquifer.* Journal of Hydrology 560: 56–74.

Gabrovšek, F., Petrič, M., Ravbar, N., Blatnik, M., Mayaud, C., Prelovšek, M., Kogovšek, B., Mulec, J., Šebela, S. & G. Vižintin, 2019: *Raziskave možnih rezervnih vodnih virov za oskrbo občin Postojna in Pivka*. Project report, pp. 84.

Gams, I., 1965: *On the Quarternary geomorphogenesis of the area among the karst poljes of Postojna, Planina and Cerknica* (In Slovene, English Summary). Geografski vestnik 37: 61–101.

Gams, I., 1978: *The polje: the problem of definition: with special regard to the Dinaric karst*. Zeitschrift für Geomorphologie 22:170–181.

Gams, I., 2004: *Kras v Sloveniji v prostoru in času*. Založba ZRC, pp. 515, Ljubljana.

Gospodarič, R., 1981: *Morfološki in geološki položaj kraških votin v ponornem obrobju Planinskega polja*. Acta Carsologica 10: 157–172.

Gospodarič, R. & P. Habič, (Eds.), 1976: *Underground water tracing: Investigations in Slovenia 1972–1975*. Third International Symposium of Underground Water Tracing (3. SUWT), pp. 312, Ljubljana, Bled.

Habič, P., (Ed.) 1973*: Speleološka karta – List Vrhnika 2-D*. Inštitut za raziskovanje krasa ZRC SAZU, pp. 156, Postojna.

Habič, P., 1984: *Vodna gladina v Notranjskem in Primorskem krasu Slovenije*. Acta Carsologica13: 37–78.

Jurkovšek, B., Biolchi, S., Furlani, S., Kolar-Jurkovšek, T., Zini, L., Jež, J., Tunis, G., Bavec, M. & F. Cucchi, 2016: *Geology of the Classical Karst Region (SW Slovenia - NE Italy).* Journal of maps 12: 352–362.

Kaufmann, G., Gabrovšek, F. & J. Turk, 2016: *Modelling flow of subterranean Pivka River in Postojnska Jama, Slovenia*. Acta Carsologica 45 (1): 57–70.

Kaufmann, G., Mayaud, C., Kogovšek, B. & F. Gabrovšek, 2020: *Understanding the temporal variation of flow direction in a complex karst system (Planinska Jama, Slovenia).* Acta Carsologica 49/2-3: 213–228.

Kogovšek, B., 2022: *Characterization of a karst aquifer in the recharge area of Malenščica and Unica springs based on spatial and temporal variations of natural tracers.* PhD thesis. University of Nova Gorica, pp. 242.

Kogovšek, J., 1999: *Nova spoznanja o podzemnem pretakanju vode v severnem delu Javornikov (Visoki kras).* Acta Carsologica 28 (1): 161–200.

Kovačič, G., 2010: *An attempt towards an assessment of the Cerknica Polje water balance*. Acta Carsologica 39 (1): 39–50.

Kovačič, G., 2011: *Kraški izvir Malenščica in njegovo zaledje : hidrološka študija s poudarkom na analizi časovnih vrst*. Univerza na Primorskem, Znanstveno-raziskovalno središče, Univerzitetna založba Annales, pp. 408, Koper.

Kovačič, G. & N. Ravbar, 2010: *Extreme hydrological events in karst areas of Slovenia, the case of the Unica River basin*. Geodinamica Acta 23/1–3: 89–100.

Krivic, P., Verbovšek, R. & F. Drobne, 1976: *Hidrogeološka karta 1: 50 000*. In: Gospodarič, R. & P. Habič (Eds.): *Underground water tracing: Investigations in Slovenia 1972–1975*. Inštitut za raziskovanje krasa ZRC SAZU, Postojna.

Mayaud, C., Gabrovšek, F., Blatnik, M., Kogovšek, B., Petrič, M. & N. Ravbar, 2019: *Understanding flooding in poljes: A modelling perspective.* Journal of Hydrology 575: 874-889.

Mihevc, A., 2001: *Speleogeneza Divaškega krasa*. Založba ZRC SAZU, pp. 180, Ljubljana.

Mihevc, A., Prelovšek, M., & N., Zupan Hajna, 2010*: Introduction to Dinaric Karst*.- Založba ZRC SAZU, pp. 71., Ljubljana.

Petrič, M., 2010: *Characterisation, exploitation, and protection of the Malenščica karst spring, Slovenia*. In: Kresic, N. & Z. Stevanovic (Eds.) *Groundwater Hydrology of Springs. Engineering, Theory, Management and Sustainability*. Butterworth-Heinemann, pp. 428–441, Burlington.

Petrič, M., Kogovšek, J., & N. Ravbar, 2018: *Effects of the vadose zone on groundwater flow and solute transport characteristics in mountainous karst aquifers–the case of the Javorniki–Snežnik massif (SW Slovenia).* Acta Carsologica 47 (1): 35–51.

Placer, L., 2008: *Principles of the tectonic subdivision of Slovenia = Osnove tektonske razčlenitve Slovenije*. Geologija 51 (2): 205–217.

Placer, L., Vrabec, M. & B. Celarc, 2010: *The bases for understanding of the NW Dinarides and Istria Peninsula tectonics.* Geologija 53 (1): 55–86.

Placer, L., 2015: *Simplified structural map of Kras*. Geologija 58 (1): 89–93.

Pivetta, T., Braitenberg, C., Gabrovšek, F., Gabriel, G. & B. Meurers, 2021: *Gravity as a tool to improve the hydrologic mass budget in karstic areas*. Hydrology and Earth System Sciences 25: 6001-6021.

Putick, V., 1889: *Die hydrologischen Geheimnisse des Karstes und seine unterirdischen Wasserläufe : auf Grundlage der neuesten hydrotechnischen Forschungen*. Himmel und Erde, pp. 13, Berlin.

Ravbar, N., Barberá, J.A., Petrič, M., Kogovšek, J. & A. Bartolomé, 2012: *The study of hydrodynamic behaviour of a complex karst system under low-flow conditions using natural and artificial tracers (the catchment of the Unica River, SW Slovenia).* Environ Earth Sciences 65: 2259–2272.

Ravbar, N., Mayaud, C., Blatnik, M. & M. Petrič, 2021: *Determination of inundation areas within karst poljes and intermittent lakes for the purposes of ephemeral flood mapping.* Hydrogeology Journal 29 (1): 213–228.

Ravnik, D., 1976: *Kameninska podlaga Planinskega polja*. Geologija 19: 291–315.

Savnik, R., 1960: *Hidrografsko zaledje Planinskega polja*. Geografski vestnik 32: 212–224.

Shaw, T. & A. Čuk, 2015: *Slovene karst and caves in the past*. Inštitut za raziskovanje krasa ZRC SAZU, pp. 464, Postojna.

Šebela, S., 2009: *Structural geology of the Škocjan Caves.* Acta Carsologica 38 (2-3): 165–177.

Šušteršič, F., 1996: *Poljes and caves of Notranjska*. Acta Carsologica 25: 251–290.

Šušteršič, F., 1999*: Speleogenesis of the Ljubljanica River Drainage Basin, Slovenia*. In: Klimchouk, A.B., Ford, D.C., Palmer, A.N. & W. Dreybrodt (Eds.): *Speleogenesis: Evolution of Karst Aquifers*. NSS, Huntsville, Alabama, 397–406.

Šušteršič, F., 2002: Where does Underground Ljubljanica Flow? RMZ Materials and Geoenvironment 49 (1): 61–84.

Šušteršič, F., 2006: *Relationships between deflector faults collapse dolines and collector channel formation.* International Journal of Speleology 35: 11–12.

Turk, J., 2010: *Dynamics of underground water in the karst catchment area of the Ljubljanica springs.* Carsologica 11, Založba ZRC, pp. 136, Ljubljana.

Vrabec, M., 1994: *Some thoughts on the pull-apart origin of karst poljes along the Idrija strike-slip fault zone in Slovenia.* Acta Carsologica 23: 155–167.

Žvab Rožič, P., Čar, J. & B. Rožič, 2015: *Geological Structure of the Divača Area and its Influence on the Speleogenesis and Hydrology of Kačna jama*.

STRATIGRAPHY AND STRUCTURE OF THE JULIAN ALPS IN NW SLOVENIA

STRATIGRAFIJA IN STRUKTURA JULIJSKIH ALP V SEVEROZAHODNI SLOVENIJI

Špela GORIČAN[1,2*], Aleksander HORVAT[1,2], Duje KUKOČ[3] & Tomaž VERBIČ[4]

http://dx.doi.org/10.3986/fbg0098

ABSTRACT

Stratigraphy and structure of the Julian Alps in NW Slovenia

The Julian Alps belong to the eastern Southern Alps where the South-Alpine and the Dinaric structures now overlap. In Mesozoic times, this area was part of the northeastern Adriatic continental margin, which was facing the Neotethys Ocean but was also close to the Alpine Tethys. The Mesozoic distribution of basins and swells on the continental margin determined variations in the stratigraphic record and also controlled the structural evolution of the later thrust belt. The most general tectonic subdivision in the Julian Alps is the distinction between the Tolmin nappes derived from the Slovenian Basin and the Julian nappes derived from the Julian High and its surroundings. This paper focuses on the Julian nappes. The Mesozoic stratigraphic record is linked with the available structural data to propose a robust subdivision in four nappes that were emplaced in the early Paleogene. From bottom to top these nappes and their corresponding paleotopographic units are: The Tamar Nappe (Tarvisio Basin), the Krn Nappe (western part of the Julian High) with the overlying Travnik Thrust Sheet (Bovec Basin), the Jelovica Nappe together with the Zlatna Klippe and the equivalent smaller klippen (eastern Julian High) and the Pokljuka Nappe (Bled Basin).

The second part of the paper deals with the description of field-trip stops. The panoramic view from the mountain ridge south of Lake Bohinj is presented to explain the general structure of the Julian Alps. The second half of the field-trip is devoted to the Jurassic and Cretaceous stratigraphy of the Bled Basin as the paleogeographically most internal unit with clear affinities with the central Dinarides.

Key words: Mesozoic, Cenozoic, Southern Alps, Dinarides, stratigraphy, nappe structure

IZVLEČEK

Stratigrafija in struktura Julijskih Alp v severozahodni Sloveniji

Julijske Alpe so del vzhodnih Južnih Alp, kjer se danes križajo južnoalpske in starejše dinarske strukture. V mezozoiku je bilo ozemlje del severovzhodnega kontinentalnega roba Jadranske plošče med Neotetido na vzhodu in Alpsko Tetido na zahodu. Razporeditev globokomorskih bazenov in relativno dvignjenih planot na mezozojskem kontinentalnem robu se odraža v raznolikem stratigrafskem zapisu, od mezozojskih prelomov in razlik v stratigrafskih zaporedjih pa je bil odvisen tudi nadaljnji strukturni razvoj ozemlja. Generalno so Julijske Alpe razdeljene na Tolminske in na Julijske pokrove. Stratigrafska zaporedja Tolminskih pokrovov so bila paleogeografsko del Slovenskega bazena, v Julijskih pokrovih pa so ohranjena zaporedja Julijskega praga in bazenov, ki so ga obkrožali. Poudarek članka je na Julijskih pokrovih. Na osnovi mezozojske stratigrafije in obstoječih strukturnih podatkov predlagamo grobo delitev Julijskih pokrovov na štiri pokrove iz Dinarskega faze narivanja, tako da vsakemu pokrovu ustreza določena mezozojska paleotopografska enota. Najnižji je Tamarski pokrov z zaporedji Trbiškega bazena. Sledi Krnski pokrov (zahodni del Julijskega praga) s Travniško lusko oziroma zaporedjem Bovškega bazena. Nad Krnskim pokrovom je Jelovški pokrov (vzhodni del Julijskega praga), ki mu pripadajo še Zlatenska plošča in nekaj manjših tektonskih krp. Strukturno najvišji je bil v paleogenu Poklјuški pokrov, sestavljen iz kamnin Blejskega bazena.

V drugem delu članka so opisane ogledne točke ekskurzije. Razgled z Vogla in Šije smo uporabili za razlago generalne strukture Julijskih Alp. Druga polovica ekskurzije je posvečena stratigrafiji jurskih in krednih plasti Blejskega bazena, ki je bil paleogeografsko relativno interna enota, po stratigrafiji primerljiva z enotami centralnih Dinaridov.

Ključne besede: mezozoik, kenozoik, Južne Alpe, Dinaridi, stratigrafija, pokrovna zgradba

[1] ZRC SAZU, Paleontološki inštitut Ivana Rakovca, Novi trg 2, SI-1000 Ljubljana, Slovenia. spela.gorican@zrc-sazu.si; aleksander.horvat@zrc-sazu.si

[2] Podiplomska šola ZRC SAZU, Novi trg 2, SI-1000 Ljubljana, Slovenia.

[3] Hrvatski geološki institut, Ul. Milana Sachsa 2, HR-10000 Zagreb, Croatia. dkukoc@hgi-cgs.hr

[4] Tomaž Verbič, Cesta dveh cesarjev 15a, SI-1000 Ljubljana, Slovenia. tomazver@gmail.com

INTRODUCTION

The eastern Southern Alps (including the Julian Alps in NW Slovenia) are part of a complex, more than 300 km long transition zone between the Alps and the Dinarides (Figure 1). Westwards, in northern Italy, an overlap of South-Alpine and Dinaric structures has been established (Doglioni 1987; Doglioni & Siorpaes 1990) and a strong influence of Mesozoic stratigraphy on the structural evolution of the thrust belt has been demonstrated (Doglioni 1992; Doglioni & Carminati 2008, and references therein). An overlap of the Dinaric and younger Alpine structures was also confirmed at the boundary between the Southern Alps and the Dinarides in Slovenia (Placer & Čar 1998). Recent studies revealed that the zone of interference extends far eastwards to the Internal Dinarides in northern Croatia (van Gelder et al. 2015).

The nappe system in the research area was derived from the continental margin of the Adriatic microplate. In the Middle and Late Jurassic, this part of the margin was located between two oceanic domains: The Alpine Tethys and the Meliata-Maliac-Vardar branch of the Neotethys (in the sense of Schmid et al. 2008) (Figure 2a). The Mesozoic successions consist of a variety of facies ranging from platform carbonates to deep-marine radiolarian cherts. Due to extensive stratigraphic research, the local basin-and-swell configuration of the continental margin through the Mesozoic is now relatively well known (Goričan et al. 2012a with references; Gale et al. 2015; Goričan et al. 2018). On the other hand, the complex structure and the polyphase deformation history of the area have not been sufficiently explored yet. Although several thrust faults have been recognized by early researchers (e.g. Kossmat 1913; Winkler 1923) and confirmed during the systematic geological mapping at scale 1:100,000 (Jurkovšek 1986; Buser 1987), a clear differentiation between the Paleogene (Dinaric) and younger structures is still missing.

The aim of this paper is to relate the well-established Mesozoic stratigraphy to the present-day structure and to propose a subdivision in which each Mesozoic paleotopographic unit (basin or swell) corresponds to a separate thrust sheet of the initial Dinaric nappe stack. The field trip will start south of Lake Bohinj at Mt. Šija (1880 m altitude), which offers a nice view of the general nappe structure in the Julian Alps. In the afternoon, the

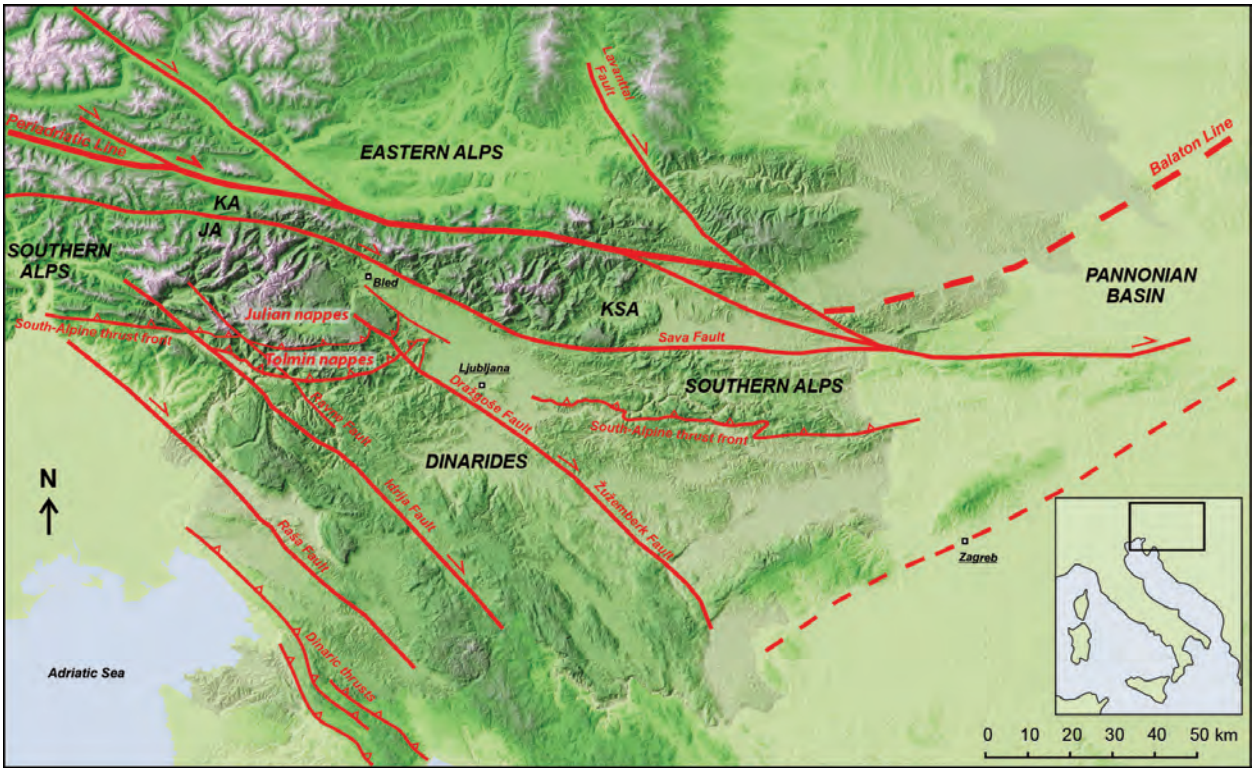

Figure 1: Eastern Southern Alps and adjacent tectonic units with the location of the Julian and Tolmin nappes. Abbreviations: KA Karavanke Mountains, JA Julian Alps, KSA Kamnik–Savinja Alps.

Jurassic – Cretaceous stratigraphy of the highest nappe, the Pokljuka Nappe, will be visited. This stratigraphic succession defines the Bled Basin, which occupied the most internal position in the area and is characterized by Lower Cretaceous ophiolite-bearing flysch-type deposits correlative to the Bosnian Flysch in the central Dinarides.

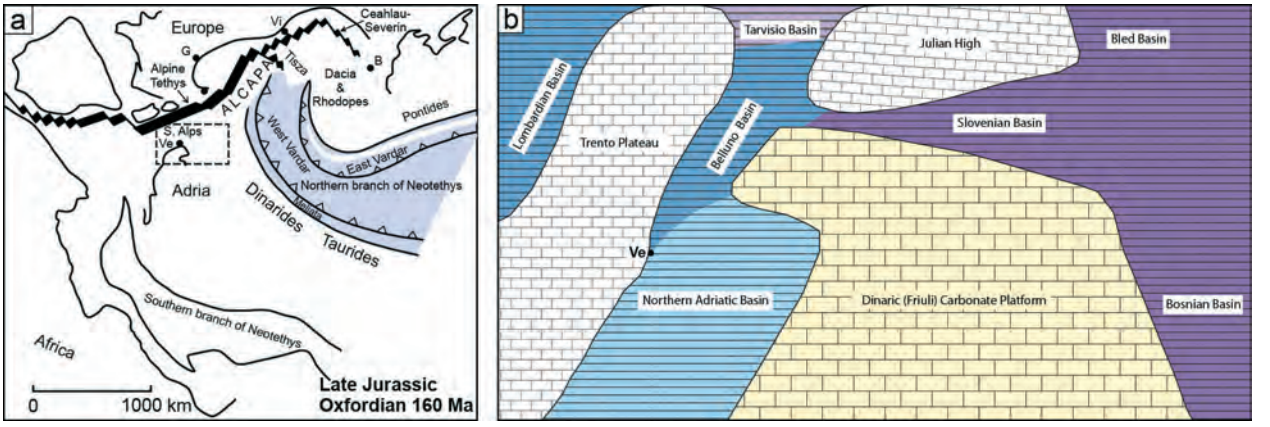

Figure 2a: Paleogeographic map in the Late Jurassic (after Schmid et al. 2020). The dashed rectangle indicates the location of the map on the right (Ve = Venice).
2b: Local configuration of the Adriatic continental margin (Belluno Basin and Northern Adriatic Basin simplified according to Masetti et al. 2012). The colors in 2b correspond to the time of basin formation. The Bled, Slovenian and Bosnian basins formed in the Middle Triassic and the Tarvisio Basin in the Late Triassic. The Belluno Basin subsided in the Hettangian and the Northern Adriatic Basin around the Sinemurian–Pliensbachian boundary (Masetti et al. 2012).

REGIONAL GEOLOGICAL SETTING

The Southern Alps are bounded to the north by the Periadriatic Fault and extend southwards to the South-Alpine front, where they are in direct thrust contact with the External Dinarides (Figure 1). The Sava Fault, a branch of the Periadriatic fault system, internally separates the Julian Alps from the South Karavanke Mountains and the Kamnik-Savinja Alps.

The Julian Alps are traditionally subdivided into the Tolmin Nappe and the overlying Julian Nappe (Placer 1999; Figure 1). Since both consist of several nappe units, it is preferable to use the names Tolmin nappes and Julian nappes as collective plural terms.

The Tolmin nappes are composed of several superposed E-W trending south-vergent second-order nappes (Cousin 1981; Buser 1986, 1987). The stratigraphic successions of these nappes are ascribed to the Tolmin Basin (Cousin 1981), which represents the western part of the Slovenian Basin (in the sense of Buser 1989). The sediments are typically deeper marine (shale, chert, pelagic limestone, carbonate turbidites) from a Middle Triassic volcano-sedimentary succession up to Campanian-Maastrichtian flysch. The Mesozoic successions of the Tolmin nappes exhibit a considerable thermal overprint (Rainer et al., 2002, 2016).

The Julian nappes are stratigraphically more complex and structurally less well known. The area is now dominated by Triassic platform carbonates but deep-water Jurassic–Cretaceous and also Upper Triassic sediments also exist. Significant lateral variations in thickness and facies types indicate that the Julian nappes originated from several paleotopographic units. The Julian Carbonate Platform that in the Jurassic evolved to submerged submarine high, the Julian High (Buser 1996), and remnants of the surrounding basins are preserved.

The overall shape of the Julian nappes is an approximately E-W oriented dish-like synform (Placer 2009). The Zlatna Klippe (Zlatnaplatte of Kossmat 1913) in the central, highest part of the Julian Alps around Mt. Triglav (Figure 3) is well differentiated and the sub-horizontal contact with the underlying nappe is preserved. In remaining portions of the Julian Alps, the nappe structure is strongly obliterated by younger deformation. The area is dissected by a set of NE-SW striking faults (Jurkovšek 1986; Buser 2009; Goričan et al.

Figure 3: Aerial view of the central Julian Alps towards south. The Zlatna Klippe is outlined in red.

2018). Some of these faults have a prominent reverse-slip component. Well-exposed normal faults with the same orientation have also been observed.

The NE-SW striking faults are cross-cut by sub-vertical NW-SE oriented faults; some are evidently still active as dextral strike-slip faults (Kastelic et al. 2008; Atanackov et al. 2021). The most prominent of these is the Sava Fault whose right lateral displacement is estimated at 30–60 km (Vrabec & Fodor 2006) or even 70 km (Placer 1996). These young faults are well-marked on satellite and digital relief images and are directly linked to the system of NW-SE dextral faults in the External Dinarides (the Raša, Idrija, Ravne and Dražgoše–Žužemberk faults in Figure 1).

MESOZOIC STRATIGRAPHY OF THE JULIAN ALPS

An overview of the stratigraphic successions characteristic of different paleogeographic units in the area is presented graphically (Figure 4). Only the most distinctive formations are highlighted in the text but sufficient references are cited to provide the relevant source of more detailed information.

Since the study area was part of a continental margin between the Alpine Tethys and the Neotethys (Figure 2a), the correlative stratigraphic units exist in the Southern Alps in Italy, in the Northern Calcareous Alps in Austria, in the Transdanubian Range in Hungary and in the Dinarides. For a Triassic to end Cretaceous correlation of the Julian Alps with the neighboring units in the Southern Alps (Trento Plateau and Belluno Basin in Figure 2b) the reader is referred to Goričan et al. (2012a) and references therein. More recent studies (Goričan et al. 2018) focused on correlation with the other three mountain chains that preserve stratigraphic successions of Neotethyan affinity.

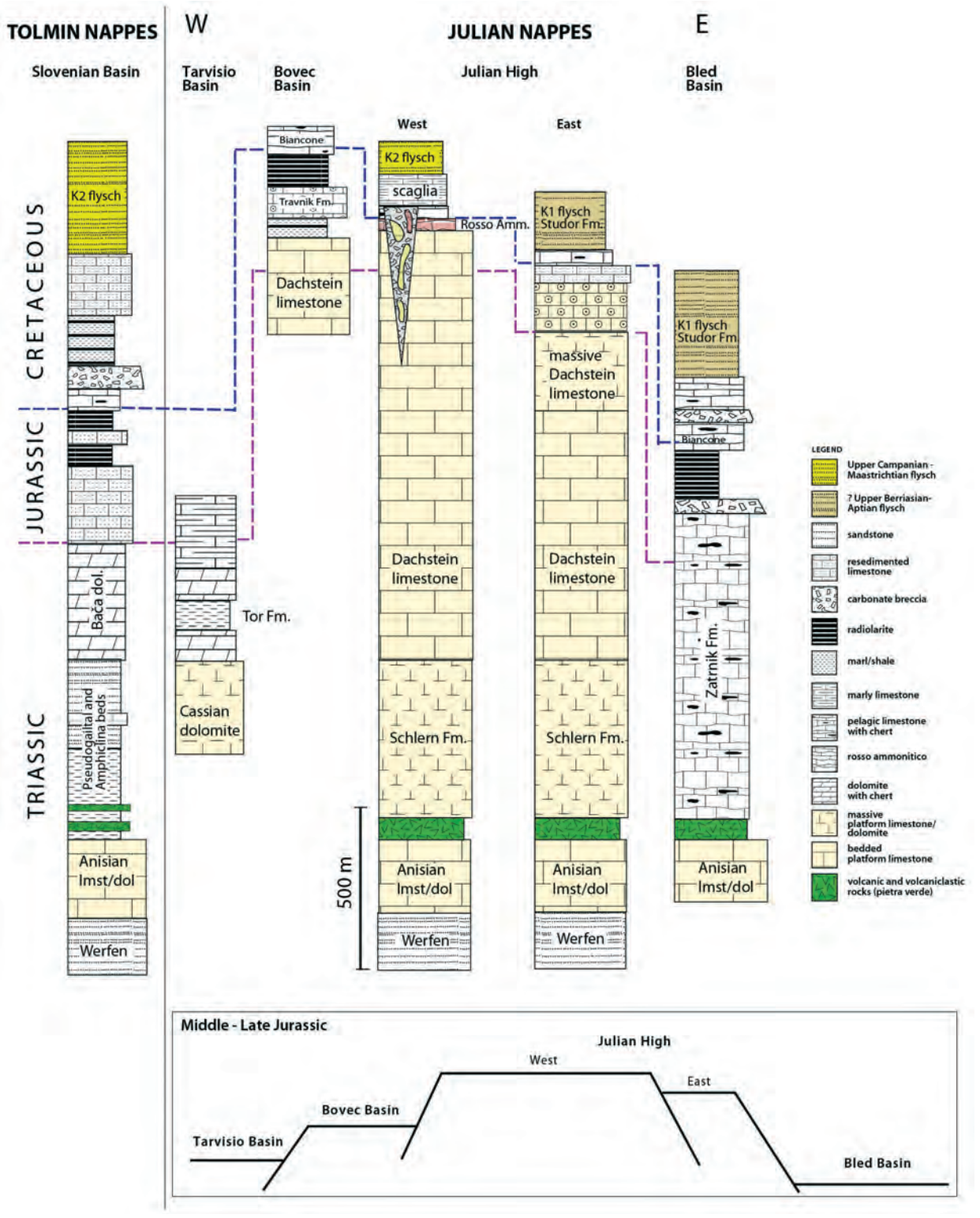

Figure 4: Stratigraphic overview of different tectonic/paleogeographic units in the Julian Alps. The Tolmin nappes are represented by a single synthetic log because the successions of different thrust sheets are basically identical; only the thickness of individual formations varies in relation to proximity of adjacent carbonate platforms. The Julian nappes, on the other hand, show great variations in the stratigraphic record suggesting a complex topography of a submarine high surrounded by deeper basins (a simple 2D sketch is presented below the stratigraphic logs). References to stratigraphy are given in the text.

Three main paleotopographic units with their distinct stratigraphic record have been differentiated in the Julian nappes (Figures 2b, 4) – the Tarvisio Basin, the Julian High and the Bled Basin.

The sediments of the Tarvisio Basin are now exposed in the Carnic Alps (NE Italy), in the NW Julian Alps, and in the Southern Karavanke Mountains. The most distinctive units of this stratigraphic succession are the uppermost Julian–lower Tuvalian carbonate-siliciclastic Tor Formation (formerly known as the Raibl beds) and the upper Tuvalian to Rhaetian carbonates rich in organic matter and chert nodules (Gale et al. 2015). Lower Jurassic rocks of this basin consist of a thick pile of thin-bedded lime mudstone and are exposed only in the Karavanke Mountains (Krystyn et al. 1994). The Tarvisio Basin formed in the Carnian apparently as a west-east oriented intra-platform basin (Gale et al. 2015). In the Jurassic it may have been connected to the Belluno Basin, which subsided in the Hettangian (Masetti et al. 2012).

The sediments of the Julian High rest upon a thick pile of Upper Triassic to Lower Pliensbachian platform limestones that constitute the core of the Julian nappes. The post-Pliensbachian sections are all composed of deeper-water facies but differ in thickness and the degree of condensation.

Three characteristic successions are distinguished. The most continuous succession, best exposed in the Travnik structural unit at Mt. Mangart saddle, pertained to the deeply subsided block of the former carbonate platform; the term Bovec Basin designates this paleogeographic unit (Cousin 1981). The succession shows first a gradual transition from shallow to deeper-marine facies through the Pliensbachian and Lower Toarcian that ends with a discontinuity surface. Black shales with interbedded radiolarian-rich siliceous limestone characterize the Lower Toarcian (Goričan et al. 2003; Šmuc & Goričan 2005; Sabatino et al. 2009). This lower part is overlain by typical basinal deposits ranging in age from the Bajocian to the Early Hauterivian (Šmuc 2005; Šmuc & Goričan 2005). The most distinguishing Jurassic facies are oolitic megabeds (Member 2 of the Travnik Formation) evoking the Vajont Limestone of the Belluno Basin in northern Italy (e.g. Bosellini et al. 1981).

The strongly condensed Middle to Upper Jurassic sections consist of Rosso Ammonitico type limestone (the Prehodavci Formation) that does not exceed 20 m in thickness; ferromanganese mineralisations are common and mark distinctive discontinuity sufaces at certain stratigraphic levels (Šmuc 2005; Šmuc & Rožič 2010). The overlying Biancone limestone also is a thin (only a few meters thick) pelagic sequence. The condensed Rosso Ammonitico type limestone was widely deposited but is now poorly preserved with laterally continuous exposures occurring only in the Triglav Lakes Valley just below the thrust-fault contact with the Zlatna Klippe.

The condensed Jurassic sections are in places associated with up to several hundred meters deep neptunian dykes filled with chaotic blocky breccias. Such breccias are well known on Mt. Mangart (Šmuc 2005; Črne et al. 2007) and at Lužnica Lake (Babić 1981; Cousin 1981) but have been also mapped in other localities west of the Zlatna Klippe (Jurkovšek 1986; Jurkovšek et al. 1990). The Scaglia variegata of Albian age directly overlies the breccias in places (Cousin 1981; Goričan & Šmuc 2004) and provides good age control on the formation of these deep neptunian dykes. The Scaglia variegata is followed by Turonian to Senonian red pelagic limestone (Scaglia rossa) and by upper Campanian – Maastrichtian flysch (Cousin 1981; Jurkovšek 1986; Buser 1987; Kocjančič et al. 2022).

The stratigraphy of the Julian High at its eastern border is fundamentally different. The post-Pliensbachian succession is extremely thin, reduced to a few meters of the Biancone limestone (Rožič et al. 2014) and is overlain by Lower Cretaceous mixed carbonate-siliciclastic flysch-type deposits of the Studor Formation (Goričan et al. 2018). This stratigraphically incomplete succession and the age of flysch indicate the transition to the Bled Basin.

The Bled Basin (Cousin 1981) formed during the Middle Triassic rifting event. The entire upper Anisian to Lower Cretaceous succession consists of deep-water sediments. The more than 600 m thick Zatrnik Limestone spans the long stratigraphic interval from the Ladinian to the Lower Jurassic and consists mostly of bedded micrite with chert nodules (Cousin 1981; Goričan et al. 2018; Gale et al., 2019, 2021). The limestone is generally light gray, rarely reddish in color. This limestone clearly contrasts with the time equivalent formations of the Tarvisio Basin that are darker (bituminous) and usually dolomitized. The Zatrnik Limestone is overlain by Pliensbachian carbonate breccia, Upper Bajocian to Lower Tithonian bedded radiolarian cherts and shales, Upper Tithonian–Berriasian Biancone limestone ending with carbonate breccia and calcarenite (the Bohinj Formation), marly limestone with scarce siliciclastic admixture, and finally Berriasian?–Hauterivian mixed carbonate-siliciclastic turbidites with ophiolite debris (the Studor Formation) (Goričan et al. 2018, with references). It is well established that the Lower Cretaceous flysch of the Julian Alps corresponds to the Bosnian Flysch (Cousin 1981; Kukoč et al. 2012). Moreover, the entire

succession is in good agreement with that of the median Bosnian Zone in the central Dinarides (Goričan et al. 2018).

The Mesozoic stratigraphy of the Tolmin nappes is typical of a deep basin that also formed in the Middle Triassic and persited until the end of the Cretaceous. The Triassic to Cretaceous stratigraphy and sedimentary evolution have been described in great detail in several recently published papers (Rožič 2009; Rožič et al. 2009, 2017, 2018; Gale 2010, Gale et al., 2012; Goričan et al. 2012a, b). Paleogeographically, the area belonged to the Tolmin Basin, which was located between the Julian Carbonate Platform / Julian High and the Dinaric Carbonate Platform. The Tolmin Basin is regarded as the western part of the Slovenian Basin (*sensu* Cousin 1970 and Buser 1989), which is now exposed in a longer facies belt running in W-E direction through all of central Slovenia. In the Tolmin Basin, the onset of flysch-type deposits is, similar to the western Julian High, dated upper Campanian to Maastrichtian (Caron & Cousin 1972; Cousin 1981; Buser 1987). In the underlying succession, we note the upper Aptian to Turonian Lower flyschoid formation, which is composed of basal calcareous breccia, shale, marl, and limestone turbidites but devoid of sand-sized siliciclastic material and cannot be considered flysch in the proper sense (Caron & Cousin 1972).

In summary, we can emphasize that flysch deposits of the Julian Alps are clearly related to two separate orogenic phases. Their distribution allows us to distinguish a relatively internal Dinaric sector with Lower Cretaceous flysch and a more external sector where the oldest flysch is Campanian-Maastrichtian in age (Figure 4). The two orogenic phases have been well documented throughout the Dinarides and Hellenides (Schmid et al. 2020, with references). The first phase started with emplacement of ophiolites on the Adriatic continental margin; deep-sea foreland basins were then created in front of the obducted ophiolite nappes and filled with flysch-type deposits from the Tithonian–Berriasian (Mikes et al. 2008). The second phase was related to the Late Cretaceous – Paleogene continental collision of the African and Eurasian plates. The widespread flysch sedimentation of Campanian age in all the internal Dinarides marks the beginning of this tectonic phase (Nirta et al. 2020; Schmid et al. 2020) with deformation that propagated towards SW and continued to the Eocene.

MAIN STRUCTURAL ELEMENTS

The initial nappe structure related to the Dinaric thrusting phase was strongly controlled by inherited Mesozoic normal faults and facies variations across these faults. Based on the compiled stratigraphic data and available structural evidence we present a generalized tectonic map and a profile perpendicular to the NE-SW trending faults (Figures 5a, b). A tentative reconstruction of the Dinaric-phase nappe emplacement is also presented (Figure 6).

The present-day morphology of the Julian nappes is mainly determined by the deformation along steep reverse and normal faults. Except for the central part of the study area and a few other exceptions (Figure 5a) the initial nappe contacts are located below surface and the boundaries among different nappes in map-view now coincide with the post-nappe faults. The structural elements of the South-Alpine contraction phase are clearly differentiated from the first-phase nappe contacts and are generally easy to recognize in the field, especially when well-bedded lithologies (e.g. the Dachstein limestone) are involved. Some typical examples are illustrated in Figures 7 to 9. A well-defined distinction among different stratigraphic successions as shown in Figure 4 is also of prime importance to map the nappes.

The Pokljuka Nappe is the highest of the Julian nappes but is now preserved only in a relatively subsided block, separated by steep boundary faults from the originally underlying nappe (Goričan et al. 2018). Goričan et al. (2018) suggested that the previously defined Krn Nappe (Buser 1986) could be subdivided into two nappes – the lower (western) Krn Nappe *sensu stricto* and the upper (eastern) Krn Nappe, which directly underlies the Pokljuka Nappe. Here we retain this distinction but, instead of the "eastern Krn Nappe", we use the name Jelovica Nappe, a name that was previously applied to the southeastern part of this structural unit (Grad & Ferjančič 1976; Demšar 2016).

The Zlatna Klippe was possibly connected to the Jelovica Nappe as suggested by its structural position on top of the Krn Nappe (Figure 5a). Stratigraphically it is less distinctive because it is composed almost exclusively of the upper Ladinian–Carnian massive carbonates of the Schlern Formation; only at Begunjski vrh along the northern contact of this klippe, some meters of heavily folded older Ladinian rocks (bedded limestone, sandstone and tuff) occur (Ramovš 1990). Smaller Zlatna-type klippen, composed only of the Schlern Formation are present west of the Zlatna

Klippe (two are rather clear and are indicated in Figure 5a; one is illustrated in Figure 9a). The Viševnik Klippe (Jurkovšek 1987), which now constitutes a footwall syncline below a steep SE vergent reverse fault (Figures 8a, b) can be also related to the Zlatna Klippe. The oldest rocks of this klippe are Lower Triassic brownish-gray fossiliferous marly limestones (Kolar-Jurkovšek et al. 2013), in classical stratigraphy of the Southern Alps known as the Campil beds of the Werfen Formation. The well-exposed contacts of

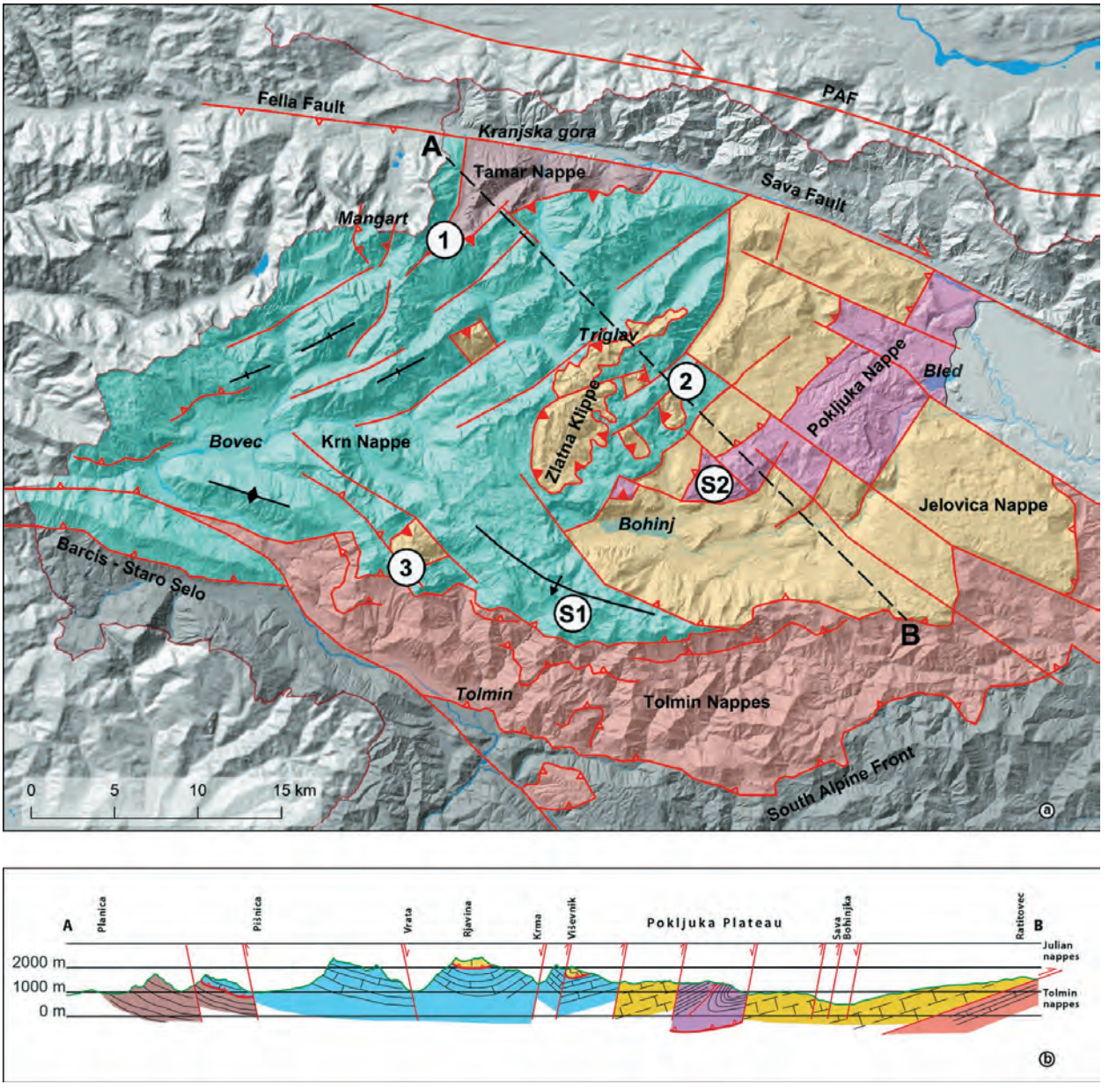

Figure 5a: Generalized tectonic map with emphasis on subdivision into Dinaric-phase nappes (solid triangles – Dinaric-phase nappe contacts; empty triangles – high- and low-angle reverse faults of the South-Alpine phase). The numbers in circles correspond to localities shown in Figures 7 to 9 (1 = Tamar Valley, 2 = Viševnik, 3 = Jezero v Lužnici-Rdeči rob) and to the field-trip stops (S1 and S2).
5b: Profile AB perpendicular to the NE-SW trending post-nappe faults. Note that the reverse faults are doubly-verging: they are directed towards SE to S in the eastern part of the study area and have the opposite direction NW of the Zlatna Klippe.
Based mainly on Geological Map of Slovenia 1:250,000 (Buser 2009). The Pokljuka Nappe in Figure 5a and the south-eastern half of the profile in Figure 5b are from Goričan et al. (2018).

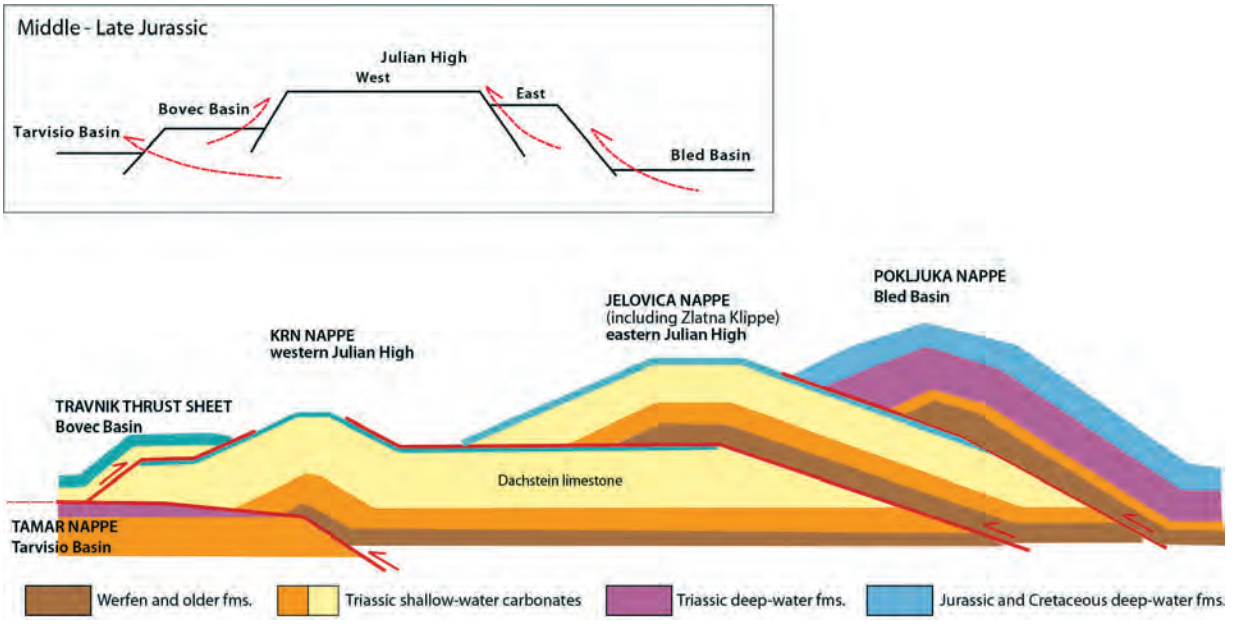

Figure 6: Tentative reconstruction after the Dinaric-phase nappe emplacement and its relation to pre-orogenic topography. The back-thrusting of the Travnik thrust sheet (the type locality of the Bovec Basin stratigraphy) is suggested by its position on top of the condensed succession of the western Julian High as demonstrated on Mt. Mangart (Šmuc 2005; see Figure 5a for the location of Mt. Mangart). The contact between the Krn and Tamar nappes is visible in the entire SE wall of the Tamar Valley (Figure 7a, see also Figure 8 in Celarc et al. 2013); the incompetent terrigenous sediments of the Raibl Group and the Norian-Rhaetian marly carbonates were the main horizon allowing for the displacement along thrust fault that cut through the inherited Mesozoic normal faults.

the Zlatna Klippe and its equivalents thus suggest a hanging-wall ramp position for the central Julian Alps. The ramp cuts through the Lower Triassic to Ladinian – Carnian succession of the upper nappe whereas the underlying Krn Nappe in this central area is quasi complete, preserved to the top of the Dachstein limestone or even to the Jurassic-Cretaceous condensed facies.

The contact of the Krn Nappe with the underlying structural unit is well exposed in the Tamar Valley (Figure 7a) where the upper Tuvalian to Rhaetian deep-water sediments of the Tarvisio Basin are thrust by the Dachstein limestone (Celarc et al. 2013). This north-verging thrust was first interpreted as a possible continuation of the Val Resia–Val Coritenza backthrust (Celarc et al. 2013; Gale et al. 2015), known from the Italian part of the Julian Alps as an E-W striking Alpine-phase backthrust (Venturini & Carulli 2002; Merlini et al. 2002; Ponton 2002). The completely different Upper Triassic facies below and above the thrust plane in the Tamar Valley (basin vs. carbonate platform, Figure 7a) indicate a different paleogeographic location of the two thrust blocks in the Mesozoic and suggest that this thrust belongs to the group of pre-existing Dinaric thrusts. The Dinaric thrust could then have been steepened and probably dextrally rotated during the later Alpine phase.

The stratigraphic succession of the Bovec Basin overlying the Julian Platform (see the 3rd column in Figure 4) is limited to a tectonically complicated area near the Slovenian-Italian border (Figure 5a). On Mt. Mangart, this succession forms a separate Travnik Thrust Sheet on top of the massive Dachstein limestone (Šmuc 2005). The plausible explanation for this tectonic superposition is a Dinaric-phase backthrust along an inverted Mesozoic normal fault that was dipping opposite to the dip of normal faults in the eastern part of the Julian High (Figure 6). This original geometry was cross-cut by steep reverse faults and was heavily folded during the Alpine contraction (for photographs of folds and a detailed map see Šmuc 2005).

The Tolmin nappes (paleogeographically the Slovenian Basin) are a composite south-verging tectonic unit between the External Dinarides below and the Julian nappes above (Figures 1, 5a). Individual nappes within this system are largely discontinuous laterally but allow a general subdivision into three superposed units. From bottom to top these are the Podmelec Nappe, the Rut Nappe and the Kobla Nappe (Buser 1986, 1987). The generally E-W striking thrust faults

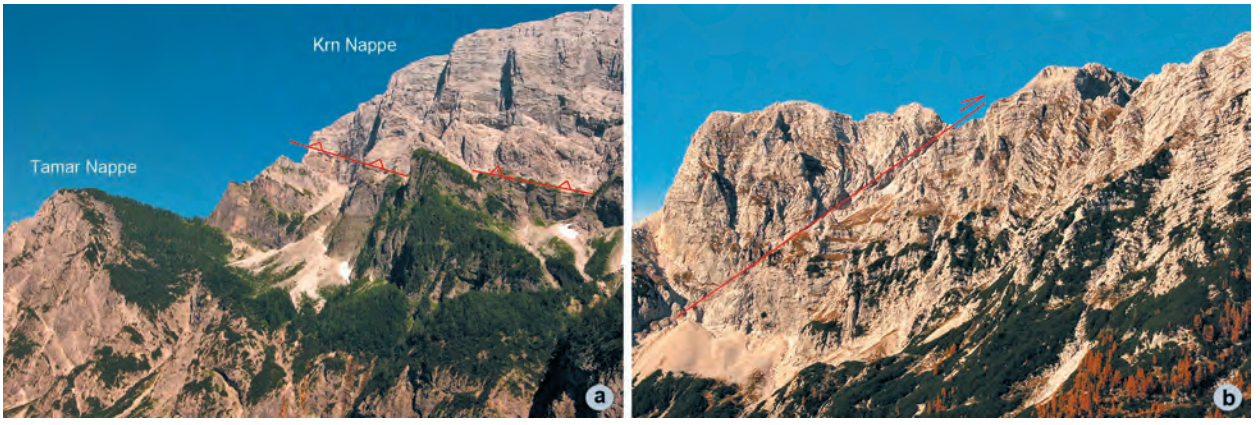

Figure 7: Dinaric and South-Alpine deformation in the Tamar Valley, locality no. 1 in Figure 5a.
7a: Dinaric-phase thrust contact between the deep-water Norian-Rhaetian limestone of the Tamar Nappe and the Dachstein limestone of the Krn Nappe; SE wall of the Tamar Valley. 7b: Post-nappe north vergent reverse fault in the Dachstein limestone of the Krn Nappe; W wall of the Tamar Valley.

Figure 8: Viševnik Klippe, locality no. 2 in Figure 5a.
8a: Panoramic view of the Dinaric thrust plane; the Werfen Formation lies on top of the Dachstein limestone. This thrust plane was bent during the South-Alpine shortening along steep SE directed reverse faults.
8b: The same locality seen from NW to SE. The thrust plane separating the Werfen and the Dachstein formations is easily visible.

(Buser 1986) indicate that the Tolmin nappes mainly resulted from the N–S, i.e. South-Alpine shortening. Further structural analysis could unravel an older deformational phase but has not been carried out yet.

TIMING OF TECTONIC EVENTS

The nappe emplacement can be broadly attributed to the Maastrichtian to Eocene top-to-SW thrusting phases observed throughout the Dinarides (Tari 2002; Ilić & Neubauer 2005; Schmid et al. 2008, 2020; Žibret & Vrabec 2016). Considering the striking similarity in stratigraphy and facies between the Bled Basin and the Bosnian Basin, a pre-Maastrichtian emplacement of the Pokljuka Nappe is unlikely although the Upper Cretaceous deposits are actually missing. The Upper Campanian – Maastrichtian flysch deposits of

Figure 9: Jezero v Lužnici – Rdeči rob, locality no. 3 in Figure 5a.
9a: Panoramic view showing 3 phases of deformation: 1= Dinaric thrust (Schlern Formation on top of the Dachstein limestone); 2 = steep reverse fault of the South-Alpine phase; 3 = younger normal fault.
9b: Enlargement of the fold in the Scaglia rossa; 2nd deformation phase.
9c: C-S structures in the Scaglia rossa indicate top-to-the-south sense of shear that is compatible with the thrusting direction of the Julian nappes over the Tolmin nappes (see Figure 5a).

the Julian High and the Slovenian Basin (Figure 4) were not necessarily shed coevally with the emplacement of the Pokljuka Nappe but may have originated from a more internal part of the Dinarides. The upper age limit for the emplacement of the Julian nappes is provided in the Southern Karavanke Mountains by middle Eocene molasse-type deposits with abundant mollusks (Mikuž 1979).

The first post-nappe contraction, reflected in NE-SW striking reverse faults can be attributed to the late Oligocene–early Miocene southward to SE-ward South-Alpine thrusting (Doglioni 1987; Doglioni & Siorpaes 1990; Fodor et al. 1998; Castellarin & Cantelli 2000; Bartel et al. 2014; van Gelder et al. 2015). South and east of the Zlatna Klippe the faults of this group are associated with S to SE vergent folds, whereas the folds and the steepened beds west and north of the Zlatna Klippe have the opposite vergence (Figures 5a, b; 7b). South of Bohinj, closer to the Tolmin nappes, the faults are NW-SE trending and the associated folds are S to SSW vergent. This pattern suggests an overall pop-up structure and probably CW rotation of internal smaller-scale fault blocks. The style of deformation within the Julian nappes is predominantly brittle, determined by the thick pile of platform carbonates. Larger-scale, low-angle thrusts were created in the Tolmin nappes where the Mesozoic sediments of the Slovenian Basin were overridden by the entire Julian nappe-stack and internally dissected into several approximately E–W oriented thrust sheets.

The South-Alpine thrusting is generally thought to have been associated with dextral transpression concentrated on the Periadriatic (Insubric) Lineament (Doglioni 1987; Fodor et al. 1998; Bartel et al. 2014). The shear zone in the study area encompasses the Julian nappes but most probably also includes the Tolmin nappes. This zone between the Sava Fault and the South-Alpine Front has a lenticular outline (Figure 5a) and is comparable to the adjacent Sava-PAF "shear lens" (Vrabec & Fodor 2006), which is composed of the Southern Karavanke Mountains and the Kamnik-Savinja Alps (Figure 1).

The subsequent short-lasting extension is evidenced by normal faults, which were documented at several locations (e.g., Celarc & Herlec 2007; Goričan et al. 2018) but the overall pattern of the extensional structures throughout the Julian Alps has not been determined. It is thus not yet clear to what extent the normal faults were determined by the structures inherited from the preceding contraction stage. The event is ascribed to the Early-Middle Miocene extension widely documented in the Dinarides and classically interpreted in relation to the formation of the Pannonian Basin (Ilić & Neubauer 2005; van Gelder et al. 2015; Žibret & Vrabec 2016). The extension was followed by a renewed shortening, which started in the latest Miocene and is still active. The last stage of deformation in the Julian Alps is the strike-slip reactivation of both sets of pre-existing faults (Goričan et al. 2018). This deformation fits well into the recent inversive/transpressive tectonic phase, documented in a wider South-Alpine – NW Dinarides territory (Tomljenović & Csontos 2001; Bartel et al. 2014; Žibret & Vrabec 2016).

DESCRIPTION OF STOPS

Stop 1. General view on the Julian Alps from Mt. Šija

(Location: N 46°14'19.23", E 13°50'2.45, altitude 1880 m, Figure 10)

Mt. Šija is part of the Lower Bohinj Ridge, a high mountain ridge south of Lake Bohinj. Its western part belongs to the Krn Nappe (Figure 5a). The overall structure of this ridge is a south-verging monocline, which formed as a fault-propagation fold above the thrust over the Tolmin nappes.

The upper Vogel cable car station offers a magnificent view to the north to the Bohinj area and to the central Julian Alps with Triglav and other mountains of the Zlatna Klippe (Figure 11). On a walk towards the top of the ridge we will cross first the gently north dipping beds of the Dachstein limestone and then the steeply south dipping beds of the southern limb of the anticline. From the top of Mt. Šija almost the entire ridge is visible (Figures 12, 13, 14). The morphological contrast with vegetated low hills of the Tolmin nappes is also apparent (Figure 13).

Stop 2. Jurassic and Cretaceous of the Bled Basin

The stratigraphy of the Bled Basin will be visited at three nearby outcrops located north of Srednja Vas and Studor, between the Ribnica Valley and the road to Uskovnica (Figures 10, 15a, b).

Stop 2.1 – The Ribnica Valley (Pliensbachian to Tithonian) (Location: N 46° 18.190', E 13° 54.821')

General description: The Lower Jurassic Ribnica Breccia and the overlying Middle to Upper Jurassic radiolarian cherts (Figure 15a) are best exposed at the first waterfall in the Ribnica Valley. The lowermost part of the section is composed of calcarenite with more than 50% echinoderms and rare foraminifers. The calcarenite is followed by a 0.5 m thick layer of greenish marly limestone and a 20 cm thick layer of reddish filament-bearing limestone, which also contains echinoderms and foraminifers.

The Ribnica Breccia (Cousin 1981; Kukoč 2014) consists of several beds. The first is 1 m thick and con-

Figure 10: Topographic map 1:50,000 of the Julian Alps around Lake Bohinj with location of field-trip stops S1 and S2.

Figure 11: Panoramic view from the upper Vogel cable car station to Lake Bohinj and the central part of the Julian Alps. The red line indicates the contact between the Krn Nappe and the Zlatna Klippe. Dashed line means that the contact runs behind the hills in foreground.

Figure 12: View from Mt. Šija towards west. The mountains in the foreground belong to the western part of the Bohinj Ridge (see Figures 5a and 10 for location). The Dachstein limestone beds along the ridge are dipping steeply towards south to south-west and constitute the forelimb of a larger fault-propagation fold, which was formed during the South-Alpine thrusting phase.

Figure 13: View from Mt. Šija towards southwest (left of Figure 12). The difference between the Krn Nappe and the underlying Tolmin nappes is well expressed in the landscape. Note the change in dip of the Dachstein limestone across the steep fault. The beds are dipping towards south on Mt. Vogel and towards NW on Mt. Žabiški Kuk. This deviation can be ascribed to the transpressive dextral shear that accompanied the general N–S directed shortening during the South-Alpine phase.

Figure 14: Oblique view from SE to the fault-propagation fold in the Dachstein limestone at the southern edge of the Krn Nappe. The thrust contact with the Tolmin nappes below is indicated but is actually located just below the view of the photograph. The change from SSW dipping beds on Mt. Vrh nad Škrbino to almost horizontal bedding is marked by a shelf (the hinge of the syncline is indicated with a dashed red line). The opposite side of Vrh nad Škrbino is illustrated in Figure 12.

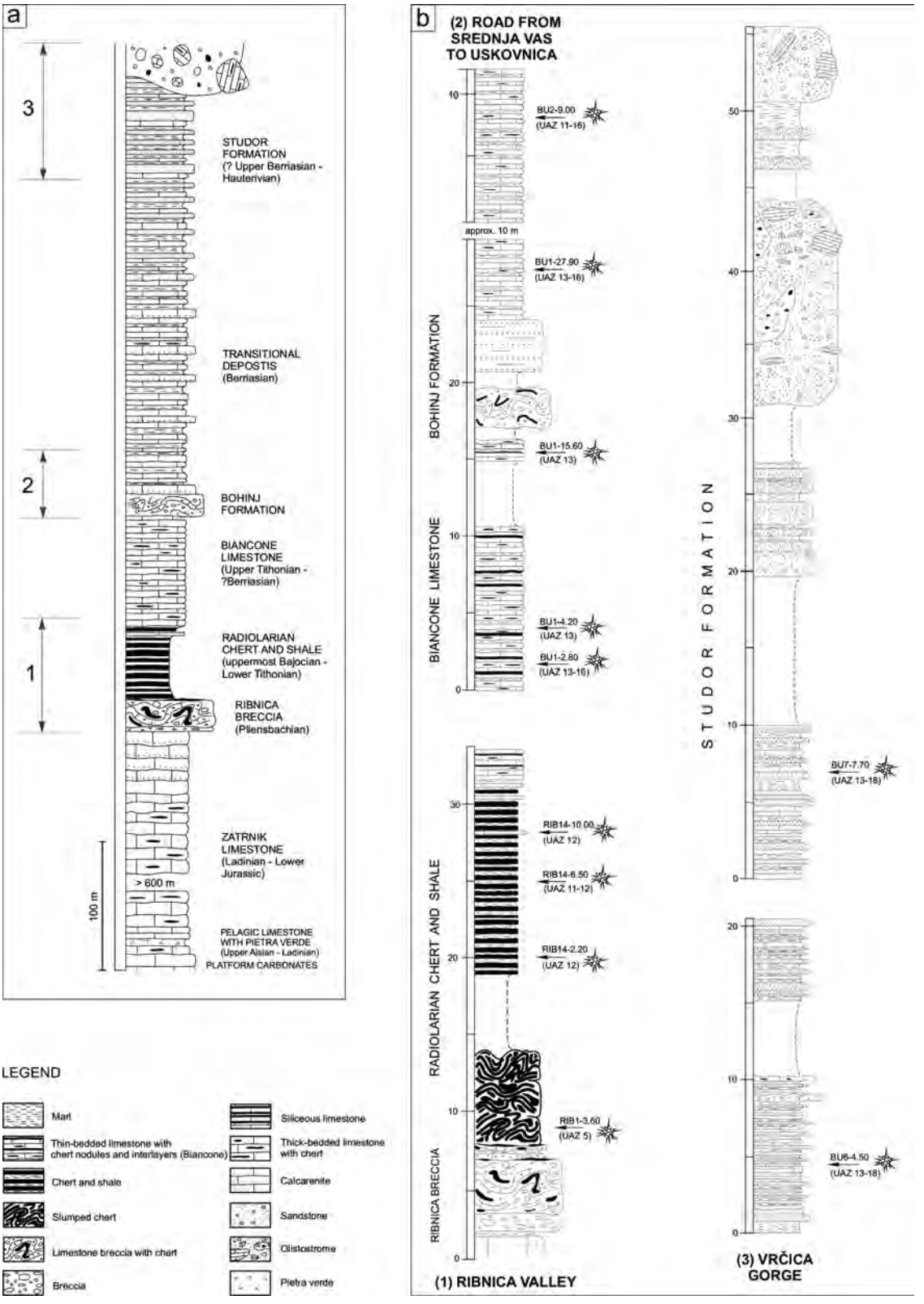

Figure 15a: General stratigraphy of the Bled Basin. The stratigraphic position of stops 2.1, 2.2 and 2.3 is indicated. 15b: Detailed stratigraphy of the three stops with position of radiolarian samples and their assignment to UA Zones of Baumgartner *et al. (1995).*

tains limestone clasts up to 40 cm in size, but no chert. The overlying bed is thinner (0.5 m) with smaller limestone clasts. The upper part of the Ribnica Breccia is an approximately 5 m thick chaotic bed containing large limestone and chert clasts, and also irregularly shaped folded layers of chert up to 1 m in size. The upper bedding plane is in places silicified and covered by a 10 cm thick horizon of gray marl. The topmost breccia bed is 0.5 m thick and contains a high amount of chert (app. 50%) in the form of folded nodules and layers.

The most common microfacies of the breccia clasts is bioclastic wackestone-packstone with abundant echinoderms and foraminifers (e.g., *Involutina liassica* (Jones)). Ammonite and gastropod shells also occur. Some clasts are wackestones with radiolarians and sponge spicules. Glauconite grains are rare but present throughout the Ribnica Breccia.

The overlying succession is dominated by radiolarian chert (Figure 15b). It starts with a 6 m thick slumped interval of dark-green bedded chert. The shale interlayers constitute less than 10% of the sequence. The transition to the overlying bedded chert is not exposed; presumably mostly shales occur in this covered interval. The upper part of the succession consists of dark-brownish-red bedded chert and shale. The content of shale in this part of the succession is high and reaches up to 60%. Individual chert beds are 3 to 5 cm thick and generally laminated. In places, normal grading and channel structures clearly indicate that the chert beds were deposited as low-density turbidites. In the upper part of the section carbonate content increases again. Gray laminated siliceous-limestone beds, up to 10 cm thick, are intercalated in the dark-gray shale. Limestone microfacies is wackestone-packstone with radiolarians and sponge spicules. Parallel lamination and normal grading again indicate deposition as low-density turbidites. The content of shale decreases upsection and the succession ends with thin-bedded laminated siliceous radiolarian-bearing limestones. The entire thickness of the laminated limestones is estimated to 50 m but is not visible at this outcrop.

Age: The diagnostic foraminifer *Involutina liassica* (Jones) in the breccia clasts indicates an Early Jurassic age. The maximum range of this species is from the Upper Norian to the lowermost Toarcian (Bassoullet 1997). Based on regional stratigraphic correlations, the Pliensbachian is the most probable age of the Ribnica breccia. The slumped cherts above the breccias yielded a latest Bajocian to early Bathonian radiolarian assemblage (UA Zone 5 of Baumgartner et al. 1995) based on the occurrence of *Hemicryptocapsa tetragona* (Matsuoka). These two age constraints suggest that a significant stratigraphic gap occurs between the Ribnica Breccia and the overlying radiolarian cherts. The upper part of the chert/shale succession in the Ribnica Valley is dated as early to early late Tithonian (UA Zone 12) based on co-occurrence of *Protunuma japonicus* Matsuoka & Yao and *Eucyrtidiellum pyramis* (Aita).

Stop 2.2 – Along the road from Srednja vas to Uskovnica (Tithonian and Lower Cretaceous)
(Location N 46° 17.992‘, E 13° 55.069‘)

General description: An approximately 40 m thick section of pelagic limestones, including carbonate gravity-flow deposits (Figure 15b), is exposed along the road from Srednja Vas to Uskovnica. This section is subdivided into three lithostratigraphic units: 1) the Biancone limestone; 2) carbonate gravity-flow deposits (the Bohinj Formation); and 3) siliceous limestone with marl.

The Biancone limestone is characterized by thin- to medium-bedded light gray to white limestone with individual beds up to 20 cm thick; up to 5 cm thick discontinuous beds of dark-gray chert and irregularly shaped chert nodules are common. Intercalations of marl are also present. The predominant microfacies are radiolarian-rich wackestone and packstone with parallel lamination in some layers. In some places, normally graded calcarenites occur as several centimeters thick intercalations in micrite beds and contain up to 5 mm large intraclasts of wackestone with radiolarians and chert clasts in the basal part.

The second lithostratigraphic unit is the Bohinj Formation (Kukoč et al. 2012). At the type locality, the Bohinj Formation consists of 3 m of carbonate breccia and 4 m of calcarenite. Slump folds are present in the breccia. The calcarenite is massive and shows no internal folding or bedding.

The third lithostratigraphic unit is reddish siliceous limestone similar to the Biancone limestone, but with a higher proportion of marl and red color. At this section the transition into overlying deposits is covered.

Composition of the breccia and calcarenite: The breccia consists primarily of matrix-supported angular to subangular shallow-water carbonate clasts up to 2 cm in diameter. The matrix is radiolarian-rich lime mudstone with sponge spicules and scarce calpionellids. Most limestone clasts are bioclastic grainstones and bioclastic-peloidal packstones. The skeletal grains in these clasts are miliolid and textulariid foraminifers, echinoderm fragments and algal fragments. Clasts of algal wackestone and oncoid packstone are also

present but rare. The dasyclad algae *Clypeina jurassica* Favre, characteristic of the upper Kimmeridgian to lowest Berriasian, is found both in the clasts of algal wackestone and in the form of isolated fragments. Intraclasts of pelagic calpionellid wackestone with sponge spicules and rare planktonic foraminifers are also present. Callpionellid species *Calpionella alpina* Lorenz, ranging from the late Tithonian to earliest Valanginian has been recognized. Single bioclasts are common and include fragments of *Clypeina jurassica* Favre, the green algae *Cayeuxia*, and fragments of sponges, bryozoans, echinoderms and thick-shelled bivalves. Well-developed concentric and radial ooids and oncoids are present as isolated grains. Rare chert grains and lithic grains of igneous origin, including basalt, also occur in the breccia.

Calcarenite is predominantly composed of shallow-water skeletal fragments and lithoclasts similar to those found in the breccia. Lithic grains of igneous origin, grains of chert and opaque grains are present but are less abundant than carbonate components.

The microfacies analysis reveals that the main source area of the resedimented limestone was a penecontemporaneous carbonate platform. Limestone clasts and isolated grains from the outer platform prevail, but lagoonal facies (algal wackestone) is also present. Grains of basalt indicate ophiolitic origin.

Age: Radiolarians from the Biancone limestone below the Bohinj Formation indicate a latest Tithonian to earliest Berriasian age (UA Zone 13) based on co-occurrence of *Eucyrtidiellum pyramis* (Aita) with *Hiscocapsa kaminogoensis* (Aita), *Parapodocapsa furcata* Steiger and *Praeparvicingula columna* (Rüst). Radiolarians in samples above the Bohinj Formation may range into the early Valanginian, with *Fultacapsa tricornis* (Jud) having the shortest range (UA Zones 13-16). Typical genera first appearing in the late Valanginian (e.g. *Cana*, *Crolanium* and *Pseudocrolanium*) have not been found.

Significance for local paleogeography: The Bohinj Formation provides evidence of a carbonate platform that must have been located more internally but is now not preserved. This inferred platform (named the Bohinj Carbonate Platform by Kukoč et al. 2012) may have developed on top of a nappe stack that formed during the early emplacement of the internal Dinaric units onto the continental margin. The platform correlates regionally with genetically similar isolated carbonate platforms of the Alpine – Dinaride – Carpathian orogenic system, e.g., with the Plassen Carbonate Platform in the Northern Calcareous Alps (Gawlick & Schlagintweit 2006) and the Kurbnesh Carbonate Platform in Albania (Schlagintweit et al. 2008).

Stop 2.3 – Along the road from Srednja vas to Uskovnica – Vrčica Gorge (Lower Cretaceous)
(location N 46° 17‘50.51“, E 13° 54‘49.48“)

General description: Mixed carbonate-siliciclastic deposits of the Studor Formation (Kukoč 2014, Goričan et al. 2018; Figure 15b) are exposed in the Vrčica Gorge. By its lithological characteristics the Studor Formation represents a unique and easily distinguishable lithostratigraphic unit in the wider area. The formation starts with 5–10 cm thick beds of light gray radiolarian wackestone/packstone intercalated with thin-bedded sandstone, which is less frequent in the lower part of the formation. Calcarenite beds are rare. Micrite beds in places contain chert. In the upper part of the formation the proportion of marl is higher and micrite and calcarenite beds are subordinate to sandstone. Thickness of sandstone beds in this part reaches up to 1 m. Horizontal and cross lamination is observed. The uppermost part of the formation is composed of two olistostrome layers composed of centimeter- to meter-sized blocks of different litologies in a dark gray sandy matrix. Laminated micritic limestone with radiolarians (Biancone facies) prevails among these olistolithes. Carbonate breccia with limestone and chert clasts is also present as well as smaller, decimeter-sized clasts of dark green and red chert.

Composition of sandstone: Carbonate lithic grains prevail in sandstone (approximately 40% of all lithic grains). Most are small micrite grains, however larger grains of peloidal and bioclastic grainstone and packstone also occur. Isolated bioclasts and echinoderm fragments are rare. Non-carbonate components include predominantly fragments of mafic rocks. Grains of basalts with intersertal and spherulitic texture predominate. Grains of serpentinite, chert, amphibolite, phyllites, quartzite, granitoid rocks and grains of quartz sandstone are also present. Quartz grains represent approximately 10–20% of grains and are mostly monocrystalline, however polycrystalline quartz of metamorphic origin also occurs. Heavy minerals make up less than 10% of all grains. The sandstone matrix is micritic with admixture of clay component.

Sandstones of the Studor Formation were deposited by turbidity currents. Composition of sandstone indicates a composite source of material. Shallow-water carbonate clasts, specially isolated bioclasts indicate proximity of an active carbonate platform while siliciclastic admixtures indicate erosion of ophiolites and underlying metamorphic soles. Olistostromes were deposited as a debris-flow.

Age: Radiolarian samples from the lower part of the Studor Formation yielded poorly preserved radio-

larian faunas assigned to a relatively broad range from the latest Tithonian–earliest Berriasian (UAZ13) to the latest Valanginian–earliest Hauterivian (UAZ18) based on the occurrence of *Svinitzium depressum* (Baumgartner). Similar as below, typical genera first appearing in the late Valanginian have not been found. This may indicate that the lower part of the Studor Formation is of late Berriasian to early Valanginian age. Valanginian-Hauterivian age of the Studor Formation was previously obtained with nannoplankton (Buser et al. 1979).

ACKNOWLEDGEMENTS

This paper is dedicated to the memory of our friend Bogomir Celarc who passed away on October, 30th 2021. Bogomir Celarc was an outstanding geologist with a special passion for stratigraphy and structure of Slovenian mountains. He was a highly valued colleague to whom we owe a great deal of knowledge on the Julian Alps.

This study was financed by the Slovenian Research Agency, through the program P1-0008 Paleontology and Sedimentary Geology and the project J1-1714 Mesozoic stratigraphy and tectonic evolution of the Southern Alps in Slovenia. We thank Vida Bitenc (GeoPodobe s.p.) for visualization of the relief maps. Reviewers Jan Pleuger and Elizabeth S. Carter are acknowledged for their constructive comments and corrections.

REFERENCES

Atanackov, J., Jamšek Rupnik, P., Jež, J., Celarc, B., Novak, M., Milanič, B., Markelj, A., Bavec, M. & Kastelic, V., 2021: *Database of Active Faults in Slovenia: Compiling a New Active Fault Database at the Junction Between the Alps, the Dinarides and the Pannonian Basin Tectonic Domains*. Frontiers in Earth Science 9: 604388. doi: 10.3389/feart.2021.604388

Babić, L., 1981: *The origin of "Krn Breccia" and the role of the Krn area in the Upper Triassic and Jurassic history of the Julian Alps*. Vjestnik Zavoda za geološka i geofizička istraživanja, ser. A Geologija 38/39: 59–87.

Bartel, E.M., Neubauer, F., Genser, J. & Heberer, B., 2014: *States of paleostress north and south of the Periadriatic fault: comparison of the Drau Range and the Friuli Southalpine wedge.* Tectonophysics 637: 305–327.

Bassoullet, J.P., 1997: *Les grands foraminifères.* In: Cariou, E. & Hantzpergue, P. (coord.), *Biostratigraphie du Jurassique ouest-européen et méditerranéen, Zonation parallèles et distribution des invertébrés et microfossiles*. Bull. Centres Rech. Explor.- Prod., Mém. 17: 293–304.

Baumgartner, P.O., Bartolini, A., Carter, E.S., Conti, M., Cortese, G., Danelian, T., De Wever, P., Dumitrica, P., Dumitrica-Jud, R., Goričan, Š., Guex, J., Hull, D.M., Kito, N., Marcucci, M., Matsuoka, A., Murchey, B., O'Dogherty, L., Savary, J., Vishnevskaya, V., Widz, D. & Yao, A., 1995: *Middle Jurassic to Early Cretaceous radiolarian biochronology of Tethys based on Unitary Associations*. In: Baumgartner, P.O., O'Dogherty, L., Goričan, Š., Urquhart, E., Pillevuit, A. & De Wever, P. (Eds.). *Middle Jurassic to Lower Cretaceous Radiolaria of Tethys: Occurrences, Systematics, Biochronology.* Mémoires de Géologie (Lausanne) 23: 1013–1048.

Bosellini, A., Masetti, D. & Sarti, M., 1981: *A Jurassic "Tongue of the ocean" infilled with oolitic sands: the Belluno Trough, Venetian Alps, Italy.* Marine Geology 44: 59–95.

Buser, S., 1986: *Osnovna geološka karta SFRJ 1: 100 000. Tolmač listov Tolmin in Videm (Udine)*. Zvezi geološki zavod, Beograd, pp 1–103.

Buser, S., 1987: *Osnovna geološka karta SFRJ 1: 100 000, list Tolmin in Videm*. Zvezni geološki zavod, Beograd.

Buser, S., 1989: *Development of the Dinaric and the Julian carbonate platforms and of the intermediate Slovenian Basin (NW Yugoslavia)*. Memorie della Società Geologica Italiana 40 (1987): 313–320.

Buser, S., 1996: *Geology of western Slovenia and its paleogeographic evolution*. In: Drobne, K., Goričan, Š. & Kotnik, B. (Eds.): *The Role of Impact Processes in the Geological and Biological Evolution of Planet Earth)*, 111–123, International workshop, ZRC SAZU, Ljubljana.

Buser, S., 2009: *Geological map of Slovenia 1: 250,000*. Geološki zavod Slovenije, Ljubljana.

Buser, S., Pavšič, J. & Radoičić, R., 1979: *Spodnjekredne plasti v Bohinju*. Rudarsko-metalurški zbornik 26 (4): 385–393.

Caron, M. & Cousin, M., 1972: *Le sillon slovène: les formations terrigènes crétacées des unités externes au Nord-Est de Tolmin (Slovénie occidentale)*. Bulletin de la Société Géologique de France 14: 34–45.

Castellarin, A. & Cantelli, L., 2000. *Neo-Alpine evolution of the Southern Eastern Alps*. Journal of Geodynamics 30: 251–274.

Celarc, B. & Herlec, U., 2007. *Nariv Slatenske plošče na jurske apnence v Kanjavcu*. 18. posvetovanje slovenskih geologov, Geološki zbornik 19, 9–11.

Celarc, B., Vrabec, M., Rožič, B., Kralj, P., Jamšek Rupnik, P., Kolar-Jurkovšek, T., Gale, L., Šmuc, A. 2013: *Field trip A1: Southern Alps of Slovenia in a nutshell: paleogeography, tectonics, and active deformation*. In: Schuster, R. (Ed.): 11th Workshop on Alpine Geological Studies & 7th European Symposium on Fossil Algae, Schladming, September 2013. Abstracts and field guides, Ber. Geol. Bundesanst. 99, 135—168.

Cousin, M., 1970: *Esquise géologique des confins italo-yougoslaves: leur place dans les Dinarides et les Alpes méridionales*. Bulletin de la Société Géologique de France, Sér. 7, XII (6), 1034–1047.

Cousin, M., 1981: *Les rapports Alpes-Dinarides. Les confins de l'Italie et de la Yougoslavie*. Société géologique du Nord, Publ 5, Vol. I:1–521, Vol. II Annexe:1–521.

Črne, A. E., Šmuc, A. & Skaberne, D., 2007: *Jurassic neptunian dikes at Mt. Mangart (Julian Alps, NW Slovenia)*. Facies 53, 249–265.

Demšar, M., 2016: *Geološka karta Selške doline 1 : 25 000*. Geološki zavod Slovenije, Ljubljana.

Doglioni, C., 1987: *Tectonics of the Dolomites (Southern Alps, Northern Italy)*. Journal of Structural Geology 9 (2): 181–193.

Doglioni, C., 1992: *Relationship between Mesozoic extensional tectonics, stratigraphy and Alpine inversion in the Southern Alps*. Eclogae geologicae Helvetiae 85 (1): 105–126.

Doglioni, C. & Carminati, E., 2008: *Structural styles & Dolomites Field Trip*. Memorie Descrittive della Carta Geologica d'Italia 82: 1–299.

Doglioni, C. & Siorpaes, C., 1990: *Polyphase deformation in the Col Bechei area (Dolomites –Northern Italy)*. Eclogae geologicae Helvetiae 83: 701–710.

Fodor, L., Jelen, B., Márton, E., Skaberne, D., Čar, J. & Vrabec, M., 1998: *Miocene-Pliocene tectonic evolution of the Slovenian Periadriatic fault: Implications for Alpine-Carpathian extrusion models*. Tectonics 17(5): 690–709.

Gale, L., 2010: *Microfacies analysis of the Upper Triassic (Norian) "Bača Dolomite": early evolution of the western Slovenian Basin (eastern Southern Alps, western Slovenia)*. Geologica Carpathica 61: 293–308.

Gale, L., Kolar-Jurkovšek, T., Šmuc, A. & Rožič, B., 2012: *Integrated Rhaetian foraminiferal and conodont biostratigraphy from the Slovenian Basin, eastern Southern Alps*. Swiss Journal of Geosciences 105: 435–462.

Gale, L., Celarc, B., Caggiati, M., Kolar-Jurkovšek, T., Jurkovšek, B. & Gianolla, P., 2015: *Paleogeographic significance of Upper Triassic basinal succession of the Tamar Valley, northern Julian Alps (Slovenia)*. Geologica Carpathica 66 (4), 269–283.

Gale, L., Kolar-Jurkovšek, T., Karničnik, B., Celarc, B., Goričan, Š. & Rožič, B., 2019: *Triassic deep-water sedimentation in the Bled Basin, eastern Julian Alps, Slovenia*. Geologija 62 (2): 153–173.

Gale, L., Kukoč, D., Rožič, B. & Vidervol, A., 2021: *Sedimentological and paleontological analysis of the Lower Jurassic part of the Zatrnik Formation on the Pokljuka plateau, Slovenia*. Geologija 64 (2): 173–188.

Gawlick, H.J. & Schlagintweit, F., 2006: *Berriasian drowning of the Plassen carbonate platform at the type – locality and its bearing on the early Eoalpine orogenic dynamics in the Northern Calcareous Alps (Austria)*. International Journal of Earth Sciences 95: 451–462.

Goričan, Š. & Šmuc, A., 2004: *Albian Radiolaria and Cretaceous stratigraphy of Mt. Mangart (western Slovenia)*. Razprave IV. Razreda SAZU 45 (3): 29–49.

Goričan, Š., Šmuc, A. & Baumgartner, P.O., 2003: *Toarcian Radiolaria from Mt. Mangart (Slovenian-Italian border) and their paleoecological implications*. Marine Micropaleontology 49: 275–301.

Goričan, Š., Košir, A., Rožič, B., Šmuc, A., Gale, L., Kukoč, D., Celarc, B., Črne, A.E., Kolar-Jurkovšek, T., Placer, L. & Skaberne, D., 2012a: *Mesozoic deep-water basins of the eastern Southern Alps (NW Slovenia)*. 29th IAS Meeting of Sedimentology – Field Trip Guides, Journal of Alpine Geology 54: 101–143.

Goričan, Š., Pavšič, J., & Rožič, B., 2012b: *Bajocian to Tithonian age of radiolarian cherts in the Tolmin Basin (NW Slovenia)*. Bulletin de la Société Géologique de France 183: 369–382.

Goričan, Š., Žibret, L., Košir, A., Kukoč, D. & Horvat, A., 2018: *Stratigraphic correlation and structural position of Lower Cretaceous flysch-type deposits in the eastern Southern Alps (NW Slovenia)*. International Journal of Earth Sciences 107: 2933–2953.

Grad, K. & Ferjančič, L., 1976: *Osnovna geološka karta SFRJ 1:100 000. Tolmač za list Kranj.* Zvezni geološki zavod, Beograd.

Ilić, A. & Neubauer, F., 2005: *Tertiary to recent oblique convergence and wrenching of the Central Dinarides: Constraints from paleostress study.* Tectonophysics 410: 465–484.

Jurkovšek, B., 1986: *Osnovna geološka karta SFRJ 1: 100.000, list Beljak in Ponteba*. Zvezni geološki zavod, Beograd.

Jurkovšek, B., 1987: *Osnovna geološka kata SFRJ 1: 100.000. Tolmač listov Beljak in Ponteba*. Zvezi geološki zavod, Beograd.

Jurkovšek, B., Šribar, L., Ogorelec, B. & Kolar-Jurkovšek, T., 1990: *Pelagic Jurassic and Cretaceous beds in the western part of the Julian Alps.* Geologija 31/32: 285–328.

Kastelic, V., Vrabec, M., Cunningham, D. & Gosar, A., 2008: *Neo-Alpine structural evolution and present-day tectonic activity of the eastern Southern Alps: The case of the Ravne Fault, NW Slovenia.* Journal of Structural Geology 30: 963–975.

Kocjančič, A., Petrizzo, M.R. & Horvat, A., 2022: *Pregled zgornjekrednih pelagičnih sedimentov na območju Krnskega pogorja.* Abstract Book, 6th Slovenian Geological Congress, Rogaška Slatina.

Kolar-Jurkovšek, T., Vuks, V.J., Aljinović, D., Hautmann, M., Kaim, A. & Jurkovšek, B., 2013: *Olenekian (Early Triassic) fossil assemblage from eastern Julian Alps (Slovenia).* Annales Societatis Geologorum Poloniae 83: 213–227.

Kossmat, F., 1913: *Die adriatische Umrandung in der alpinen Faltenregion*. Mitteilungen der Geologischen Gesellschaft in Wien 6: 61–165, pls. 1–3.

Krystyn, L., Lein, R., Schlaf, J. & Bauer, F.K., 1994: *Über ein neues obertriadisch-jurassisches intraplattformbecken in den Südkarawanken.* Jubiläumsschrift 20 Jahre Geologische Zusammenarbeit Österreich—Ungarn 2: 409—416, Wien.

Kukoč, D., 2014: *Jurassic and Cretaceous radiolarian stratigraphy of the Bled Basin (northwestern Slovenia) and stratigraphic correlations across the Internal Dinarides.* Dissertation, University of Ljubljana.

Kukoč, D., Goričan, Š. & Košir, A., 2012: *Lower Cretaceous carbonate gravity-flow deposits from the Bohinj area (NW Slovenia): evidence of a lost carbonate platform in the Internal Dinarides.* Bulletin de la Société Géologique de France 183 (4): 383–392.

Masetti, D., Fantoni, R., Romano, R., Sartorio, D. & Trevisani, E., 2012: *Tectonostratigraphic evolution of the Jurassic extensional basins of the eastern southern Alps and Adriatic foreland based on an integrated study of surface and subsurface data.* AAPG Bulletin 96 (11): 2065–2089.

Merlini, S., Doglioni, C., Fantoni, R. & Ponton, M., 2002: *Analisi strutturale lungo un profilo geologico tra la linea Fella-Sava e l'avampaese adriatico (Friuli Venezia Giulia – Italia).* Memorie della Società Geologica Italiana 57: 293–300.

Mikes, T., Christ, D., Petri, R., Dunkl, I., Frei, D., Báldi-Beke, M., Reitner, J., Wemmer, K., Hrvatović, H. & von Eynatten, H. 2008: *Provenance of the Bosnian Flysch*. Swiss Journal of Geosciences 101: S31–S54.

Mikuž, V., 1979: *Srednjeeocenski moluski iz Lepene (Middle Eocene molluscan fauna from Lepena).* Geologija 22 (2): 189–224.

Nirta, G., Aberhan, F., Bortolotti, V., Carras, N., Menna, F. & Fazzuoli, M., 2020: *Deciphering the geodynamic evolution of the Dinaric orogen through the study of the 'overstepping' Cretaceous successions.* Geological Magazine 157 (8), 1238–1264.

Placer, L., 1996: *O premiku ob Savskem prelomu*. Geologija 39: 283–287.

Placer, L., 1999: *Contribution to the macrotectonic subdivision of the border region between Southern Alps and External Dinarides.* Geologija 41(1998): 223–255.

Placer, L., 2009: *Tectonic subdivision of Slovenia*. In: Pleničar, M., Ogorelec, B. & Novak, M. (Eds.), The Geology of Slovenia, Geološki Zavod Slovenije, 43–58.

Placer, L. & Čar, J., 1998: *Structure of Mt. Blegoš between the Inner and Outer Dinarides*. Geologija 40: 305–323.

Ponton, M., 2002: *La tettonica del gruppo del M. Canin e la linea Val Resia-Val Coritenza (Alpi Giulie occidentali).* Memorie della Società Geologica Italiana 57: 283–292.

Rainer, T., Herlec, U., Rantitsch, G., Sachsenhofer, R.F. & Vrabec, M., 2002: *Organic matter maturation vs clay mineralogy: A comparison for Carboniferous to Eocene sediments from the Alpine – Dinaride junction (Slovenia, Austria).* Geologija 45: 513–518.

Rainer, T., Sachsenhofer, R.F., Green, P.F., Rantitsch, G., Herlec, U. & Vrabec, M., 2016: *Thermal maturity of Carboniferous to Eocene Sediments of the Alpine-Dinaric Transition Zone (Slovenia)*. International Journal of Coal Geology 157: 19–38.

Ramovš, A., 1990: *Razvoj ladinijske stopnje v severnih Julijskih Alpah (Ausbildung der Ladin-Stufe (Mitteltrias) in den nördlichen Julischen Alpen)*. Geologija 31–32: 241–266.

Rožič, B., 2009: *Perbla and Tolmin formations: revised Toarcian to Tithonian stratigraphy of the Tolmin Basin (NW Slovenia) and regional correlations.* Bulletin de la Société Géologique de France 180: 411–430.

Rožič, B., Kolar-Jurkovšek, T. & Šmuc, A., 2009: *Late Triassic sedimentary evolution of Slovenian Basin (eastern Southern Alps): description and correlation of the Slatnik Formation.* Facies 55: 137–155.

Rožič, B., Venturi, F. & Šmuc, A., 2014: *Ammonites from Mt Kobla (Julian Alps, NW Slovenia) and their significance for precise dating of Pliensbachian tectono-sedimentary event.* RMZ – Materials and Geoenvironment 61(2–3):191–201.

Rožič, B., Kolar-Jurkovšek, T., Žvab Rožič, P. & Gale, L., 2017: *Sedimentary record of subsidence pulse at the Triassic/Jurassic boundary interval in the Slovenian Basin (eastern Southern Alps)*. Geologica Carpathica 68 (6): 543–561.

Rožič, B., Gerčar, D., Oprčkal, P., Švara, A., Turnšek, D., Kolar-Jurkovšek, T., Udovč, J., Kunst, L., Fabjan, T., Popit, T. & Gale, L., 2018: *Middle Jurassic limestone megabreccia from the southern margin of the Slovenian Basin*. Swiss Journal of Geosciences 112: 163–180.

Sabatino, N., Neri, R., Bellanca, A., Jenkyns, H., Baudin, F., Parisi, G. & Masetti, D., 2009: *Carbon-isotope records of the Early Jurassic (Toarcian) oceanic anoxic event from the Valdorbia (Umbria-Marche Apennines) and Monte Mangart (Julian Alps) sections: palaeogeographic and stratigraphic implications.* Sedimentology 56: 1307–1328.

Schlagintweit, F., Gawlick, H.J., Missoni, S., Hoxha, L., Lein, R. & Frisch, W., 2008: *The eroded Late Jurassic Kurbnesh carbonate platform in the Mirdita Ophiolite Zone of Albania and its bearing on the Jurassic orogeny of the Neotethys realm*. Swiss Journal of Geosciences 101, 125–138.

Schmid, M.S., Bernoulli, D., Fügenschuh, B., Maţenco, L., Schefer, S., Schuster, R., Tischler, M. & Ustaszewski, K., 2008: *The Alpine-Carpathian-Dinaridic orogenic system: correlation and evolution of tectonic units.* Swiss Journal of Geosciences 101: 139–183.

Schmid, M.S., Fügenschuh, B., Kounov, A., Maţenco, L., Nievergelt, P., Oberhänsli, R., Pleuger, J., Schefer, S., Schuster, R., Tomljenović, B., Ustaszewski, K. & van Hinsbergen, D.J.J., 2020: *Tectonic units of the Alpine collision zone between Eastern Alps and western Turkey.* Gondwana Research 78: 308–374.

Šmuc, A., 2005: *Jurassic and Cretaceous stratigraphy and sedimentary evolution of the Julian Alps, NW Slovenia.* Založba ZRC/ZRC Publishing, Ljubljana.

Šmuc, A. & Goričan, Š., 2005: *Jurassic sedimentary evolution of a carbonate platform into a deep-water basin, Mt. Mangart (Slovenian-Italian border).* Rivista Italiana di Paleontologia e Stratigrafia 111: 45–70.

Šmuc, A. & Rožič, B., 2009: *Tectonic geomorphology of the Triglav Lakes Valley (easternmost Southern Alps, NW Slovenia).* Geomorphology 103: 597–604.

Šmuc, A. & Rožič, B., 2010: *The Jurassic Prehodavci Formation of the Julian Alps: easternmost outcrops of Rosso Ammonitico in the Southern Alps (NW Slovenia).* Swiss Journal of Geosciences 103: 241–255.

Tari, V., 2002: *Evolution of the northern and western Dinarides: a tectonostratigraphic approach*. In: Bertotti, G., Schulmann, K. & Cloetingh, S. (Eds.), *Continental collision and the tectono-sedimentary evolution of forelands.* EGU Stephan Mueller Special Publication Series 1: 223–236.

Tomljenović, B. & Csontos, L., 2001: *Neogene-Quaternary structures in the border zone between Alps, Dinarides and Pannonian Basin (Hrvatsko Zagorje and Karlovac Basins, Croatia)*. International Journal of Earth Sciences 90: 560–578.

van Gelder, I. E., Matenco, L., Willingshofer, E., Tomljenović, B., Andriessen, P.A.M., Ducea, M.N., Beniest, A. & Gruić, A., 2015: *The tectonic evolution of a critical segment of the Dinarides-Alps connection: Kinematic and geochronological inferences from the Medvednica Mountains, NE Croatia*. Tectonics 34(9): 1952–1978.

Venturini, C. & Carulli, G.B., 2002: *Neoalpine structural evolution of the Carnic Alps central core (Mt. Amariana, Mt. Plauris, Mt. San Simeone)*. Memorie della Società Geologica Italiana 57: 273–281.

Vrabec, M. & Fodor, L., 2006: *Late Cenozoic tectonics of Slovenia: structural styles at the northeastern corner of the Adriatic Microplate.* In: Pinter, N., Grenerczy, G., Weber, J., Stein, S. & Medak, D. (Eds.), *The Adria*

Microplate: GPS Geodesy, Tectonics and Hazards. NATO Science Series: IV: Earth and Environmental Sciences, Springer, 151–168.

Winkler, A., 1923: *Ueber den Bau der östlichen Südalpen*. Mitteilungen der Geologischen Gesellschaft in Wien 16: 1–272, pl. 1–4.

Žibret, L. & Vrabec, M., 2016: *Palaeostress and kinematic evolution of the orogen-parallel NW-SE striking faults in the NW External Dinarides of Slovenia unraveled by mesoscale fault-slip data analysis*. Geologia Croatica 69 (3): 295–305.

MESOZOIC BASINS ON THE ADRIATIC CONTINENTAL MARGIN – A CROSS-SECTION THROUGH THE DINARIDES IN MONTENEGRO

MEZOZOJSKI BAZENI NA KONTINENTALNEM ROBU JADRANSKE PLOŠČE – PRESEK ČEZ DINARIDE V ČRNI GORI

Špela GORIČAN[1,2], Martin ĐAKOVIĆ[3], Peter O. BAUMGARTNER[4], Hans-Jürgen GAWLICK[5], Tim CIFER[1,2], Nevenka DJERIĆ[6], Aleksander HORVAT[1,2], Anja KOCJANČIČ[1,2], Duje KUKOČ[7] & Milica MRDAK[3,6]

http://dx.doi.org/10.3986/fbg0099

ABSTRACT

Mesozoic basins on the Adriatic continental margin – a cross-section through the Dinarides in Montenegro

The Dinarides, together with the Albanides and Hellenides, preserve stratigraphic successions derived from the eastern margin of the Adriatic microplate and remnants of ophiolites obducted from the Maliac-Vardar branch of the Neotethys Ocean. The main stages in the Mesozoic geodynamic history are: 1) rifting leading to opening of the Maliac Ocean in the Late Anisian, 2) onset of an east-dipping intraoceanic subduction in the Early-Middle Jurassic and seafloor spreading in a supra-subduction setting (Vardar Ocean), 3) formation of ophiolitic mélanges in trench-like basins, westward obduction of young supra-subduction ophiolites in the Middle-Late Jurassic and accumulation of flysch-type deposits in foreland basins in the latest Jurassic to Early Cretaceous, 4) subaerial exposure of the newly formed nappes followed by middle to Late Cretaceous transgression, and 5) continental collision in the Maastrichtian and Paleogene. On the continental margin, the Middle Triassic to Early Jurassic extension created a complex horst-and-graben geometry that is apparent in the stratigraphic record. The present day NW-SE striking tectonic units are in rough accordance with the Mesozoic paleogeography. Hence, the inferred configuration for the most complete SW to NE transect through Montenegro and Serbia is as follows:

IZVLEČEK

Mezozojski bazeni na kontinentalnem robu Jadranske plošče – presek čez Dinaride v Črni gori

V Dinaridih, Albanidih in Helenidih so ohranjena stratigrafska zaporedja vzhodnega roba Jadranske mikroplošče in ostanki ofiolitov, narinjenih na kontinent iz oceana Maliak-Vardar, ki je bil del Neotetide. Glavne stopnje v mezozojski geodinamični evoluciji tega ozemlja so bile: 1) rifting, ki je v zgornjem aniziju privedel do odprtja oceana Maliak, 2) v spodnji do srednji juri začetek intraoceanske subdukcije in raztezanje oceanskega dna v suprasubdukcijskem okolju Vardarskega oceana, 3) v srednji do zgornji juri formacija ofiolitnega melanža v jarkom podobnih bazenih in obdukcija mladih suprasubdukcijskih ofiolitov proti zahodu ter na koncu jure in v spodnji kredi akumulacija flišnih sedimentov v predgornih bazenih, 4) emerzija novo nastalih pokrovov in nato transgresija v srednji do zgornji kredi, 5) kolizija kontinentov v maastrichtiju in paleogenu. Kontinentalni rob se je med ekstenzijo od srednjega triasa do spodnje jure diferenciral na horste in grabne, kar se odraža v stratigrafskem zapisu. Današnje NW-SE usmerjene tektonske enote v Dinaridih se v grobem ujemajo z mezozojsko paleogeografijo, iz česar sklepamo, da je bila konfiguracija kontinentalnega roba v prečnem preseku čez Črno goro in Srbijo naslednja: Dalmatinska karbonatna platforma, Budvanski bazen, karbonatna platforma Visokega Krasa, Bosanski bazen, Durmi-

[1] ZRC SAZU, Paleontološki inštitut Ivana Rakovca, Novi trg 2, SI-1000 Ljubljana, Slovenia. spela.gorican@zrc-sazu.si; tim.cifer@zrc-sazu.si; aleksander.horvat@zrc-sazu.si; anja.kocjancic@zrc-sazu.si

[2] Podiplomska šola ZRC SAZU, Novi trg 2, SI-1000 Ljubljana, Slovenia.

[3] Geological Survey of Montenegro, Jaglike Adžić bb, 81000 Podgorica, Montenegro. comanski@gmail.com; mrdak.milica@yahoo.com

[4] Institut des Sciences de la Terre ISTE, Université de Lausanne, Géopolis, CH-1015 Lausanne, Switzerland. peter.baumgartner@unil.ch

[5] Montanuniversitaet Leoben, Department of Applied Geosciences and Geophysics, Petroleum Geology, Peter-Tunner Strasse 5, 8700 Leoben, Austria. E-mail: Hans-Juergen.Gawlick@unileoben.ac.at

[6] University of Belgrade, Faculty of Mining and Geology, Kamenička 6, 11000 Belgrade, Serbia. nevenka.djeric@rgf.bg.ac.rs

[7] Hrvatski geološki institut, Ul. Milana Sachsa 2, HR-10000 Zagreb, Croatia. dkukoc@hgi-cgs.hr

The Dalmatian Carbonate Platform, the Budva Basin, the High Karst Carbonate Platform, the Bosnian Basin, the Durmitor High, the Lim Basin, the Drina-Ivanjica High, and the deep-marine distal continental-margin domain.

We present a short description of the stratigraphy for these tectonic/paleogeographic units and discuss their possible connection with other units of the Dinarides and Hellenides. The field guide focuses on deep-water deposits, in which radiolarians are the crucial tool for dating. We describe the complete Mesozoic succession of the Budva Zone, the Middle Triassic pelagic episode of the High Karst Zone, the Upper Triassic and Jurassic pelagic rocks of the Lim Zone and two localities with radiolarites associated with ophiolites.

The largest part of the guide is devoted to the Budva Zone, a deeply rifted trough in the continuation of the Pindos Basin. The Budva Zone with its external location in the Dinaric orogen was a site of continuous pelagic sedimentation from the Middle Triassic to the end Cretaceous. Radiolarites characterize the Middle Triassic, Hettangian–Sinemurian, Aalenian to Tithonian, and Hauterivian–Barremian to lower Turonian; pelagic limestones prevail in the Upper Triassic, Berriasian–Valanginian and upper Turonian to Maastrichtian. Calcareous turbidites from the adjacent High Karst Carbonate Platform are interstratified in all units and completely replace radiolarites in the Pliensbachian.

Pelagic sequences also occur in the High Karst Zone, but are confined to the Middle Triassic syn- and early postrift deposits. A 20 m thick unit of Middle Triassic nodular limestone and radiolarite within shallow-water carbonates is a typical example.

More internally, the western Ćehotina Subzone of the Lim Zone records pelagic sedimentation from the Middle Triassic to early Cretaceous, when synorogenic mixed carbonate-siliciclastic deposition began. This zone has been less investigated than the Budva Zone. A 100 m thick Norian to Rhaetian succession of limestone with chert nodules is dated with conodonts. A Callovian-early Oxfordian age of limefree cherts is determined with radiolarians. The Mihajlovići Subzone that may have been part of the Drina-Ivanjica paleogeographic unit shows Triassic shallow-water carbonates and a Jurassic deepening upward sequence ending with Oxfordian radiolarites.

The last two field-trip stops show upper Bathonian-lower Callovian radiolarites in an ophiolitic mélange and upper Anisian radiolarites in direct contact with basalt. These ages, obtained in the south-westernmost ophiolite remnants of the Dinarides, agree with previously documented ophiolite ages in the wider region.

In comparison with the Southern Alps and the Apennines, pelagic deposits of the Dinarides are characterized by an earlier onset and considerably higher proportions of silica with respect to carbonate throughout the Mesozoic. The Dinaric basins were connected with the central Neotethys, where the high fertility of surface waters enabled radiolarite formation since the oceanisation (Anisian or earlier) until the early Late Cretaceous, when planktonic foraminifera and calcareous nannoplankton began to dominate worldwide.

Key words: Dinarides, Neotethys, radiolarites, continental margin, ophiolitic mélange

torski prag, Limski bazen, prag Drina-Ivanjica in globokomorski distalni kontinentalni rob.

V članku je najprej na kratko opisan stratigrafski razvoj tektonskih oziroma paleogeografskih enot tega preseka in domnevna povezava z drugimi enotami v Dinaridih in Helenidih. V nadaljevanju so opisane ogledne točke ekskurzije s poudarkom na globokomorskih sedimentnih kamninah, ker so za določanje starosti teh kamnin radiolariji najpomembnejši in pogosto edini fosili. Podrobno predstavljamo celotno mezozojsko zaporedje Budvanske cone, srednjetriasno pelagično epizodo v coni Visokega Krasa, zgornjetriasne in jurske pelagične kamnine Limske cone in dve lokaliteti z radiolariti v ofiolitih.

Največji del vodnika je posvečen Budvanski coni v Zunanjih Dinaridih. V mezozoiku je bila ta cona globokomorski jarek v nadaljevanju bazena Pindos s kontinuirano pelagično sedimentacijo od srednjega triasa do konca krede. Radiolariti so značilni za obdobje srednjega triasa, hettangija in sinemurija, aalenija do tithonija ter hauterivija-barremija do spodnjega turonija. Pelagični apnenci prevladujejo v zgornjem triasu, berriasiju in valanginiju ter od zgornjega turonija do maastrichtija. Karbonatni turbiditi, prinešeni s sosednje karbonatne platforme Visokega Krasa, so interstratificirani v vseh formacijah, v pliensbachiju pa prevladujejo in popolnoma izpodrinejo pelagične sedimente.

Pelagična zaporedja v coni Visokega Krasa so omejena na sinriftne in zgodnje postriftne sedimente. Kot tipičen primer predstavljamo 20 m debelo zaporedje srednjetriasnih gomoljastih apnencev in radiolaritov znotraj plitvovodnih karbonatov.

V bolj interni Limski coni je za podcono Ćehotina značilna pelagična sedimentacija od srednjega triasa do začetka krede, ko so se začeli odlagati sinorogeni mešani karbonatno-siliciklastični sedimenti. Stratigrafsko zaporedje te podcone do sedaj ni bilo podrobneje proučeno. V članku je prvič datiran 100 m debel profil apnencev z gomolji roženca, ki smo ga s konodonti uvrstili v norij in retij. Z radiolariji smo dokazali callovijsko do spodnjeoksfordijsko starost plastovitih rožencev brez karbonata. V podconi Mihajlovići je stratigrafski razvoj podoben kot v enoti Drina-Ivanjica. Triasnim plitvovodnim karbonatom sledijo jurski apnenci, ki kažejo na postopno poglabljanje sedimentacijskega okolja. Zaporedje se konča z oxfordijskimi radiolariti.

V Črni gori so ohranjeni najbolj jugozahodno ležeči ostanki ofiolitov v Dinaridih. Zadnji dve točki prikazujeta bathonijske do spodnjecallovijske radiolarite v ofiolitnem melanžu in zgornjeanizijske radiolarite v kontaktu z bazaltom. Te starosti se ujemajo z do sedaj znanimi datacijami v ofiolitih širše regije.

V primerjavi z Južnimi Alpami in Apenini je za pelagične sedimente Dinaridov značilno, da so se začeli odlagati prej in da so skozi ves mezozoik vsebovali znatno višji delež kremenice glede na karbonat. Dinarski bazeni so bili povezani s centralno Neotetido, kjer je visoka produktivnost površinskih voda omogočala nastanek radiolaritov od oceanizacije (v aniziju ali še prej) do sredine zgornje krede, ko so po vsem svetu začeli prevladovati foraminifere in kalcitni nanoplankton.

Ključne besede: Dinaridi, Neotetida, radiolariti, kontinentalni rob, ofiolitni melanž

1 INTRODUCTION

The Dinarides, Albanides and Hellenides (Figure 1) form a single mountain chain that shares a common Mesozoic history of rifted continental margins of the Adria microcontinent, facing branches of the Neotethys Ocean (Stampfli & Borel 2004). After the closure of the Paleotethys, at least two successive small branches of the Neotethys opened during the Middle Triassic. Towards the SW (W in present day coordinates) the short-lived Pindos Ocean in the Montenegro transect is merely represented by a deeply rifted trough, the

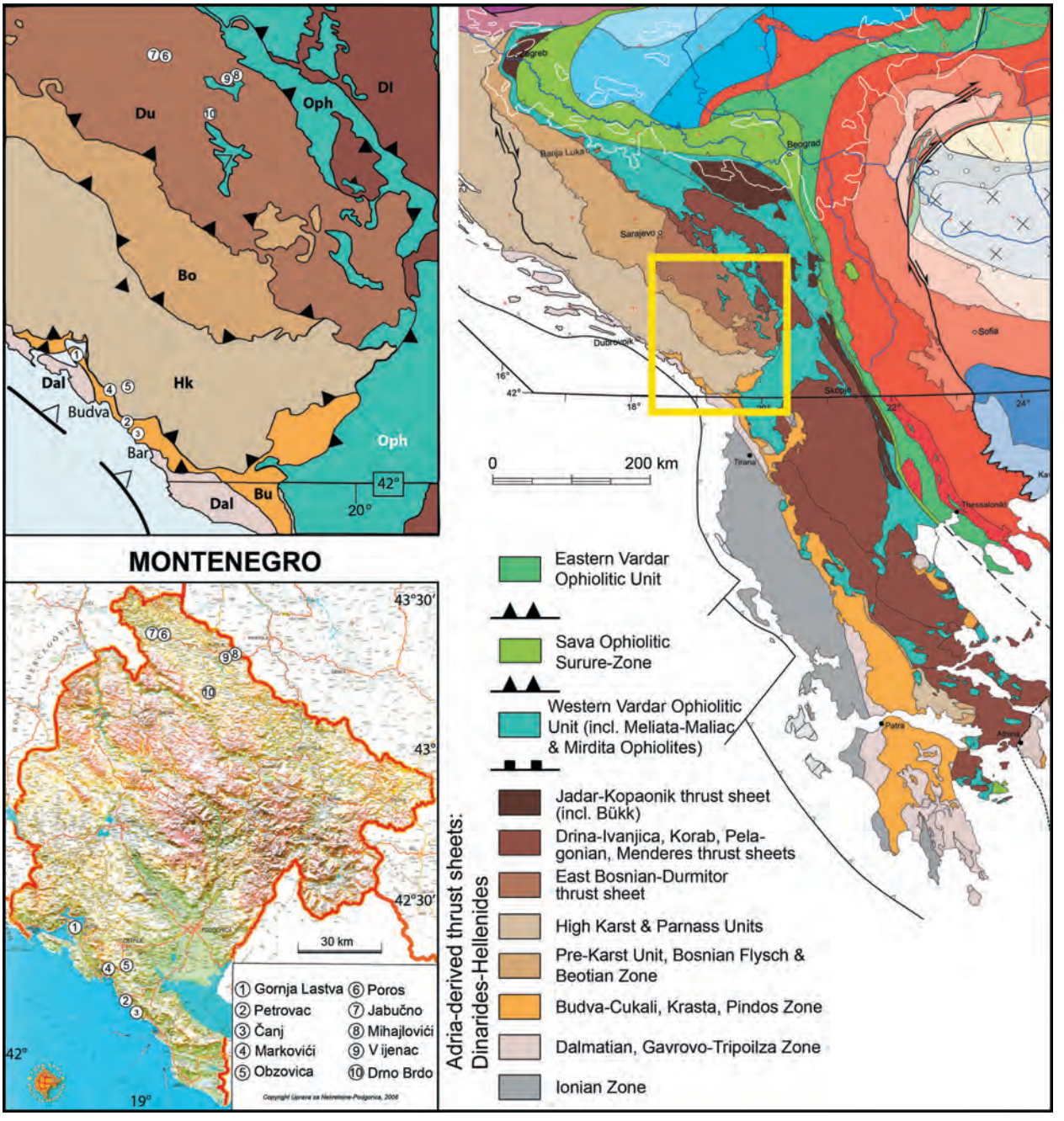

Figure 1: Right: Tectonic map of the Dinarides–Hellenides after Schmid et al. (2008, 2020, polygons courtesy of S. Schmid), showing the continuity of large scale tectonic/paleogeographic units. Yellow rectangle marks location of inset to the left with field stops marked 1–10.

Budva Zone, whereas in southern Greece and Crete, ophiolite remnants testify for an oceanic basement.

To the N (NE in present day coordinates) the main branch of the Neotethys, called the Maliac Ocean by many authors (Ferrière et al. 2016) or Vardar by others (Robertson et al. 2013) or jointly Meliata-Maliac-Vardar (Schmid et al. 2008, 2020), opened in the late Anisian-early Ladinian (Ferrière et al. 2015) (Figure 2). The ophiolite nappes of the Dinarides-Hellenides were, for a large majority of authors, derived from this eastern oceanic realm (Bernoulli & Laubscher 1972; Bortolotti et al. 2013, Schmid et al. 2008; Gawlick & Missoni 2019). The Pindos-Budva paleogeographic realm cannot be the origin of the ophiolites because this realm is materialized by a contiguous, conformable Middle Triassic to Paleogene pelagic sequence, unaffected by Jurassic nappe emplacement.

Between these two oceanic realms, Middle Triassic to Early Jurassic extension produced a system of tectonic highs (horsts) covered by carbonate platforms, and troughs (grabens) filled with pelagic sediments. This realm has been associated with the Pelagonian *s.l.* microcontinent in the Hellenides (Robertson et al. 1991; Robertson & Karamata 1994; Dilek et al. 2005). It is preserved today in a SW-vergent nappe stack with excellent outcrops in the Montenegro transect. Classically, each tectonic unit was defined by distinct Mesozoic facies and paleogeography ("zones isopiques" of Aubouin et al. 1970). This is still a valid first order concept. In contrast, major paleo-fault zones such as the Skutari–Peć Line in northern Albania and the Sperchios fault zone in Central Greece, dissect the paleogeographic domains and have been interpreted as ancient transform faults that affected the Mesozoic margin (Dercourt 1968). As a consequence, the external Triassic–Paleogene carbonate platforms are discontinuous: The Parnassos platform of Central Greece exists only south of the Sperchios line largely disconnected from the High Karst Zone in a similar paleogeographic position. The more internal Durmitor Platform

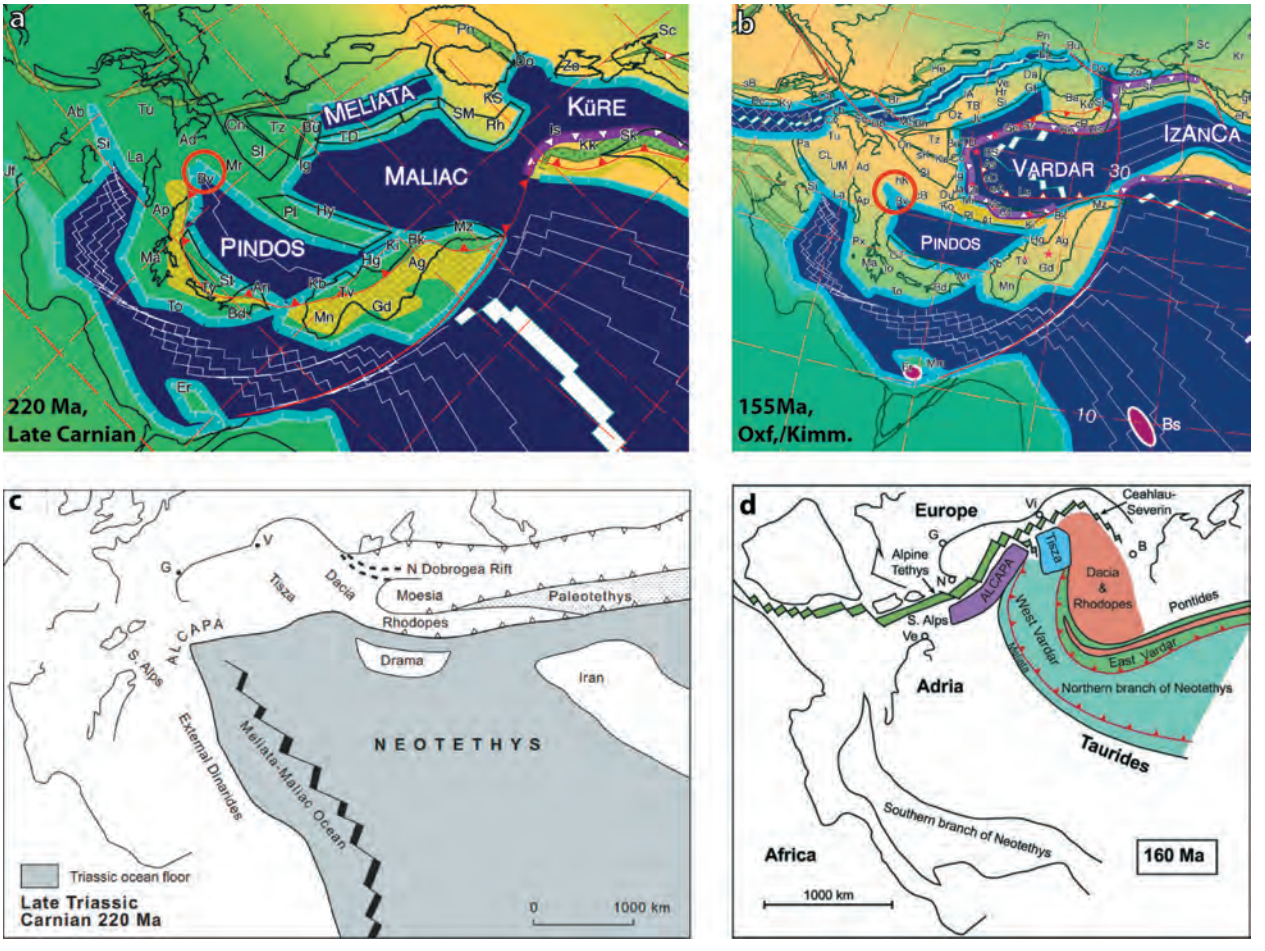

Figure 2: Paleogeographic reconstructions for the Late Triassic (a, c) and the Late Jurassic (b, d). (a, b: from Stampfli & Borel 2004, c: from Schmid et al. 2008, d: from Schmid et al. 2020). Paleogeographic location of field trip marked with a red circle.

has no similar equivalent in Greece, since the Pelagonian margin became successively pelagic during the Jurassic (Baumgartner 1985; Scherreiks et al. 2010).

Progressive closure of the Eastern ("Maliac") oceanic realm began in the Middle Jurassic as an eastward dipping, intra-oceanic subduction outboard of the Pelagonian-Korab-Durmitor-Drina-Ivanjica margin that became the lower plate (Figure 3). A consequence of this subduction was the creation of supra-subduction ocean floor of Middle Jurassic age, often associated with the name Vardar, today represented by the main ophiolite nappes of the Dinarides (e.g. Schmid et al. 2008, 2020).

Convergence progressively consumed the Triassic Maliac ocean floor and seamounts were accreted in a wedge, now represented by accretionary mélanges of Middle Jurassic age. Some of the Triassic ocean floor remained in the upper plate (e.g. Furka Unit, Othris, Central Greece, Ferrière et al. 2016; parts of the Vardar Zone in western Serbia, Vishnevskaya et al. 2009; Medvednica and Kalnik in the Internal Dinarides in Croatia, Halamić & Goričan 1995). When the Pelagonian-Korab-Durmitor-Kuci margin became the lowermost unit of this wedge, subduction ceased and the young Vardar backarc spreading centre obducted over the accretionary wedge, including the margin. Further westward thrusting of composite units (mostly during Late Cretaceous–Early Cenozoic) emplaced composite ophiolite nappes as far as the external Pindos-Cukali-Budva zones. Emplacement and exposure/erosion of the ophiolites during the Middle to Late Jurassic is largely diachronous along the Pelagonian-Korab-Durmitor margin and is in part synchronous with the ongoing formation of Vardar (suprasubduction) oceanic crust. Ophiolitic debris continued during the Early Cretaceous to be shed in the tectonic foreland of the Jurassic orogen ("Premier Flysch du Pinde", Boeotian Flysch, Bosnian Flysch).

Radiolarian biostratigraphy has been fundamental for the reconstruction of the paleogeographic and paleotectonic history of the area, since both the oceanic realms and the rifted troughs commonly are represented by radiolarian-bearing pelagic sediments, largely radiolarites, typical for the Ladinian, lowest Jurassic, and Middle Jurassic to Lower Cretaceous intervals.

The present day NW-SE striking tectonic units of the Dinarides are in rough accordance with the Mesozoic paleogeography and allow for a relatively easy palinspastic restoration. Each tectonic zone corresponds to a different facies belt on the continental margin. Regional studies in the 1970s (Aubouin et al. 1970; Rampnoux 1974; Blanchet 1975; Cadet 1978; Charvet 1978) provided a good stratigraphic framework for the continental-margin Mesozoic successions and also demonstrated the horst-and-graben topography that was created during the Middle Triassic to Early Jurassic rifting. The deeply subsided rift basins that existed through most of the Mesozoic were recognized but the pelagic successions could not be precisely dated because at that time radiolarians were too poorly known to be widely used in biostratigraphy. Radiolarian research in Montenegro was initiated in the late 1980s (Goričan 1987, 1994; Obradović & Goričan 1988) and is ongoing (Gawlick et al. 2012; Kukoč 2014).

The complete SW to NE transect through Montenegro and Serbia preserves the following paleotopographic units (Figure 3): The Dalmatian Carbonate Platform, the Budva Basin, the High Karst Carbonate Platform (also called the Dinaric Carbonate Platform), the Bosnian Basin, the Durmitor High, the Lim Basin, the Drina-Ivanjica High, the deep-marine environment of the distal continental margin, and the oceanic crust, whose remnants are now preserved in the structurally overlying ophiolite nappe. The proximal margin from the Budva Basin to the Lim Basin and the ophiolitic mélange will be visited. The field trip aims to discuss the sedimentary evolution of these Mesozoic basins and to stress the importance of radiolarians for accurate dating. Regional geodynamic setting is introduced to understand to what extent the stratigraphic record was controlled by synsedimentary tectonic events. A Tethyan-wide stratigraphic correlation with other deep-marine basins is presented to place the local radiolarian-bearing pelagic sediments within an interregional paleogeographic and paleoceanographic framework.

2 GEOLOGICAL AND PALEOGEOGRAPHICAL OUTLINE

During the past decades, a general consensus has been reached on the regional arrangement of ocean realms and continental margins. Nevertheless, the Mesozoic geodynamic evolution is still actively debated. Palaeogeographic reconstructions contrast (Figure 2), but agree on a northeastern origin of the obducted ophiolites representing remnants of Neotethys.

The Dinarides-Albanides-Hellenides in the western Neotethys realm underwent in Triassic to Early Cretaceous times more or less the same geodynamic history,

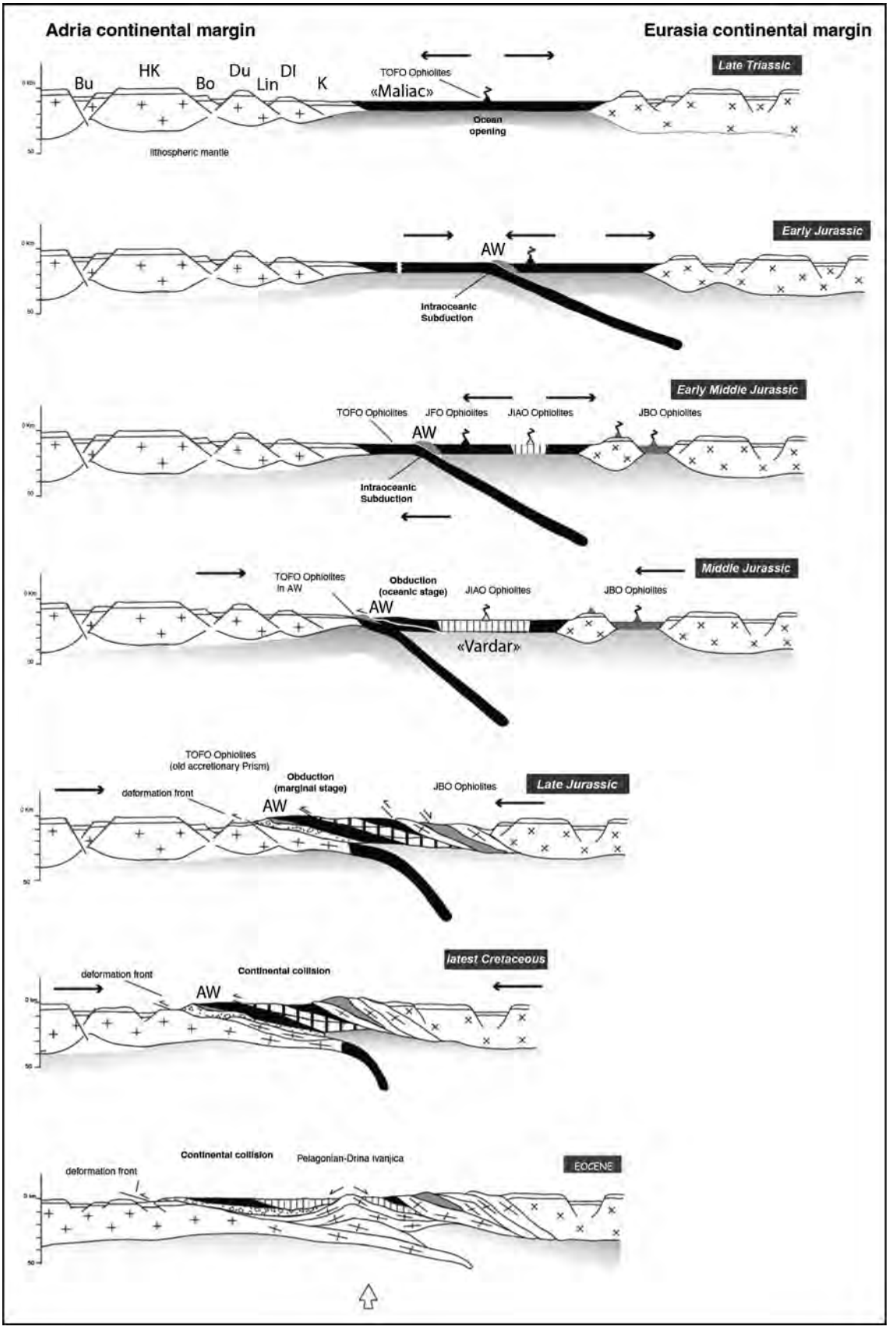
Adria continental margin
Eurasia continental margin
Late Triassic
Bu
HK
Bo
Du
Lin
DI
K
TOFO Ophiolites
«Maliac»
Ocean opening
lithospheric mantle
Early Jurassic
AW
Intraoceanic Subduction
Early Middle Jurassic
TOFO Ophiolites
JFO Ophiolites
JIAO Ophiolites
JBO Ophiolites
AW
Intraoceanic Subduction
Middle Jurassic
TOFO Ophiolites in AW
Obduction (oceanic stage)
JIAO Ophiolites
JBO Ophiolites
AW
«Vardar»
TOFO Ophiolites (old accretionary Prism)
deformation front
Obduction (marginal stage)
JBO Ophiolites
Late Jurassic
AW
latest Cretaceous
deformation front
Continental collision
AW
Continental collision
Pelagonian-Drina ivanjica
EOCENE
deformation front

reflecting a complete Wilson cycle from initial rifting to ophiolite obduction, erosion and formation of flysch and molasse basins:

1. Late Permian to Middle Anisian rift stadium with sedimentation of siliciclastics and carbonate ramp deposits.
2. Middle Anisian to Middle Jurassic passive margin evolution following the late Anisian oceanic breakup. A complex configuration of the continental margin from the inner shelf (platform facies) to the outer shelf (open-marine facies) was established in the Middle to Late Triassic; pelagic platforms were formed in the Early to Middle Jurassic.
3. Middle to Late Jurassic convergent tectonic regime initiated by an intraoceanic subduction and followed by obduction of young, suprasubduction ophiolites ("active continental margin evolution"); the process includes thrusting, trench and trench-like basin formation, and the onset and growth of carbonate platforms on top of the newly formed nappes.
4. Erosion of the Jurassic nappe stack from the Kimmeridgian/Tithonian boundary onwards and filling of the deeply submerged foreland basins with the erosional products of the uplifted orogeny.

In the late Early Cretaceous a new tectonic cycle began which resumed in the Paleogene with thrusting and the formation of new foreland basins.

2.1 Middle Triassic rifting

The Dinarides consist of a number of superposed SW-vergent nappes derived from the Adriatic continental margin (Figures 1, 2c–d, 3). The differentiation of the relatively uniform area of shallow-marine carbonates started in the Anisian. The upper Middle to Upper Anisian Bulog Formation (red nodular limestone), indicating platform drowning, was more than a century ago dated with ammonoids (e.g. Hauer 1888). Further stratigraphic research on deep-water Middle Triassic sedimentary sequences and research on petrology of associated volcanic rocks (Pietra Verde) enabled inferences on rifting processes ascribed either to continental breakup (e.g., Bechstädt et al. 1978; Pamić 1984) or to formation of inter-arc basins in a convergent setting related to the subduction of the Paleotethys realm (e.g., Bébien et al. 1978; Stampfli & Borel 2004). The first biostratigraphic constraints on Triassic age of sedimentary cover of MOR basalts were published in the 1980s, first in Hungary (De Wever 1984; Kozur & Réti 1986), then in Serbia (Obradović & Goričan 1988). Since then, good age constraints have been obtained for a continuous sea-floor spreading from the Late Anisian to the Norian along the entire length of this oceanic branch, i.e. from southern Slovakia and Hungary through Croatia, Serbia, Albania, and Greece (e.g., Ozsvárt & Kovács 2012; Goričan et al. 2005; Chiari et al. 2012; Gawlick et al. 2008, 2016 a, b; Ferrière et al. 2015, 2016, with references). A considerable dataset on the age and geochemistry of Triassic oceanic basalts is now available but the paleogeographic reconstructions are still debated. Some authors interpret the Middle Triassic events as continental rifting preceding the opening of a single oceanic branch (Pamić et al. 2002; Schmid et al. 2008, 2020; Bortolotti et al. 2013). Other authors argue for a convergent regime implying Palaeotethys subduction and opening of back-arc basins (Ziegler & Stampfli 2001; Stampfli & Borel 2004; Stampfli & Kozur 2006; Slovenec et al. 2020; for a review of different models see Robertson 2012).

On a regional scale, including the external zones, Middle Triassic magmatism is very heterogeneous, represented by basic, and more commonly by intermediate and acid plutonic and volcanic rocks with calc-alcaline affinity; pyroclastic rocks (Pietra Verde), intercalated in sedimentary sequences or in lava flows are com-

Figure 3: 2D representation of a model of the geodynamic evolution between the Adria and the Eurasian plates from Triassic to Eocene, modified after Bortolotti et al. (2013, their Figure 10). The upper left shows a simplified sketch of the rifted Adria margin, with the Budva (BU), High Karst (HK), Bosnian (Bo), Durmitor (Du), Lim (Lim), Drina-Ivanjica (DI), and Kopaonik (K) paleogeographic domains. Note that in the Budva and Bosnian realms rifting must have thinned the continental crust. The Triassic ocean-floor ophiolites (TOFO) are here termed "Maliac" (Ferrière et al. 2016). During initial, intra-oceanic subduction an accretionary wedge (AW) developed. During the Early-Middle Jurassic fore-arc (JFO), and intra-oceanic-arc (JIAO) ophiolites formed, here termed "Vardar" (Stampfli & Borel 2004). Jurassic back-arc basin ophiolites (JBO, Guevgueli) formed within the Eurasian margin. During the late Middle to Late Jurassic the AW reached and incorporated the Adria margin. Obduction initiated. The AW then included from top to bottom: JIAO, JFO, metamorphic soles, TOFO, sub-ophiolitioc mélanges with a Middle Jurassic matrix and TOFO, and at its base, mixed ophiolithic-continental margin mélanges of Middle to Late Jurassic age. The short-lived JBO (Guevgueli) also became incorporated in the wedge, without forming a slab. An early Late Cretaceous development of passive margins and ocean floor volcanism along the remaining "Vardar" basin (documented in the Sava Zone, Schmid et al. 2008, 2020, and Adheres, Argolis Peninsula, Baumgartner in Ferrière et al. 2016) is not illustrated in this model. Continental collision may have started during latest Cretaceous and continued until the Eocene, when orogenic uplift separated the ophiolites into two belts.

mon (e.g., Pamić 1984). Although the composition of syn-rift volcanic rocks is in favour of subduction-related convergent movements (e.g., Bébien et al. 1978), the idea of continental rifting is a viable alternative that conforms better to field relationships with the underlying rocks of the continental crust (Cadet 1978; Pamić 1984). The considerable compositional variation can be compatible with a continental rift setting if we consider that the rifting occurred on a pre-existing Variscan orogen that could contribute an inherited subduction signature to rift-related magmas (Robertson 2012; Saccani et al. 2015).

A strong argument in favour of continental rifting is the overall architecture of horsts and grabens that is remarkably similar to that of the North Atlantic (Bernoulli & Laubscher 1972; Cadet 1978; see Peron-Pinvidic & Manatschal 2010, for the configuration of crustal blocks in the North Atlantic). If we consider that the present-day distribution of tectonic units and facies belts basically corresponds to the distribution of paleotopographic units, the margin in the transect through Montenegro and western Serbia can be divided into several basins and swells (Figure 3a). The Durmitor High and the Drina-Ivanjica High (equivalent of the Pelagonian Platform in Greece) terminate towards NW in eastern Bosnia. The High Karst Platform continues to the north but is cut-off to the south along the Skutari-Peć Line in northern Albania but may have paleogeographically equivalent platforms in continental Greece, such as the Olympus and Parnassos. Likewise, the Durmitor High has no direct continuation in the Hellenides but may be represented by shallow areas of the Pelagonian. The morphological highs were spatially limited, partially or completely isolated and the configuration varied substantially along the margin. The inferred geometry is closely similar to the present-day eastern margin of the North Atlantic, where continental ribbons (the Faroes, Hatton Bank, Rockfall Bank and Porcupine Bank) are surrounded by deep basins (Peron-Pinvidic & Manatschal 2010). We further notice that, like in the North Atlantic, the basins in the studied transect were V-shaped. They were oriented parallel to the mid-ocean ridge but with opposite direction of the "V" – the Budva Basin and possibly also the Lim Basin widened towards south, whereas the Bosnian Basin was wider to the north and disappeared towards south.

2.2 Middle to Late Jurassic intra-oceanic subduction and obduction

The closing of the Neotethys (Meliata-Maliac) Ocean started in the Early-Middle Jurassic with the onset of an east-dipping intra-oceanic subduction (Figure 3). In the mean time sea-floor spreading (Vardar) occurred in a supra-subduction setting. The majority of the ophiolite sequences preserved in the Dinarides and Hellenides, especially those including mantle rocks belong to the Jurassic SSZ ophiolites. On the western (Adriatic) side of the ocean, trench and trench-like basins were formed and were filled with ophiolitic mélange (see figures 19 B, C in Gawlick & Missoni 2019). On the eastern (Eurasian) side, an island arc formed on continental crust and a short-lived back-arc basin with supra-subduction ophiolites (Guevgueli Ophiolite Complex; Eastern Vardar ophiolites of Schmid et al. 2008, 2020) evolved behind the arc (Figure 3) (Saccani et al. 2008).

Ophiolite obduction on the Adriatic continental margin is diachronous and lasted from the Late Jurassic to the earliest Cretaceous (Schmid et al. 2008, 2020) or, according to some authors, may have started already in the Middle Jurassic (Gawlick et al. 2016b, 2020; Gawlick & Missoni 2019). The progressive development of trench-like basins in front of the propagating nappes is best documented in the age and composition of sedimentary mélanges; towards west, mélanges become younger and contain less ophiolite-derived material but more and more blocks reworked from the continental margin. Gawlick and co-workers (Gawlick et al. 2017b; Gawlick & Missoni 2019) distinguished two types of mélanges: 1) the ophiolitic mélange composed of serpentinites, basalts, cherts and in places carbonate blocks, and 2) the Hallstatt Mélange containing continental-margin limestone and chert blocks in a radiolaritic-argillaceous matrix. They further subdivided the Hallstatt Mélange according to the provenance of continental-margin blocks; mélanges with outer-shelf Hallstatt-limestone blocks were deposited during the Bathonian to Oxfordian and those containing Triassic reef blocks were formed in the Callovian to Oxfordian.

The Jurassic ophiolites were first dated radiometrically; igneous ages and ages of metamorphic soles are closely similar (approximately 160–180 Ma) implying that the initial obduction movements occurred when the ophiolites were still young and hot (Spray et al. 1984). In the 1980s, the first Middle Jurassic radiolarian age in ophiolitic units were obtained in the Argolis Peninsula in Greece (Baumgartner 1984, 1985), now considered as dating the sedimentary cover of an intraoceanic accretionary wedge. A large number of radiolarian dates are now available from Jurassic ophiolites in Greece, Albania, Serbia, Bosnia and Herzegovina, and Croatia (Halamić et al. 1999; Chiari et al. 2003, 2004; Bortolotti et al. 2008; Gawlick et al. 2009; Nirta et al. 2010; Šegvić et al. 2014). The documented ages consistently range from latest Bajocian –

early Bathonian (UAZ 5) to late Bathonian – early Callovian (UAZ 7) according to the zonation of Baumgartner et al. (1995), both in the sedimentary cover of basalts and in the ophiolite-bearing sedimentary mélanges. Radiometric and biostratigraphic dates together with data on petrology, geochemistry and sedimentology were summarized by Bortolotti et al. (2013), but new data have been published since then. The most recently obtained radiolarians from the matrix of the Hallstatt Mélange in Serbia are assigned to UAZ 5–7 (Gawlick et al. 2016b, 2017a, b, c) and UAZ 6–7 (based on *Kilinora spiralis* (Matsuoka) reported by Gawlick et al., 2018). A comprehensive review on mélange units from the entire Meliata-Maliac-Vardar branch of the Neotethys has been also published (Gawlick & Missoni 2019) but the exact depositional age of the ophiolitic mélanges is still a matter of debate (compare e.g. Schmid et al. 2020 and Gawlick et al. 2020). Since these chaotic units are often pervasively sheared, it is not always clear in the field whether the embedded radiolarian chert is the matrix of the mélange or part of a deformed slide block, which could be markedly older.

In a larger regional picture (Figures 2b, d), it is important to note that the onset of intra-oceanic subduction and the formation of ophiolitic mélange in the Neotethys are contemporaneous with the opening of the Alpine Tethys (Liguria-Piemont Ocean, named the Alpine Atlantic by Gawlick & Missoni 2019), where very slow sea-floor spreading began in the Bajocian and continued until the Tithonian (Bill et al. 2001).

For the origin of the Dinaric-Hellenic ophiolites that occur in two separate ophiolite belts (Figure 1) two basic models have been proposed – the first implying a single oceanic basin (the Vardar Ocean) and the second one implying two oceans (Pindos and Vardar oceans separated by the Pelagonian microcontinent). In the one-ocean model, the ophiolites were generated in the Vardar Ocean, located between the Pelagonian continental margin as part of Adria, and the continental margin of Eurasia (Baumgartner 1985; Bortolotti et al. 2005; Schmid et al. 2008, 2020; Saccani et al. 2011; Ferrière et al. 2016; Chiari et al. 2011; Gawlick & Missoni 2019 with references). This hypothesis was first formulated by Bernoulli & Laubscher (1972) who interpreted the Dinaric-Hellenic ophiolite belts as far-travelled nappes thrust over the Pelagonian unit. The alternative model considers the Pelagonian unit as a microcontinent between the Pindos Ocean in the west and the Vardar Ocean in the east; ophiolites from both oceans were obducted with opposite vergence onto the Pelagonian microcontinent (Robertson et al. 1991; Robertson & Karamata 1994; Robertson & Shallo 2000; Dilek et al. 2005). A comparison of both basic models and their modifications are discussed in detail in several papers (Saccani et al. 2011; Robertson 2012; Gawlick et al., 2017b, 2018). The interpretation that both ophiolite belts were derived from one oceanic basin located to the east of the Pelagonian domain has been widely accepted in recent literature and is also adopted in this paper (Figure 3). We only note that the common origin of ophiolites from the eastern ocean does not contradict the existence of a western ocean-like Pindos Basin whose oceanic basement may have been entirely consumed by underthrusting (e.g. Stampfli & Borel 2002; Ferrière et al. 2012; Argnani 2018).

2.3 From obduction to continental collision (Late Jurassic to Paleogene)

The orogeny occurred in two main phases. The first phase of orogenic deformation was the emplacement of ophiolites on top of the Adriatic continental margin that is well documented in different types of mélange deposited in trench-like basins in front of the advancing nappes (Gawlick & Missoni 2019 with references). Isolated carbonate platforms evolved internally in the uplifted areas of the newly formed nappe stacks. These platforms were first documented in the Northern Calcareous Alps (Schlagintweit et al. 2005; Gawlick & Schlagintweit 2006). In the Dinarides–Hellenides genetically similar carbonate platforms are known indirectly from reworked clasts in gravity-flow deposits of the adjacent basins (Schlagintweit et al. 2008; Kukoč et al. 2012; Gawlick et al. 2020 with references). On the foreland (western) side, the load of the ophiolite nappe induced lithospheric doming of the continental crust and local emersion events on the external carbonate platform (Vlahović et al. 2005 with references). In the foreland basin, the accumulation of flysch-type deposits, the Bosnian Flysch, started in the Tithonian–Berriasian (Blanchet et al. 1969; Mikes et al. 2008 with references). The convergence between Adria and Europe continued into the Early Cretaceous and, in the internal parts of the orogen, resulted in further nappe stacking, burial and green-schist facies metamorphism dated to an interval of early Eoalpine ages between 135 and 110 Ma (Valanginian to early Albian) (Borojević Šoštarić et al. 2012; van Gelder et al. 2015). The mountain chain that resulted from this orogenic episode was named the Paleodinarides (Rampnoux 1970; Aubouin et al. 1970).

The Paleodinarides were subaerially exposed for a prolonged period as evidenced by wide spread laterites on top of the ophiolites. The overstepping successions, in literature also known as the Gosau-type deposits, consist of basal conglomerates followed by a fining-upward

sequence of fluvial deposits and then by shallow-marine mixed carbonate-clastic sediments or carbonates including Turonian rudist reefs (Schmid et al. 2008; Chiari et al. 2011; Nirta et al. 2020). The mid-Cretaceous transgression marked by the onset of marine sedimentation is slightly diachronous along the Dinarides-Hellenides and varies from the early Aptian to the late Albian (Nirta et al. 2020 with references). The Upper Cretaceous part of the succession is in places entirely of deep-water origin and is composed of calcareous turbidites and cherty limestone, which yielded Santonian to early Campanian radiolarians (Djerić et al. 2009; Bragina et al. 2014, 2018, 2020; Đerić & Gerzina 2014).

In the Maastrichtian and Paleogene, flysch deposition was dominant throughout the Dinarides and was linked to the final closure of the Neotethys oceanic realm in the area and to the continental collision of the Adriatic and European plates (Schmid et al. 2008, 2020; Ustaszewski et al. 2009). The Sava Zone, best exposed in inselbergs between Zagreb and Belgrade (Figure 1) is considered the Paleogene suture zone between the two continents (Schmid et al. 2008). This zone includes a Campanian back-arc igneous succession proving that the oceanic domain was open in the Late Cretaceous (Ustaszewski et al. 2009). The timing of collision throughout the Dinarides and Hellenides is still debated. Schmid et al. (2008, 2020) inferred that the continent-continent collision occurred in the latest Cretaceous to Paleogene along the entire orogen. Contrary to this, some authors working in Albania and Greece (e.g. Bortolotti et al. 2013), concluded that the ocean was completely closed after the ophiolite obduction, already in the latest Jurassic – Early Cretaceous. Combining both hypotheses, Nirta et al. (2018) proposed that the continental collision was diachronous, earlier in the south and later in the northern sector of the Dinarides–Hellenides.

2.4 Nappe emplacement and post-orogenic evolution (Paleogene to Recent)

The collision propagated from NE to SW and lasted from the Campanian-Maastrichtian to the Eocene (see Figure 4 to compare the time span of flysch deposition between the internal and external zones). This main thrusting phase was followed by the late Oligocene-Miocene extension which was contemporaneous and partly related to the formation of the Pannonian Basin (Matenco & Radivojević 2012). The extension was mainly NE–SW directed, perpendicularly to the strike of the orogen (Van Unen et al. 2019). This extension affected all areas of the Dinarides and created a system of intramontane lakes with a high degree of endemism (Harzhauser & Mandić 2008). Some of these basins accumulated up to 2000 m of sediments (Hrvatović 2006). Thick Miocene lacustrine deposits also occur in NE Montenegro around Berane and Pljevlja and are economically interesting for coal exploitation.

The Miocene extension was followed by an overall inversion that started in the latest Miocene and is still active. This contraction, expressed in strike slip, thrusting, or reverse faulting and folding has a N-S to NNE-SSW direction and is not intrinsic to the Dinarides but is interpreted in relation to the much larger regional Africa-Europe convergence (Van Unen et al. 2019).

3 STRATIGRAPHY OF TECTONIC UNITS IN THE MONTENEGRO–SERBIA TRANSECT

Stratigraphy is described from the external to the internal units in the SW to NE direction (Figure 1) and graphically summarized in Figure 4. The nomenclature and definition of the first-order tectonic units follow the review papers by Schmid et al. (2008, 2020). The reader is referred to these papers to obtain a wider regional framework of tectonic units from the Alps to western Turkey. Abundant references relevant to the units of the described transect and their equivalents outside this transect are cited in these reviews and will not be fully repeated here. Other review papers on the Dinarides were previously provided by Dimitrijević (1997), Pamić et al. (2002) and Karamata (2006), and a review on the history of research was presented by Charvet (2013). More detailed local tectonic subdivisions (Rampnoux 1974; Cadet 1978) are also considered in order to point out stratigraphic (and paleotopographic) variability within a single first-order unit.

The **Dalmatian Zone** is the most external zone in Montenegro and extends from the Montenegro coast further north along the Croatian coast to Split. This unit, equivalent of the Kruja Zone in Albania and the Gavrovo–Tripolitza Zone in Greece, is composed entirely of Mesozoic and lower Paleogene shallow-water carbonates that are followed by Eocene flysch. In Montenegro, only Upper Cretaceous and Paleogene deposits are exposed, and Lower Cretaceous limestones are known from the boreholes. Middle Miocene shallow marine sandstones and limestones from the surroundings of Ulcinj belong to this unit.

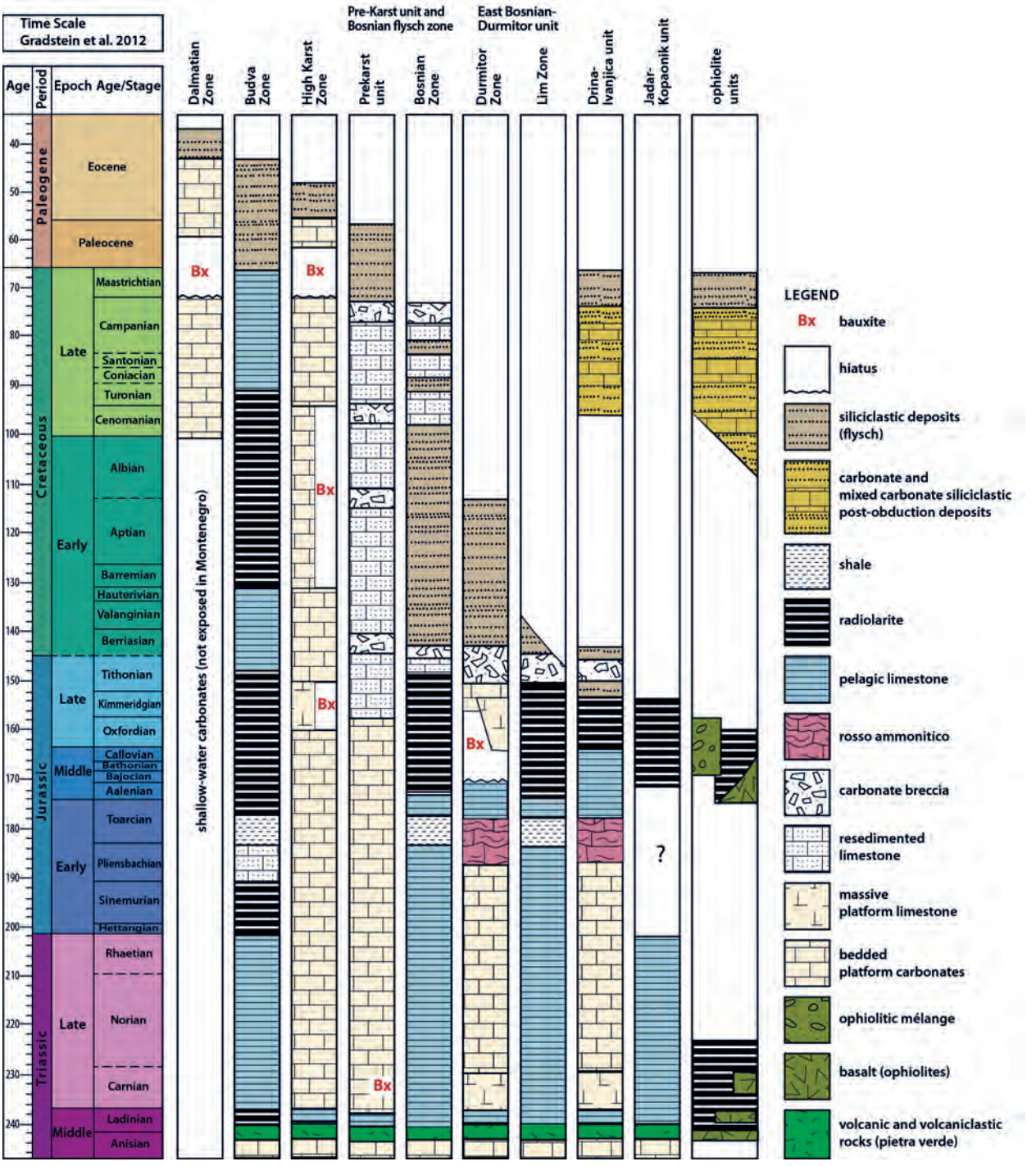

Figure 4: Chronostratigraphic overview of the formations in the Montenegro – west Serbia transect (for location of the transect see Figure 1; references on stratigraphy are given in the text). The stratigraphic column of the Bosnian Zone is compiled from data in Bosnia and Herzegovina because in Montenegro this zone is tectonically reduced and differentiated by the Lower Cretaceous flysch deposits only.

The overlying **Budva Zone** is characterized by deeper-marine sediments from the Middle Triassic to the Paleogene. The Middle Triassic synrift sediments are the nodular Bulog Limestone and a thick clastic unit informally called the "Anisian Flysch". These deposits are overlain by a volcano-sedimentary sequence. The Upper Triassic to Maastrichtian succession displays and alternation of pelagic limestones, radiolarites and resedimented carbonates. The succession ends with Paleocene to lower Eocene flysch. The Budva Zone continues to the south to the Krasta–Cukali Zone in Albania and to the Pindos Zone in Greece. To the north, it wedges out near Konavlje, about 20 km north of the Montenegro-Croatian border. The Dalmatian Zone is northwards in a direct thrust contact with the High Karst Zone as far as Split, where it runs offshore.

The **High Karst Zone** consists of a several thousand-meters thick series of Triassic to Upper Cretaceous platform carbonates, overlain by Paleogene flysch. In certain stratigraphic levels (e.g. Anisian–Ladinian, Cenomanian–Turonian) pelagic facies locally occur. Some other levels (e.g. Upper Jurassic, Aptian–Albian) are characterized by local occurrences of lagoonal to lacustrine facies with charophytes and/or bauxite. The High Karst Zone extends far north to Slovenia and north-eastern Italy. Paleogeographically it represents a large carbonate platform, known as the High Karst or Dinaric Carbonate Platform or, mostly in the Italian literature, also as the Friuli Carbonate Platform. The Dalmatian and the High Karst platforms, when regarded as one paleogeographic entity are called the Adriatic Carbonate Platform (Vlahović et al. 2005). This view is justified in Croatia but is not applicable in Montenegro, where the Budva Basin divides the "single" platform in two units. To the SE, the High Karst Zone abruptly ends at the Skutari–Peć Line. The Skutari–Peć transverse zone in northern Albania (Figure 1) now separates the Dinarides from the Hellenides but its location is paleogeographically predetermined (e.g. Dercourt 1968; Bernoulli & Laubscher 1972). The only possible southern equivalent of the High Karst Zone is the Parnassos Zone (Aubouin et al. 1970), a relatively small isolated unit of platform carbonates located north of the Gulf of Corinth.

The **Pre-Karst Subzone** (defined as a subzone of the High Karst Zone by Blanchet et al. 1970) is composed of several thrust sheets that constitute the NE border of the High Karst Zone along its entire length. The Triassic facies are identical to those of the High Karst Zone, whereas the Jurassic and Cretaceous are slope facies with resedimented carbonates originating from the High Karst Platform. Coarse-grained breccias and calcareous turbidites with interlayers of variegated pelagic limestone are common in the Cretaceous (Cadet 1978). The typical siliciclastic flysch is Maastrichtian to Paleocene in age (Cadet 1978; Mirković 1983). This flysch is well exposed on Mt. Durmitor and is traditionally called the Durmitor flysch (e.g., Mirković 1983; Dimitrijević 1997). The name Durmitor flysch entered common usage (e.g., Schmid et al. 2008, 2020) but one should bear in mind that this formation is not part of the Durmitor nappe.

The **Bosnian Zone** is an almost continuous facies belt in front of the Durmitor nappe, extending from the Albanian Alps to central Bosnia and the Pannonian Basin. This zone is best discriminated in southern Bosnia and Herzegovina where complete Mesozoic successions are exposed (described in Cadet 1978). The post-Anisian sediments are exclusively deep marine and include pelagic limestones, radiolarian cherts and turbidites. The most characteristic lithostratigraphic unit is the Bosnian Flysch, which records an early arrival of siliciclastics with ophiolite debris already in the Berriasian. The Bosnian Flysch is subdivided into the lower, predominantly siliciclastic Vranduk Formation (Berriasian to Cenomanian) (Rampnoux 1974; Cadet 1978), and the upper carbonate-dominated Ugar Formation (Cenomanian? to Maastrichtian) (Charvet 1978; Hrvatović 2006; Mikes et al. 2008 with references).

In Montenegro, the Bosnian Zone is tectonically reduced to a narrow NW-SE trending belt, which disappears below the Durmitor Mountain, along a distance of approximately 50 km, so that the Pre-Karst and the Durmitor units are in a direct contact (see tectonic maps in Aubouin et al. 1970; Rampnoux 1974; Cadet 1978). The stratigraphic succession is also incomplete. Mostly the Bosnian Flysch is exposed; pelagic Triassic rocks occur only in a half-window near Kolašin in central Montenegro (Rampnoux 1974). The thrust contact with the underlying Pre-Karst unit is difficult to recognize because it juxtaposes highly deformed flysch deposits of both tectonic units. Biostratigraphic studies demonstrated that the Berriasian to Cenomanian Bosnian Flysch tectonically overlies the Maastrichtian flysch of the Pre-Karst Zone (Rampnoux 1974). The thrust contact with the overlying Durmitor nappe is everywhere clearly expressed in landscape because it brings a thick succession of platform carbonates on top of flysch deposits. Lateral equivalents of the Bosnian Flysch are the Vermoshi Flysch in northern Albania (Marroni et al. 2009) and the Boeotian Flysch in Greece (Nirta et al. 2015, 2018). The Lower Cretaceous flysch deposits can be traced to the Hellenides but we note that there is no evidence of Triassic pelagic rocks in the corresponding zones south of Montenegro. It is possible that the Bosnian Basin, which originated in the Middle Triassic, was

initially smaller and was prolonged southwards only later, during subsequent subsidence pulses in the Jurassic and Cretaceous.

According to Schmid et al. (2008, 2020) the **Pre-Karst unit and the Bosnian flysch zone** are together considered as a single first-order tectonic unit (Figure 1a). The next structurally higher first-order unit, the **East Bosnian-Durmitor** unit, mainly corresponds to the unit of the same name defined by Dimitrijević (1997), but includes also more internal tectonic units that are overthrust by ophiolitic mélange and were by Dimitrijević (1997) discriminated as the Dinaric Ophiolite Belt. The East Bosnian-Durmitor unit is a synonym of the Serbian Zone (*sensu* Aubouin et al. 1970), which was subdivided in two zones – the Durmitor Zone and the Lim Zone (Rampnoux 1970, 1974; Figure 5). Schmid et al. (2008, 2020) considered these two zones as sub-units and thus did not differentiate them in the geological map (Figure 1).

The **Durmitor Zone** extends from the "Sarajevo sigmoid" (Dimitrijević 1997), an S-shaped north-western thrust contact with the underlying Bosnian Flysch, to the Skutari-Peć transverse zone (Figure 1). No proper equivalent of the Durmitor Zone exists in the Hellenides. The stratigraphic succession (Rampnoux 1970, 1974; Mirković 1983) is characteristic of a morphological high and consists mainly of shallow-water Triassic and Jurassic carbonates. "Ammonitico rosso" facies occurs in the upper Anisian and in the Toarcian. The Toarcian to Middle Jurassic sequence is reduced to a few meters and is disconformably overlain by Upper Jurassic reef and *Clypeina*-bearing limestone. The disconformity is marked by a considerable erosion, in places cutting down to the Middle Triassic, and locally also by bauxite deposits. The Upper Jurassic reef limestone is overlain first by coarse-grained conglomerate and then by Berriasian flysch-type sediments. The stratigraphic succession of the Durmitor Zone differs from that of the High Karst Zone by a much earlier onset of flysch deposition (Berriasian vs. Maastrichtian in the Pre-Karst unit). On the other hand, the Upper Jurassic bauxite and reefs distinguish the Durmitor Zone from the more in-

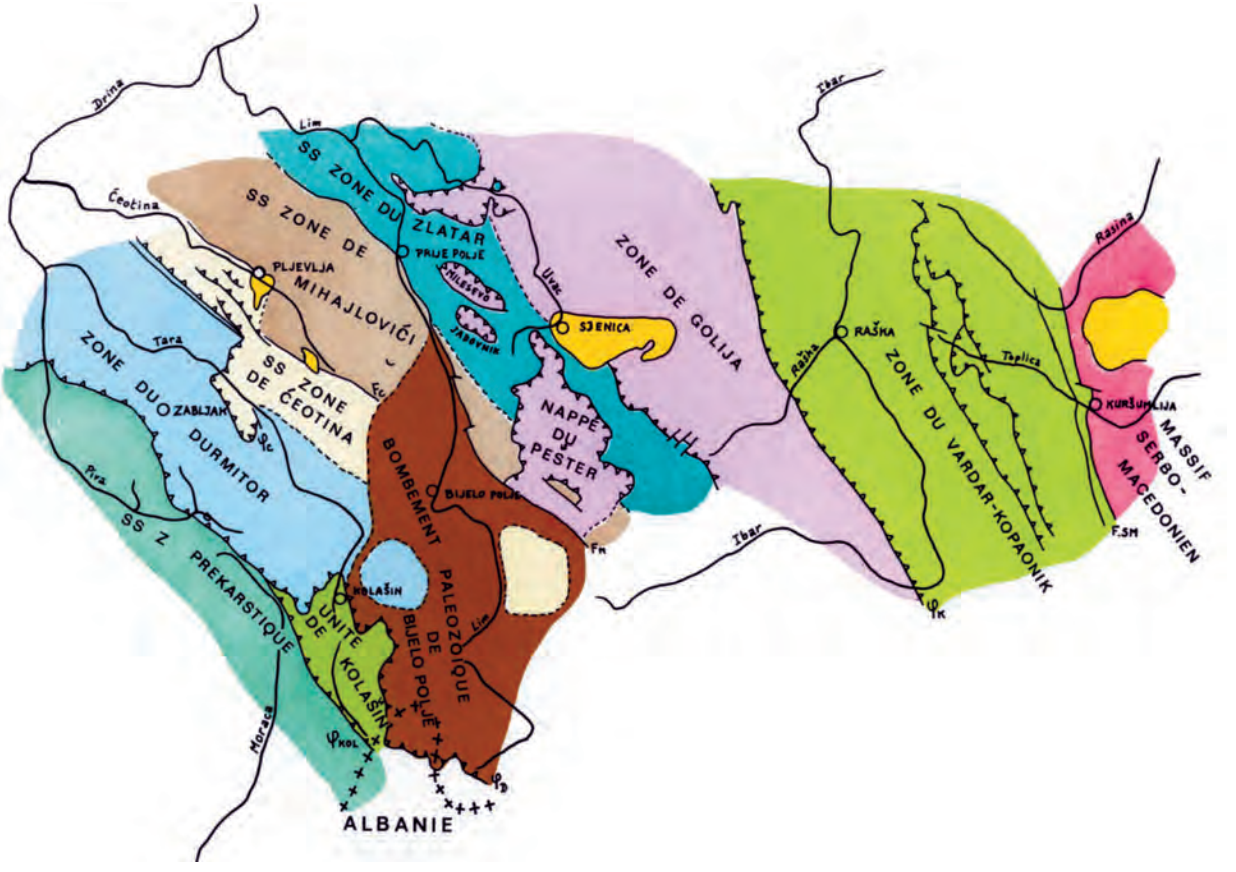

Figure 5. Tectonic sketch of northern Montenegro and south-western Serbia (reproduced from Rampnoux 1974). The dark yellow areas indicate Miocene lacustrine deposits.

ternal Drina-Ivanjica Zone, in which no shallow-water carbonates younger than the Toarcian occur.

The **Lim Zone** was subdivided into three subzones. From SW to NE these subzones are the Ćehotina Subzone, the Mihajlovići Subzone and the Zlatar Subzone (Rampnoux 1970, 1974; Figure 5). The Mihajlovići Subzone disappears towards NW in Bosnia, where only an external and an internal domain within the Lim Zone are distinguished (Cadet 1978). The stratigraphic evolution of the Mihajlovići Subzone is characteristic of a Triassic–Early Jurassic carbonate platform that submerged in the Pliensbachian. The Ćehotina and Zlatar subzones that border the Mihajlovići Subzone to SW and NE, respectively, are characterized by deep-water sediments from the Middle Triassic to the beginning of the Cretaceous. These three subzones are stratigraphically clearly distinguished but their structural superposition is less evident because the gently dipping thrust contacts are strongly obliterated by steep younger faults. It is thus possible that the Mihajlovići Subzone is not placed structurally below the Zlatar Subzone but was originally a klippe of the next higher Drina-Ivanjica unit (Figure 1), which is stratigraphically nearly identical. Moreover, several relatively large klippen of the Drina-Ivanjica unit have already been mapped on top of the Lim Zone, e.g. the Pešter Nappe in western Serbia (Rampnoux 1974; Figure 5) and the Semeć Nappe in Bosnia (Cadet 1978). In terms of paleogeography, this reinterpretation implies that the Mihajlovići Subzone is not necessarily a remnant of a separate Mesozoic submarine high but was more probably part of the larger Drina-Ivanjica continental ribbon.

The **Drina-Ivanjica thrust sheet** (the Drina-Ivanjica Element of Dimitrijević 1997) is a synonym of the Golija Zone of the French authors (Figure 5, Rampnoux 1969, 1974; Aubouin et al. 1970). This unit is characterized by a pre-Mesozoic basement followed by a Triassic–Jurassic succession typical of a morphological high. The late Anisian rifting-related drowning event is evidenced by red nodular limestone (Bulog facies) or by grey cherty limestones with shallow-water debris (Rid Formation of Sudar et al. 2013) on top of a Steinalm-type carbonate ramp. Upsection, Upper Anisian to Lower Ladinian hemipelagic limestones occur and are then followed by Wetterstein and Dachstein-type platform facies (Missoni et al. 2012; Sudar et al. 2013; Gawlick et al. 2017a). Jurassic rocks are preserved in a few outcrops in the external parts of this zone. Rampnoux (1970, 1974) regarded the Krš Gradac locality as the typical Jurassic succession of his Golija Zone. The section, later re-studied several times, overlies the Dachstein Limestone and consists of Lower Jurassic oncoidal limestone, Toarcian ammonitico rosso, Bathonian to Oxfordian/Kimmeridgian radiolarite, and Tithonian polymictic carbonate turbidites (with Cr spinels) overlain by radiolarites with intercalations of ophiolitic sandstones (Radoičić et al. 2009; Gawlick et al. 2009, 2017a, 2020).

The Drina-Ivanjica unit continues to the Korab unit in Albania, Kosovo and North Macedonia and further south to the Pelagonian unit in North Macedonia and Greece (Aubouin et al. 1970). The stratigraphic succession consists of Upper Triassic to Lower Jurassic platform limestones, Middle Jurassic open-marine facies and Oxfordian–Kimmeridgian debris flow deposits with reef fragments; laterites, indicating a Callovian subaerial unconformity, occur below the reefs (Scherreiks et al. 2010). Schmid et al. (2008, 2020) linked the Drina-Ivanjica and Korab units to the Upper Pelagonian, which is characterized by weak to strong metamorphism of the basement but the Mesozoic cover is non-metamorphic. Consistently with this correlation, they proposed that the Lower Pelagonian unit, which is entirely metamorphic and includes a several km thick sequence of Mesozoic marbles, could be the equivalent of the East Bosnian-Durmitor unit.

The **Jadar-Kopaonik thrust sheet** is the innermost composite nappe of the Dinarides and paleogeographically represents the distalmost continental margin of the Adriatic plate. A typical Mesozoic succession, exposed in the Kopaonik-Studenica area in Serbia, is composed of metasediments exhibiting carbonate platform facies up to the Anisian, which are then followed by Middle Triassic carbonate breccia and tuff, Upper Triassic pelagic limestone and presumably Jurassic radiolarian chert (Schefer et al. 2010). The northern extensions of this unit are the Medvednica Mountain in Croatia and the Bükk Mountains in northern Hungary; southwards the unit extends as a narrow belt to northern Greece (Schmid et al. 2008, 2020).

Ophiolites and ophiolitic mélanges tectonically overlie the continental-margin units. In older literature, these ophiolites and genetically related sedimentary rocks were commonly termed the Diabase-Chert Formation. Schmid et al. (2008, 2020) distinguished between western and eastern Vardar ophiolitic units (Figure 1). The Dinaric and Hellenic ophiolites are the western units that originated from the West Vardar Ocean and were emplaced onto the Adriatic continental margin (Figure 3). In present-day map view, the Western Vardar ophiolites occur in several discontinuous belts; some isolated remnants are found far west from the Sava suture zone, which is interpreted as the boundary between Adria and Europe (Schmid et al., 2008, 2020). This long-distance emplacement resulted

from Cretaceous and Cenozoic out-of-sequence thrusting of previously obducted ophiolites. In geological maps (Figure 1), the ophiolitic units include thick layers of ophiolitic mélange underlying the obducted ultramafics and their metamorphic sole. In Montenegro, the westernmost ophiolitic remnants tectonically overlie the East Bosnian-Durmitor unit or, more specifically, the outermost ultramafics occur on top of the Zlatar Subzone and the outermost mélanges on top of the Ćehotina Subzone of the Lim Zone (Rampnoux 1974). Recently, mélanges have gained an increased interest because they are not only crucial to understand the obduction history but also allow us to restore the pre-orogenic configuration of the distal passive margin. From detailed analyses of blocks in the Jurassic sedimentary mélanges of the Dinarides, a complete unmetamorphosed Triassic distal-margin stratigraphic succession could be reconstructed (Gawlick et al., 2017a, 2018; Gawlick & Missoni 2019).

A note on the tectonic units and their stratigraphy, the Mesozoic geodynamic evolution and paleogeography: One of the co-authors (HJG) disagrees with this subdivision of tectonic units, the correlation of tectonic units and in cases also with the summarized Triassic to Early Cretaceous stratigraphic and sedimentological and geodynamic evolution as presented in this field-trip guide. For a summary on the Triassic sedimentary evolution interested readers are referred to Kovács et al. (2011), and for the Jurassic sedimentary evolution to Haas et al. (2011). For the correlation of tectonostratigraphy and the geodynamic evolution interested readers are referred to Gawlick et al. (2008, 2017a, 2020), Gawlick & Missoni (2015, 2019) and references therein.

4 FIELD-TRIP DESCRIPTION

The field-trip will focus on radiolarian-bearing deposits of different tectonic units. The localities are described in SW to NE direction from the most external to more internal zones (Figures 1, 6). Ophiolitic mélanges are described together with the sedimentary succession of the Lim Zone, which they overthrust.

Montenegro is covered by 16 sheets of the Basic Geological Map 1:100,000 (available at the Geological Survey of Montenegro) and by an integral map at scale 1: 200,000 (Mirković et al. 1985). For each locality, the coordinates are given and the corresponding sheet of the Basic Geological Map is cited.

4.1 The Budva Zone

General description

The Budva Zone is a narrow, less than 10 km wide and about 100 km long belt of deep-marine Mesozoic deposits in coastal Montenegro. The zone is composed of several thrust sheets. In the Kotor area, two tectonic subunits are clearly distinguished (Figure 7). The central part between Kotor and Petrovac is more complex, composed of several smaller discontinuous recumbent folds. In general, a subdivision between a lower and an upper tectonic subunit is possible. Stratigraphic research in these units revealed that the Jurassic–Cretaceous redeposited carbonates are thicker and have a more proximal character in the upper than in the lower unit (Goričan 1994). A similar NE to SW direction towards a more distal depositional setting was recognized in Middle Triassic limestone conglomerates (Dimitrijević 1967). These observations imply that only the eastern part of the Budva Basin, which was supplied from the High Karst Carbonate Platform is now preserved in the Budva Zone.

The oldest rocks of the Budva Zone are Middle Permian dark grey shales, sandstones and calcarenites overlain by Middle to Upper Permian dark grey bioclastic limestone with algae, brachiopods, bivalves, gastropods, ammonoids and crinoids (Horacek et al. 2020). The overlying Lower Triassic deposits are sandstones, marls and calcarenites, and laterally also dolomites. The facies associations show considerable lateral variability and a general vertical change from a shallow mixed siliciclastic and carbonate Werfen-type sedimentation to deeper-water marly layers and calcareous turbidites (Krystyn et al. 2019). The lower Anisian is represented by calcareous turbidites or in places by platform limestone. The overlying Pelsonian and Illyrian deposits are limestone conglomerates (including reworked Paleozoic rocks) and mixed siliciclastic-carbonate turbidites traditionally known as the Anisian flysch (Dimitrijević 1967). The conglomerates are now named the Crmnica Formation and the turbidites the Tuđemili Formation (Čadjenović & Radulović 2018) The Crmnica Formation is defined as the basal part of this "flysch" sequence but conglomerates also occur within or on top of the finer-grained turbidites. Nodular red cephalopod limestone in places overlies these turbidites but more commonly occurs directly on top of lower Anisian platform limestones; ammonoids from the upper-

Figure 6: Road map of Montenegro with locations of field-trip sections 1–10.

most parts of "flysch" sediments are characteristic of Pelsonian age (Đaković 2018). The uppermost Anisian to Ladinian unit is a thick volcano-sedimentary sequence, which consists of volcanic and volcanoclastic rocks (Pietra Verde), alternating with radiolarian chert and limestone. Cafiero & De Capoa Bonardi (1980) described bivalves of latest Ladinian age from the uppermost part of this sequence at Bečići.

The Upper Triassic to Maastrichtian succession displays an alternation of pelagic limestones, radiolarites, and resedimented carbonates. The description of lithostratigraphic units is summarized below (according to Goričan 1994, unless otherwise specified). See Figure 8 for general stratigraphic logs of the representative sections and Figure 9 for their chronostratigraphy.

The ***Halobia* limestone** is an approximately 150 m thick succession of bedded limestone with replacement chert nodules and layers, and in places marly intercalations. The Carnian and Norian age is determined with halobiids and conodonts (Cafiero & De Capoa Bonardi 1980, 1981). From the topmost beds in the Čanj section (see Stop 3 below) radiolarians of the upper Rhaetian *Globolaxtorum tozeri* Zone were identified (Črne et al. 2011).

The **"Passée Jaspeuse"** is a unit of bedded calcareous chert alternating with shale or marl. Light grey siliceous micrite beds are intercalated. The unit is 30 to 40 m thick. It contains higher proportions of silica and clay constituents than the *Halobia* limestone and can easily be distinguished by its characteristic dark brownish red and green colours. Siliceous fossils are present in all chert and limestone beds. Sponge spicules prevail over radiolarians, which are very poorly preserved; only a few samples with identifiable specimens were found. At the base of the formation, radiolarians of the lowermost Hettangian *Canoptum merum* Zone were determined (Črne et al. 2011). The top of the formation was placed near the Sinemurian–Pliensbachian boundary.

The **Bar Limestone** is a succession of carbonate gravity-flow deposits. In contrast with the underlying "Passée Jaspeuse" the colour is light grey and the limestone beds contain only a minor amount of silica (10–20 %) in form of replacement chert layers and nodules. The age is constrained with radiolarians from underlying and overlying strata and confirmed by rare benthic foraminifera. The formation is subdivided in two members. The Lower Bar Limestone Member is 50 m to 170 m thick and occurs in the lower as well as in the upper tectonic unit of the Budva Zone. The Upper Bar Limestone Member can be more than 200 m thick and is practically restricted to the upper tectonic unit. The transition between the two members is covered, but shales and marls that overlie the Lower Member in the distal sections suggest that this transition probably correlates to widespread clay-rich deposits of the lower Toarcian.

The grain constituents in both members of the Bar Limestone show the same origin of sediment supply – penecontemporaneous platform-derived debris mixed with semilithified coeval pelagic limestone clasts. The main difference in composition is the amount of ooids. At the base of the Lower Bar Limestone Member, the ooids are rare and relatively small; from the middle part to the top of the Lower Member their proportion increases but does not exceed 40 % of shallow-water grains. In the Upper Member, on the contrary, ooid packstone facies containing only about 10 % of other grains is common. Oolites occur as part of a turbidite sequence or as independent deposits. Pure oolite beds show no grading and can be more than 20 m thick. Compared to the Lower Bar Limestone Member, the overall succession of the Upper Member exhibits a coarser grained composition, thicker bedding and proportionally less lime mudstone beds associated.

The **Lastva Radiolarite** is a sequence of rhythmically alternating chert and shale layers; beds of silici-

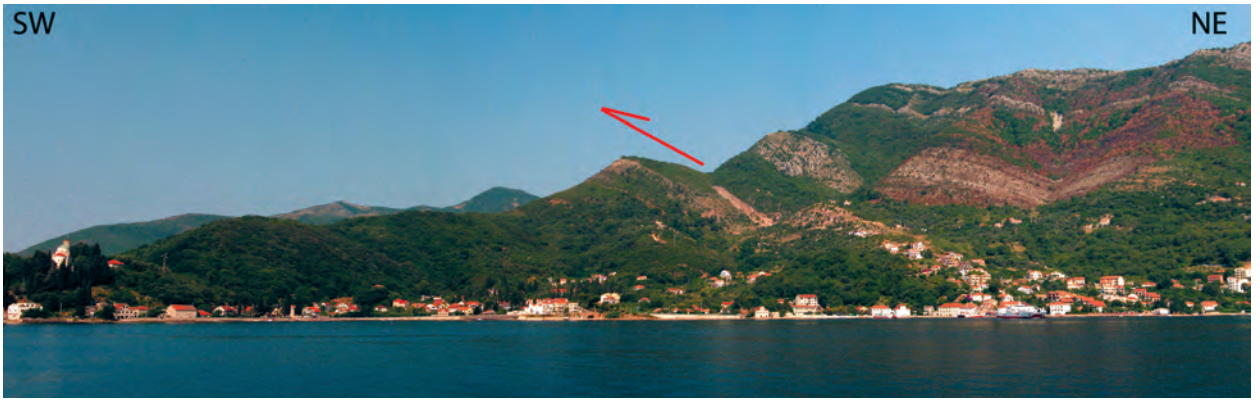

Figure 7: View to the two superposed tectonic units of the Budva Zone in NW Kotor Bay above the town of Bijela.

fied calcarenites are interstratified. The formation includes the supposedly lower Toarcian shales, which directly overlie the Lower Bar Limestone Member but are too poorly exposed to be defined as a separate lithostratigraphic unit. The oldest age determined with radiolarians is Aalenian-early Bajocian. The top of the formation is characterized by a transition to pelagic limestone and is dated to the middle Tithonian. The Lastva Radiolarite is partly the lateral equivalent of carbonate gravity-flow deposits hence, the thickness (Figure 8) and the time span (Figure 9) of this formation vary considerably across and along the basin.

Considering the colour, shale content and bedding style, several radiolarite facies can be distinguished. In all sections, these facies occur in the same stratigraphic order but are laterally diachronous and their sequence is rarely complete (Figure 9). From base to top these facies are:

The **variegated facies** (V) is in the lower part (V1) characterized by a very high proportion of dark green or

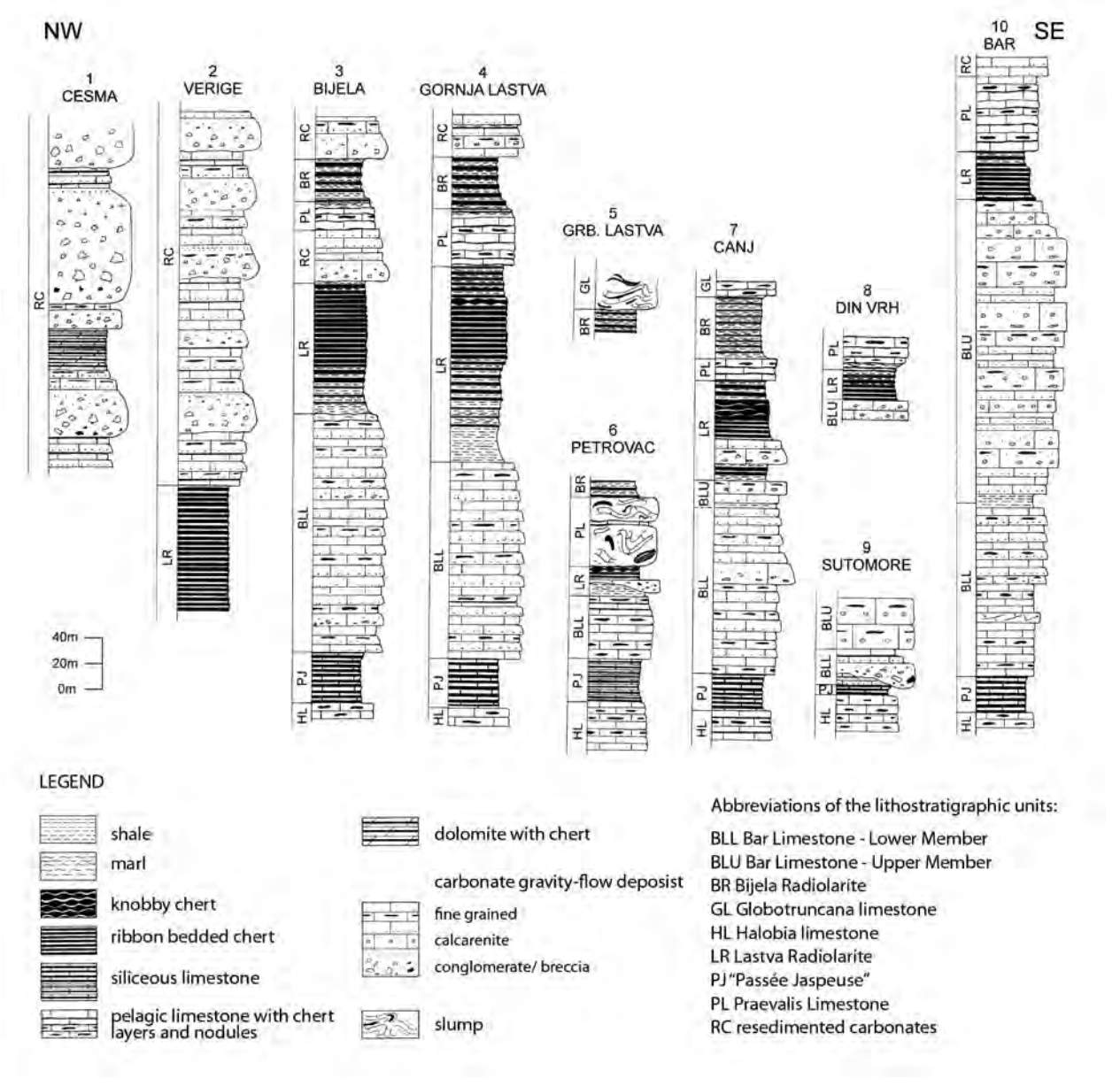

Figure 8: Schematic lithological columns of different sections in the Budva Zone (from Goričan 1994). Stratigraphic range of the formations is shown in Figure 9. For detailed columns of the field-trip sections at Gornja Lastva, Petrovac and Čanj see Figures 10, 12, 15.

brownish shale alternating with thin, about 5 cm thick grey laminated sandstone consisting of densely packed sponge spicules and radiolarians and centimeter-thick layers of dark variegated argillaceous chert. Chert beds do not exceed 30 % of the sequence. Higher in the sections (V2) the shale constituent gradually decreases. Dark reddish-green chert beds are thicker (5–10 cm), sometimes nodular, and are progressively less argillaceous. Siliceous sandstone beds disappear. Cherts represent 60 – 90 % of the sequence. The preservation of radiolarians is poor in the lower and moderate in the upper part. Some slightly argillaceous chert beds contain very well preserved and diverse fauna.

The **green radiolarite** (G) generally consists of thicker (average 10 cm) unevenly bedded, sometimes laminated greyish-green chert. Thin interlayers of slightly argillaceous yellowish-green chert are present at joints. These layers can yield pyritized radiolarians but the average preservation is poor. The content of chert varies from 95 % to 100 % of the sequence. Where the green radiolarite extends to the Kimmeridgian (Figure 9), up to 20% shale interlayers are present.

The **greenish-red** (GR) knobby radiolarite is characterized by 3 cm to 15 cm thick undulating chert beds alternating with a maximum 5 % shale. This facies is only a few meters thick and always interstratified between the green radiolarite and the red knobby radiolarite. Chert beds are red in the middle part and green at the margins. Radiolarians are abundant, diverse and well preserved.

The **red knobby** radiolarite (Rk) facies consists of decimeter-sized nodular chert beds with a high pinch

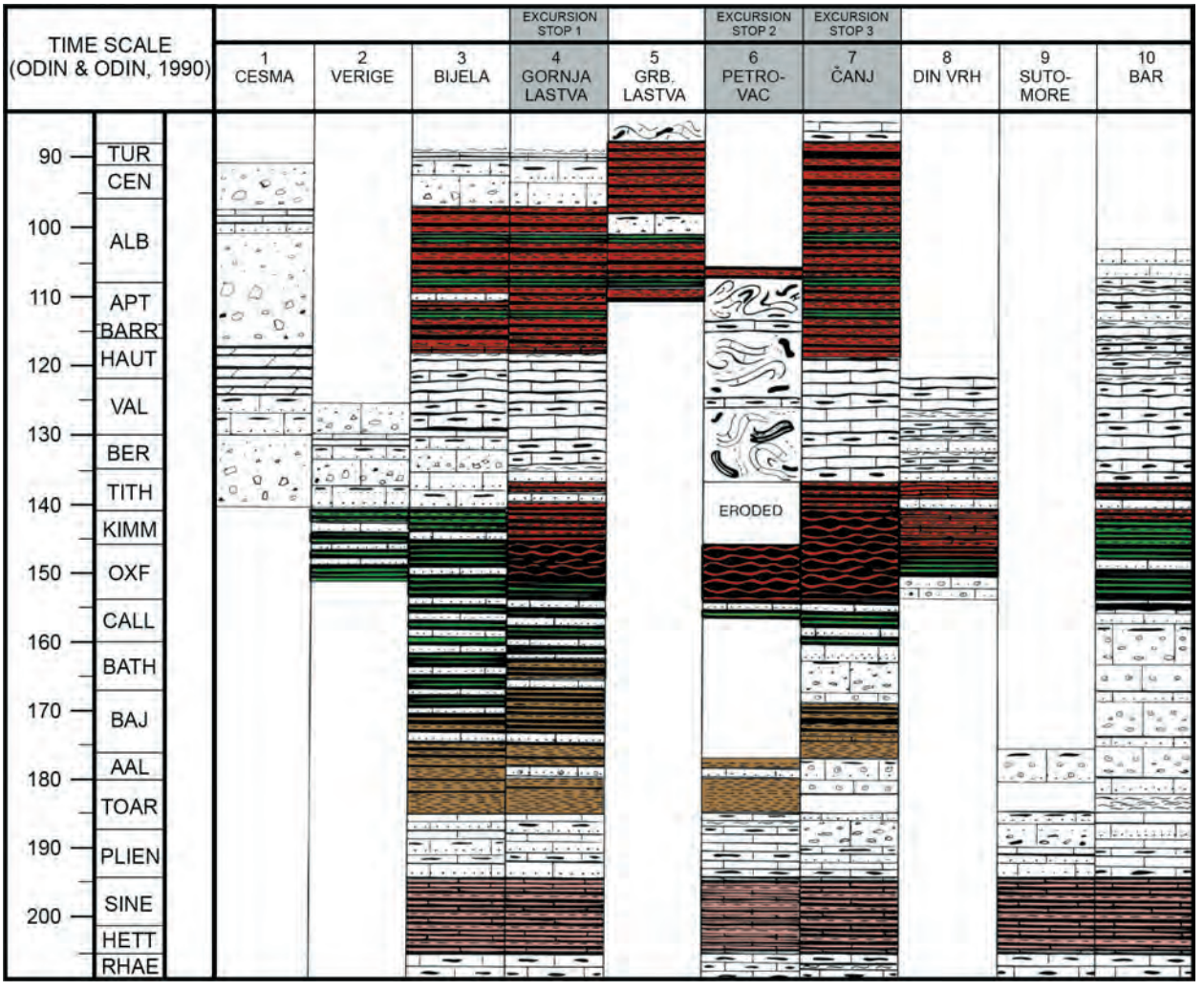

Figure 9: Chronostratigraphic view of lithofacies in the sections of Figure 8 (from Goričan 1994). Legend same as Figure 8. Radiolarian cherts and shales are colored according to their natural color. Sections 3 to 7 are part of the lower tectonic unit, other sections are part of the upper tectonic unit.

to swell ratio. No shale is interlayered. At Čanj, where this facies is best exposed, it changes from orange-red through dark red to brick-red upsection. Radiolarians are well preserved.

The **red ribbon** (Rr) radiolarite displays a very regular alternation of dark brownish-red argillaceous chert (beds 3 to 6 cm) and centimeter-sized shale interlayers. The content of chert beds varies from 80 % to 90 %. Radiolarians are abundant but moderately well preserved and usually compressed because of the compaction of the relatively clay-rich sediment.

In addition to radiolarians, sponge spicules and rhaxes occur through all the radiolarite succession. They are especially abundant in the lower variegated facies, where they prevail over radiolarians.

Carbonate gravity-flow deposits are intercalated throughout the Lastva Radiolarite. Calcarenite beds are silicified, generally 5–20 cm thick, rarely up to 30–40 cm. A few thicker graded turbidites, which escaped complete silicification are interstratified.

The **Praevalis Limestone** is composed of bedded marly micrite (beds 10–20 cm) with replacement chert nodules and layers. The general colour of limestone is light red to violet red, rarely white to pale green; cherts are vivid red. Bedding planes are undulated. In the upper part of the formation, reddish marls are intercalated. The limestone beds contain a maximum of 15 % calcified radiolarians in a mud matrix. Very rare calpionellids were found in the lower part of the formation. Relatively abundant and well-preserved radiolarians were extracted from chert nodules. The formation is up to 50 m thick and ranges from the Upper Tithonian to the Hauterivian–Barremian; in the SE part of the basin (see section Bar in Figures 8 and 9) the formation ranges to the Aptian–early Albian. The entire formation locally consists of chaotic beds interpreted as highly evolved slump to debris-flow deposits (see Stop 2 below).

The transition from the Praevalis Limestone to the overlying **Bijela Radiolarite** is gradual, marked by a progressive increase in clay and silica content. The base of the radiolarite is defined where the sequence has a typical radiolarite aspect of thin siliceous beds alternating with clayey marls. The predominant Bijela Radiolarite consists of thin-bedded (1–3 cm) dark red chert and a very high proportion of shale that makes up to 80 % of the sequence. Several levels, ranging in thickness from 0.5 to 1.5 m, of green radiolarite are interstratified. Chert beds in these green levels are also thin (1–3 cm) but the percentage of shale interlayers is much lower (5–20%) than in the red radiolarite. The maximum estimated thickness of the formation is 60 m. Cherts yield abundant but moderately preserved radiolarians and sponge spicules. The base of the Bijela Radiolarite is assigned to the Hauterivian–lower Barremian. The youngest age obtained for the top is early Turonian.

The Mesozoic succession ends with the ***Globotruncana* limestone**, a predominantly reddish Scaglia-type pelagic limestone that contains chert nodules and layers. The formation is up to 150 m thick. Planktonic foraminifera are abundant, especially in the Campanian and Maastrichtian (Danilova 1958).

Tithonian and Cretaceous resedimented carbonates are commonly interstratified in pelagic sequences and may, in the proximal sections, completely replace radiolarite and micritic limestone. The predominant deposits are turbidites consisting of graded fine breccia or calcarenite, to calcisiltite sequences, occasionally with thin marl interbeds. Up to several- meters thick debris-flow breccias are characteristic of the NW part of the Budva Zone. In contrast to the Bar Limestone, which contains penecontemporaneous platform-derived material, are the Tithonian–Maastrichtian resedimented limestones mostly composed of angular lithoclasts derived from the erosion of somewhat older platform limestones. Subrounded carbonate-mudstone clasts with pelagic fauna are very rare. Fine-grained beds are often silicified; the overall succession contains 15–25 % of replacement chert.

Stop 1: Gornja Lastva near Tivat

Lower tectonic unit, Hettangian to Upper Campanian.

Location: near Tivat, along the road from Donja Lastva to Gornja Lastva, the section starts at N 42°27'08", E 18°42'01", Basic Geological Map sheet Kotor (Antonijević et al. 1969).

A continuous Jurassic and Cretaceous section consists of 40 m of the "Passée Jaspeuse", 150 m of the Bar Limestone, 150 m of the Lastva Radiolarite, 50 m of the Praevalis Limestone, 35 m of the Bijela Radiolarite and continues with more than 70 m of carbonate gravity-flow deposits and *Globotruncana* limestone (Figure 10 a–f).

The "Passée Jaspeuse" with a sharp contact overlies grey micritic limestone (bed thickness 10–15 cm) with chert nodules. In the lowermost part some silicified calcarenites are interstratified; the remaining "Passée Jaspeuse" consists of thin-bedded brownish to greenish highly siliceous limestone. The internal part of beds usually contains replacement chert. Some beds contain less silica and are light grey in colour. The proportion of shale/marl interlayers is high; in the middle part of the section, these interlayers attain up to 60 % of the sequence. Rare decimeter-sized beds of intraformational breccia occur in the lower half of the sec-

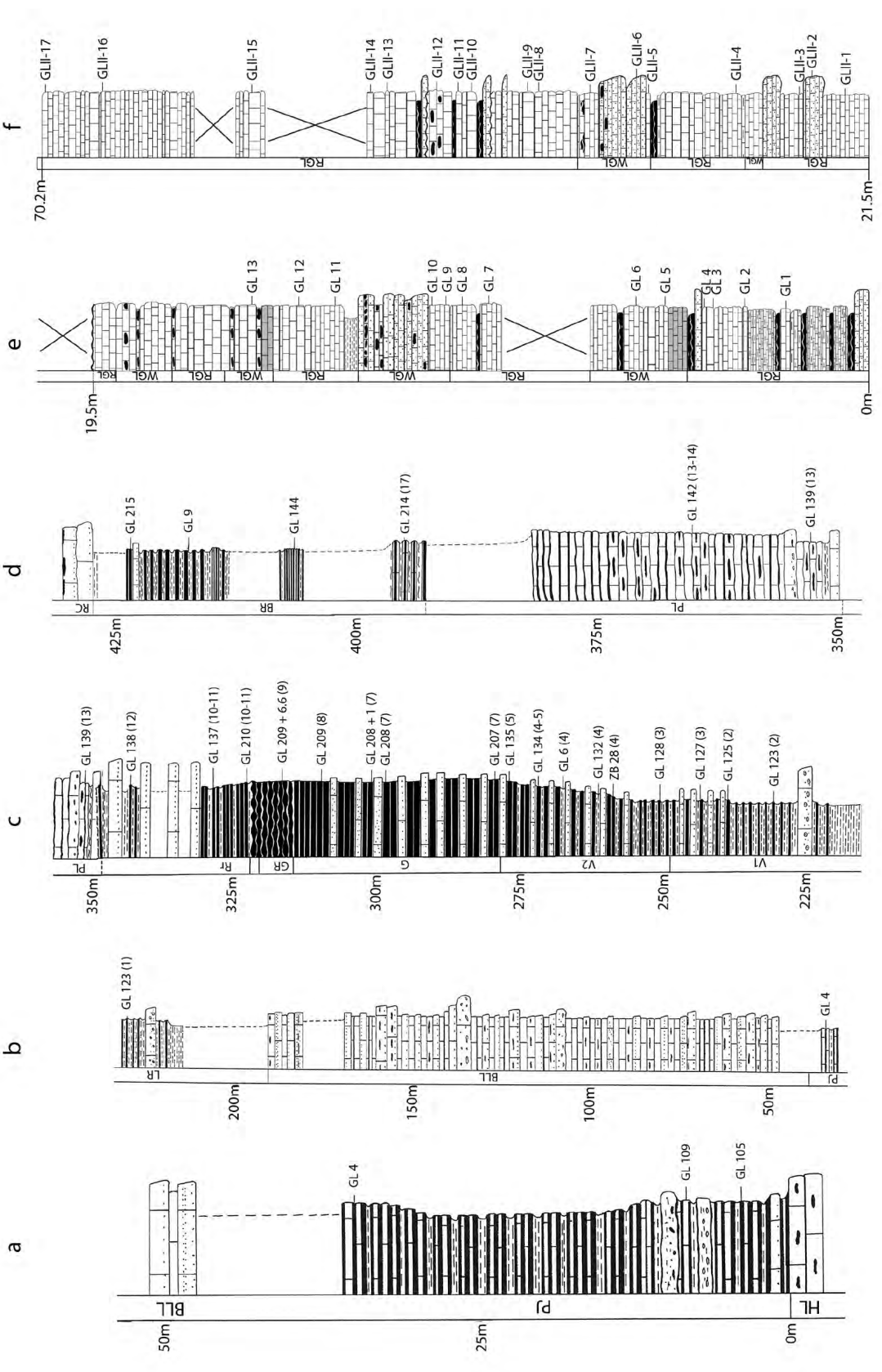

Figure 10: Lithological columns of the Gornja Lastva section (Stop 1). a) "Passée Jaspeuse" Formation, b) Bar Limestone, c) Lastva Radiolarite and transition to the Praevalis Limestone, d) Praevalis Limestone and Bijela Radiolarite, e, f) Globotruncana *limestone. Legend same as Figure 8. Note that the columns are not drawn at the same scale. Numbers in brackets refer to UA Zones of* Baumgartner *et al. (1995).*

Figure 11: Jurassic and Cretaceous formations of the Gornja Lastva section.
a) Thin-bedded siliceous limestone and intra-formational breccia with chert and micrite clasts in the "Passée Jaspeuse" formation.
b) Ripple marks in the Lower Bar Limestone Member.
c) Variegated facies of the Lastva Radiolarite.
d) Upper variegated radiolarite with a decimeter-thick bed of silicified calcarenite.
e) Bijela Radiolarite. Albian part in which the proportion of shale is the highest.
f) Bedded calcarenite with chert at the base of the Globotruncana *limestone.*

tion (Figure 11a). Three poorly preserved radiolarian assemblages were analysed from this section (Figure 10a; Goričan 1994). The samples GL 105 and GL 109 contain *Pantanellium tanuense* Pessagno & Blome, which is regarded as a Hettangian index (Pessagno et al. 1987; Carter et al. 1998). Sample GL 4 above contains the genus *Wrangellium*, whose first appearance is documented in the Late Sinemurian (O'Dogherty et al. 2009b).

The overlying Bar Limestone (Figure 10b) mostly consists of classical turbidites that start with a graded calcarenite unit. A few tens of centimeters thick bed of clast-supported conglomerate to pebbly calcarenite rarely occurs at the base. On the other hand, fine-grained turbidites composed of base-absent Bouma sequences are common and make up more than 10 meters thick packages. The entire succession is organized in roughly three larger fining-upward sequences.

This section is the type section of the Lastva Radiolarite, which here consists of the complete sequence of different facies from the lower variegated facies at the base to the red ribbon radiolarite at the top (Figures 10c, 11c, d). The lowermost productive sample GL 123, found 40 m above the top of the Bar Limestone, correlates with UA Zone 2 (Upper Aalenian) of Baumgartner et al. (1995). The uppermost sample GL 138, collected 8 m below the boundary with the Praevalis Limestone is assigned to UA Zone 12 (Lower – lower Upper Tithonian). The age assignments of all other productive samples, expressed in UA zones of Baumgartner et al. (1995), are indicated in Figure 10c. The chronostratigraphy of individual radiolarite facies and their correlation with other sections of the Budva Zone is shown in Figure 9.

The contact with the overlying Praevalis Limestone (Figure 10d) is sharp. Only the lowermost beds of micrite limestone with replacement chert nodules still contain some marly interlayers and also a thin bed of carbonate breccia. The remaining 30 m of the Praevalis Limestone are free of resedimented carbonates and consist of 5–15 cm thick beds of white or light reddish to greenish micrite and up to 5 cm thick beds, lenses and nodules of dark red replacement chert. The replacement chert makes approximately 30% of the succession. Radiolarians in sample GL 139 at the base of the formation correlate to UAZ 13 of Baumgartner et al. (1995).

The boundary with the Bijela Radiolarite (Figure 10d) is transitional and poorly exposed. The thickness of beds decreases, the silica content is higher and marly interlayers are present again. Sample GL 214 contains *Aurisaturnalis variabilis* (Squinabol) that is characteristic of the Hauterivian to early Barremian age. Higher up, the section consists of thin-bedded chert and 40–60% shale (Figure 11e). Silicified calcarenites are interstratified in the upper 8 meters of the formation. Based on *Thanarla spoletoensis* O'Dogherty, sample GL 215 near the top of the radiolarite is assigned to the Albian–lowermost Cenomanian Spoletoensis Zone of O'Dogherty (1994).

The following 70 meters of the section start with thick-bedded (60–100 cm) calcarenite with a high content of replacement chert (Figure 11f). The first planktonic foraminifera were found in light pink micrite approximately 2 m above the last thick calcarenite bed (Figure 10e, sample GL 1). The remaining part of the section consists of an alternation of *Globotruncana*-bearing micrite, marly limestone, cherts layers and calcarenite. Micritic limestone without fossils is also common. Higher in the section, reddish *Globotruncana* limestone prevails. The section is divided into several red (RGL - Red *Globotruncana* Limestone) and white to light ocher (WGL - White *Globotruncana* Limestone) units. The preliminary analysis of the planktonic foraminifera suggests that the age of the lower RGL part (Figure 10e) is Early Campanian based on rare occurrence of *Globotruncanita stuartiformis* (Dalbiez), abundant *Contusotruncana fornicata* (Plummer), *Globotruncana linneiana* (d'Orbigny), *Globotruncanita elevata*, abundant specimens of the genus *Planoheterohelix*, and the absence of marginotruncanids. Planispiral forms are also very common. The uppermost RGL towards the end of the section has abundant *Globotruncanita plummere* (Gandolfi), *Globotruncana bulloides* (Vogler) and a lesser amount of *G. elevata* (Brotzen). *Contusotruncana walfischensis* (Todd) and *Radotruncana subspinosa* (Pessagno) are also present in some samples, suggesting Late Campanian age. Further and more detailed analyses are in progress (by A.K.).

The Gornja Lastva village is built on the *Globotruncana* limestone, which is the uppermost stratigraphic unit at this locality. The Vrmac Mountain above the village belongs to the upper thrust sheet of the Budva Zone.

Stop 2: Petrovac

Lower tectonic unit, Upper Triassic to upper Aptian–lower Albian.

Location: near Petrovac, along the road from Petrovac to Podgorica, at the junction with the littoral road Budva – Bar; the section starts at N 42°12'39", E 18°56'41", Basic Geological Map sheet Budva (Antonijević et al. 1969).

The measured section consists of 35 m of the "Passée Jaspeuse", 50 m of the Bar Limestone, approximately 30 m of the Lastva Radiolarite and approximately 50 m

of the Praevalis Limestone in contact with the Bijela Radiolarite (Figures 12a–d). This succession is part of the reversed limb of a syncline, which, in addition, is intensely folded internally.

The Triassic cherty limestone at this section is well exposed in a thickness of nearly 150 m and ranges from the Middle Triassic to the Rhaetian (Cafiero & De Capoa Bonardi 1980, 1981; Goričan 1994). The "Passée Jaspeuse" contains a relatively high proportion of carbonate and is lighter in colour than in the other sections. The transition with the underlying and also with the overlying formation is thus more gradual. The sample PK 20 near the top of the formation (Figure 12a) includes the genus *Gigi*, whose FAD is in the Lower Pliensbachian (O'Dogherty et al. 2009b). It is thus possible that the "Passée Jaspeuse" ranges to the base of the Pliensbachian.

The Bar Limestone is only 50 m thick and consists of fine, often faintly laminated cherty limestone with thin interbeds of marl. In the slightly reddish upper part, bioturbation is frequent. The entire sequence is characterized by a uniform basin-plain facies association.

The overlying green and violet shale is supposedly Early Toarcian in age (Figure 13). A breccia, consisting of large blocks of limestone, radiolarite and shale follows upsection. It wedges out in a distance of a few meters. Blocks and clasts of Upper Triassic limestones are the most abundant and evoke the Hallstatt Limestone of the Northern Calcareous Alps. The Lower Norian components consist of grey radiolarian-filament bearing wackestones and correspond to the Massiger Hellkalk. The upper Lower Norian to Middle Norian components are red radiolarian-filament limestone with small chert nodules corresponding to the Hangendrotkalk. The Upper Norian to Lower Rhaetian components are radiolarian wackestones with rare filaments corresponding to the Hangendgraukalk. Rhaetian conodonts appear in grey siliceous radiolarian-rich wackestones. Spicules-rich grey siliceous components are most likely of Early Jurassic age. The reworked sed-

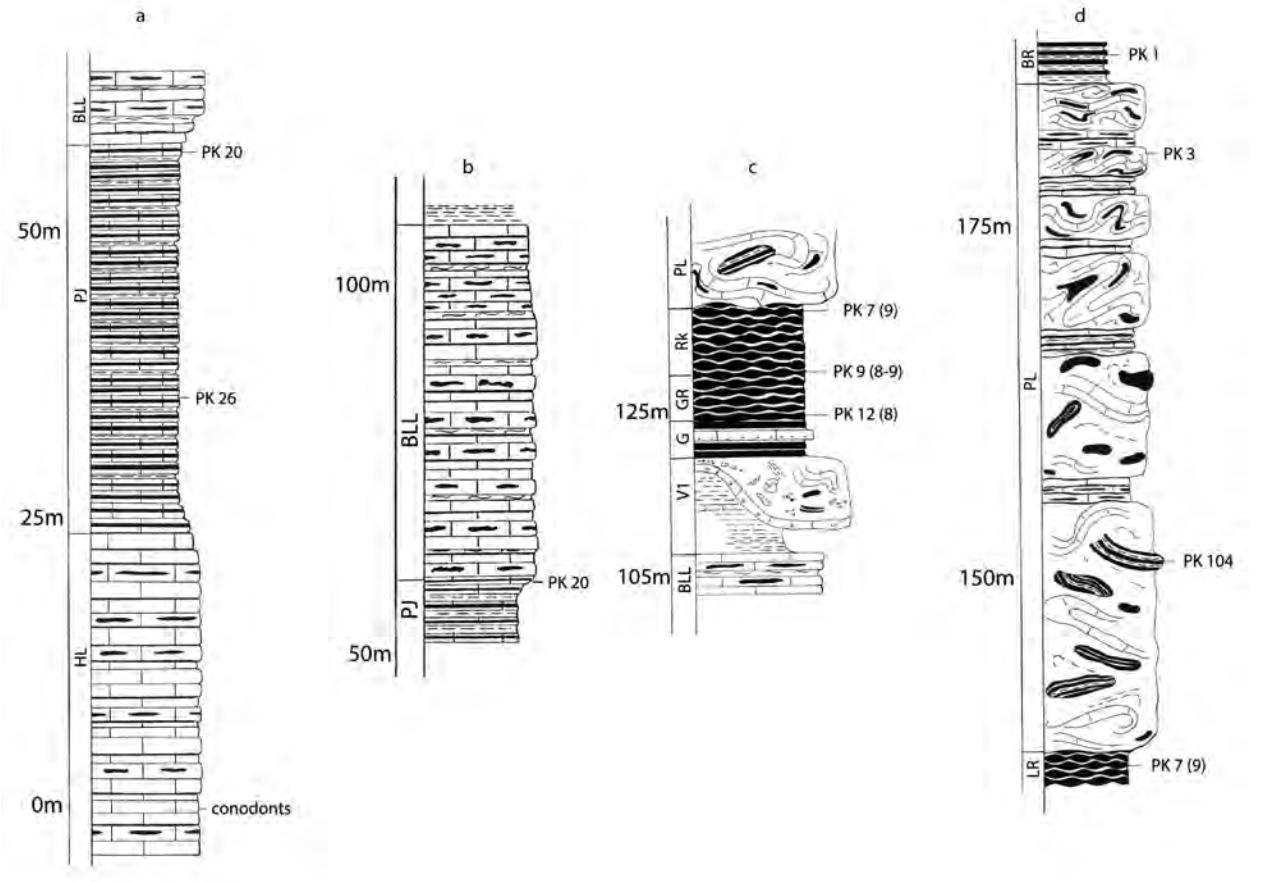

Figure 12: Lithological columns of the Petrovac section (Stop 2). a) "Passée Jaspeuse" Formation, b) Bar Limestone, c) Lastva Radiolarite and base of the Praevalis Limestone, d) Praevalis Limestone and base of Bijela Radiolarite. Legend same as Figure 8. Note that the columns are not drawn at the same scale. Numbers in brackets refer to UA Zones of Baumgartner et al. (1995).

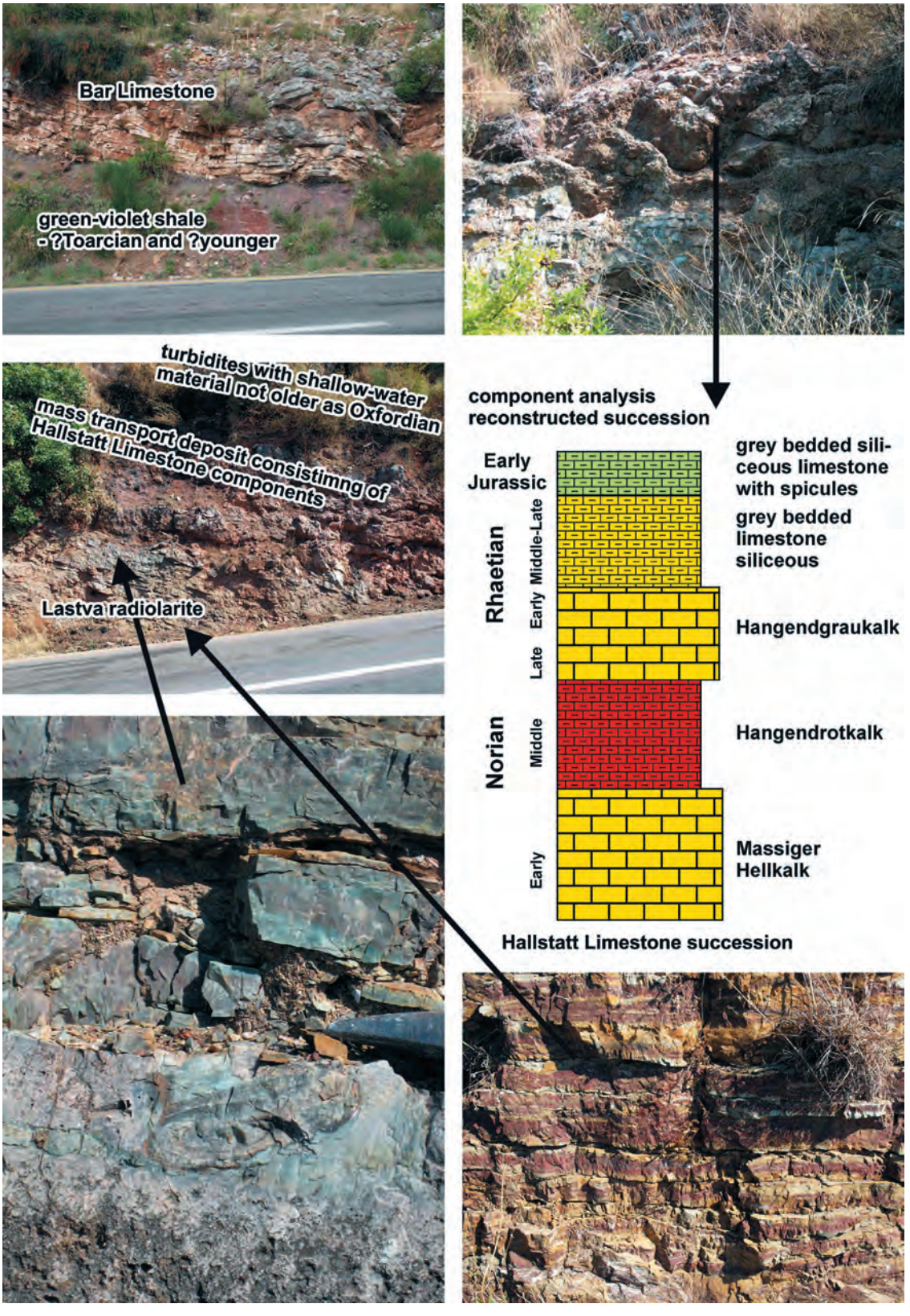

Figure 13: Jurassic formations of the Petrovac section and reconstruction of the Upper Triassic succession reworked in the Jurassic breccia. Explanation on the photographs. Note the section is in overturned position.

imentary sequence resembles a classical Hallstatt Limestone succession as known in the whole western Tethys realm (Krystyn 2008). Redeposition of this Hallstatt Limestone sequence is age equivalent with the Hallstatt Mélanges known in all mountain ranges in the eastern Mediterranean (Gawlick & Missoni 2019 and references therein). Similar Hallstatt Limestone successions are also known in the Budva unit, e.g. in the Čanj embayment (Gawlick & Missoni 2015). Below the mass transport deposit with the Hallstatt Limestone components turbiditic layers with ooids and other shallow-water grains, including *Protopeneroplis* sp., occur.

The Lastva Radiolarite consists of three facies: green, green-red knobby and red knobby radiolarite and ranges from UA Zone 8 (middle Callovian – early Oxfordian) in sample PK 12 to UA Zone 9 (middle–late Oxfordian) in sample PK 7 (Figure 12b). These data clearly show that the base and the top of the radiolarite sequence are cut-off (Figure 9).

The most conspicuous feature of the Petrovac section is thick chaotic beds of the Praevalis Limestone (Figure 12d). They are 1 m to several meters thick, separated by a few tens of centimeters of undisturbed bedded limestone. The encompassed cherts show considerable deformation; they have a form of ruptured, folded layers or rotated nodules (Figures 14a, b). In the lower part of the section, up to 1 m large clasts of Tithonian ribbon radiolarite are incorporated in these megabeds (Figure 14a). The chaotic beds at Petrovac are interpreted as highly evolved slumps to debris-flow deposits, which moving downslope eroded the underlying sediments. The base of the overlying Bijela Radiolarite (sample PK 1) is assigned to the upper Aptian-lower Albian based on *Turbocapsula costata* (Wu).

Stop 3: Čanj

Lower tectonic unit, Rhaetian to Campanian.

Location: two nearby localities near the tourist village Čanj: Pečinj Bay (N 42°09'40", E 18°59'30" E) for the Rhaetian to Pliensbachian, Čanj Beach (N 42°09'45", E 18°59'43") for the Middle Jurassic to Upper Cretaceous; Basic Geological Map sheets Budva (Antonijević et al. 1969) and Bar (Mirković et al. 1968).

The section consists of the *Halobia* limestone, 30 m of the "Passée Jaspeuse", 150 m of the Bar Limestone, 80 m of the Lastva Radiolarite (including a 20 m thick unit of resedimented carbonates), 20 m of the Praevalis Limestone, approximately 50 m of the Bijela Radiolarite, and more than 30 m of the *Globotruncana* limestone (Figures 15a–e).

The *Halobia* limestone consists of cherty micrite and fine-grained resedimented limestone beds (Figure 16a). Slump and intra-formational debris-flow deposits containing clasts of red chert occur in the upper part (Figures 15a, 16b). Thin marly intercalations are common between pelagic limestone beds. The overlying "Passee Jaspeuse" is an easily mappable dark brownish-reddish unit of siliceous limestone alternating with shale (Figures 16 c–e). Texturally, these highly siliceous limestones are mostly calcisiltites or mudstones to packstones containing radiolarians. A few beds with clasts of siliceous limestone are present in the middle part of the formation where slump folds also occur and the amount of interstratified shale is the highest (Figure 15a). Near the top of the "Passée Jaspeuse", the limestone beds are thicker and the carbonate content is higher.

A detailed 20 m thick section across the boundary between the *Halobia* limestone and the "Passée Jaspeuse" was measured and sampled bed by bed for radio-

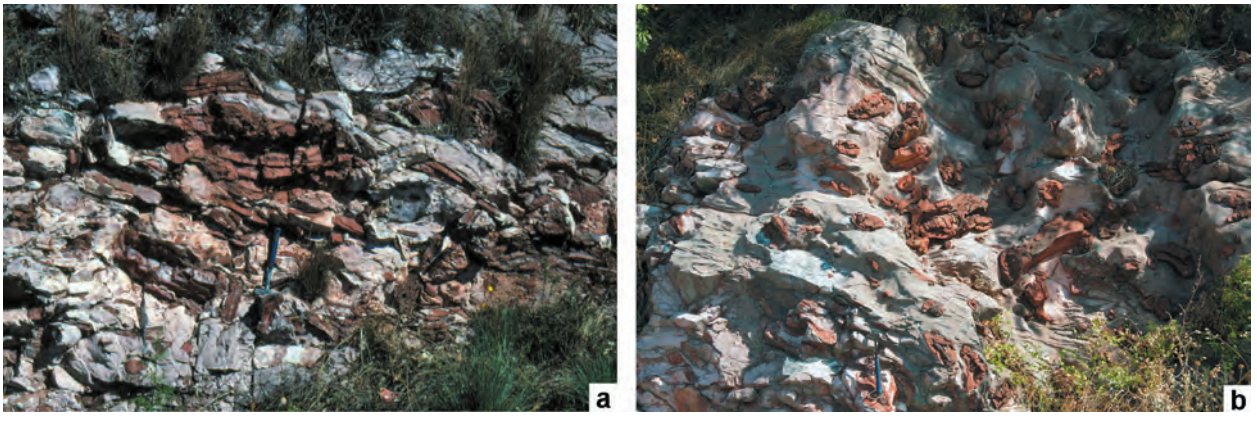

Figure 14: Lower Cretaceous Praevalis Limestone Formation, Petrovac section.
a) Large clasts of Tithonian ribbon radiolarite in the lower part of the formation (at 152 m in the lithological column, Figure 12d).
b) Folded chert layers and rotated nodules float in a deformed micritic matrix (at 160 m in the lithological column, Figure 12d).

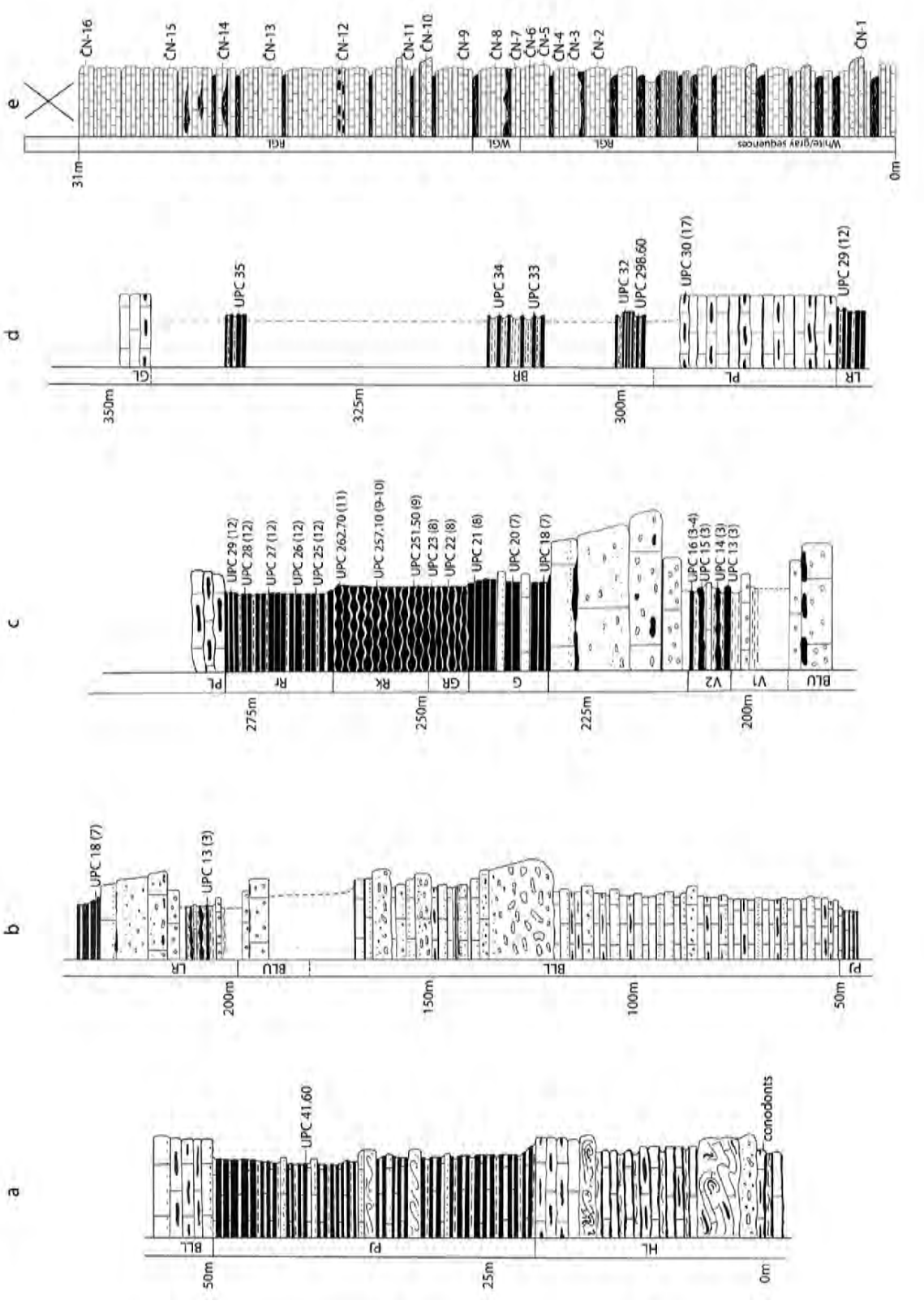

Figure 15: Lithological columns of the Čanj section (Stop 3). a) "Passée Jaspeuse", b) Bar Limestone, c) Lastva Radiolarite, d) Praevalis Limestone and Bijela Radiolarite, e) Globotruncana *limestone. Legend same as Figure 8. Note that the columns are not drawn at the same scale. Numbers in brackets refer to UA Zones of* Baumgartner *et al. (1995).*

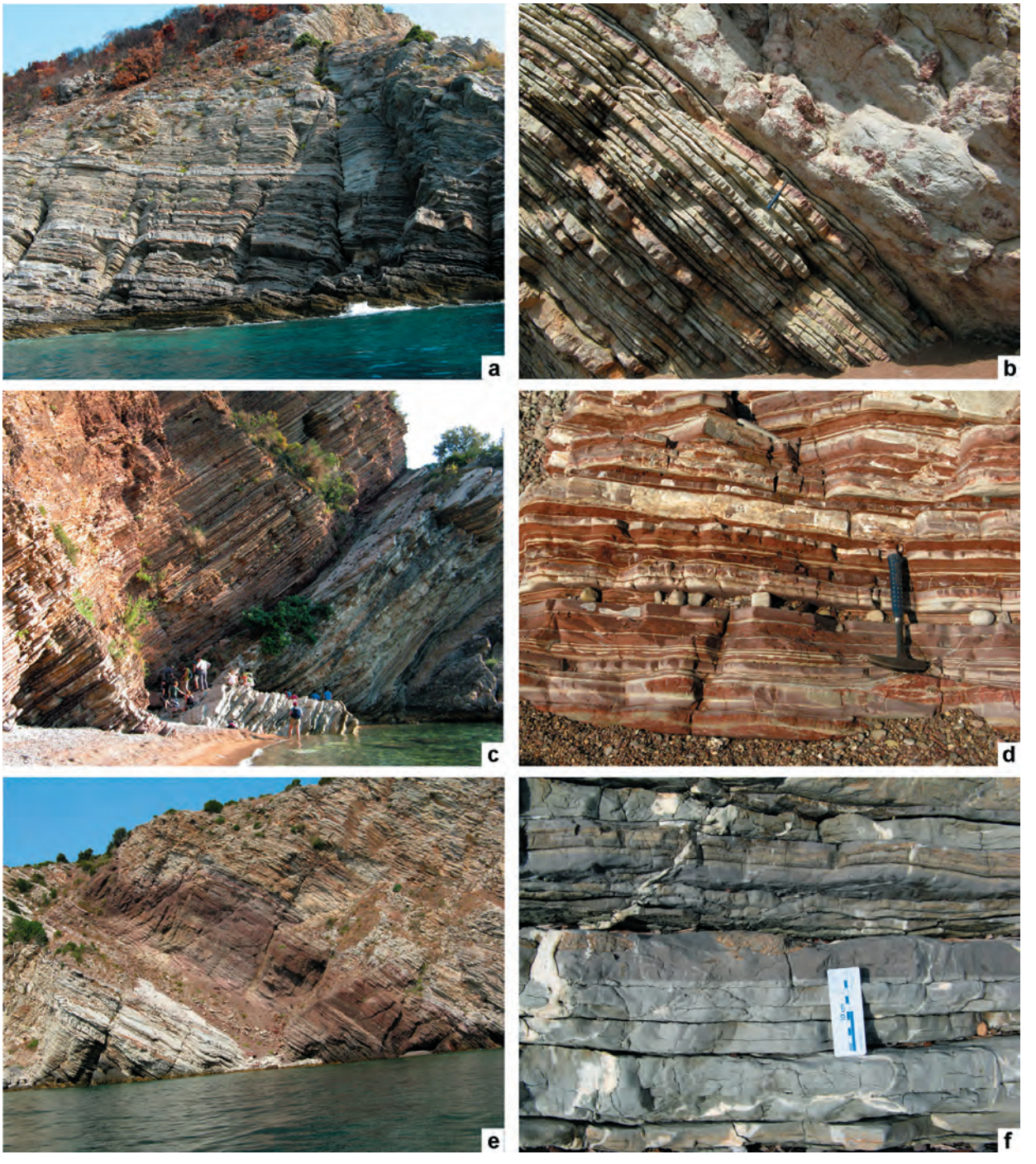

Figure 16: Upper Triassic and Lower Jurassic formations of the Čanj section.
a) Halobia *limestone; micrite with chert nodules.*
b) Closer view of the Halobia *limestone 20 m below the boundary with the "Passée Jaspeuse". Limestone beds separated by thin marly interlayers; base of an intraformational debris-flow conglomerate with clasts of red chert visible on the right.*
c) Well-exposed contact between the Halobia *limestone and the "Passée Jaspeuse". The section of Figure 17 was measured at this outcrop.*
d) Siliceous limestone and marl of the "Passée Jaspeuse".
e) The brownish unit in the middle part of the photograph is the 30 m thick "Passée Jaspeuse", which lies between the Halobia *limestone below and the Bar Limestone above.*
f) Lime-mud dominated turbidites in the lower part of the Lower Bar Limestone Member.

larians and stable carbon isotope analyses (Črne et al. 2011). The sharp lithological boundary coincides with the Triassic–Jurassic boundary as determined with radiolarians of the *Globolaxtorum tozeri* Zone near the top of the *Halobia* limestone and radiolarians of the *Canoptum merum* Zone at the base of the "Passée Jaspeuse" (see Figure 17 for the position of productive radiolarian samples). Faunal changes across the system boundary are comparable to those recognized in Haida Gwaii, British Columbia, and in Japan (Carter & Hori 2005; Longridge et al. 2007). A negative spike in the stable carbon isotope curve, measured in bulk carbonate and in bulk organic matter, was detected at the very base, in the boundary shales of the "Passée Jaspeuse" and is coincident with the rapid drop in carbonate content from more than 80 % to less than 10 % (Figure 17). The contemporaneous negative anomaly in both, bulk carbonates and bulk organic matter, as well as the comparison with other stable carbon isotope records across the Triassic–Jurassic boundary confirm that the anomaly reflects a global perturbation of the carbon cycle. The simultaneous drop in carbonate content can be a result of accelerated carbonate dissolution, or more probably a consequence of reduced carbonate input due to a biocalcification crisis. A biocalcification crisis *sensu lato* includes not only a

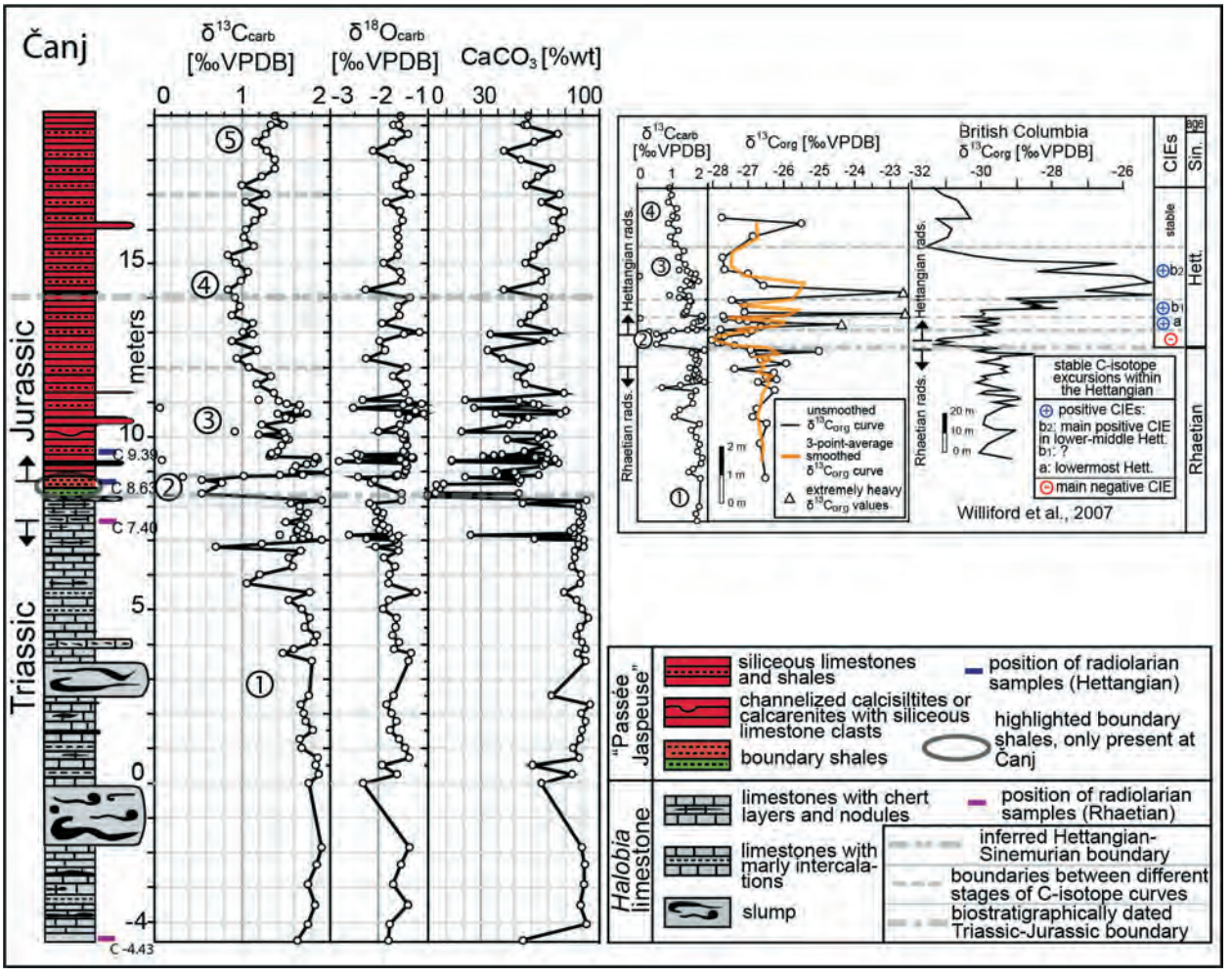

Figure 17: (reproduced from Črne et al. 2011):
Detailed stratigraphic log of the Triassic–Jurassic boundary section with stable carbon and oxygen isotope curves, carbonate content curves and marked position of radiolarian samples (red and blue bars with sample numbers). The intervals of the carbon isotope curve (1–5) were correlated with the published curves; the position of the Hettangian–Sinemurian boundary, 5.5 m above the Triassic–Jurassic boundary is based on this correlation.
Upper right frame: Stable carbon isotope curves for bulk carbonate (δ13Ccarb) and bulk organic matter (δ13Corg) from Čanj section and comparison with stable carbon isotope curve from bulk organic matter in British Columbia (Williford et al. 2007). The Triassic–Jurassic boundary of both sections is precisely dated with radiolarians.

lowered production of shallow-water carbonate but also a change in the carbonate production mode from skeletal to microbial, which would have equally led to reduced offshore shedding. Both scenarios are compatible with increased CO_2, SO_2 and CH_4 fluxes due to the Central Atlantic magmatic province volcanism causing undersaturation of ocean with respect to calcium carbonate (see Črne et al. 2011, for more details).

The lower half of the Lower Bar Limestone Member (Figure 15b) is dominated by fine-grained turbidites organized in base-cut-out Bouma sequences (Figure 16f). Medium-grained turbidites prevail in the upper part. Four levels of clast-supported conglomerates capped by normally graded pebbly mudstone are intercalated. The thickest conglomerate bed reaches 16 m and consists of large (up to 20x50 cm) densely packed calcilutite clasts (when visiting this stop, note that some plurimetric blocks broken off the thickest conglomerate unit are nicely exposed on the beach). These conglomerate levels are distal equivalents of disorganized debris-flow breccias exposed at the Sutomore section, which is located in close vicinity but is part of the upper tectonic unit (see figure 2.2 in Goričan 1994, for the correlation of these two sections).

The Upper Bar Limestone Member, well distinguished by its pure oolitic limestone beds constitutes a few-meters thick unit above a covered interval and below the first outcropping radiolarian chert (Figure 15b). Another 20 m thick unit of oolite, coarse-grained graded conglomerate and calcarenite is interstratified in the Lastva Radiolarite (Figures 15b, c); this unit was

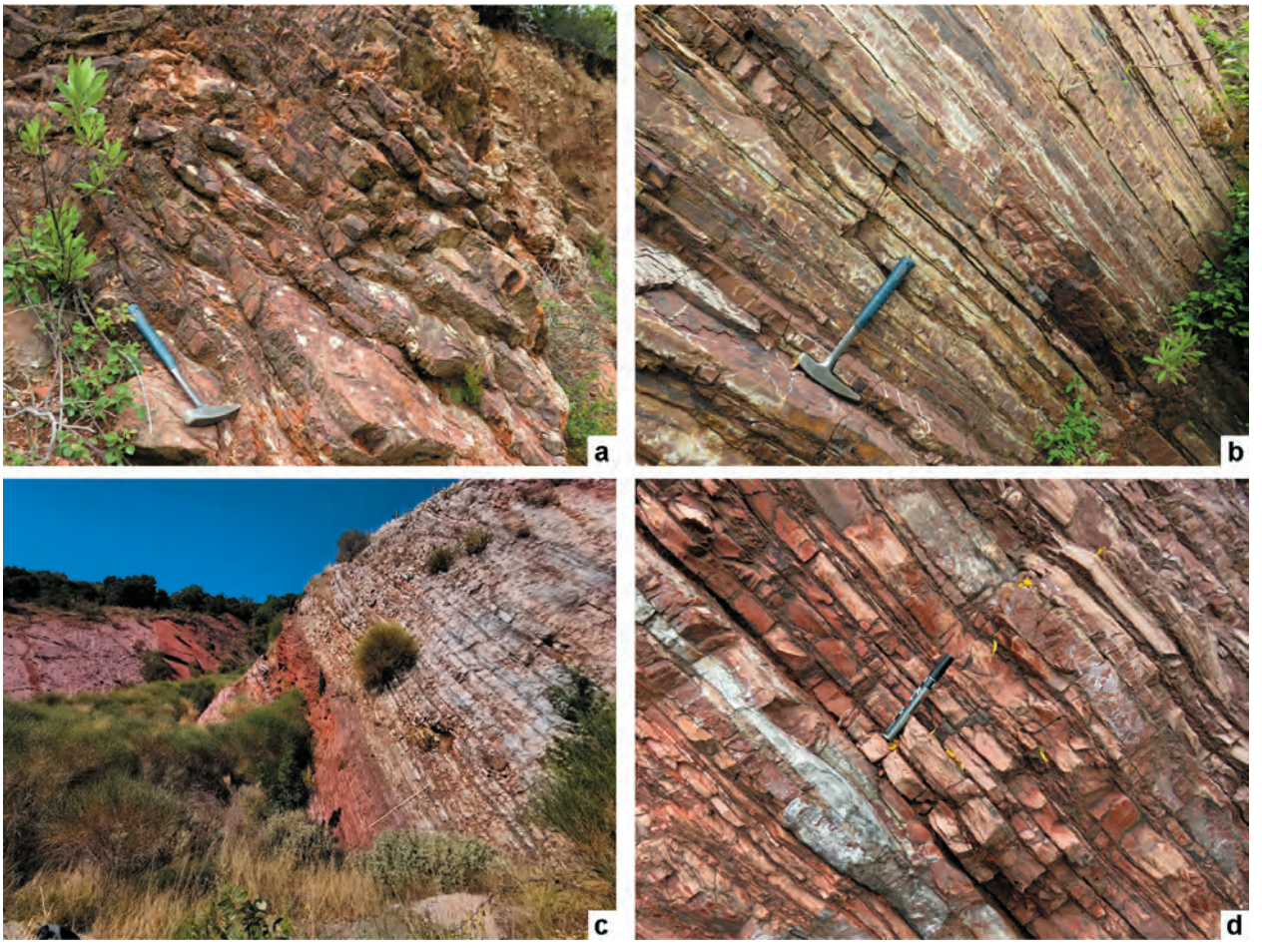

Figure 18: Upper Jurassic and Upper Cretaceous formations of the Čanj section.
a) Lastva Radiolarite Formation, red knobby radiolarite, Oxfordian–Kimmeridgian.
b) Lastva Radiolarite Formation, red ribbon radiolarite, Lower Tithonian.
c) Red and white units of the Globotruncana *limestone. The red limestone visible as dip slope in the background belongs to the Lower Cretaceous Praevalis Limestone. The mostly covered depression between the two formations corresponds to the Bijela Radiolarite.*
d) Siliceous limestone of the lower red unit of the Globotruncana *limestone.*

interpreted as a single compound gravity-flow deposit. Middle–late Bajocian radiolarians (UAZ 3 of Baumgartner et al. 1995) were found in the variegated radiolarite below the oolite. Latest Bathonian–Callovian radiolarians (UAZ 7 were found in the green radiolarite above. The remaining few meters of green radiolarites, also assigned to UAZ 7, include beds of silicified calcarenite, but the following red-green and red radiolarites (Figures 18a, b) are devoid of resedimented carbonates. The uppermost sample collected in red ribbon radiolarite 0.5 m below the boundary with the Praevalis Limestone belongs to the Lower to lower Upper Tithonian UAZ 12. For the age assignments of all productive radiolarian samples, expressed in UA zones see Figure 15c. The chronostratigraphy of individual radiolarite facies and their correlation with other sections of the Budva Zone is shown in Figure 9.

The Praevalis Limestone consists of reddish micrite with red replacement chert lenses. The overlying Bijela Radiolarite is poorly exposed; its thickness was estimated to 50 meters (Figure 15d). The radiolarian assemblage in sample 298.60 near the base of the formation contains *Aurisaturnalis carinatus perforatus* Dumitrica & Dumitrica Jud, whose range is restricted to the Upper Barremian – Lower Aptian (Dumitrica & Dumitrica Jud 1995). The topmost sample contains *Hemicryptocapsa polyhedra* Dumitrica and *Afens liriodes* Riedel & Sanfilippo that first appear in the lower Turonian (O'Dogherty 1994) together with abundant *Pseudodictyomitra pseudomacrocephala* (Squinabol) that last appears in the Turonian (Pessagno 1977). The Turonian age is the youngest age recorded in the Bijela Radiolarite (Figure 9). In comparison with other sections so far studied in the Budva Zone, the Čanj section is the only section where the entire Berriasian to Turonian succession consists exclusively of distal pelagic facies (radiolarite and pelagic limestone) without carbonate gravity-flow deposits.

The overlying *Globotruncana* limestone is subdivided into several reddish to light pink and white units (Figures 15e, 18c, d). The studied section is 31 m thick and starts with several 10 cm to 18 cm thick layers of white-gray micrite. Upward, these limestone layers reach thickness of up to 70 cm and are interbedded with thin horizons of dark gray chert and layers of resedimented carbonates up to 20 cm thick (Figure 15e; White/gray sequences). The occurrence of Upper Cretaceous planktonic foraminifera in this part of the section is rare. The exception is the first resedimented carbonate layer (Figure 15e; ČN-1), where the assemblage of planktonic foraminifera such as *Globotruncanita elevata* (Brotzen), the high abundance of *Globotruncana linneiana* (d'Orbigny), and the low abundance of *Globotruncanita stuartiformis* (Dalbiez) indicate the Early Campanian age. The following unit is an 8.4 m thick package of alternating reddish and light pink micrite (up to 20 cm thick), thin layers of reddish marly limestones, and layers of gray to reddish chert up to 30 cm thick. Planktonic foraminifera were not found in these beds. The following sequence is composed of reddish to light pink *Globotruncana* limestones (RGL), red chert beds and pink calcarenite layers with red grains. This RGL section is interrupted once by a 1.5 m thick sequence of white-grey to light ocher *Globotruncana* limestone and chert (WGL). The first occurrence of *Globotruncanita atlantica* (Caron) in the lower RGL section (Figure 15e; ČN-6) confirms the Early to Middle Campanian age. In the WGL beds (Figure 15e; ČN-8) zonal marker *Contusotruncana plummerae* (Gandolfi) appears for the first time and is present throughout the upper RGL section along with abundant *Globotruncanita stuartiformis* (Dalbiez) and decreased amount of *G. elevata* (Brotzen), suggesting the Late Campanian age. The research on the Upper Cretaceous of the Budva Zone is in progress (by A.K.). Since Coniacian and Santonian ages have not been documented, we plan to examine more closely especially the transition from the Bijela Radiolarite to the *Globotruncana* limestone.

Stop 3-supplement: Čanj center

Middle Triassic chert in a thrust sheet above the main Čanj section.

Location: Čanj village, in front of hotel Jadranski Biser (N 42°09'46", E 18°59'38"). Basic Geological Map, sheet Bar (Mirković et al. 1968).

Ladinian radiolarites occur in a deep-water succession, comparable to the succession of the outer shelf facies in the Northern Calcareous Alps and Inner Dinarides (stratigraphic log in Figure 19). Radiolarians of the Upper Ladinian *Muelleritortis cochleata* Zone (Kozur & Mostler 1994) were found in the red radiolarian cherts.

Stop 4: Markovići

Lower tectonic unit, Middle Triassic.

Location: on the road from Budva to Cetinje, about 8.5 km NE from Budva (N 42°18'06", E 18°51'25", Basic Geological Map sheet Budva (Antonijević et al. 1969).

The section consists of three units – the Tuđemili Formation in the lower part, a megabreccia in the middle, and tuffitic layers of Pietra Verde in the upper part of the section (Figure 20).

The Tuđemili Formation in this section is represented by alternation of fine calcarenites with marly layers, 19 meters in thickness, representing the distal part of this formation. Otherwise very fossiliferous, the outcrop of this formation in Markovići does not contain any megafossils. In other localities the formation is well dated with crinoids, bivalves and brachiopods (Dimitrijević 1967), and recently with ammonoids (Đaković 2018) of Pelsonian age.

Overlying the Tuđemili Formation is a megabreccia, 8 meters thick. The matrix of this bed is a gray clayey-marly sediment, similar to marls of the underlying Tuđemili Formation. Blocks in this bed are built of Permian reefal limestones (Krystyn, personal communication) along with crinoidal and brachiopod limestones, nodular limestones with ammonoids, shallow water limestones etc., all of Anisian age. A block of nodular limestone contains ammonoid species *Gymnites toulai*, *Metasturia gracilis*, *Acrochordiceras* sp. etc., of Pelsonian age (Đaković, unpublished). Considering that the limestones blocks from this megabreccia do not contain any fossils younger than Pelsonian, the assumed age of the matrix is Illyrian.

The upper part of the succession is separated by a subvertical fault from the underlying breccia and is built of green tuffs, the so-called Pietra Verde, approximately 30 m thick. This uniform series contains rare interlayers of chert or limestone, but without recognizable fossils in the Markovići section. As already indicated, Cafiero & De Capoa Bonardi (1980) described bivalves of latest Ladinian age from the uppermost part of this sequence in Bečići.

The section ends at a thrust contact with the Bijela Radiolarite. A sample in this radiolarite contained *Pseudodictyomitra macrocephala* (Squinabol) and other typical mid-Cretaceous taxa. No radiolarians have so far been extracted from the Triassic rocks of the Markovići section.

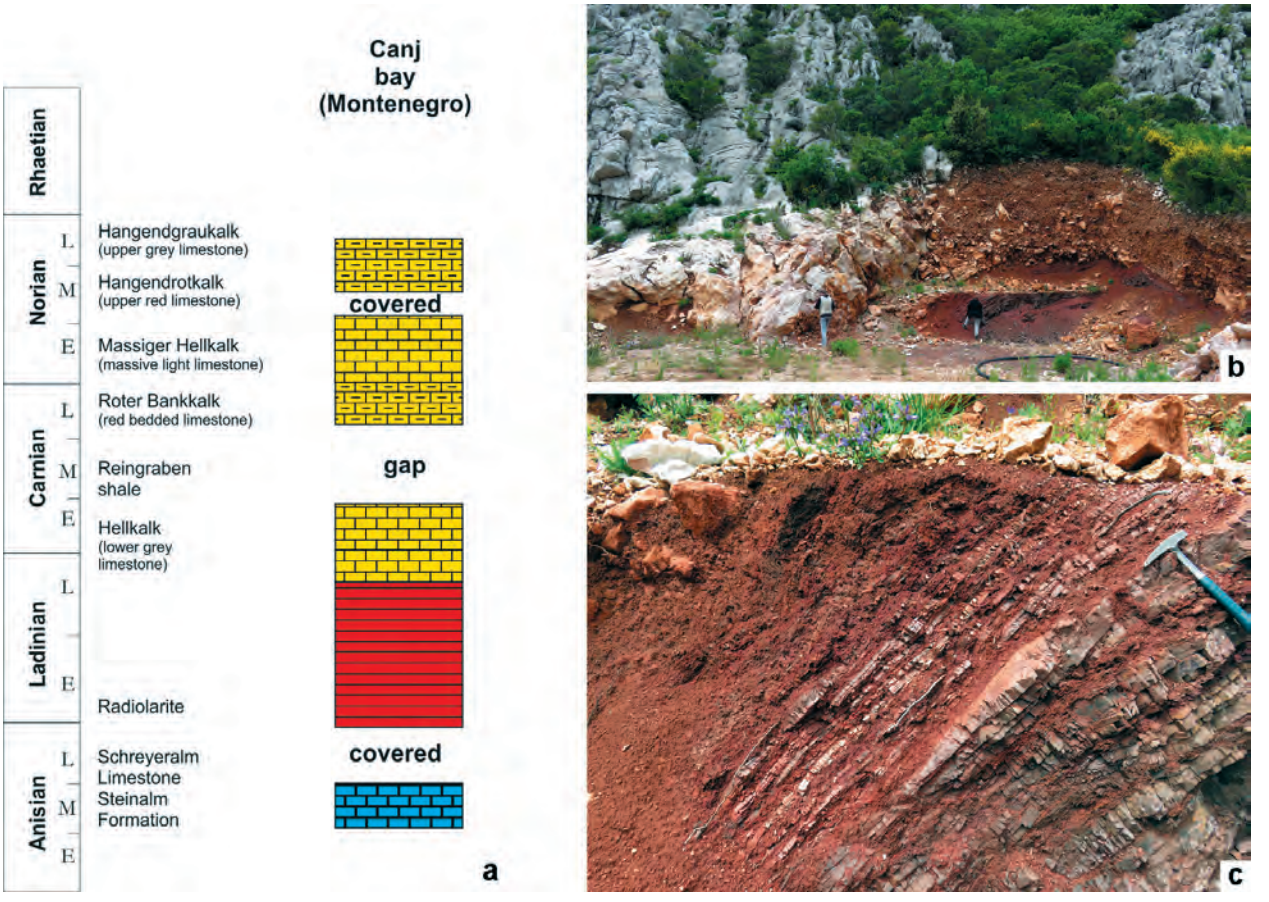

Figure 19: Triassic radiolarite in the center of village Čanj. Stratigraphic position (a), general view (b) and detail of the outcrop (c). The lithological column (a) according to Gawlick & Missoni (2015).

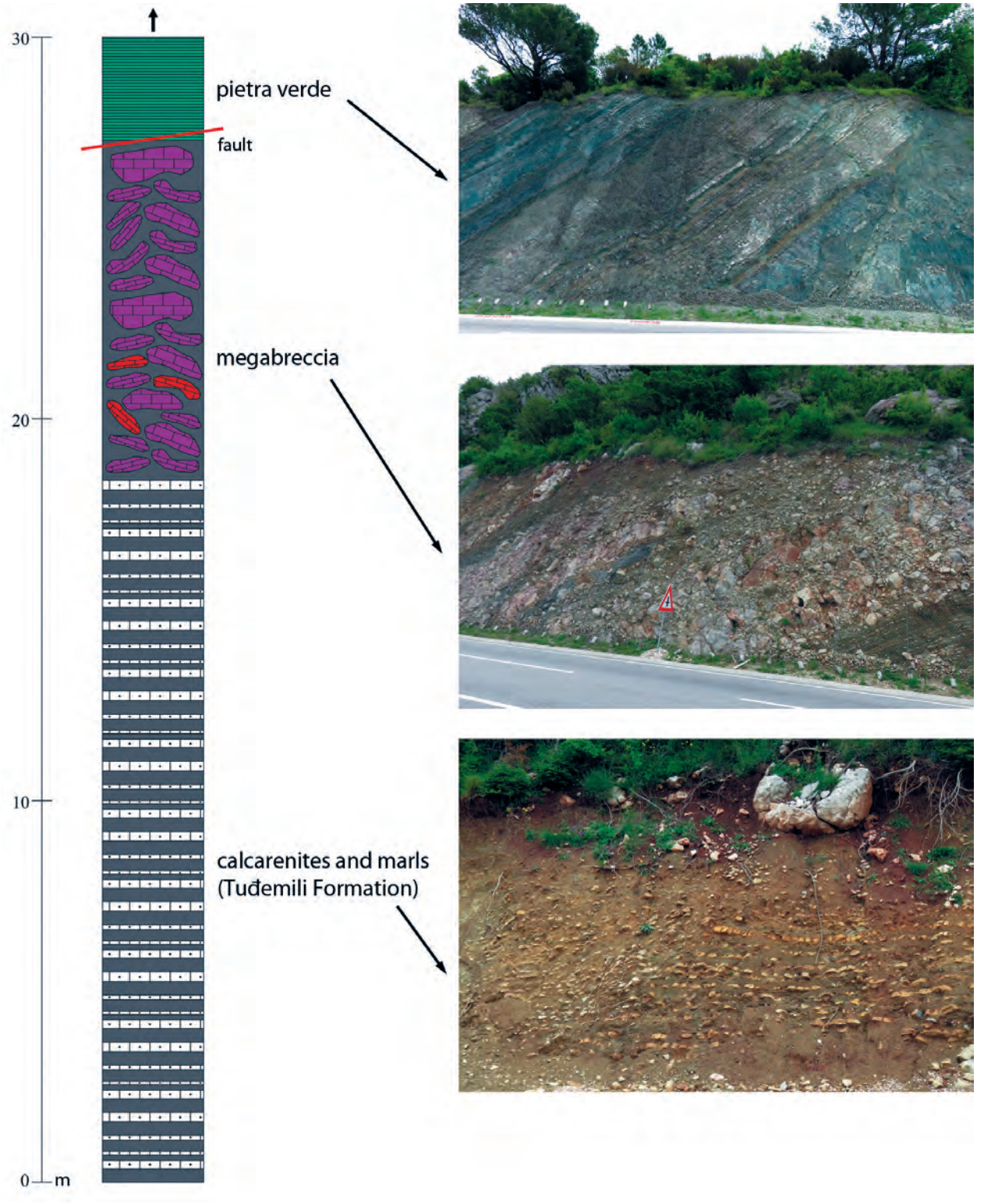

Figure 20: Lithological column of the Markovići section and field photographs of the three stratigraphic units.

Sedimentary evolution of the Budva Basin and correlation with the High Karst Carbonate Platform

Different localities across the Budva Zone preserve Mesozoic carbonate-gravity flow deposits as well as fully pelagic sequences. The correlation among these successions allows us to make inferences on local factors controlling the carbonate supply from the adjacent platform, and on regional Tethyan-wide paleoceanographical conditions affecting pelagic sedimentation.

During the Early Triassic, the areas of the present Budva and High Karst zones were occupied by a uniform sedimentation of red marine sandstones, dolomites and marly limestones (Živaljević 1989). The differentiation of this paleogeographic realm started in the Anisian with the deposition of limestone conglomerates (the Crmnica Formation) and mixed carbonate-siliciclastic Tuđemili Formation formerly known under the name "Anisian flysch". These deposits are overlain by volcanic and volcaniclastic rocks associated with limestone and chert.

A different opinion on the onset of subsidence was recently proposed by Krystyn et al. (2019) describing deeper water facies in the Lower Triassic of the Budva Zone, containing conodonts and ammonoids (Đaković et al. 2022). These sediments differ from time equivalent Werfen type deposits that can be found withing the High Karst in Brajići (Antonijević 1969) or elsewhere in the Dinarides (e.g. Aljinović et al. 2018). This would imply that the Budva Basin was already differentiated from the High Karst zone in the Smithian and that Crmnica and Tuđemili formations belong exclusively to the Budva Zone (Krystyn et al. 2019). Cherty limestones of Bithynian age, containing ammonoids and conodonts, have also been described from the Budva Zone (Đaković et al. 2018), representing a deeper water facies than the time equivalent rocks of the High Karst Zone (e.g. Čađenović et al. 2014).

The Budva Basin remained a deep-sea trough through the entire Mesozoic. In the Triassic and Jurassic, the great majority of carbonate mud in deep-sea sediments was of platform origin. It was not until the latest Jurassic that calcareous nannoplankton had their first bloom and not until mid-Cretaceous that planktonic foraminifera became an important component of pelagic limestones. The proportion of biogenic silica in sediments of deep continental-margin basins was thus primarily determined by the amount of lime mud shed from the adjacent platforms; this platform/basin correlation is well perceivable in Mesozoic deposits of the Budva Zone (Figure 21).

The prominent Rhaetian–Hettangian facies change from pelagic limestones to carbonate-poor siliceous deposits is correlated to the facies change on the margin of the High Karst Carbonate Platform, where the thick-bedded Upper Triassic Dachstein limestone with abundant Rhaetian fauna is overlain by medium-bedded Lower Jurassic micritic limestones containing almost exclusively peloids and only rare foraminifera (Črne & Goričan 2008). This facies change marks the drowning of the southwestern part of the High Karst Carbonate Platform. The drowning event on the platform margin was possibly amplified by accelerated tectonic subsidence and a sea-level rise.

The carbonate production on the platform was restored by the end of the Sinemurian. The margin of the High Karst Carbonate Platform was a southwest dipping ramp with lithiotid limestones in the inner ramp, peloidal packstones in mid-ramp and peloidal packstones with abundant chert in outer ramp; ooid banks formed in the mid-ramp setting in times of warm climate and high sea-level temperatures, i.e. in the late Early Pliensbachian (Črne 2009). During the Early Toarcian, the platform margin was flooded again; marls and marly limestones accumulated. The recovery phase from the middle Toarcian to the Aalenian was marked by deposition of bioclastic limestone with echinoderm fragments, brachiopods and filaments (Črne & Goričan 2008; Črne 2009).

The Early Toarcian flooding corresponds to the boundary between the Lower and the Upper Bar Limestone members. The Upper Member differs from the Lower Member by a higher proportion of ooids, coarser grain-size, thicker bedding and less lime-mudstone beds associated. Thick pure oolitic beds are present. Laterally, it is less expanded than the Lower Member (Figure 21). The differences in composition and lateral distribution were caused by a reorganization of the platform margin after the Toarcian. The Pliensbachian low relief carbonate ramp with smaller discontinuous oolitic shoals supplied large volumes of detritus to the relatively gentle slope and to the basin. The Middle Jurassic platform margin, in contrast, was dominated by oolitic bars (Radoičić 1982), which provided the major platform component displaced to the basin. In addition, they seem to have trapped and hampered the transport of lagoonal-mud offshore. As a consequence, the gravity flows travelled shorter distances, produced steeper slopes, and allowed the accumulation of lime-free radiolarite (Lastva Radiolarite) distally.

A radical change in platform margin architecture took place at the beginning of the Late Jurassic with the development of a coral-stromatoporoid reef complex (Radoičić 1982). Early cementation welded the reef margin into a rigid wave-resistant mass, which efficiently blocked the offshore sediment transport. The Oxford-

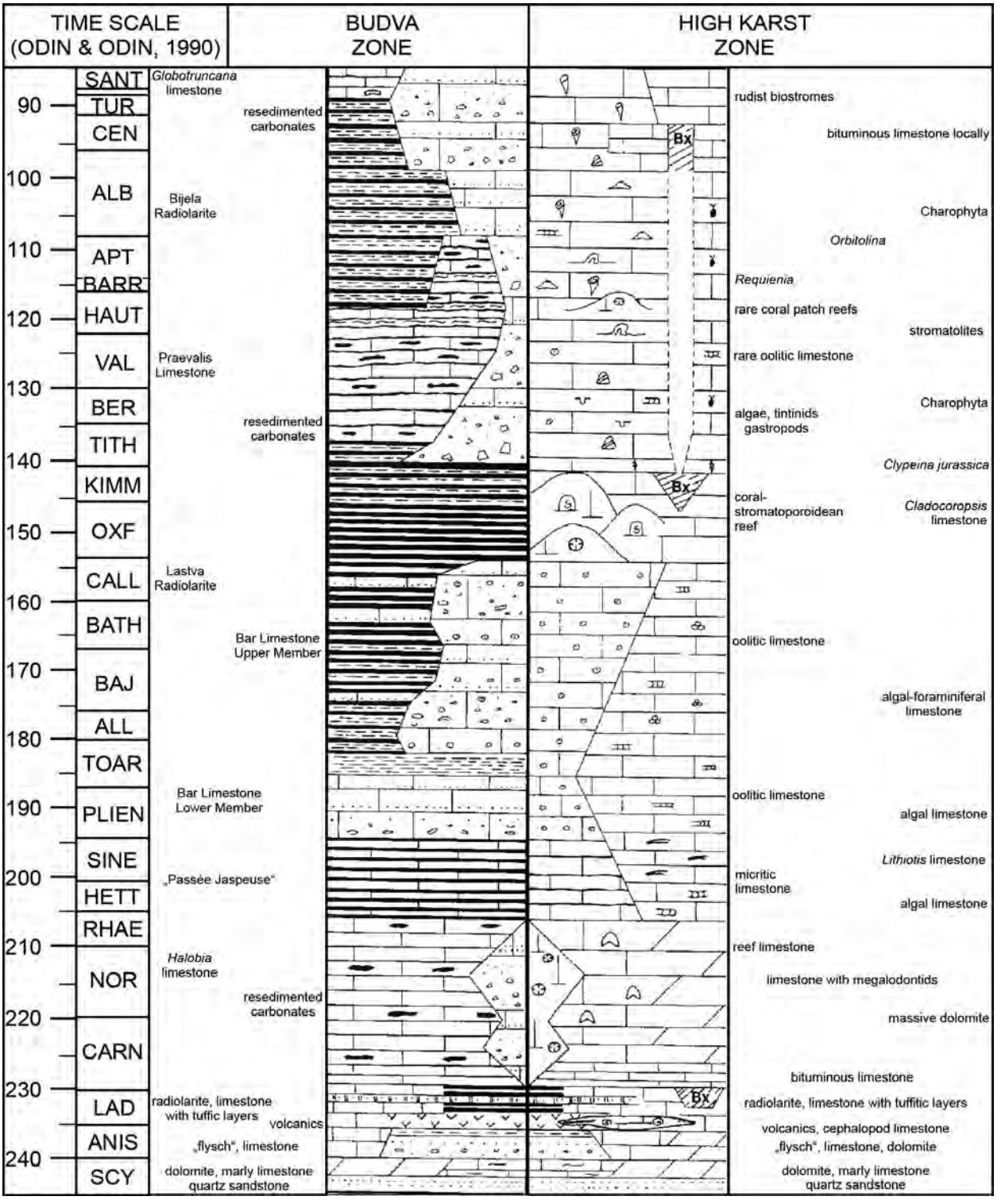

Figure 21: Basin-platform facies relationship through time between the Budva Basin and the High Karst Platform (from Goričan 1994).

ian-Kimmeridgian time interval was therefore a period of most widely expanded radiolarite sedimentation. Distal sequences, characterized by lime-free deposition from the Middle Jurassic, recorded a drastic reduction of interstratified calcarenites.

Green radiolarites, wide-spread in the Budva Basin before the Oxfordian, were replaced by red radiolarites in the Late Jurassic times. This facies change was diachronous; oxygen depleted conditions persisted longer in near-platform areas (Figures 9, 21). The Budva Basin is comparable to the Recent Guaymas Basin, Gulf of California, with the basin sill situated below the core of oxygen minimum layer (Ingle 1981). The progressive change to more expanded oxygenated conditions through the Late Jurassic may have been a result of progressively increasing bottom water circulation or lowered productivity and hence a thinner oxygen minimum layer.

In the Late Jurassic, the composition and distributional pattern of resedimented carbonates changed significantly. Prior to that time, carbonate gravity flow deposits were composed of remobilized pelagic sediments and penecontemporaneous platform debris. Contrary to this, since the Tithonian the bulk of the resedimented carbonates was derived from the erosion of lithified shallow water limestones. This facies change is related to the evolution from an extensional to a compressive regime, which, in the external zones of the foreland system induced a differential uplift of the High Karst Platform. The uplift is inferred from several charophyte-bearing horizons and well documented Upper Jurassic and mid-Cretaceous bauxite deposits (Figure 21).

During the Jurassic and Cretaceous, two different depositional areas could be recognized along the axis of the Budva Basin and, since the Tithonian, the discrepancies between the north-western and the south-eastern area were more pronounced. Abundant coarse-grained resedimented carbonates became restricted to the north-western depositional area, whereas in the south-eastern area pelagic to hemipelagic carbonates prevailed even in the environment close to the carbonate platform (Figure 22). These differences along the basin axis correlate well with the distribution of bauxite deposits, which are limited to only a part of the High Karst Zone NW of Podgorica (Burić 1966) and suggest that the tectonic uplift was more pronounced in the NW than in the SE part of the High Karst Platform.

Facies changes in distal successions of the Budva Basin reflect regional paleoceanographic conditions. In the late Tithonian, radiolarian cherts were replaced by pelagic limestones (Praevalis Limestone). In the Hauterivian–Barremian, inversely, radiolarite sedimentation (Bijela Radiolarite) replaced pelagic carbonates

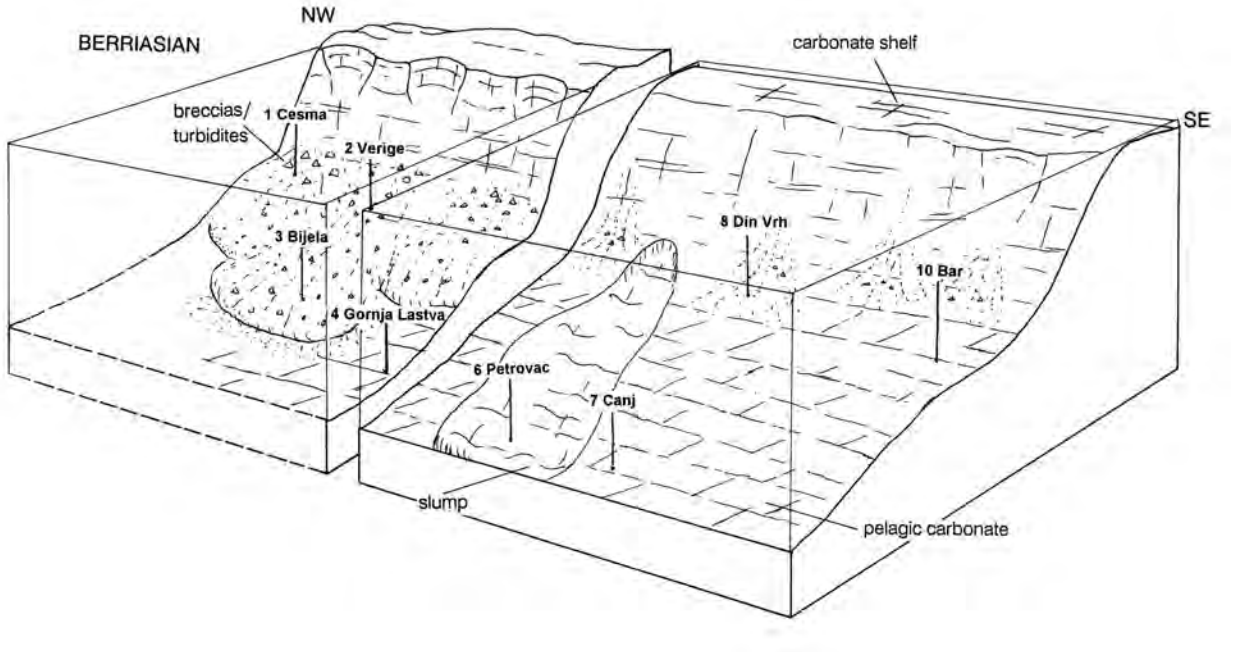

Figure 22: Reconstruction of depositional environment of the Budva Basin and the adjacent High Karst Platform margin in the Berriasian (from Goričan 1994).

and persisted to the Turonian. Meter-scale green levels in generally red Bijela Radiolarite were most probably related to mid-Cretaceous oceanic anoxic events (Figure 9). In the Turonian, pelagic sedimentation turned again to carbonate with the *Globotruncana* limestone. Comparable facies changes occur in the Southern Alps and Apennines. The first is the mid-Tithonian shift from radiolarites to the Maiolica (or Biancone) limestone, followed by a shift to lime-poor and clay rich Scisti a Fucoidi (or Scaglia variegata alpina) and then a shift back to limestones of the Scaglia Bianca and Scaglia Rossa. The Budva Basin, however, differs from other basins of the western Tethys by a higher proportion of silica in Jurassic and Cretaceous pelagic sediments. In addition, the Cretaceous shifts in carbonate/silica ratio are not exactly synchronous across different basins; in the Budva Basin, siliceous sediments were dominant through longer time intervals. Namely, the Bijela Radiolarite, which extends up to the Turonian, is time equivalent of the Scisti a Fucoidi (Aptian–lower Albian) and also of the Scaglia Bianca (upper Albian–lower Turonian).

4.2 Middle Triassic pelagic episode on the High Karst Carbonate Platform

General description

The Middle Triassic rifting-related extension and differential subsidence created a horst-and-graben topography with relatively deep basins and structural highs but the internal topography of these larger units was also differentiated. In the early-middle Anisian, prior to the main rifting phase, the future Adriatic continental margin was occupied by a uniform carbonate deposition in an epicontinental sea (Ravni Carbonate Ramp in the Dinarides, Gutenstein/Steinalm Formations in the Northern Calcareous Alps, Contrin Formation in the Southern Alps). In the late Middle Anisian (Late Pelsonian), the carbonate ramp was dissected into blocks. Some blocks drowned and the first deep-water carbonates were deposited. The elevated blocks were also flooded in the Late Illyrian so that deep-water deposition prevailed on horsts and in grabens until the Ladinian–Carnian boundary. When carbonate platforms on the elevated blocks started to prograde, they filled in the relatively shallow depressions (see Figure 23a for the general stratigraphy). In the early Carnian, the small-scale topographic differences were mostly levelled and the structural highs were again the site of shallow-water carbonate deposition (Wetterstein Formation in the Northern Calcareous Alps and in the Dinarides, Schlern Formation in the Southern Alps).

The short-lived Middle Triassic basins have been documented in the Southern Alps (e.g., Brack & Rieber 1993; Kozur et al. 1996; Celarc et al. 2013) and in the Dinarides (e.g., Goričan et al. 2005; Gawlick et al. 2012, 2017a). The typical sediments are nodular cephalopod limestones (named the Bulog Formation in the Dinarides), limestones with chert nodules and, more rarely pure radiolarian cherts. Coarse-grained breccias were deposited close to steep paleo-escarpments. Late Anisian to Ladinian volcanic and volcaniclastic rocks are widespread but may be locally absent or represented by only thin tuffaceous intercalations. In the upper shallowing-upward part of the basin fill, calcarenites with platform-derived debris prevail. The entire succession bounded by shallow-water carbonates below and above is generally a few tens of meters and only exceptionally more than one hundred meters thick. It is thus reasonable to conclude that the maximum depositional depth of these pelagic sediments was relatively shallow and did not exceed a few hundred meters (see discussion in Gawlick et al. 2012).

The example at Stop 5 – Obzovica described below is part of the High Karst Nappe. Across the Montenegro–Serbian transect (Figure 1), Middle Triassic basins of comparable stratigraphic evolution exist also in the Durmitor Zone (Rampnoux 1974; Mirković 1983), in the Drina-Ivanjica unit (Sudar et al. 2013) and as kilometer-sized blocks in mélanges (Missoni et al. 2012).

Stop 5: Obzovica

SW margin of the High Karst Zone.

Location: near the Obzovica village along the road from Budva to Cetinje (N 42°18'52", E 18°56'10"); Basic Geological Map sheet Budva (Antonijević et al. 1969).

An approximately 20 m thick Upper Anisian to Ladinian unit of hemipelagic limestone and radiolarian chert occurs within a succession of shallow-water carbonates (Figure 23b). The description is summarized from Gawlick et al. (2012) and updated.

The section above the shallow-water Ravni Formation starts with a few meters of bedded grey to red limestones with red marly intercalations (Figure 24a). The limestone beds consist of packstones with bivalves, echinoderm fragments and rare benthic foraminifera that grade into wackestone with calcified radiolarians and thin-shelled bivalves. The reddish marly limestone is composed of alternating laminae of packed thin-shelled bivalves (Figure 24b) and radiolarians.

Reddish bedded and nodular limestones below the radiolarite succession belong to the Upper Pelsonian-Illyrian Bulog Formation. A five-meters thick succession

follows that is composed of reddish and partly grey well-bedded radiolarites, silicified limestones with filaments (Figure 24c) and centimeter-thick volcanic ash layers. From the reddish radiolarites (sample MNE 80, Figure 23c) we isolated a moderately well preserved Illyrian radiolarian fauna. The stratigraphically most important species are *Baumgartneria bifurcata* Dumitrica and *Falcispongus calcaneum* Dumitrica, both restricted to the *Spongosilicarmiger italicus* Zone (Kozur & Mostler 1994). In the upper part of the radiolarite sequence, intercalated turbiditic filament-bearing limestones up to ten centimeters thick are of latest Anisian age based on radiolarians and conodonts (sample MNE 78). Radiolarian fauna in this sample is very well preserved. Nassellarians are abundant and diverse (Figure 23c), but stratigraphically important spumellarians, e.g., characteristic detached spines of Oertlispongidae, have not been found. The sample is probably still Anisian in age,

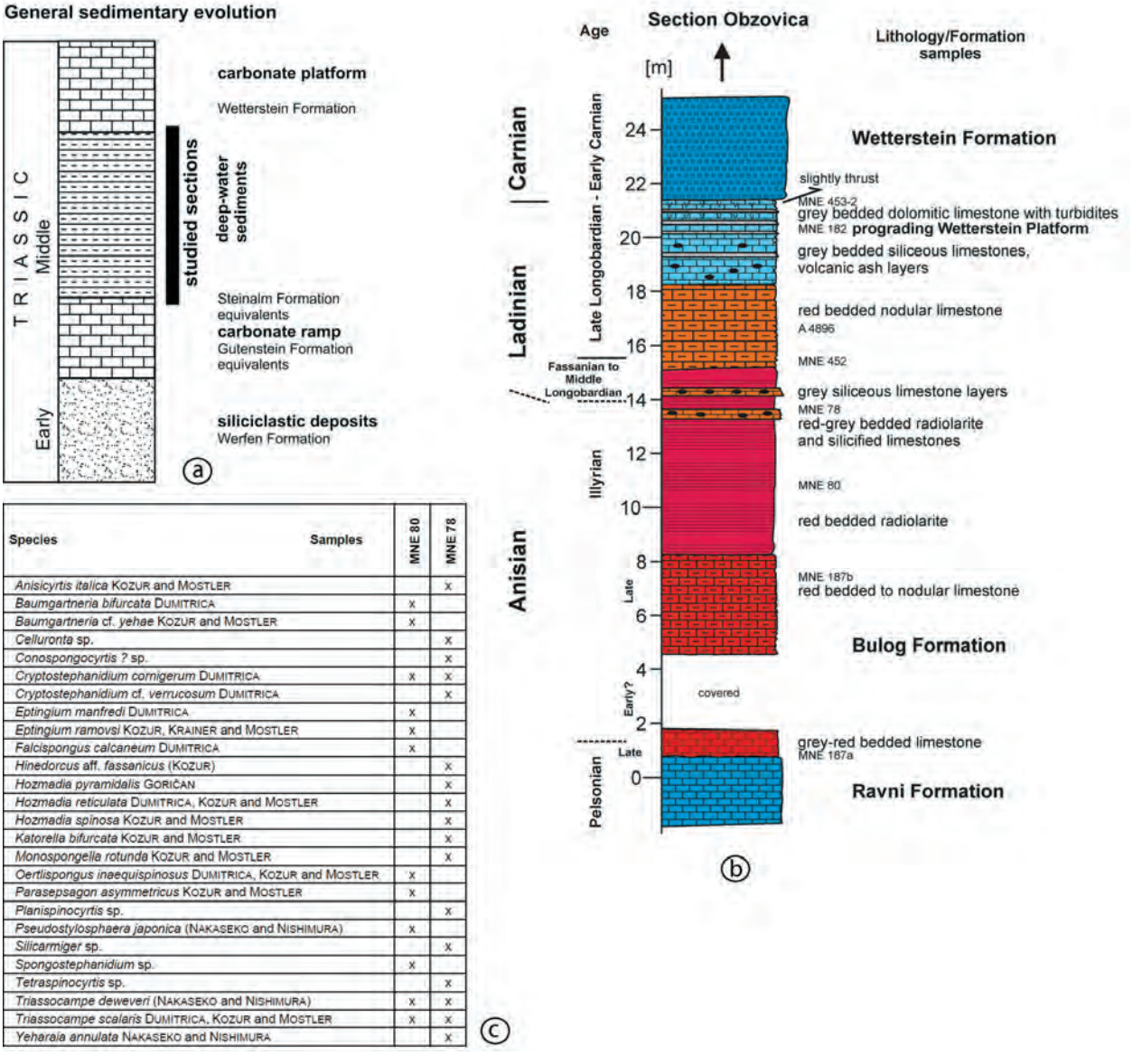

Species / Samples	MNE 80	MNE 78
Anisicyrtis italica Kozur and Mostler		x
Baumgartneria bifurcata Dumitrica	x	
Baumgartneria cf. *yehae* Kozur and Mostler	x	
Celluronta sp.		x
Conospongocyrtis ? sp.		x
Cryptostephanidium cornigerum Dumitrica	x	x
Cryptostephanidium cf. *verrucosum* Dumitrica		x
Eptingium manfredi Dumitrica	x	
Eptingium ramovsi Kozur, Krainer and Mostler	x	
Falcispongus calcaneum Dumitrica	x	
Hinedorcus aff. *fassanicus* (Kozur)		x
Hozmadia pyramidalis Goričan		x
Hozmadia reticulata Dumitrica, Kozur and Mostler		x
Hozmadia spinosa Kozur and Mostler		x
Katorella bifurcata Kozur and Mostler		x
Monospongella rotunda Kozur and Mostler		x
Oertlispongus inaequispinosus Dumitrica, Kozur and Mostler	x	
Parasepsagon asymmetricus Kozur and Mostler	x	
Planispinocyrtis sp.		x
Pseudostylosphaera japonica (Nakaseko and Nishimura)	x	
Silicarmiger sp.		x
Spongostephanidium sp.	x	
Tetraspinocyrtis sp.		x
Triassocampe deweveri (Nakaseko and Nishimura)	x	x
Triassocampe scalaris Dumitrica, Kozur and Mostler	x	x
Yeharaia annulata Nakaseko and Nishimura		x

c

Figure 23:
a) General stratigraphy of the short-lived Middle Triassic basins in the Dinarides.
b) Stratigraphic log of the Obzovica section with position of radiolarian samples (from Gawlick et al. 2012).
c) Occurrence of radiolarian species in samples MNE 80 and MNE 78.

as suggested by the well-known range of *Yeharaia annulata* Nakaseko & Nishimura (Kozur & Mostler 1994). Moreover, the genus *Anisicyrtis* does not extend above the Anisian (O'Dogherty et al. 2009a, 2010).

Upsection, the dominance of radiolarian cherts decreases rapidly and radiolarian-bearing wacke- to packstones were deposited instead. The age of these rocks is most probably Early to early Late Ladinian as indicated by the occurrence of late Longobardian conodonts from the red nodular limestones above the siliceous rocks (Figure 23b, sample MNE 452). The radiolarian-rich interval is overlain by about 5 meters of red limestones that provided a Late Ladinian age (sample A 4896). These reddish limestones pass continuously into grey deep-water limestones showing an increasing proportion of shallow-water debris of Late Ladinian age (sample MNE 182, Figure 24d), again with intercalated volcanic ash layers. This sequence is topped by reefal dolomites of Early Carnian age (sample MNE 453-2). The transition of the thick-bedded basinal dolomites with shallow-water turbidites and intercalated volcanic ash layers and the more massive dolomitized reefal rudstones of the Wetterstein Carbonate Platform is slightly tectonically overprinted.

4.3 The Lim Zone and the overlying ophiolite mélanges

General description of the Lim Basin

The Lim Basin is a typical continental-margin basin that formed during the Middle Triassic rifting and then persisted as a deep-marine basin until the arrival of the

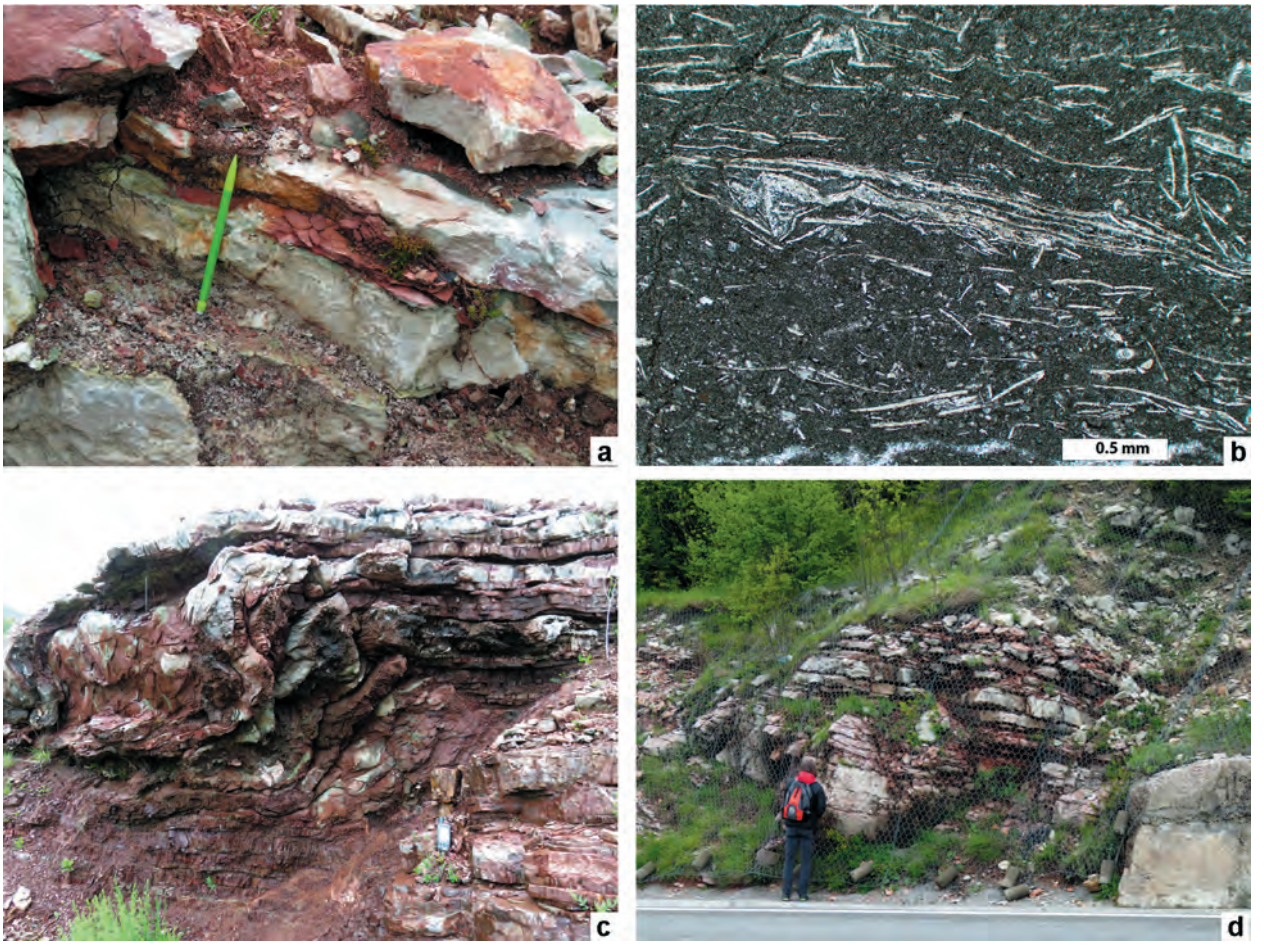

Figure 24: Middle Triassic rocks of the Obzovica section.
a) Grey bioclastic limestone with reddish marly intercalations near the base of the section.
b) Limestone rich in filaments; thin section of the 1-cm thick reddish bed in the middle of Figure 24a.
c) Radiolarian chert overlain by filament-rich cherty limestone. The cherty limestone yields well-preserved radiolarians.
d) Upper part of the section with increasing proportion of bioclastic limestone.

first synorogenic sediments in the Late Jurassic – earliest Cretaceous. The Mesozoic stratigraphy of the Lim Basin was less systematically studied than that of the Budva Basin. Here we mainly summarize the general study carried out by Rampnoux (1974) in the Ćehotina and Zlatar subzones (Figure 5) in Montenegro and western Serbia, and complement this review by some recently obtained local biostratigraphic dates (Figure 25). The Mihajlovići Subzone of Rampnoux (1974, Figure 5) is excluded from this summary and is presented separately (under Stop 8 – Mihajlovići below) because its stratigraphy is typical of a Jurassic submarine high and not of a pelagic basin.

The Lower Triassic rocks of the entire Lim Zone are bioturbated grey limestones, a characteristic lithostratigraphic unit of the Southern Alps and Dinarides, in older literature known as the upper member of the Werfen formation or the Campil beds. They locally overlie red sandstones of the lower Werfen formation or, in places, Carboniferous synorogenic Variscan Culm-type deposits. The lower Anisian unit consists of 50–200 m of massive shallow water limestone with abundant algae, gastropods and foraminifera. The first deeper-water unit is a few meters thick condensed "ammonitico rosso" type Bulog Formation, which is ascribed to the Upper Anisian Trinodosus Ammonoid Zone. The upper Upper Anisian volcanic and volcaniclastic rocks follow but laterally vary considerably and may be up to 60 m thick or completely absent. The Ladinian to Lower Jurassic unit is a uniform 200 to 350 m thick succession of bedded pelagic limestone with chert nodules. Except for the Ladinian, well dated with ammonoids and bivalves, the age of this thick formation is poorly constrained. Conodont studies have recently been introduced to refine the Upper Triassic stratigraphy in the area (see Stop 6 – Poros below). The Lower Jurassic limestones of this succession are generally thinner-bedded and more marly; rare belemnites, aptychi, calcispheres and foraminifera were found in this upper part of the succession (Rampnoux 1974). The pelagic limestones are overlain by green and red radiolarite. A few meters thick radiolarite unit was dated to the Callovian–Oxfordian (see Stop 7 – Jabučno below). In the upper part, the radiolarite is interlayered with breccia beds that contain clasts of pelagic limestone and chert but also include clasts of oolitic limestone, Upper Jurassic reef limestone with *Ellipsactinia* and *Sphaeractinia*, benthic foraminifera and the Tithonian alga *Aloisalthella sulcata* (former *Clypeina jurassica*). The topmost stratigraphic unit is a flyschoid series composed of fine sandstones, greywackes with fragments of chert and volcanic rocks, breccias with carbonate clasts,

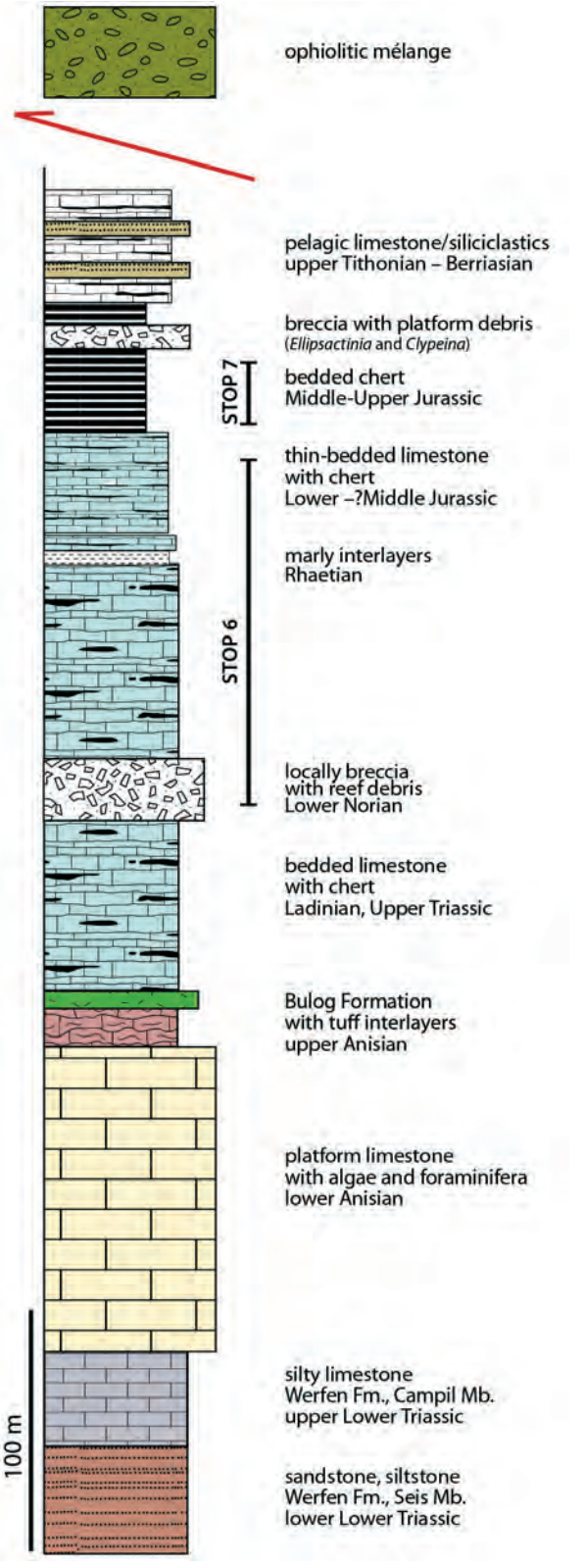

Figure 25: Schematic stratigraphic column of the Ćehotina Subzone NW of Pljevlja (according to Rampnoux 1974) with position of stops 6 and 7.

and thin-bedded pelagic limestone. Calpionellas in the pelagic limestone indicate a late Tithonian – early Berriasian age. The flyschoid series exists only in the western Ćehotina Subzone.

A part of the Ćehotina Subzone, as defined by Rampnoux (1970, 1974) is exposed in south-eastern Montenegro near Berane, but is separated from the NW part near Pljevlja by a large area where only Paleozoic rocks are exposed (Figure 5). Both parts of the Ćehotina Subzone are composed of deep-water sediments from the Anisian to the end of the Jurassic and thus correlate well in general outlines but may differ in details. Lime-free radiolarites are probably thicker and have a longer range in the southern sector. Near Berane, the oldest radiolarian cherts, which characteristically occur in a shale-dominated interval, are Aalenian in age; upsection, red radiolarian cherts with rare calcarenite intercalations were assigned to the latest Bajocian – early Bathonian (Kukoč 2014).

Stop 6: Poros

Ćehotina Subzone.

Location: W of Pljevlja, along the road from Gradac to Šuplja Stijena (N 43°24'03", E 19°08'45"); Basic Geological Map sheet Pljevlja (Mirković et al. 1978).

A more than 120 m thick overturned Upper Triassic succession of reef limestone and bedded siliceous limestones (Figures 26, 27) is exposed. The section is slightly tectonized, with folded slump deposits in the central part, so that only some parts of the section can be accurately measured. The results presented here are the first results of the current study by one of us (M.M.).

The section starts with a roughly 20 m thick reef to fore-reef limestone succession with deep-water matrix in the upper part (Lacian 2 in age with conodonts *Epigondolella rigoi* and *Norigondolella* sp.). Near the base the reef limestone is thick bedded to massive, higher up in the section variously bedded. We consider these reef limestones as part of the Dachstein Reef Limestone, interestingly with a deepening upward sequence from the middle Lower Norian onwards. Around the Lacian 2-3 boundary the depositional characteristics change relatively abruptly. The next 30 m thick part consists of dm-bedded limestones with chert nodules and layers, grey limestones and reddish limestones. Conodont dating shows that the age of this part of the section is Lacian 3 to Alaunian 3 in the upper part (dated by *Epigondolella abneptis, E. spatulata* to *E. slovakensis* and *E. serrulata*). The higher Alaunian 3 to Sevatian (with *E. bidentata*) is characterized by a thick series of slump deposits with carbonate turbidite intercalations. In these slumps, mainly grey siliceous thin-bedded limestones of the higher Alaunian, dated with e.g. *E. slovakensis*, appear. Polymictic breccias (debris flows) and turbiditic microbreccias with older (Lacian and Alaunian proven with conodonts) open-marine hemipelagic components follow upsection. The overlying dm-bedded grey-reddish siliceous limestones with red chert nodules are Rhaetian in age dated with the appearance of *Misikella posthernsteini*. The higher Lacian to Upper Norian part of the succession corresponds to the reef-near facies belt in open shelf position, known in the type-area in the Northern Calcareous Alps as the Gosausee Limestone facies. The section Poros shows during the Norian a general deepening trend.

Bedded grey siliceous and slightly marly limestones (bed thickness 5–10 cm) follow upsection in a thickness of less than 20 m and are overlain by roughly 10 m of dm-bedded red-grey siliceous limestones with red marl to claystone intercalations. These reddish limestones are again overlain by bedded grey siliceous and slightly marly limestones. An exact age of this part of the series could not be determined; only conodont multielements could be isolated in several parts of the succession. The age is most likely Rhaetian 2-3, but earliest Jurassic for some parts of the folded sequence cannot be excluded.

The upper part of the section consists of dark red highly siliceous thin-bedded limestone (Figures 28 a, b). Replacement chert nodules and layers are more abundant than in the limestones below. Ten samples from this and the previous unit have been processed to extract siliceous microfauna. Sponge spicules are abundant but no radiolarians have been found.

Stop 7: Jabučno

Ćehotina Subzone.

Location: Along the road from Gradac to Šuplja Stena, 6 km west from Stop 6, N 43°24'26", E 19°05'44"; Basic Geological Map sheet Pljevlja (Mirković et al. 1978).

An isolated 5 m thick outcrop of variegated chert; according to Rampnoux (1974), this chert occurs above a stratigraphic succession similar to that of the Poros section (Stop 6) in the general stratigraphic column of the Ćehotina Subzone (Figure 25).

The outcropping section (Figures 29a–c) consists of green, variegated green and red, and violet red weathered cherts. These cherts contain no dispersed carbonate and the succession is also devoid or resedimented carbonates. Four samples have been processed with diluted hydrofluoric acid. Sponge spicules (mostly small and large monaxones) are abun-

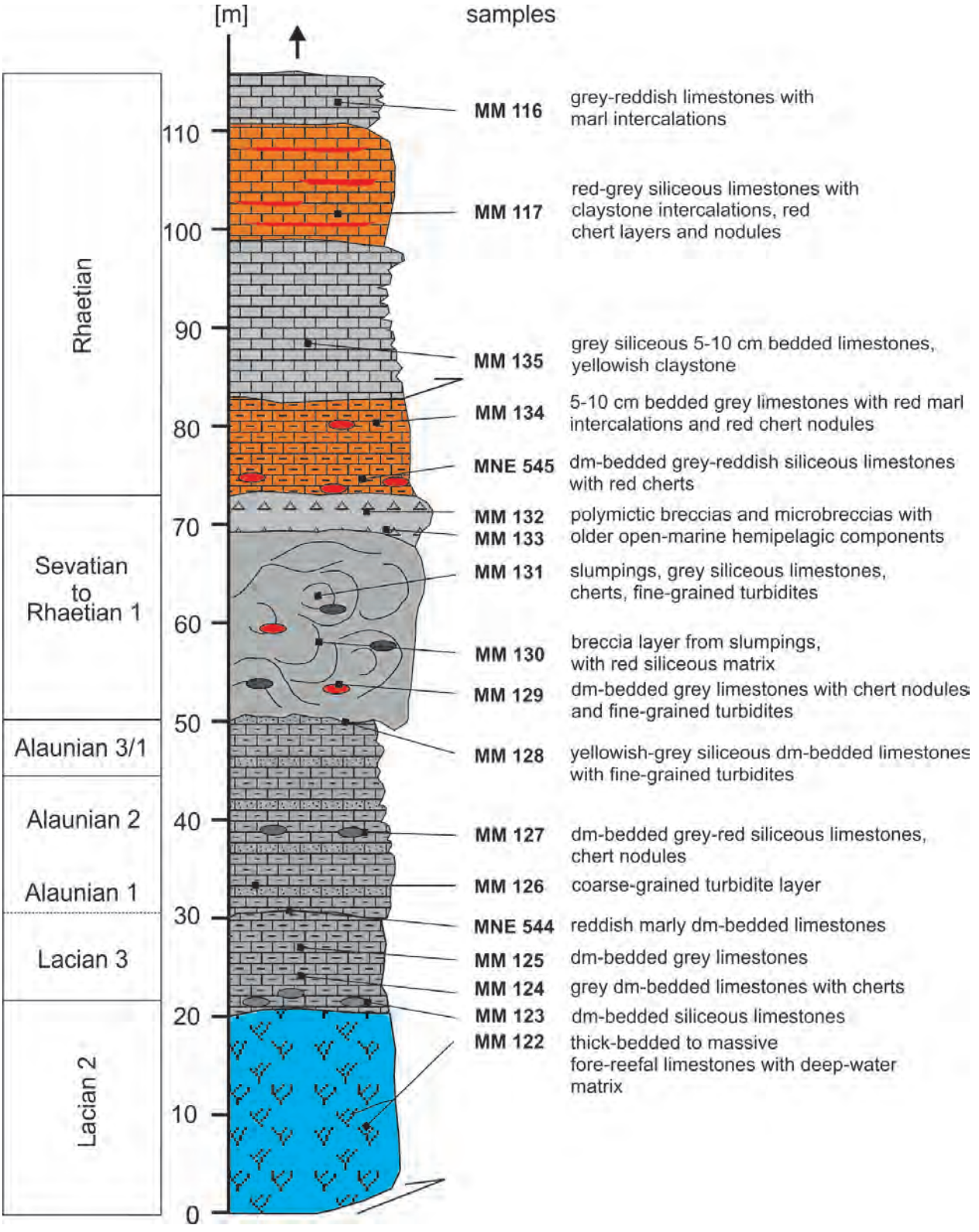

Figure 26: The nearly 120 m thick overturned Late Triassic sedimentary sequence of the reef to reef near facies belt in the Poros area.

dant and practically rock-forming in all samples. Only one sample (no. JB 3) yielded some determinable radiolarians. Also in this sample, sponge spicules account for more than 95% of the siliceous fauna. Among the identified radiolarians (Figure 30), the co-occurrence of *Cinguloturris carpatica* Dumitrica (FAD in UAZ 7) and *Hemicryptocapsa marcucciae* (Cortese) (LAD in UAZ 8) indicates a late Bathonian-early Callovian to middle Callovian-early Oxfordian age according to Baumgartner et al. (1995).

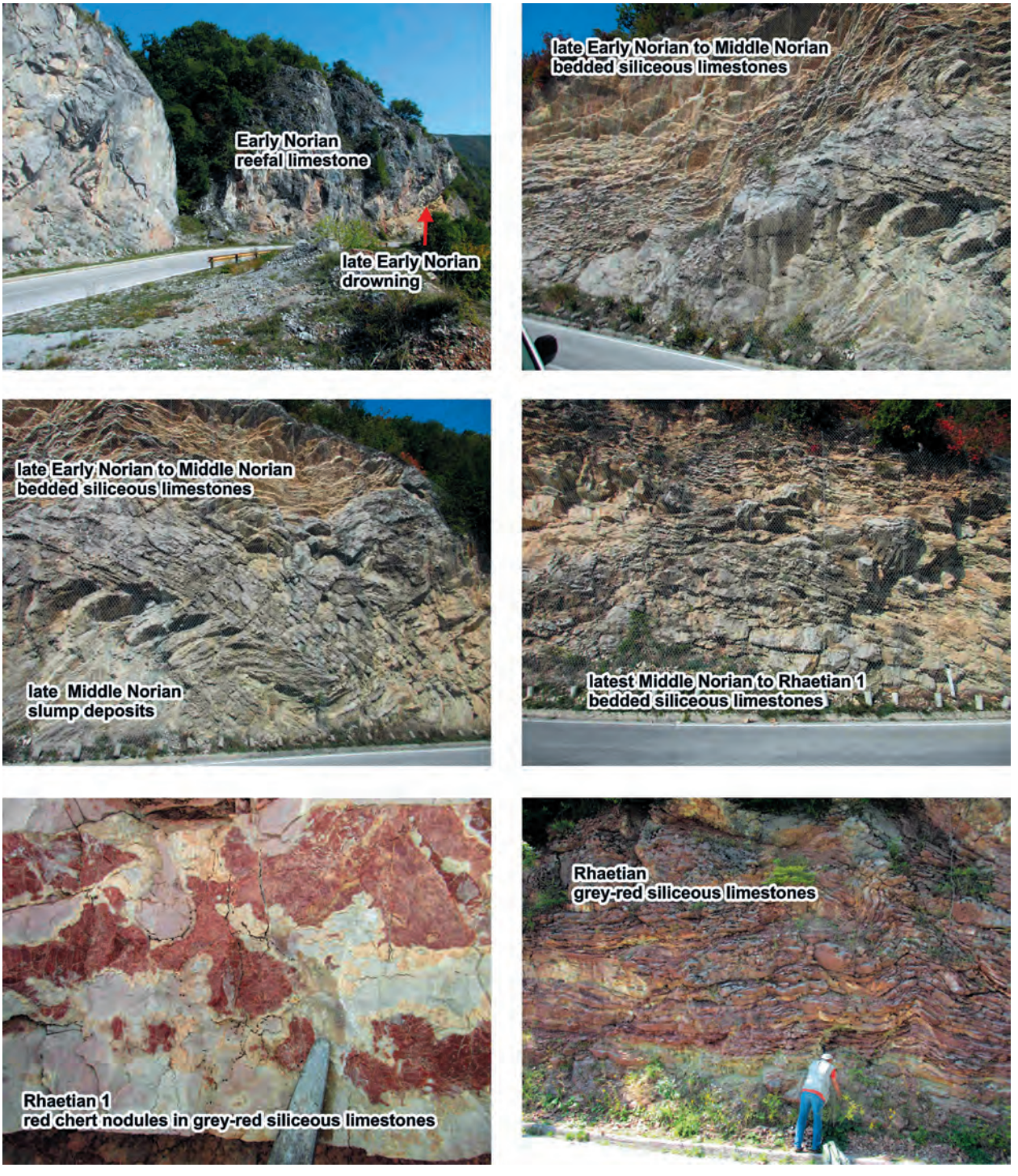

Figure 27: Field views of the Upper Triassic Poros section. Explanation in the photos.

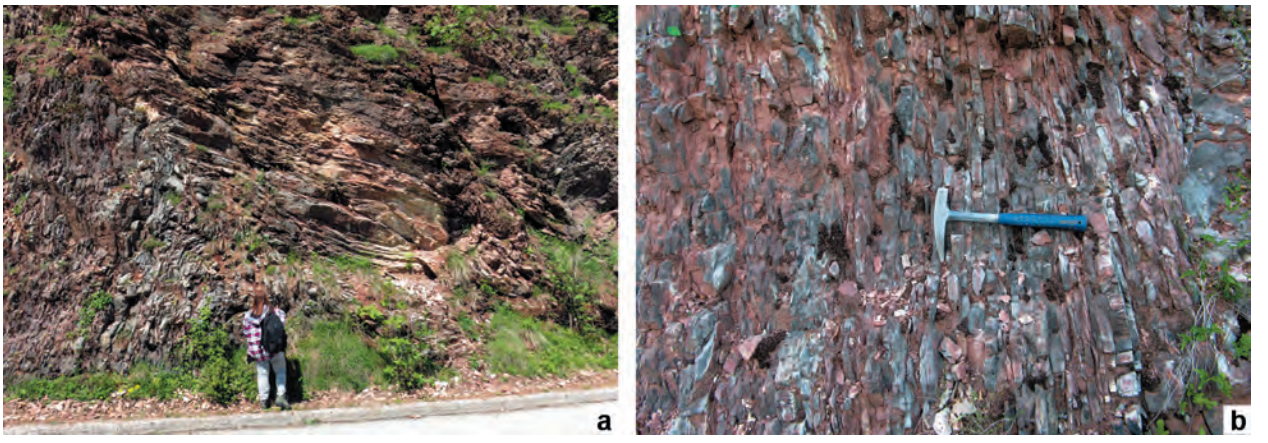

Figure 28: Upper part of the Poros section.
a) Lower Jurassic thin-bedded highly siliceous limestone cut with E–W striking subvertical faults.
b) Close up of figure a. The limestone is rich in sponge spicules but devoid of radiolarians.

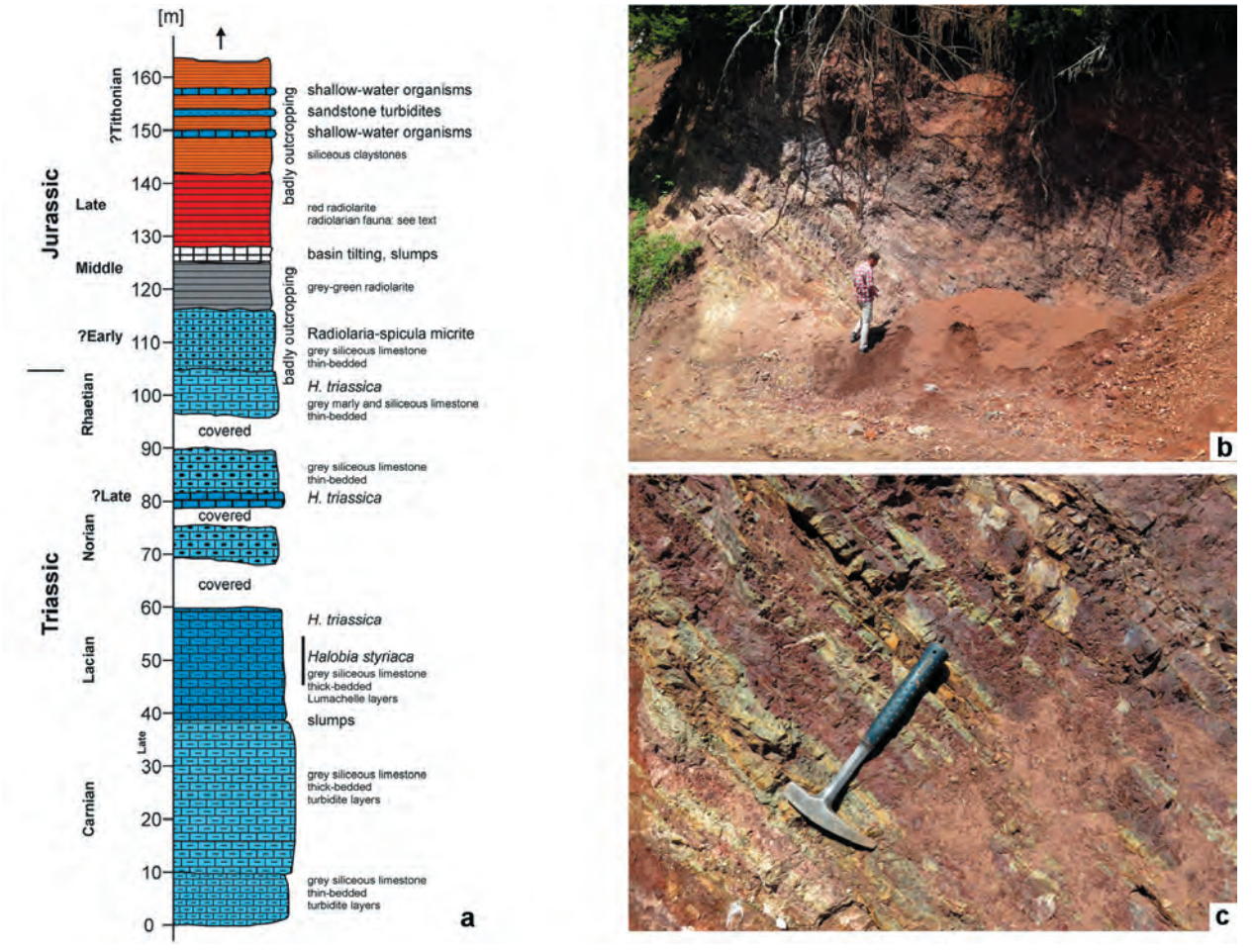

Figure 29: Jurassic radiolarite at Jabučno.
a) Stratigraphic column of the Jabučno area; the radiolarite of b–c is marked in red.
b) General view of the outcrop.
c) Red and green cherts in the lower part of the outcrop in b.

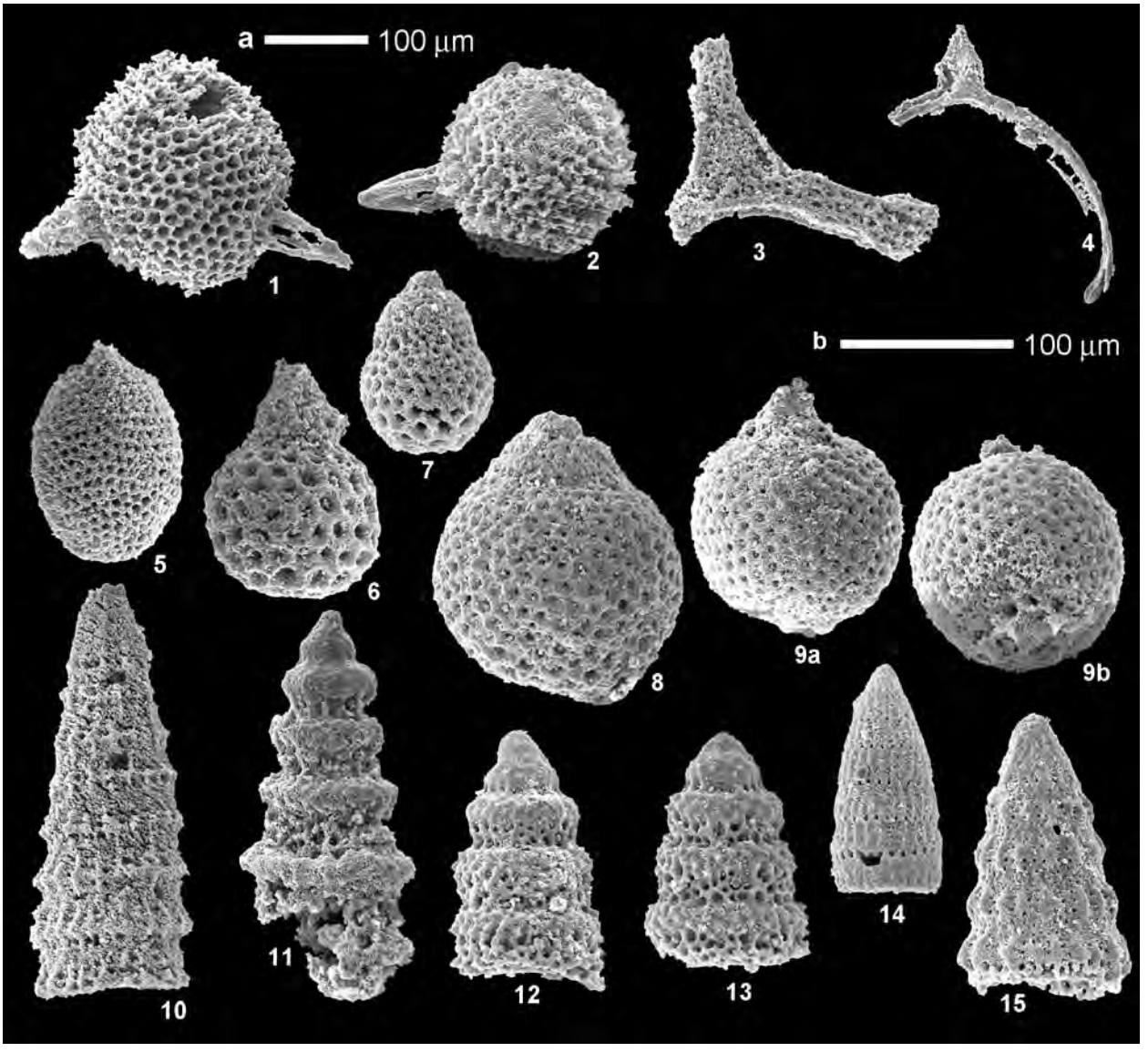

Figure 30: Late Bathonian – early Callovian to middle Callovian – early Oxfordian (UAZ 7–8) radiolarians from sample JB 3 at Jabučno.
1: Triactoma enzoi *Beccaro, scale bar a.*
2: Triactoma blakei *(Pessagno), scale bar a.*
3: Angulobracchia *cf.* digitata *Baumgartner, scale bar a.*
4: Dicerosaturnalis angustus *(Baumgartner), scale bar a.*
5: Kilinora *cf.* spiralis *(Matsuoka), scale bar b.*
6: Crococapsa *cf.* hexagona *(Hori), scale bar b.*
7: Theocapsomella? kiesslingi *(Hull), scale bar b.*
8: Zhamoidellum ventricosum *Dumitrica, scale bar b.*
9a-b: Hemicryptocapsa marcucciae *(Cortese), a: lateral view, b: antapical view, scale bar b.*
10: Transhsuum brevicostatum *(Ožvoldova), scale bar b.*
11–13: Cinguloturris carpatica *Dumitrica, scale bar b.*
14: Loopus venustus *(Chiari, Cortese & Marcucci), scale bar b.*
15: Transhsuum crassum *Chiari, Marcucci & Prela, scale bar b.*

The rocks directly underlying these radiolarites are not exposed, but the Upper Triassic succession in the continuation below is somewhat different from the Poros section; no reef limestone, which is well marked in the Poros section occurs below the Jabučno section. The Triassic section (work in progress by H.-J.G. and M.M.) starts with a thick-bedded (10–25 cm) series of bedded slightly siliceous limestones with very fine-grained carbonate turbidite intercalations, but without shallow-water grains (only automicrite clasts). The dipping in the upper part changes rapidly without any clear direction indicating slump deposits. The age of this part of the section cannot be exactly determined, conodont samples yielded only multielements, but is most likely Late Carnian (Tuvalian). Higher up in the succession a series of lumachelle layers with predominantly *Halobia* aff. *styriaca* indicate a lowermost Norian age. Above these lumachelle layers follow a roughly 40 m thick series of grey siliceous limestones, in cases with chert nodules and chert layers. Generally, the series is in that part thin-bedded (5–10 cm), turbidites are generally missing with one exception in the middle part of this series. This fine-grained turbidite layer with filaments most likely corresponds to the resedimentation event in the latest Middle to Late Norian.

Also this part of the section cannot be exactly dated by conodonts: the sediments consist of radiolarian biomicrites without resediments. Only *Hindeodella triassica*, indicating a Late Triassic age, could be isolated, also in the more marly thin-bedded part in the highest part of this series. On top of these marly siliceous limestones appears a 1–2 cm thick layer of grey claystones, which marks an abrupt change in the microfacies characteristics. Upsection follow grey thin-bedded biomicrites rich in radiolarians and sponge spicules that resemble the Lower Jurassic successions known widespread in the Western Tethys realm. The Triassic part of the section can be attributed to the Grivska Formation.

Stop 8: Mihajlovići

Mihajlovići Subzone

Location: Along the road from Pljevlja to Jabuka, about 10 km east-southeast from Pljevlja, several outcrops between N 43°20'19", E 19°27'08' and N 43°20'28.5", E 19°27'09". Basic Geological Map sheet Pljevlja (Mirković et al. 1978).

The succession consists of Triassic shallow-water limestone and a Jurassic deepening-upward sequence, overthrust by ophiolitic mélage (Figure 31). This succession was first described nearly a hundred years ago; the Lower to Middle Jurassic sequence has been recently well dated with ammonites and foraminifera (Rabrenović et al. 2012; Metodiev et al. 2013; Gawlick et al. 2020; Đaković et al. 2021; see the last two publications for the complete list of references).

The Upper Triassic is represented by Norian-Rhaetian Dachstein Limestone developed in an open lagoonal facies. The Lower to Middle Jurassic rocks belong to the Krš Gradac Formation and represent a stepwise deepening sequence in the transitional facies belt between the Adriatic Carbonate Platform (*sensu lato*) basement and the Neo-Tethys open shelf (Đaković et al. 2021). The formation is subdivided into four members reflecting the deepening.

The ?Middle/Upper Hettangian–Sinemurian member consists of shallow-subtidal micro-oncoidal limestones, mainly grain- and packstones with abundand benthic foraminifera, crinoids and only a few open-marine organisms. Foraminifera assemblages from these limestones (Rabrenović et al. 2012; Gawlick et al. 2020) have a wider biostratigraphic range, but are most common during Hettangian and Sinemurian of the Eastern Alps, Dinarides etc. (Đaković et al. 2021 and references therein). The lower part of this unit is dominated by large micro-oncoids with several layers. The number of layers/laminae decreases upsection. Contrary to this, the variability of the benthic foraminifera and the amount of crinoid fragments increase, indicating a slight deepening trend during the ?Middle/Late Hettangian-Sinemurian.

Following a hardground/gap, Pliensbachian is represented by wackestones with thick shells (brachiopods, ?bivalves), crinoids, some foraminifera and ammonoid shells, and only a few levels with micro-oncoids, mainly with foraminifera as core. In the uppermost level of this member ammonoids of *Fuciniceras lavinianum* Zone were found, below the upper hardground surface with the Middle Toarcian ammonoids. According to these finds, the age of this member was assigned to ?Early Pliensbachian to early Late Pliensbachian (Đaković et al. 2021). The hardground at the base of this member may represent a gap of the uppermost Sinemurian to the Early Pliensbachian. The hardground above the early Late Pliensbachian ammonoids would represent a longer gap in the depositional history, i.e. the rest of the Pliensbachian and the lowermost Toarcian. Around the level with the Early Domerian ammonoids the limestones are more condensed, represented by densely packed ammonoid-crinoid-foraminifera packstones. These microfacies types point to deposition in a relatively low-energy deeper-water enviroment, indicating ongoing deepening.

The Toarcian part of the Lower Jurassic succession at Mihajlovići is represented by deeper open-marine

nodular, condensed limestones. The lowermost layer contains a rich Middle Toarcian ammonoid fauna (Rabrenović et al. 2012; Metodiev et al. 2013; Đaković et al. 2021). The hardground consists of a Fe/Mn-crust indicating a lithified sea floor and a gap in deposition. Ammonoids appear slightly above this hardground again in a micro-oncoidal facies and in crinoid-framinifera-ammonoid limestones. These micro-oncoids are much smaller, not as common as in the ?Upper Hettangian–Sinemurian and have mainly only

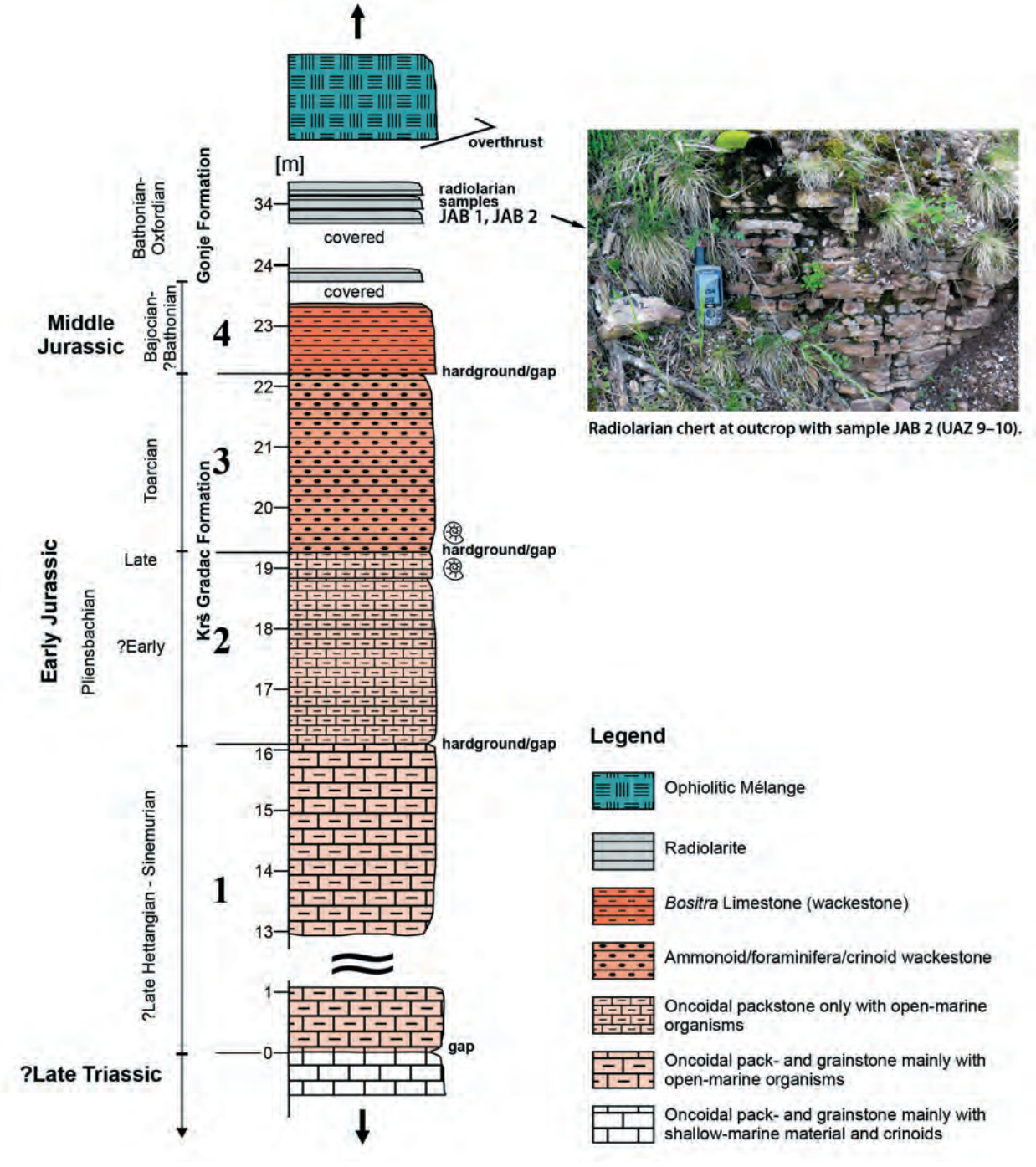

Figure 31: Stratigraphic column of the Mihajlovići section (from Gawlick et al. 2020; Đaković et al. 2021) and field photograph of Oxfordian radiolarite in the upper part of the section.

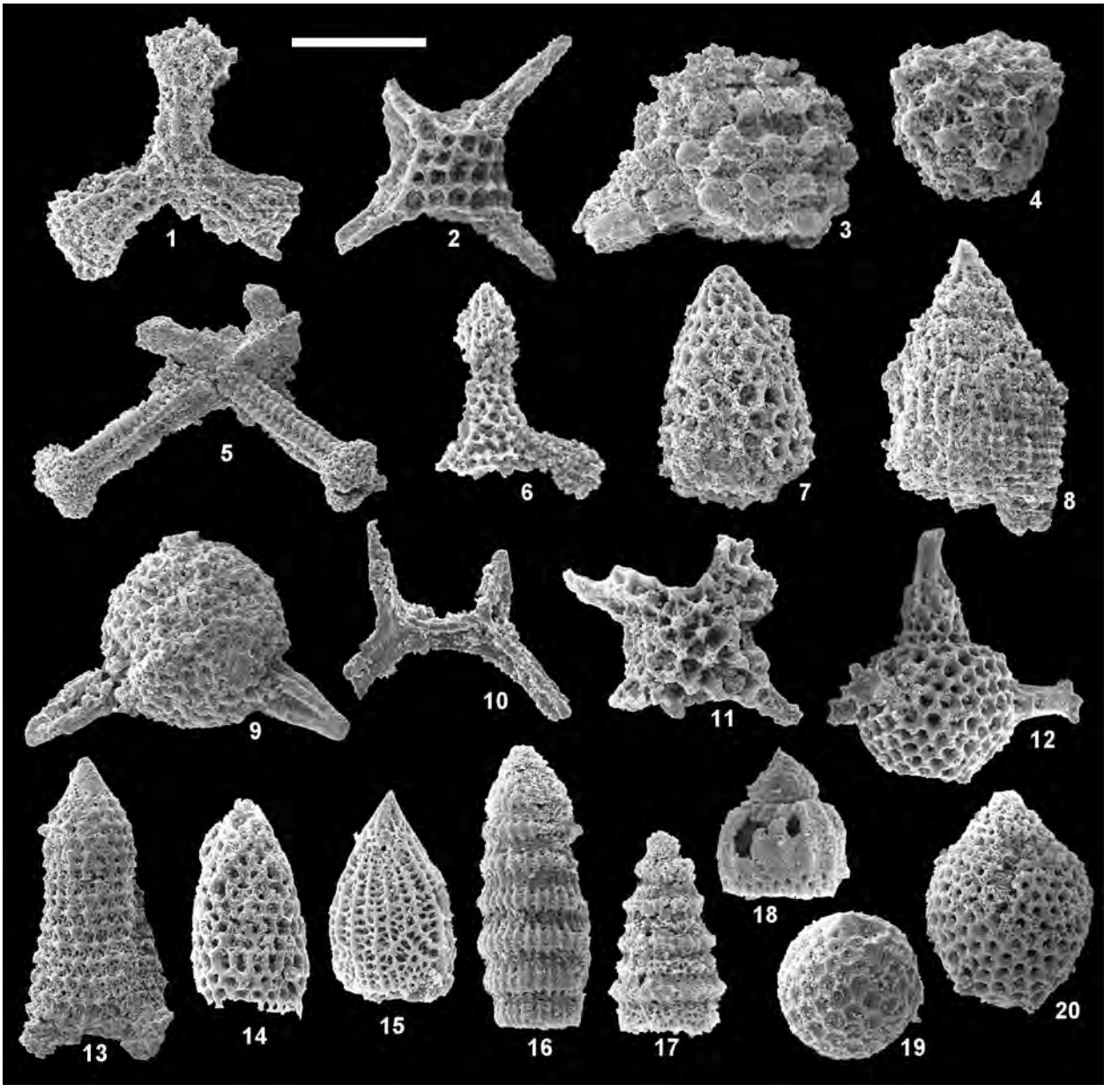

Figure 32: Late Jurassic radiolarians from samples JAB 1 (1–8) and JAB 2 (9–20) at Mihajlovići.
Sample JAB 1 (UAZ 10–11).
1: Tritrabs exotica *(Pessagno), scale bar 133 μm.*
2: Emiluvia sedecimporata *(Rüst), scale bar 133 μm.*
3–4: Emiluvia orea ultima *Baumgartner & Dumitrica, scale bar 133 μm.*
5: Tetratrabs bulbosa *Baumgartner, scale bar 266 μm.*
6: Angulobracchia *sp., scale bar 133 μm.*
7: Campanomitra tuscanica *(Chiari, Cortese & Marcucci), scale bar 100 μm.*
8. Parahsuum *sp., scale bar 100 μm.*

Sample JAB 2 (UAZ 9–10).
9: Triactoma blakei *(Pessagno), scale bar 133 μm.*
10: Hexasaturnalis nakasekoi *Dumitrica & Dumitrica-Jud, scale bar 100 μm.*
11: Emiluvia bisellea *Danelian, scale bar 133 μm.*
12: Spinosicapsa spinosa *(Ožvoldova), scale bar 133 μm.*
13: Ristola altissima *Rüst, scale bar 200 μm.*
14: Campanomitra tuscanica *(Chiari, Cortese & Marcucci), scale bar 133 μm.*
15: Hsuum obispoense *Pessagno, scale bar 133 μm.*
16: Archaeodictyomitra minoensis *(Mizutani), scale bar 100 μm.*
17: Cinguloturris carpatica *Dumitrica, scale bar 100 μm.*
18: Eucyrtidiellum ptyctum *(Riedel & Sanfilippo), scale bar 100 μm.*
19: Gongylothorax favosus *Dumitrica, scale bar 100 μm.*
20: Zhamoidellum ovum *Dumitrica, scale bar 100 μm.*

one or two rims. Wacke- to packstones with common ammonoid fragments, foraminifera and crinoids are the dominant microfacies throughout the Toarcian part of the section. A prolonged hardground formation is indicated by common lithoclasts, in cases with Fe/Mn-crusts, shells with indications of boring organisms and layered hardgrounds. Gastropods and benthic foraminifera are also common. This microfacies indicates deposition in a low-energy relatively deep-water environment (open shelf environment).

Following a long stratigraphic gap, the Toarcian red nodular limestones are overlain by Middle Jurassic (Bajocian-?Bathonian) *Bositra* Limestone characterized by condensed red nodular limestones with juvenile ammonoids, crinoids and *Bositra* shells. The microfacies with a lot of lithoclasts, Fe/Mn crusts and the extreme enrichment of shells indicate a very slow depositional rate, as typical of hemipelagic open marine settings with less carbonate production causing stratigraphic condensation. Important to note, that radiolarians, normally quite typical of the *Bositra* facies, are rare or practically missing. Deposition of such limestones started after the Toarcian Oceanic Anoxic Event in the Late Toarcian (Böhm 1992) and prevail until the Kimmeridgian in cases. The *Bositra* Limestone in the Mihajlovići section is of Bajocian/?Bathonian age, confirmed with *Globochaete alpina* Lombard, *Globuligerina oxfordiana* (Grigelis) and *Trochammina globoconica* Tyszka & Kaminski from the upper part of the *Bositra* Limestone (Rabrenović et al. 2012).

The uppermost part of the succession is dark gray and dark red radiolarites of the Middle–Upper Jurassic Gonje Formation (Gawlick et al. 2020). The Lower–Middle Jurassic limestones and the radiolarites crop out at several places along the Pljevlja–Jabuka road, but the contacts are poorly preserved and the radiolarites are never exposed in thickness of more than three meters. The radiolarians presented herein (Figure 32) were collected a few kilometers east of the Mihajlovići section described by Gawlick et al. (2020) and Đaković et al. (2021).

We studied two samples (JAB 1 and JAB 2) of dark red laminated chert (Figure 31) from two separate outcrops. In both samples radiolarians are moderately well preserved (Figure 32); large sponge spicules and rhaxes co-occur. The age of sample JAB 1 is determined to UAZ 10–11 (late Oxfordian–early Kimmeridgian to late Kimmeridgian–early Tithonian) with the range of *Emiluvia orea ultima* Baumgartner & Dumitrica. The age of sample JAB 2 is constrained to UAZ 9–10 (middle-late Oxfordian to late Oxfordian–early Kimmeridgian) based on first appearance of *Archaeodictyomitra minoensis* (Mizutani) and last appearance of *Gongylothorax favosus* Dumitrica.

Stop 9: Vijenac

Ophiolitic mélange, tectonically overlying the Mihajlovići Subzone.

Location: (N 43°20'35", E 19°25'51"). Basic Geological Map sheet Pljevlja (Mirković et al. 1978).

The ophiolitic mélange ovethrusts the succession described in the previous section. The contact is covered today, but it was in the past visible and described (Nöth 1956).

The mélange consists of plurimetric blocks of radiolarite, sandstone and basalt in a shaley matrix (Figure 33). A block of dark grey chert yielded a radiolarian assemblage dominated by small nassellarians (Figure 34). The assemblage is assigned to UAZ 7 (Late Bathonian–early Callovian) based on *Cinguloturris carpatica* Dumitrica that first appears and several species that last appear in this zone. These species are *Kilinora spiralis* (Matsuoka), *Striatojaponocapsa naradaniensis* (Matsuoka), *Striatojaponocapsa conexa* (Matsuoka), and *Mizukidella kamoensis* (Mizutani & Kido).

Stop 10: Drno Brdo

Blocks in ophiolitic mélange, tectonically overlying the Ćehotina Subzone (Rampnoux 1974), part of the East-Bosnian Durmitor unit (Figure 1).

Location: Along the road from Pljevlja to Žabljak near Eco Camp Drno Brdo (N 43°12'57.78"; E 19°20'41.58"), Basic Geological Map sheet Žabljak (Mirković & Vujisić 1989).

Middle Triassic radiolarian chert and basalt with gabbroic dykes.

The basalts at the Drno Brdo locality cover a surface of approximately 6 by 3 km and represent one of the largest blocks/slides of volcanic rocks in the ophiolitic mélange of Montenegro (Mirković et al. 1985). Contrary to the Jurassic ophiolitic rocks and radiolarites that were incorporated in the mélange as olistoliths originating from the accretionary prism, the large Triassic blocks of basalt and pelagic sediments must have been scraped off the old oceanic crust or the distal continental slope (Gawlick et al. 2017a; Schmid et al. 2020).

Two outcrops 150 m apart have been inspected for radiolarians. The first outcrop is a block of radiolarite incorporated in a sandy-shaley matrix (Figure 35, sample ZAB 1). In the second outcrop, radiolarian chert (sample ZAB 4) is an interpillow sediment in direct contact with basalt, which is penetrated by gabbroic dykes (Figure 36). Both radiolarian samples are dark red chert without filaments; radiolarians are rare and

poorly preserved. The age of sample ZAB 4 (Figure 37: 1–6) is based on *Oertlispongus inaequispinosus* Dumitrica, Kozur & Mostler, which spans the Late Anisian and Early Ladinian (Stockar et al. 2012). Sample ZAB 1 (Figure 37: 7–13) contains only Oertlispongidae with straight spines (*Paroertlispongus*) that are less diagnostic for age determination. The most useful element of this assemblage is the genus *Celluronta*, which

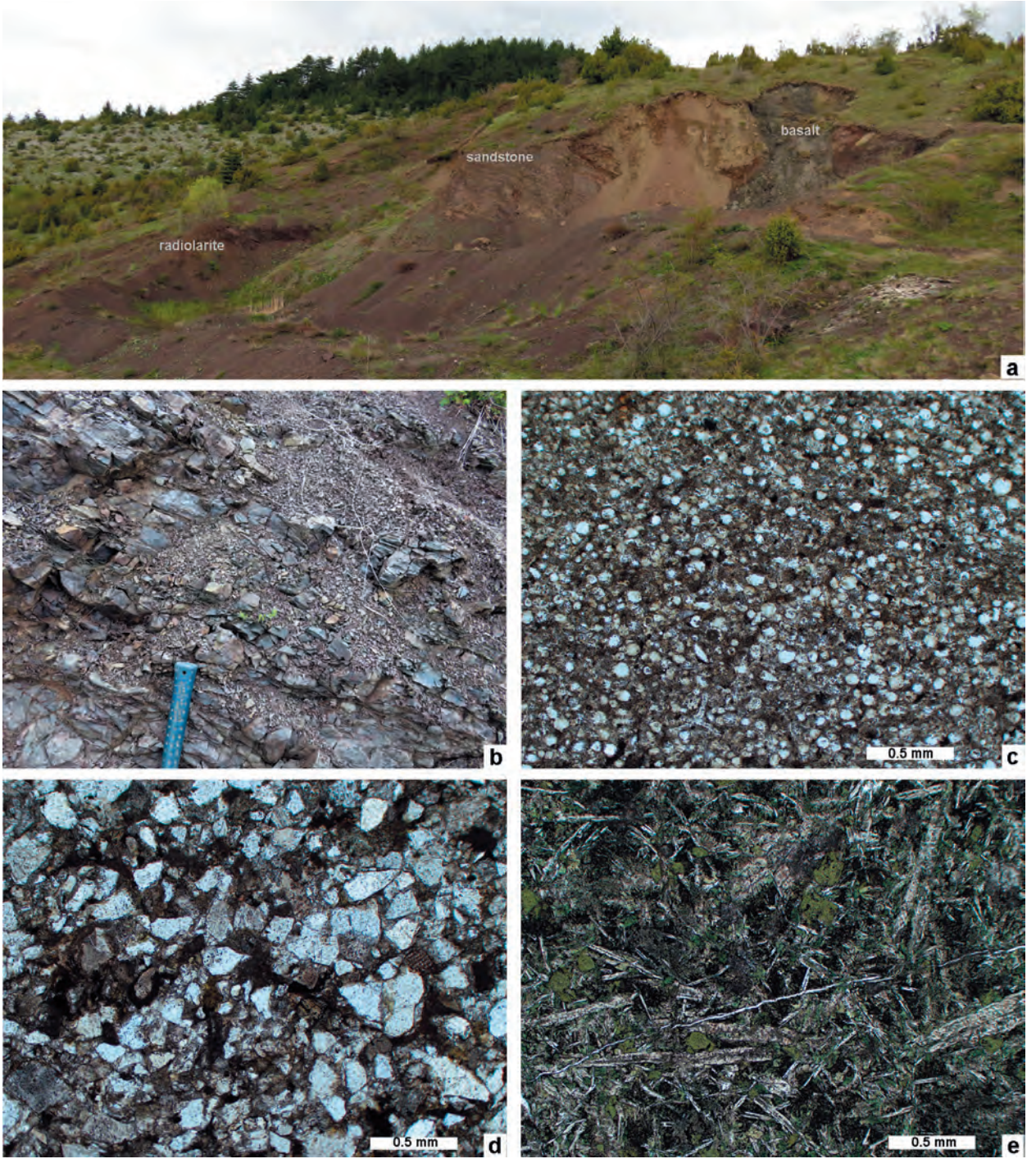

Figure 33: Ophiolitic mélange at Vijenac with blocks of radiolarite, sandstone and basalt (a).
Close up of radiolarian chert with sample JAB 3 (b) and microfacies of this chert with densely packed radiolarians (c). Photomicrographs of quartz sandstone (d) and basalt (e).

is known from the Anisian and Early Ladinian (Dumitrica 2017). The Late Anisian–Early Ladinian age is in good agreement with the oldest age documented for sea-floor spreading in the Dinarides–Hellenides, e.g. in the Fourka Unit of Othris (Ferrière et al. 2015) and the Miraka section in Albania (Gawlick et al. 2008).

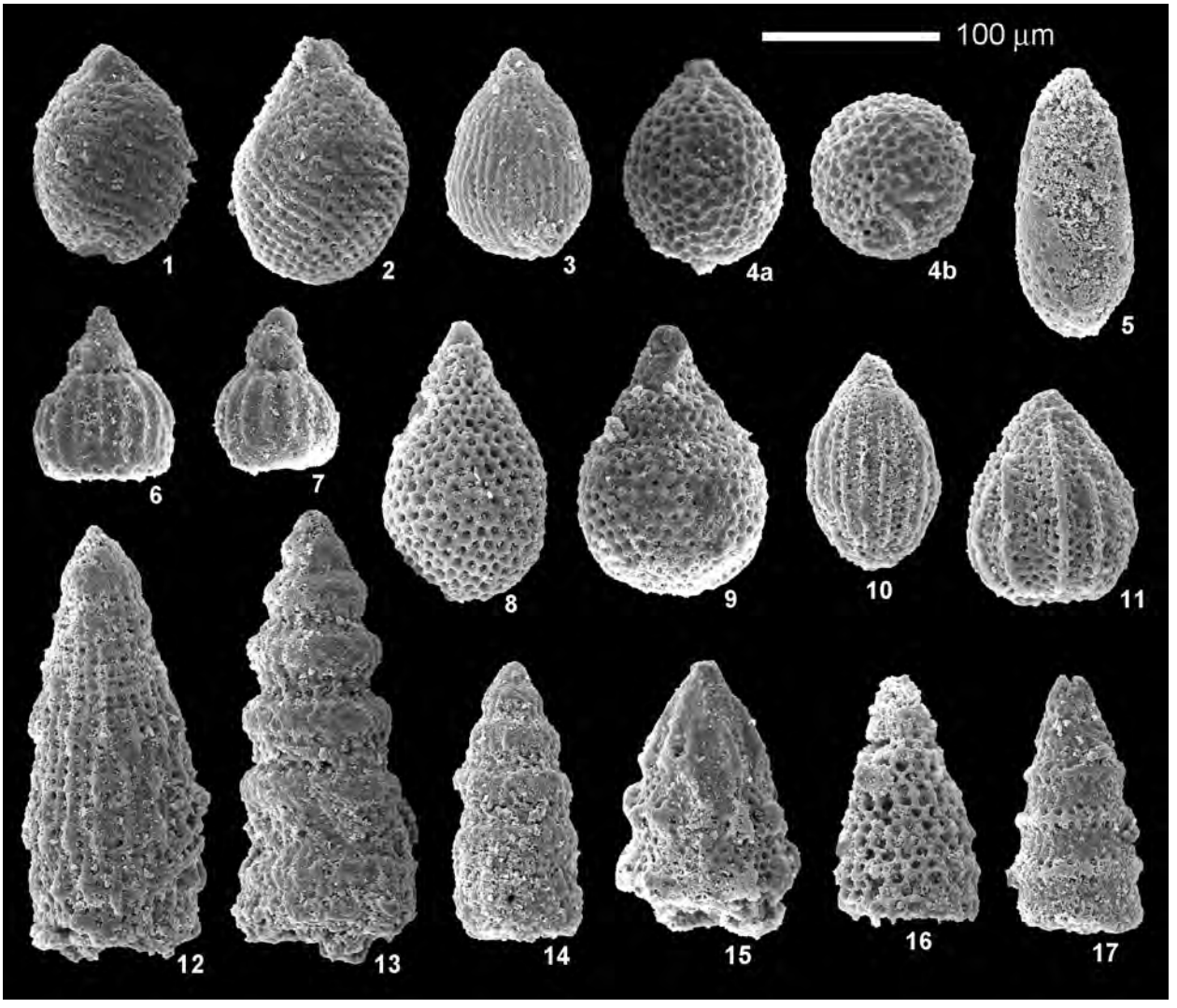

Figure 34: Late Bathonian – early Callovian (UAZ 7) radiolarians from sample JAB 3, Vijenac.
Scale bar 100 µm for all illustrations.
1–2: Kilinora spiralis *(Matsuoka)*
3: Striatojaponocapsa naradaniensis *(Matsuoka)*
4a–b: Striatojaponocapsa conexa *(Matsuoka), a: lateral view, b: antapical view.*
5: Guexella nudata (Kocher)
6–7: Eucyrtidiellum ptyctum *(Riedel & Sanfilippo)*
8–9: Praewilliriedellum convexum *(Yao)*
10: Protunuma japonicus *Matsuoka & Yao*
11: Unuma gordus *Hull*
12: Transhsuum maxwelli *(Pessagno)*
13–14: Cinguloturris carpatica *Dumitrica*
15: Xitus skenderbegi *(Chiari, Marcucci & Prela)*
16: Takemuraella *cf.* schardti *(O'Dogherty, Goričan & Dumitrica)*
17: Mizukidella kamoensis *(Mizutani & Kido)*

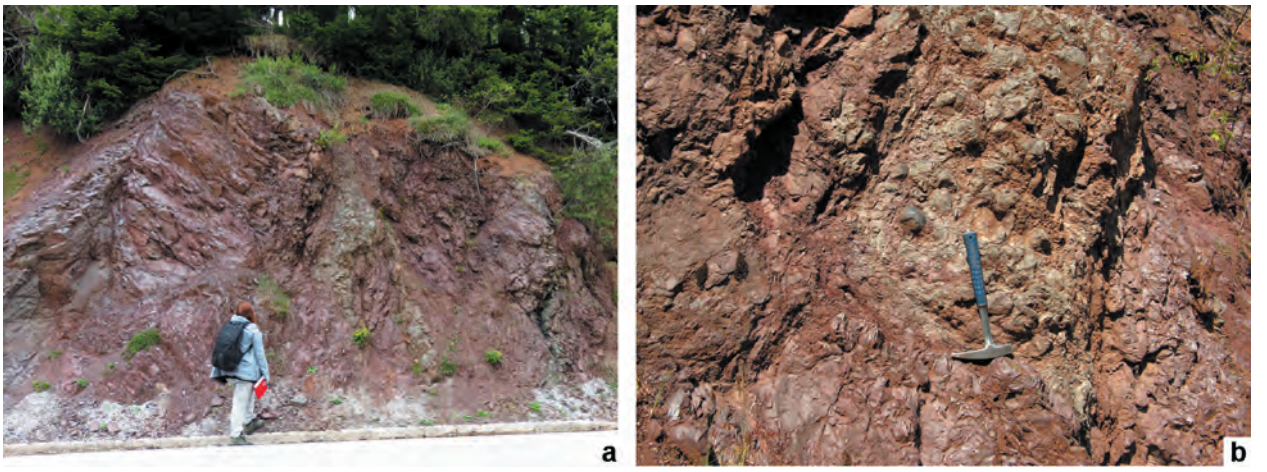

Figure 35: Block of Triassic chert at Drno Brdo (a) and a detail of block showing conglomerate with clasts of basalt (b). Radiolarian sample Z1 (Figure 37: 7–13) was collected in this block.

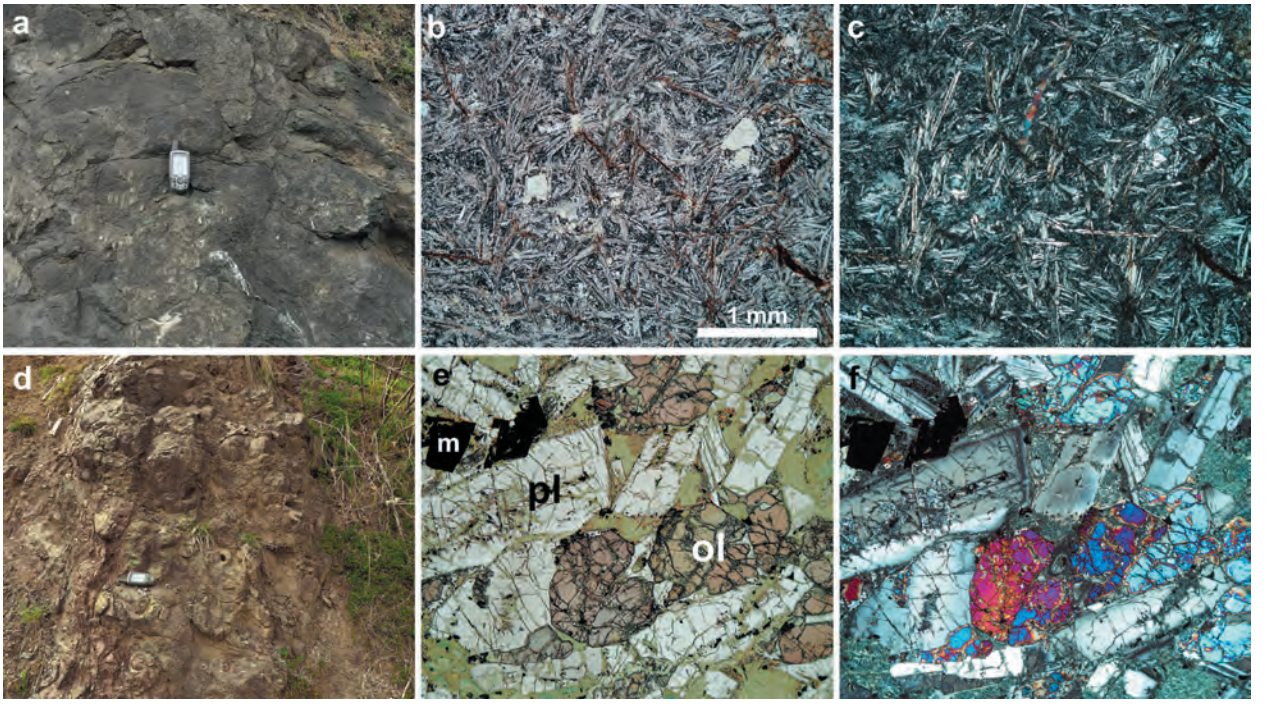

Figure 36: Ophiolite lithologies with radiolarites in sedimentary contact along the road from Pljevlja to Žabljak near Eco Camp Drno Brdo, about 150 m E of radiolarites in Figure 35.
a-c) basaltic pillow lava, a: outcrop, b: normal, c: cross polarized light, photomicrographs of a thin section showing an intersertal texture of plagioclase needles, the dark matrix represents volcanic glass replaced by secondary minerals.
d-f) same locality, a disrupted olivine bearing micro-grabbro dyke cutting through radiolarite. e: normal, f: cross polarized light, photomicrographs of a thin section showing plagioclase (pl), fresh olivine (ol), magnetite (m) and secondary epidote and chlorite in the light green patches in normal light.

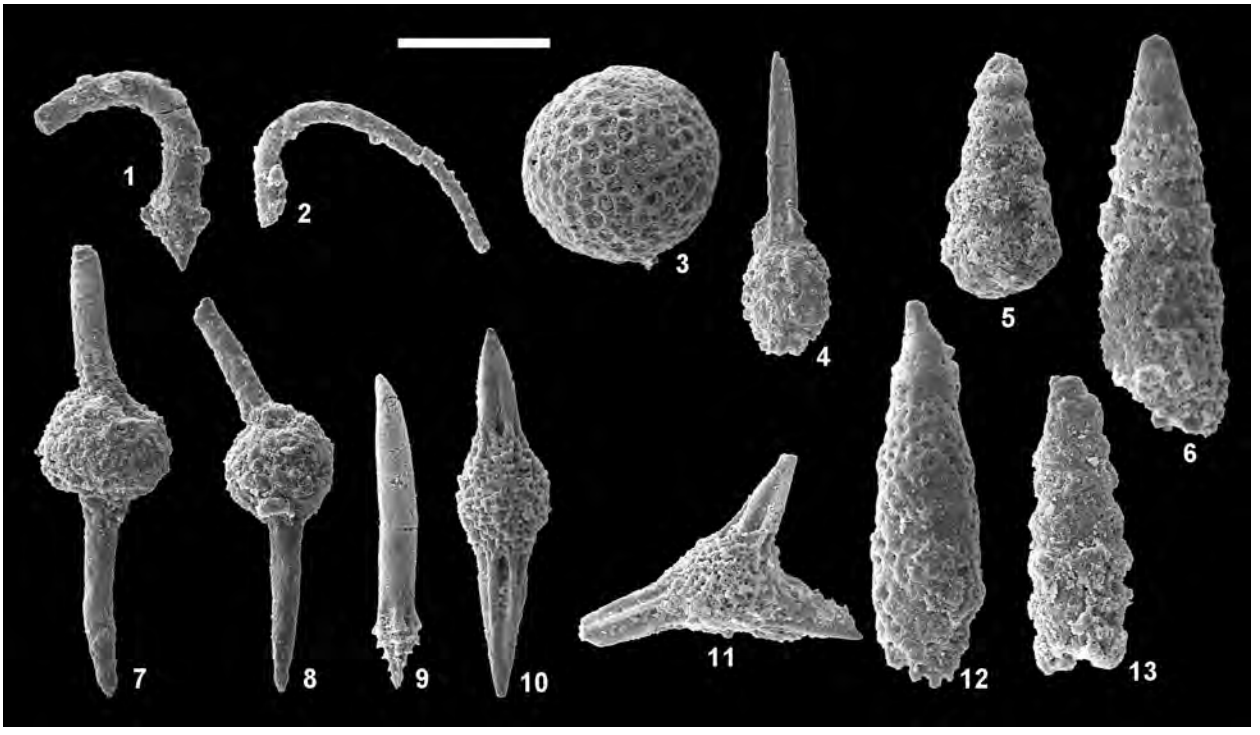

Figure 37: Late Anisian radiolarians from samples Z4 (1–6) and Z1 (7–13), Drno Brdo.
Sample Z4 (N 43°13'02.1"; E 19°20'47.46"):
1–2: Oertlispongus inaequispinosus *Dumitrica, Kozur & Mostler, scale bar 133 μm.*
3: Arhaeocenosphaera *sp., scale bar 133 μm.*
4: Pseudostylosphaera *sp., scale bar 200 μm.*
5: Pararuesticyrtium *sp., scale bar 100 μm.*
6: Triassocampe scalaris *Dumitrica, Kozur & Mostler, scale bar 100 μm.*
Sample Z1 (N 43°12'57.78"; E 19°20'41.58"):
7–8: Paroertlispongus *aff.* diacanthus *(Sugiyama), scale bar 133 μm. This species differs from typical* P. diacanthus *by having shorter and thicker spines.*
9: Paroertlispongus *sp., scale bar 133 μm.*
10: Pseudostylosphaera acrior *(Bragin), scale bar 133 μm.*
11: Eptingium manfredi *Dumitrica, scale bar 133 μm.*
12: Celluronta donax *Sugiyama, scale bar 100 μm.*
13: Pararuesticyrtium *sp., scale bar 100 μm.*

5 DINARIC BASINS, REGIONAL PALEOCEANOGRAPHY AND RADIOLARITES

The paleoceanography of Dinaric basins is discussed in the regional context both for Mesozoic rift basins underlain by thinned continental crust and for branches of the Neotethys underlain by oceanic crust such as the Meliata-Maliac, the Vardar oceans and the more southern Pindos ocean, a mere rift trough in the Montenegro transect. Pelagic oceanography and sedimentary processes are independent from their substrate, once it is below the thermocline. In contrast, the proximity of shallow margins may largely modify pelagic sedimentation by the input of peri-platform ooze or detrital clay preventing the formation of bedded cherts.

Mesozoic radiolarians are fundamental for the chronology of these basins. They have been recovered from both pelagic siliceous limestones, siliceous mudstones and from radiolarites wherein they are the main constituent. More recently, a case has been made for the presence of *Synechococcus*, a photosynthetic picocyanobacterium that produces, when degrading, EPS with Si-nanoparticles, even under highly Si-undersaturated conditions (Baines et al. 2012; Tang et al. 2014). This organism is thought to have existed since the Proterozoic to Recent, and may constitute an important proportion of the microcrystalline matrix of radiolarian cherts.

Radiolarian productivity is a function of local, regional, and global fluctuations of sea-surface fertility (Baumgartner 1987; DeWever et al. 1994). Radiolarites did not form in "Intra-Pangean" basins, such as the Jurassic Central Atlantic and the Proto-Caribbean (Figure 38). Middle Jurassic to Early Cretaceous radiolarites reported from several Antillean islands belong to exotic terranes of

Pacific origin (Bandini et al. 2011). These basins were poorly connected with the world ocean and had an anti-estuarine circulation pattern, resulting in relatively low surface fertility (Baumgartner 1987, 2013). The abundance of clays during the Middle Jurassic and the onset of oligotrophic nannoplankton productivity did not allow for the formation of ribbon-bedded radiolarites.

In Western Tethys, a "radiolarite window", ranging from early Bajocian to late Tithonian, seems to be related to regional sea-surface fertility changes, explained by Baumgartner (2013) by the "Caribbean River Plume Model" (Figure 39), rather than regional upwelling unlikely in the complicated paleogeography of Western Tethyan basins. Classical concepts (e.g. Bosellini & Winterer 1975; Bernoulli & Jenkyns 2009) interpreted the paleogeographic distribution of pelagic limestone vs. siliceous mudstone/radiolarite in Western Tethys as the result of tectonic subsidence of distal marginal and oceanic seafloors beneath a shallow CCD. Later, radiolarian biochronology revealed that condensed pelagic limestone sedimentation on highs was coeval with rapid basal radiolarite sedimentation (Baumgartner 1990), which could not be explained as a dissolution-resistant residue of marginal carbonates. Baumgartner (2013, p. 312) concluded for the Western Tethyan Middle–Late Jurassic "radiolarite window": "The spatio-temporal distribution of carbonate and silica on Tethyan margins cannot be ex-

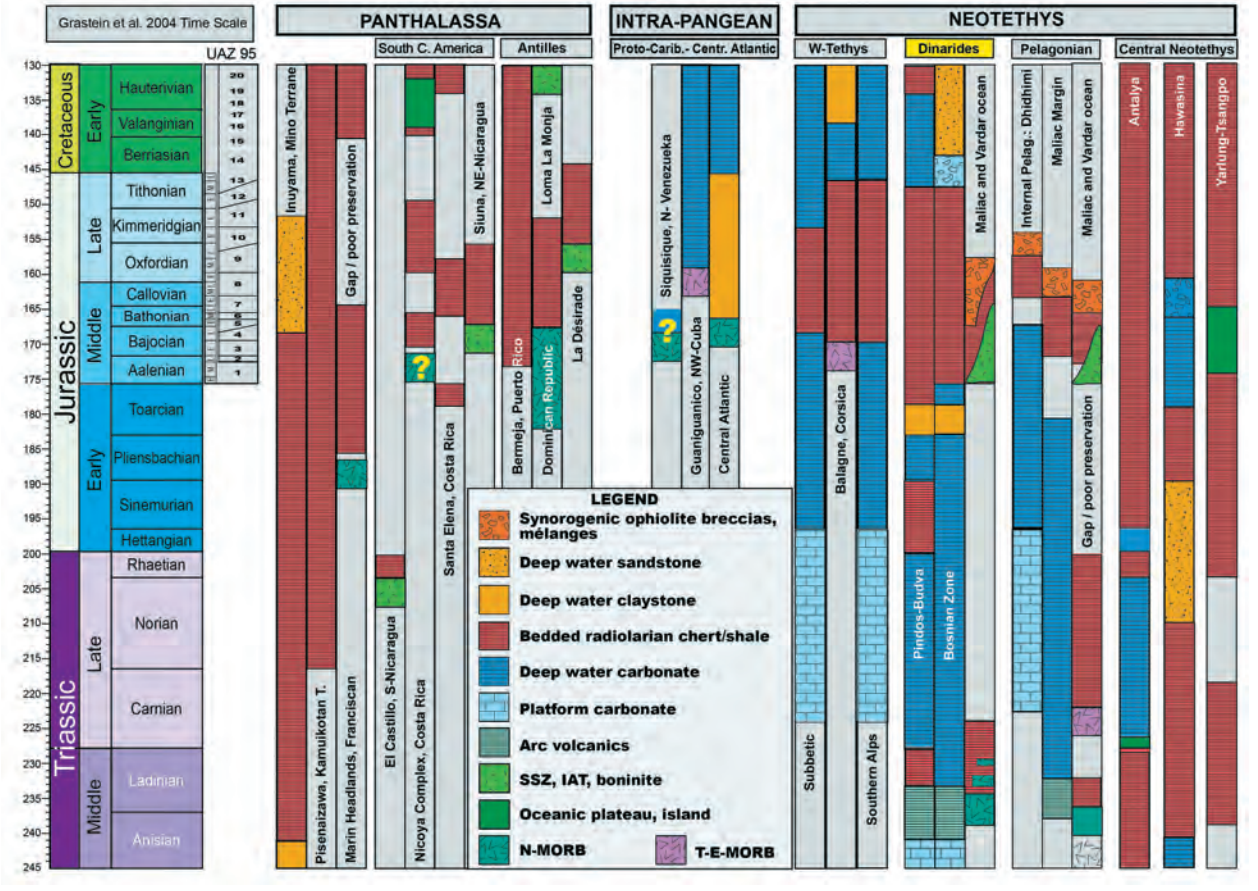

Figure 38: Middle Triassic-Early Cretaceous chronostratigraphy of pelagic facies in typical sections from Panthalassa to the E, through the intra-Pangean basins to Neotethys (modified after Baumgartner et al. 2017). Note the absence of ribbon radiolarites in the intra-Pangean proto-Caribbean and Central Atlantic. In the Dinarides-Hellenides the Western Tethyan Bajocian-Tithonian "radiolarite window" is observed in basins underlain by (thinned) continental crust in the proximity of carbonate platforms. The Budva-Pindos Basin and the Neotehyan Ocean remnants may contain radiolarites since the Middle Triassic. (Sources: Panthalassa: Murchey 1984, Ikeda et al. 2010, Ikeda & Tada 2014; S. central America: Baumgartner et al. 2008; Antilles: Bandini et al. 2011, Baumgartner et al. 2018; Intra-Pangean: Baumgartner 1984, Sandoval Gutierrez 2015; W Tethys: Baumgartner 1984, 1987, 2013; Dinarides: Goričan 1994; Vishnevskaya et al. 2009; Chiari et al. 2011; Pelagonian: Baumgartner 1985; Ferrière et al. 2015; Central Neotethys: Tekin 1999; Blechschmidt et al. 2004; Wang et al. 2002; Ziabrev et al. 2004).

plained by the palaeodepth of the calcite compensation depth (CCD) alone. Extensive lateral transport of radiolarian tests from topographic highs to the basins, and early diagenetic replacement on the highs by calcite may explain the absence of silica and the formation of condensed pelagic limestones coeval with basinal radiolarites. On a larger scale, palaeoclimatic changes, recorded in the carbon isotope curve (e.g., Jenkyns et al. 2002), rather than palaeotectonic changes, seem to have triggered major changes in surface fertility which, in turn, brought about the facies changes observed in Tethyan marginal basins. Regional platform demise, possibly due to eutrophication and a diachronous onset of radiolarites since the Early Bajocian, can be correlated with a positive shift in $\delta^{13}C$ values whereas platform recovery and the end of radiolarite accumulation correlates with a gradual drop-off of $\delta^{13}C$ values," and the installation of the Tithonian dry event (Price et al. 2016).

In the Dinaric basins underlain by Triassic carbonate platforms radiolarite accumulation began somewhat earlier (Figure 4). The Budva-Pindos Basin, that widens towards the SE into an ocean, contains the first radiolarites in the Middle Triassic and continuous radiolarite formation from earliest Hettangian to early Turonian, interrupted only by Pliensbachian carbonate resediments and late Tithonian to early Hauterivian pelagic limestones. The Budva-Pindos Basin was certainly connected with the central Neotethys where radiolarites formed, far from carbonate margins, since its oceanisation (Anisian or earlier) until the early Late Cretaceous, when planktonic foraminifera and calcareous nannoplankton began to

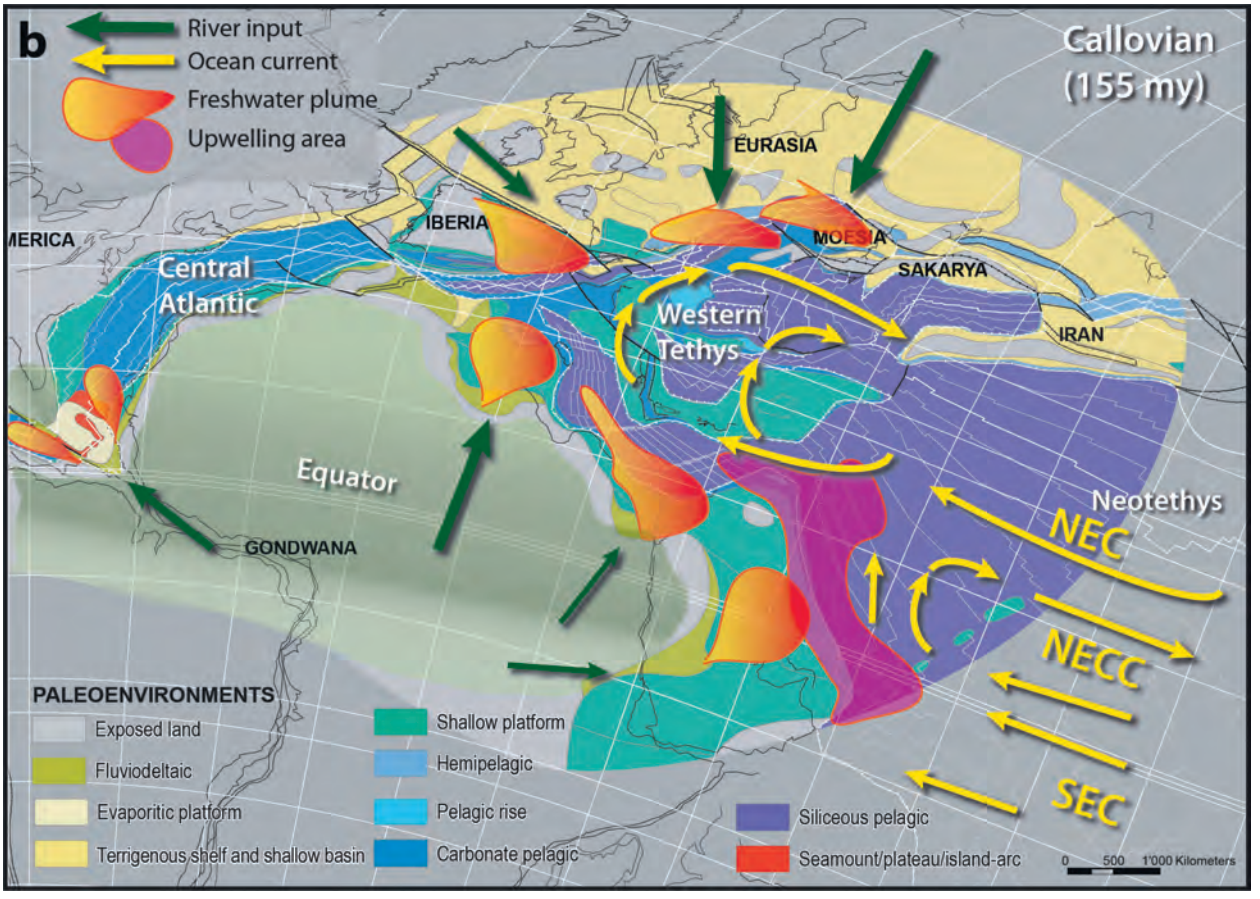

Figure 39: The River Plume Model (after Baumgartner 2013, his Figure 6b). Callovian (155 Ma) reconstruction (after Stampfli & Borel, 2002) of Western Tethys and Central Atlantic with simplified principal sedimentary palaeoenvironments (compiled by C. Wilhem, personal communication). The equatorial current system impinges on the Arabian Margin and is partly deflected into the Western Tethyan realm. Rivers draining tropical Africa and temperate Europe produce river plumes carrying dissolved organic matter that is distributed by anticyclonic surface circulation over the entire realm, including oceanic and epicontinental areas. The Central Atlantic and Proto-Caribbean are restricted 'Mediterranean' basins likely to have experienced excess evaporation, water stratification and widespread dysoxic bottom conditions trapping organic matter (and nutrients).

dominate worldwide. Late Paleozoic to early Late Cretaceous ranges of radiolarites are common in circum-Pacific remnants of Panthalassa (Figure 38). Several authors have inferred a monsoonal climate regime (DeWever et al. 1994, 2014; Arias 2008; Baumgartner 2013; Ikeda et al. 2017) that produced seasonally opposed trade winds over the Neotethys, bounded by the jaws of Eurasia to the north and Gondwana to the south (Figure 40). This regime may have produced important high productivity upwelling systems on both margins, in addition to upwelling beneath the peri-equatorial current system. The Jurassic convergence in the Dinarides-Hellenides, excluding the external Budva-Pindos and High Karst realms, makes an abrupt end to radiolarite deposition in this area, while oceanic crust continued to be formed to the southeast and radiolarites continued to form until the early Late Cretaceous also on the continental margin (e.g., Antalya nappes in southern Turkey, Yurtsever et al. 2003; Pichakun nappes in Iran, Robin et al. 2010; Hawasina units in Oman, Blechschmidt et al. 2004).

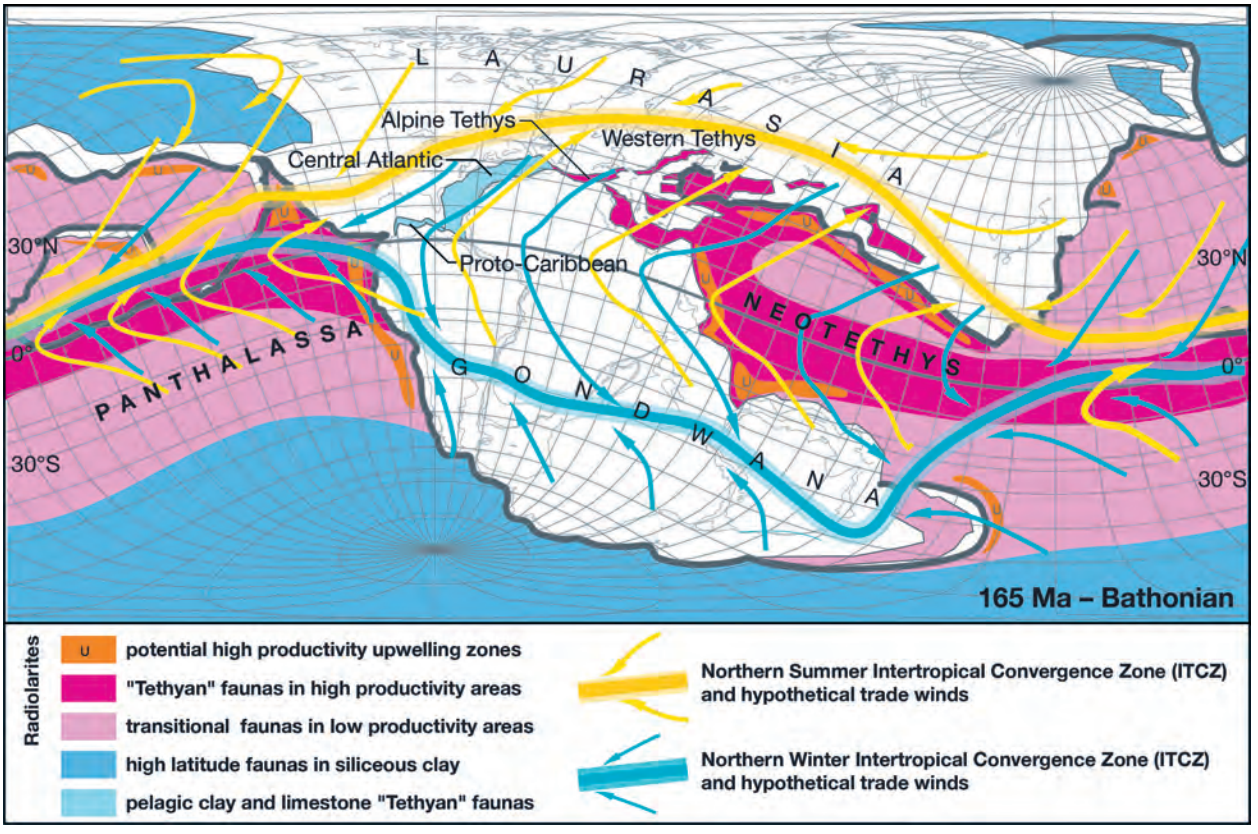

Figure 40: Paleogeographic map for 165 Ma (Bathonian) after Baumgartner et al. (2018) adapted from Bandini et al. (2011b) and Baumgartner (2013), showing major oceanic radiolarian bio-provinces and low/high accumulation of radiolarites. Epicontinental seas and continents are shown in white. Neotethys and Panthalassa oceans were covering wide paleo-latitudes and were well connected with each other. The "Intra-Pangean Basins", i.e. the Central Atlantic and the initial Proto-Caribbean, formed a low-fertility 'Mediterranean' sea with restricted connections to the world ocean. Middle Jurassic radiolarian faunas of that sea are very similar to those of the Tethys–Panthalassan low latitude belt, but accumulation rates were much smaller and episodic, not allowing for radiolarite formation. Northern summer (yellow) and Northern winter (blue) Intertropical Convergence Zones and associated (hypothetical) trade winds are shown, suggesting a "mega-monsoon" situation in Neotethys (Ikeda et al. 2017).

ACKNOWLEDGEMENTS

This study was for the most part financed by the Slovenian Research Agency, through the program P1-0008 Paleontology and Sedimentary Geology. Elizabeth S. Carter is acknowledged for her constructive comments and corrections.

REFERENCES

Aljinović, D., Horacek, M., Krystyn, L., Richoz, S., Kolar-Jurkovšek, T., Smirčić, D. & Jurkovšek, B., 2018: *Western Tethyan epeiric ramp setting in the Early Triassic: An example from the Central Dinarides (Croatia).* Journal of Earth Sciences 29 (4): 806–823.

Antonijević, R., Pavić, A & Karović, J., 1969: *Osnovna geološka karta 1:100 000, listovi Kotor i Budva.* Savezni geološki zavod, Beograd.

Argnani, A., 2018: *Subduction evolution of the Dinarides and the Cretaceous orogeny in the Eastern Alps: Hints from a new paleotectonic interpretation*. Tectonics 37: 621–635.

Arias, C., 2008: *Palaeoceanography and biogeography in the Early Jurassic Panthalassa and Tethys Oceans.* Gondwana Research 14 (3): 306–315.

Aubouin, J., Blanchet, R., Cadet, J.-P., Celet, P., Charvet, J., Chorowicz, J., Cousin, M. & Rampnoux, J.-P., 1970: *Essai sur la géologie des Dinarides.* Bull. Soc. géol. France sér. 7, XII (6): 1060–1095.

Baines, S.B., Twining, B.S., Brzezinski, M.A., Krause, J.W., Vogt, S., Assael, D. & McDaniel, H., 2012: *Significant silicon accumulation by marine picocyanobacteria*. Nature Geoscience 5: 886–891.

Bandini, A.N., Baumgartner, P.O., Flores, K., Dumitrica, P., Hochard, C., Stampfli, G.M. & Jackett, S.J., 2011: *Aalenian to Cenomanian Radiolaria of the Bermeja Complex (Puerto Rico) and Pacific origin of radiolarites on the Caribbean Plate*. Swiss Journal of Geosciences 104: 367–408.

Baumgartner, P.O., 1984: *A Middle Jurassic – Early Cretaceous low-latitude radiolarian zonation based on unitary associations and age of Tethyan radiolarites*. Eclogae geologicae Helvetiae 77: 729–837.

Baumgartner, P.O., 1985: *Jurassic sedimentary evolution and nappe emplacement in the Argolis Peninsula (Peloponnesus, Greece).* Mémoires de la Société helvétique des Sciences Naturelles 99: 1–111.

Baumgartner, P.O., 1987: *Age and genesis of Tethyan Jurassic radiolarites*. Eclogae geologicae Helvetiae 80, 831–879.

Baumgartner, P.O., 1990: *Genesis of Jurassic Tethyan radiolarites – the example of Monte Nerone (Umbria-Marche Apennines).* Atti 2. Convegno, Fossili Evoluzione Ambiente. Editore Comitato Centenario Raffaele Piccinini, Pergola, 19–32.

Baumgartner, P.O., 2013: *Mesozoic radiolarites – accumulation as a function of sea surface fertility on Tethyan margins and in ocean basins.* Sedimentology 60, 292–318.

Baumgartner, P.O., Bartolini, A., Carter, E.S., Conti, M., Cortese, G., Danelian, T., De Wever, P., Dumitrica, P., Dumitrica-Jud, R., Goričan, Š., Guex, J., Hull, D.M., Kito, N., Marcucci, M., Matsuoka, A., Murchey, B., O'Dogherty, L., Savary, J., Vishnevskaya, V., Widz, D. & Yao, A., 1995: *Middle Jurassic to Early Cretaceous radiolarian biochronology of Tethys based on Unitary Associations*. In: Baumgartner, P.O., O'Dogherty, L., Goričan, Š., Urquhart, E., Pillevuit, A. & De Wever, P. (Eds.), *Middle Jurassic to Lower Cretaceous Radiolaria of Tethys: Occurrences, Systematics, Biochronology.* Mémoires de Géologie (Lausanne) 23: 1013–1048.

Baumgartner, P.O., Flores, K., Bandini, A., Girault, F. & Cruz, D., 2008: *Upper Triassic to Cretaceous Radiolaria from Nicaragua and northern Costa Rica: the Mesquito composite oceanic terrane.* Ofioliti 33: 1–19.

Baumgartner, P. O., Andjic, G., Sandoval-Gutierez, M., Bandini-Maeder, A., Diserens, M.-O., Baumgartner-Mora, C. & Kukoc, D., 2018: *Radiolarian biochronology and paleoceanography of Pacific Terranes in Central America and the Caribbean.* In AAPG Hedberg Research Conference, *Geology of Middle America – the Gulf of Mexico, Yucatán, Caribbean, Grenada and Tobago Basins and Their Margins*, Siguenza, Spain, 10–16, AAPG Datapages, Search and Discovery Article #90330, Tulsa.

Bébien, J., Blanchet, R., Cadet, J.-P., Charvet, J., Chorowicz, J., Lapierre, H. & Rampnoux, J.-P. 1978: *Le volcanisme triasique des Dinarides en Yougoslavie : sa place dans l'évolution géotectonique péri-méditerranéenne*. Tectonophysics 47: 159–176.

Bechstädt, T., Brandner, R., Mostler, H. & Schmidt, K., 1978: *Aborted rifting in the Triassic of the eastern and southern Alps.* N. Jb. Geol. Paläont. Abh. 156 (2): 157–178.

Bernoulli, D. & Laubscher, H., 1972: *The palinspastic problem of the Hellenides*. Eclogae Geologicae Helvetiae 65: 107–118.

Bernoulli, D. & Jenkyns, H.C., 2009: *Ophiolites in ocean–continent transitions: from the Steinmann Trinity to sea-floor spreading.* C.R. Geoscience 341: 363–381.

Bill, M., O'Dogherty, L., Guex, J., Baumgartner, P.O. & Masson, H., 2001: *Radiolarite ages in Alpine-Mediterranean ophiolites: Constraints on the oceanic spreading and the Tethys-Atlantic connection*. GSA Bulletin 113 (1): 129–143.

Blanchet, R., 1970: *Sur un profil des Dinarides, de l'Adriatique (Split-Omiš, Dalmatie) au Bassin pannonique (Banja Luka – Doboj, Bosnie)*. Bull. Soc. géol. France sér. 7, XII (6): 1010–1027.

Blanchet, R., 1975: *De l'Adriatique au Bassin pannonique. Essai d'un modèle de chaîne alpine*. Mémoires de la Société géologique de France 120, 172 pp., 4 pls, 1 map.

Blanchet, R., Cadet, J.-P., Charvet, J. & Rampnoux, J.-P., 1969: *Sur l'existence d'un important domaine de flysch tithonique–crétacé inférieur en Yougoslavie: l'unité du flysch bosniaque.* Bull. Soc. *Géol.* France sér. 7, XI (6): 871–880.

Blechschmidt, I., Dumitrica, P., Matter, A., Krystyn, L. & Peters, T., 2004 : *Stratigraphic architecture of the northern Oman continental margin – Mesozoic Hamrat Duru Group, Hawasina Complex, Oman*. GeoArabia 9: 81–132.

Böhm, F., 1992: *Mikrofazies and Ablagerungsmilieu des Lias und Dogger der Nordöstlichen Kalkalpen*. Erlanger Geol. Abh. 121: 55–217.

Borojević Šoštarić, S., Neubauer, F., Handler, R. & Palinkaš, L.A., 2012. *Tectonothermal history of the basement rocks within the NW Dinarides: new 40Ar/39Ar ages and synthesis*. Geologica Carpathica 63 (6): 441–452.

Bortolotti, V., Marroni, M., Pandolfi, L. & Principi, G., 2005: *Mesozoic to Tertiary tectonic history of the Mirdita ophiolites, northern Albania*. The Island Arc 14: 471–493.

Bortolotti, V., Chiari, M., Marcucci, M., Photiades, A., Principi, G. & Saccani, E., 2008: *New geochemical and age data on the ophiolites from the Othrys area (Greece): implication for the Triassic evolution of the Vardar Ocean*. Ofioliti 33: 135–151.

Bortolotti, V., Chiari, M., Marroni, M., Pandolfi, L., Principi, G. & Saccani, E., 2013. *Geodynamic evolution of ophiolites from Albania and Greece (Dinaric-Hellenic belt): one, two, or more oceanic basins?* International Journal Earth Sciences 102, 783–811.

Bosellini, A. & Winterer, E.L., 1975: *Pelagic limestone and radiolarite of the Tethyan Mesozoic: a genetic model*. Geology 3: 279–282.

Brack, P. & Rieber, H., 1993: *Towards a better definition of the Anisian/Ladinian boundary: New biostratigraphic data and correlations of boundary sections from the Southern Alps*. Eclogae geologicae Helvetiae 86 (2): 415–527.

Bragina, L.G., Bragin, N.Yu., Djerić, N. & Gajić, V., 2014: *Late Cretaceous Radiolarians and Age of Flyschoid Sediments in the Struganik Section (Western Serbia)*. Stratigraphy and Geological Correlation 22 (2): 202–218.

Bragina, L.G., Bragin, N.Yu., Kopaevich, L.F. & Beniamovsky, V.N., 2018: *Santonian Radiolarians and Foraminifers from Brežđe Section, Western Serbia*. Moscow University Geology Bulletin 73 (4): 333–345.

Bragina, L.G., Bragin, N.Yu., Kopaevich, L.F., Djerić, N. & Gerzina Spajić, N., 2020: *Stratigraphy and Microfauna (Radiolarians and Foraminifera) of the Upper Cretaceous (Upper Santonian–Lower Campanian) Carbonate Deposits in the Area of Struganik Village, Western Serbia)*. Stratigraphy and Geological Correlation 28 (1): 65–87.

Burić, P., 1966: *Geologija ležišta boksita Crne Gore (Géologie des gîtes de bauxite du Monténégro, Yougoslavie)*. Geološki glasnik, Sarajevo, Posebna izdanja 8: 1–277.

Cadet, J.-P., 1978: *Essai sur l'évolution alpine d'une paléomarge continentale: les confins de la Bosnie-Herzégovine et du Monténégro (Yougoslavie)*. Mémoires de la Société géologique de France (nouvelle série) 133: 1–83, pls. 1–4.

Cafiero, B. & De Capoa Bonardi, P., 1980: *Stratigraphy of the pelagic Triassic in the Budva-Kotor area (Crna Gora, Montenegro, Yugoslavia).* Bolletino della Società Paleontologica Italiana 19 (2): 179–204.

Cafiero, B. & De Capoa Bonardi, P., 1981: *I Conodonti dei calcari ad* Halobia *del Trias superior del Montenegro (Crna Gora, Jugoslavia)*. Rivista Italiana di Paleontologia 86 (3): 563–576.

Carter, E.S. & Hori, R.S., 2005: *Global correlation of the radiolarian faunal change across the Triassic-Jurassic boundary.* Canadian Journal of Earth Sciences 42: 777–790.

Carter, E.S., Whalen, P.A. & Guex, J., 1998: *Biochronology and paleontology of Lower Jurassic (Hettangian and Sinemurian) radiolarians, Queen Charlotte Islands, British Columbia*. Geological Survey of Canada, Bulletin 496: 1–162.

Celarc, B., Goričan, Š. & Kolar-Jurkovšek, T., 2013: *Middle Triassic carbonate-platform break-up and formation of small-scale half-grabens (Julian and Kamnik–Savinja Alps, Slovenia).* Facies 59: 583–610.

Charvet, J., 1978: *Essai sur un orogène alpin. Géologie des Dinarides au niveau de la transversale de Sarajevo (Yougoslavie)*. Société géologique du Nord Publ 2:1–554, pls. 1–21.

Charvet, J., 2013: *Le développement géotectonique des Dinarides: évolution des idées et apport des équipes françaises.* Travaux du Comité français d'Histoire de la Géologie. In: Comité français d'Histoire de la Géologie 3ème série 27 (7): 163–220.

Chiari, M., Bortolotti, V., Marcucci, M., Photiades, A. & Principi, G., 2003: *The Middle Jurassic siliceous sedimentary cover at the top of the Vourinos Ophiolite (Greece)*. Ofioliti 28: 95–103.

Chiari, M., Marcucci, M. & Prela, M., 2004: *Radiolarian assemblages from the Jurassic cherts of Albania: new data*. Ofioliti 29: 95–105.

Chiari, M., Djerić, N., Garfagnoli, F., Hrvatović, H., Krstić, M., Levi, N., Malasoma, A., Marroni, M., Menna, F., Nirta, G., Pandolfi, L., Principi, G., Saccani, E., Stojadinović, U. & Trivić, B., 2011: *The geology of the Zlatibor-Maljen area (western Serbia): A geotraverse across the ophiolites of the Dinaric-Hellenic collisional belt*. Ofioliti 36 (2): 139–166.

Chiari, M., Bortolotti, V., Marcucci, M., Photiades, A., Principi, G. & Saccani, E., 2012: *Radiolarian biostratigraphy and geochemistry of the Koziakas massif ophiolites (Greece).* Bulletin de la Société géologique de France 183(4): 287–306.

Čadjenović, D. & Radulović, N., 2018: *The distribution of terrigenous clastics of Anisian: slope, submarine fan, basins of Crmnica in Montenegro*. 17th Serbian Geological Congress, Book of Abstracts, 91–97.

Čađenović, D., Milutin, J., Đaković, M. & Radulović, N., 2014: *Anisian carbonates of Crmnica and surroundings in Montenegro*. 16th Serbian Geological Congress, Proceedings: 63–71 (In Serbian, English summary).

Črne, A.E., 2009: *Depositional model of Lower Jurassic carbonates on the Dinaric Carbonate Platform margin*. Dissertation, University of Ljubljana, 185 pp.

Črne, A.E. & Goričan, Š., 2008: *The Adriatic-Dinaric Carbonate Platform margin in the Early Jurassic: a comparison between successions in Slovenia and Montenegro*. Bollettino della Società Geologica Italiana 127: 389–405.

Črne, A.E., Weissert, H., Goričan, Š. & Bernasconi, S.M., 2011: *A biocalcification crisis at the Triassic–Jurassic boundary recorded in the Budva Basin (Dinarides, Montenegro)*. GSA Bulletin 123 (1–2): 40–50.

Danilova, A., 1958: *Mikropaleontološki prikaz zona višeg senona u Boki Kotorskoj*. Geološki glasnik Titograd 11: 223–232, pl. 23–27.

Đaković, M., 2018: *Stratigraphy of Triassic formations with ammonoids between Virpazar and Bar (Montenegro).* Unpublished dissertation, University of Belgrade, 238 pp. (In Serbian, with English abstract).

Đaković, M., Gawlick, H.-J., Čađenović, D., Missoni, S., Milić, M. & Krystyn, L., 2018: *Bithynian cherty limestones of the Rosni virovi locality, Budva zone (southern Montenegro).* XXI International Congress of the CBGA, Abstracts, p. 64.

Đaković, M., Gawlick, H.-J. & Sudar, M., 2021: *Early-Middle Jurassic stepwise deepening in the transitional facies belt between the Adriatic Carbonate Platform Basement and Neo-Tethys open shelf in northeastern Montenegro evidenced by new ammonoid data from the early Late Pliensbachian (Lavinianum Zone).* Geološki anali Balkanskoga poluostrva 82 (1): 1–25.

Đaković, M., Krystyn, L. & Sudar, M., 2022: *The Middle Smithian (Early Triassic) ammonoids of Gornji Brčeli (Southern Montenegro)*. Rivista Italiana di Paleontologia e Stratigrafia 128 (2): 427–446.

Dercourt, J., 1968: *Sur l'accident de Scutari-Peć, la signification paléogéographique de quelques séries condensées en Albanie septentrionale*. Annales de la Société géologique du Nord 88: 109–117.

Đerić, N. & Gerzina, N., 2014: *New data on the age of an Upper Cretaceous clastic-carbonate succession in Brežđe (Western Serbia)*. Geologia Croatica 67 (3): 163–170.

Djerić, N., Gerzina, N., Gajić, V. & Vasić, N., 2009: *Early Senonian radiolarian microfauna and biostratigraphy from the Western Vardar Zone (Western Serbia).* Geologica Carpathica 60 (1): 35–41.

De Wever, P., 1984: *Triassic radiolarians from the Darnó area (Hungary).* Acta geol. Hungarica 27 (3), 295–306.

De Wever P., Azéma, J. & Fourcade, E., 1994: *Radiolaires et radiolarites: production primaire, diagenèse et paléogéographie.* Bulletin des Centres de Recherches Exploration-Production Elf Aquitaine 18 (1): 315–379.

De Wever, P., O'Dogherty, L. & Goričan, Š., 2014: *Monsoon as a cause of radiolarite in the Tethyan realm*. C. R. Geoscience 346 : 287–297.

Dimitrijević, M., 1967: *Sedimentološko-stratigrafski problemi srednjetrijaskog fliša u terenima između Skadarskog jezera i Jadranskog mora*. Geološki glasnik Titograd 5: 223–275.

Dimitrijević, M.D., 1997: *Geology of Yugoslavia*. Geological Institute GEMINI Special Publication, Belgrade, 187 pp.

Dilek, Y., Shallo, M. & Furnes, H., 2005: *Rift-drift, seafloor spreading, and subduction tectonics of Albanian ophiolites.* International Geology Review 47: 147–176.

Dumitrica, P., 2017: On the status of the Triassic Nassellarian radiolarian family Tetraspinocyrtiidae Kozur and Mostler and description of some related taxa. Revue de micropaléontologie 60: 33–85.

Dumitrica, P. & Dumitrica Jud, R., 1995: Aurisaturnalis carinatus *(Foreman), an example of phyletic gradualism among Saturnalid-type radiolarians*. Revue de Micropaléontologie 38 (3): 195–216.

Ferrière, J., Chanier, F. & Ditbanjong, P., 2012: *The Hellenic ophiolites: eastward or westward obduction of the Maliac Ocean, a discussion*. International Journal of Earth Sciences 101: 1559–1580.

Ferrière, J., Chanier, F., Baumgartner, P.O., Caridroit, M., Bout-Roumazeilles, V., Graveleau, F., Danelian, T. & Ventalon, S., 2015: *The evolution of the Triassic–Jurassic oceanic lithosphere: insights from the supra-ophiolitic series of Othris (continental Greece)*. Bull. soc. géol. France 186 (6): 71–84.

Ferrière, J., Baumgartner, P.O. & Chanier, F., 2016: *The Maliac Ocean: the origin of the Tethyan Hellenic ophiolites*. International Journal of Earth Sciences 105: 1941–1963.

Gawlick, H.-J. & Missoni, S., 2015: *Middle Triassic radiolarite pebbles in the Middle Jurassic Hallstatt Mélange of the Eastern Alps: implications for Triassic-Jurassic geodynamic and palaeogeographic reconstructions of the western Tethyan realm*. Facies 61 (13): 19 pages. DOI 10.1007/s10347-015-0439-3

Gawlick, H.-J. & Missoni, S., 2019: *Middle–Late Jurassic sedimentary mélange formation related to ophiolite obduction in the Alpine-Carpathian-Dinaridic Mountain Range*. Gondwana Research 74: 144–172.

Gawlick, H.-J. & Schlagintweit, F., 2006: *Berriasian drowning of the Plassen carbonate platform at the type-locality and its bearing on the early Eoalpine orogenic dynamics in the Northern Calcareous Alps (Austria)*. International Journal of Earth Sciences 96: 451–462.

Gawlick, H.J., Frisch, W., Hoxha, L., Dumitrica, P., Krystyn, L., Lein, R., Missoni, S. & Schlagintweit, F., 2008: *Mirdita Zone ophiolites and associated sediments in Albania reveal Neotethys Ocean origin*. International Journal of Earth Sciences 97: 865–881.

Gawlick, H.J., Sudar, M., Suzuki, H., Djerić, N., Missoni, S., Lein, R. & Jovanović D., 2009: *Upper Triassic and Middle Jurassic radiolarians from the ophiolitic mélange of the Dinaridic Ophiolite Belt, SW Serbia*. Neues Jahrbuch für Geologie und Paläontologie, Abhandlungen 253 (2–3), 293–311.

Gawlick, H.-J., Goričan, Š., Missoni, S. & Lein, R., 2012: *Late Anisian platform drowning and radiolarite deposition as a consequence of the opening of the Neotethys ocean (High Karst nappe, Montenegro)*. Bulletin de la Société géologique de France 183 (4): 349–358.

Gawlick, H.-J., Goričan, Š., Missoni, S., Dumitrica, P., Lein, R., Frisch, W. & Hoxha, L., 2016a: *Middle and Upper Triassic radiolarite components from the Kcira-Dushi-Komani ophiolitic mélange and their provenance (Mirdita Zone. Albania)*. Revue de micropaléontologie 59: 359–380.

Gawlick, H.-J., Missoni, S., Suzuki, H., Sudar, M., Lein, R. & Jovanović, D., 2016b: *Triassic radiolarite and carbonate components from a Jurassic ophiolitic mélange (Dinaridic Ophiolite Belt)*. Swiss Journal of Geosciences 109: 473–494.

Gawlick, H.-J., Sudar, M.N., Missoni, S., Suzuki, H., Lein, R., Jovanović, D., 2017a: *Triassic-Jurassic geodynamic evolution of the Dinaridic Ophiolite Belt (Inner Dinarides, SW Serbia)*. Journal of Alpine Geology 55, 1–167.

Gawlick H.-J., Djerić N., Missoni S., Bragin N. Yu., Lein R., Sudar M. & Jovanović D., 2017b: *Age and microfacies of oceanic Late Triassic radiolarite components from the Middle Jurassic ophiolitic mélange in the Zlatibor Mountains (Inner Dinarides, Serbia) and their provenance*. Geologica Carpathica 68 (4): 350–365.

Gawlick, H.-J., Missoni, S., Sudar, M.N., Goričan, Š., Lein, R., Stanzel, A.I. & Jovanović, D., 2017c: *Open-marine Hallstatt Limestones reworked in the Jurassic Zlatar Mélange (SW Serbia): a contribution to understanding the orogenic evolution of the Inner Dinarides*. Facies 63: 29 (25 p.).

Gawlick, H.-J., Missoni, S., Sudar, M.N., Suzuki, H., Méres, Š., Lein, R. & Jovanović, D. 2018: *The Jurassic Hallstatt Mélange of the Inner Dinarides (SW Serbia): implications for Triassic–Jurassic geodynamic and palaeogeographic reconstructions of the Western Tethyan realm*. Neues Jahrbuch für Geologie und Paläontologie, Abhandlungen 288 (1): 1–47.

Gawlick, H.-J., Sudar, M., Missoni, S., Aubrecht, R., Schlagintweit, F., Jovanović, D. & Mikuš, T., 2020. *Formation of a Late Jurassic carbonate platform on top of the obducted Dinaridic ophiolites deduced from the analysis of carbonate pebbles and ophiolitic detritus in southwestern Serbia*. International Journal of Earth Sciences 109: 2023–2048.

Goričan, Š., 1987: *Jurassic and Cretaceous radiolarians from the Budva Zone (Montenegro, Yugoslavia)*. Revue de Micropaléontologie 30: 177–196.

Goričan, Š., 1994: *Jurassic and Cretaceous radiolarian biostratigraphy and sedimentary evolution of the Budva Zone (Dinarides, Montenegro)*. Mémoires de Géologie (Lausanne) 18, 177 pp.

Goričan, Š., Halamić, J., Grgasović, T. & Kolar-Jurkovšek, T. 2005: *Stratigraphic evolution of Triassic arc--backarc system in northwestern Croatia*. Bull. Soc. géol. France 176: 3–22.

Gradstein, F.M., Ogg, J.G., Schmitz, M.D. & Ogg, G.M., 2012: *The geological time scale 2012*. Elsevier, Amsterdam.

Haas, J., Kovács, S., Gawlick, H.-J., Gradinaru, E., Karamata, S., Sudar, M., Péró, C., Mello, J., Polák, M., Ogorelec, B. & Buser, S., 2011: *Jurassic evolution of the tectonostratigraphic units of the Circum-Pannonian Region*. Jahrbuch der Geologischen Bundesanstalt 151: 281–354.

Halamić, J. & Goričan, Š., 1995: *Triassic radiolarites from Mts. Kalnik and Medvednica (northwestern Croatia).* Geologia Croatica 48: 129–146.

Halamić, J., Goričan, Š., Slovenec, D. & Kolar-Jurkovšek, T., 1999: *A Middle Jurassic Radiolarite-Clastic Succession from the Medvednica Mt. (NW Croatia)*. Geologia Croatica 52, 29–57.

Harzhauser, M. & Mandić, O., 2008: *Neogene lake systems of central and South-Eastern Europe: Faunal diversity, gradients and interrelations*. Paleogeography, Paleoclimatology, Paleoecology 260 (3–4): 417–434.

Hauer, F.v., 1888: *Die Cephalopoden des bosnischen Muschelkalkes von Han Bulog bei Sarajevo*. Denkschr. K. Akad. Wiss., math.-natw. Kl., 54: 1–50.

Horacek, M., Đaković, M. & Krystyn, L., 2020: *The Permian of the Budva Zone, Montenegro, western Tethys*. Permophiles 69: 32–36.

Hrvatović, H., 2006: *Geological guidebook through Bosnia and Herzegovina*. Geological Survey of Federation Bosnia and Herzegovina, Sarajevo, 172 pp.

Ikeda, M. & Tada, R., 2014: *A 70 million year astronomical time scale for the deep-sea bedded chert sequence (Inuyama, Japan): Implications for Triassic–Jurassic geochronology*. Earth and Planetary Science Letters 399: 30–43.

Ikeda, M., Tada, R. & Sakuma, H., 2010: *Astronomical cycle origin of bedded chert: A middle Triassic bedded chert sequence, Inuyama, Japan*. Earth and Planetary Science Letters 297: 369–378.

Ikeda, M., Tada, R. & Ozaki, K., 2017: *Astronomical pacing of the global silica cycle recorded in Mesozoic bedded cherts*. Nature Communications 8:15532, DOI: 10.1038/ncomms15532.

Ingle, J.C. Jr., 1981: *Origin of Neogene diatomites around the North Pacific Rim*. In: Garrison, R.E., Douglas, R.G. et al. (Eds.): *The Monterey Formation and Related Siliceous Rocks of California*. Spec. Publ. Pac. Sect. Soc. econ. Paleont. Miner., Los Angeles, 159–179.

Jenkyns, H.G., Jones, C.E., Gröcke, D.R., Hesselbo, S.P. & Parkinson, D.N., 2002: *Chemostratigraphy of the Jurassic System: applications, limitations and implications for palaeoceanography*. Journal of the Geological Society London 159: 351–378.

Karamata, S., 2006: *The geological development of the Balkan Peninsula related to the approach, collision and compression of Gondwanan and Eurasian units*. In: Robertson, A.H.F. & Mountrakis, D., (Eds.): *Tectonic Development of the Eastern Mediterranean Region*. Geological Society London Special Publications 260: 155–178.

Kozur, H. & Mostler, H., 1994: *Anisian to Middle Carnian radiolarian zonation and description of some stratigraphically important radiolarians*. Geologisch-Paläontologische Mitteilungen Innsbruck Sonderband 3: 39–255.

Kozur, H. & Réti, Z., 1986: *The first paleontological evidence of Triassic ophiolites in Hungary*. N. Jb. Geol. Paläont. Mh. 5: 284–292.

Kozur, H.W., Krainer, K. & Mostler, H., 1996: *Radiolarians and Facies of the Middle Triassic Loibl Formation, South Alpine Karawanken Mountains (Carinthia, Austria)*. Geologisch-Paläontologische Mitteilungen Innsbruck Sonderband 4, 195–269.

Kovács S., Sudar M., Grădinaru E., Gawlick H.-J., Karamata S., Haas J., Péró C., Gaetani M., Mello J., Polák M., Aljinović D., Ogorelec B., Kolar-Jurkovšek T., Jurkovšek B. & Buser S. 2011. *Triassic Evolution of the Tectonostratigraphic Units of the Circum-Pannonian Region*. Jahrbuch der Geologischen Bundesanstalt 151 (3–4): 199–280.

Krystyn, L., 2008: *The Hallstatt pelagics—Norian and Rhaetian Fossillagerstaetten of Hallstatt*. Berichte Geologische Bundesanstalt 76: 81–98.

Krystyn, L., Brandner, R., Đaković, M. & Horacek, M. 2019: *The Lower Triassic of Budva Zone*. Geološki Glasnik 17: 9–22.

Kukoč, D., 2014: *Jurassic and Cretaceous radiolarian stratigraphy of the Bled Basin (northwestern Slovenia) and stratigraphic correlations across the Internal Dinarides*. Dissertation, University of Ljubljana, 257 pp.

Kukoč, D., Goričan, Š. & Košir, A., 2012: *Lower Cretaceous carbonate gravity-flow deposits from the Bohinj area (NW Slovenia): evidence of a lost carbonate platform in the Internal Dinarides*. Bull. Soc. géol. France 183 (4): 383–392.

Longridge, L.M., Carter, E.S., Smith, P.L. & Tipper, H.W., 2007: *Early Hettangian ammonites and radiolarians from the Queen Charlotte Islands, British Columbia and their bearing on the definition of the Triassic–Jurassic boundary*. Palaeogeography, Palaeoclimatology, Palaeoecology 244: 142–169.

Matenco, L. & Radivojević, D., 2012: *On the formation and evolution of the Pannonian Basin: Constraints derived from the structure of the junction area between the Carpathians and Dinarides.* Tectonics 31, TC6007. https://doi.org/10.1029/2012TC003206

Marroni, M., Pandolfi, L., Onuzi, K., Palandri, S. & Xhomo, A., 2009: *Ophiolite-bearing Vermoshi Flysch (Albanian Alps, northern Albana): elements for its correlation in the frame of Dinaric-Hellenic belt*. Ofioliti 34 (2): 95–108.

Metodiev, L., Rabrenović, D., Mojsić, I., Ivanova, D., Koleva-Rekalova, E. & Radulović, V., 2013: *The ammonites of the Bifrons Zone (Toarcian, Lower Jurassic) from Mihailovići (Northern Montenegro)*. Comptes rendus de l'Académie bulgare des Sciences 66 (1): 67–76.

Mikes, T., Christ, D., Petri, R., Dunkl, I., Frei, D., Báldi-Beke, M., Reitner, J., Wemmer, K., Hrvatović, H. & von Eynatten, H., 2008: *Provenance of the Bosnian Flysch*. Swiss Journal of Geosciences 101: S31–S54.

Mirković, M., 1983: *Geološki sastav i tektonika planina Durmitora, Pivske planine i Volujaka (Geology and tectonics of Durmitor, Piva and Volujak mountains)* (in Serbian with English summary). Zavod za geološka istraživanja SR Crne Gore, Posebna izdanja Geološkog glasnika 5, 116 pp., 4 foldouts in appendix.

Mirković, M. & Vujisić, P., 1989: *Osnovna geološka karta 1:100 000, list Žabljak*. Savezni geološki zavod, Beograd.

Mirković, M., Kalezić, M. & Pajović, M., 1968: Osnovna geološka karta 1:100 000, list Bar. Savezni geološki zavod, Beograd.

Mirković, M., Pajović, M., Buzaljko, R., Kalezić M. & Živaljević, M., 1978: *Osnovna geološka karta 1:100 000, list Pljevlja*. Savezni geološki zavod, Beograd.

Mirković, M., Živaljević, M., Đokić, V., Perović, Z., Kalezić, M. & Pajović, M., 1985: Geološka karta Crne Gore, 1:200.000. RSIZ za geološka istraživanja, Titograd.

Missoni, S., Gawlick, H.-J., Sudar, M.N., Jovanović, D. & Lein, R., 2012: *Onset and demise of the Wetterstein Carbonate Platform in the mélange areas of the Zlatibor Mountain (Sirogojno, SW Serbia)*. Facies 58: 95–111.

Murchey, B. M., 1984: *Biostratigraphy and lithostratigraphy of chert in the Franciscan Complex, Marin Headlands, California*. In: Blake, Jr. M. C. (Ed.), F*ranciscan Geology of Northern California*. Pacific Section Society of Economic Paleontologists and Mineralogists 43: 51–70.

Nirta G., Bortolotti V., Chiari M., Menna F., Saccani E., Principi G. & Vannucchi P., 2010: *Ophiolites from the Grammos-Arrenes area, northern Greece: geological, paleontological and geochemical data*. Ofioliti 35: 103–115.

Nirta, G., Moratti, G., Piccardi, L., Montanari, D., Catanzariti, R., Carras, N. & Papini, M., 2015: *The Boeotian flysch revisited: new constraints on ophiolite obduction in Central Greece.* Ofioliti 40 (2): 107–123.

Nirta, G., Moratti, G., Piccardi, L., Montanari, D., Carras, N., Catanzariti, R., Chiari, M. & Marcucci, M., 2018: *From obduction to continental collision: new data from Central Greece*. Geological Magazine 155 (2): 377–421.

Nirta, G., Aberhan, F., Bortolotti, V., Carras, N., Menna, F. & Fazzuoli, M., 2020: *Deciphering the geodynamic evolution of the Dinaric orogen through the study of the 'overstepping' Cretaceous successions*. Geological Magazine 157 (8): 1238–1264.

Nöth, L., 1956: *Beiträge zur Geologie von Nordmontenegro. Oberlias in der Umgebung von Pljevlja*. Raimund von Klebelsberg-Festschrift der Geologischen Gesellschaft in Wien 48, 167–191.

Obradović, J. & Goričan, Š., 1988: *Siliceous Deposits in Yugoslavia: Occurrences, Types and Ages.* In: Hein, J. R. & Obradović, J. (Eds.): *Siliceous Deposits of the Tethys and Pacific Regions*. Springer Verlag: 51–64.

O'Dogherty, L., 1994: *Biochronology and Paleontology of Mid-Cretaceous Radiolarians from Northern Apennines (Italy) and Betic Cordillera (Spain)*. Mémoires de Géologie (Lausanne) 21: 1–415.

O'Dogherty, L., Carter, E.S., Dumitrica, P., Goričan, Š., De Wever, P., Hungerbühler, A., Bandini, A.N. & Takemura A., 2009a: *Catalogue of Mesozoic radiolarian genera. Part 1: Triassic*. Geodiversitas 31: 213–270.

O'Dogherty, L., Carter, E.S., Dumitrica, P., Goričan, Š., De Wever, P., Bandini, A.N., Baumgartner, P.O. & Matsuoka, A., 2009b: *Catalogue of Mesozoic radiolarian genera. Part 2, Jurassic–Cretaceous*. Geodiversitas 31, 271–356.

O'Dogherty, L., Carter, E. S., Goričan, Š. & Dumitrica, P., 2010: *Triassic radiolarian biostratigraphy.* In: Lucas, S.G. (Ed.), *The Triassic Timescale*. Geological Society London, Special Publication 334: 163–200.

Ozsvárt, P. & Kovács, S., 2012: *Revised Middle and Late Triassic radiolarian ages for ophiolite mélanges: implications for the geodynamic evolution of the northern part of the early Mesozoic Neotethyan subbasins*. Bull. Soc. géol. France 183 (4): 273–286.

Pamić, J., 1984: *Triassic magmatism of the Dinarides in Yugoslavia*. Tectonophysics 109: 273–307.

Pamić, J., Tomljenović, B. & Balen, D., 2002: *Geodynamic and petrogenetic evolution of Alpine ophiolites from the central and NW Dinarides: an overview*. Lithos 65: 113–142.

Peron-Pinvidic, G. & Manatschal, G., 2010. *From microcontinents to extensional allochthons: witnesses of how continents rift and break apart?* Petroleum Geoscience 16, 1–10.

Pessagno, E.A. 1977: *Lower Cretaceous radiolarian biostratigraphy of the Great Valley Sequence and Franciscan Complex, California Coast Ranges*. Cushman Foundation for foraminiferal Research, Special Publication 15:1–87.

Pessagno, E.A.Jr., Blome, C.D., Carter, E.S., MacLeod, N., Whalen, P. & Yeh, K.-Y., 1987: *Studies of North American Jurassic Radiolaria. Part II. Preliminary radiolarian zonation for the Jurassic of North America*. Cushman Foundation Spec. Publ. 23: 1–18.

Price, G.D., Főzy, I. & Pálfy, J., 2016: *Carbon cycle history through the Jurassic-Cretaceous boundary: A new global δ13C stack*. Palaeogeography, Palaeoclimatology, Palaeoecology 451: 46–61.

Rabrenović, D., Metodiev, L.S., Ivanova, D.K., Koleva-Rekalova, E.K., Radulović, V. & Mojsić, I., 2012: *The Lower and the Middle Jurassic facies and biostratigraphy (ammonites and foraminifers) of the Lim River area (Internal Dinarides), Montenegro.* Comptes rendus de l'Académie bulgare des Sciences 65 (12): 1705–1716.

Radoičić, R., 1982. *Carbonate platforms of the Dinarides: the example of Montenegro – west Serbian sector.* Bulletin de l'Académie Serbe des Sciences et des Arts 80, Classe des Sciences naturelles et mathématiques 22: 35–46.

Radoičić, R., Jovanović, D. & Sudar, M., 2009: *Stratigraphy of the Krš Gradac section (SW Serbia)*. Geološki anali Balkanskoga poluostrva 70: 23–41.

Rampnoux, J.-P., 1969: *La géologie du Sandjak: mise en evidence de la nappe du Pešter: confins serbo-monténégrins (Yougoslavie).* Bull. Soc. géol. France sér. 7, XI (6): 881–893.

Rampnoux, J.-P., 1970: *Regards sur les Dinarides internes yougoslaves (Serbie-Monténégro oriental): stratigraphie, evolution paléogéographique, magmatisme*. Bull. Soc. géol. France sér. 7, XII (6): 948–966.

Rampnoux, J.-P., 1974: *Contribution à l'étude géologiqe des Dinarides: un secteur de la Serbie méridionale et du Monténégro oriental (Yougoslavie). Mémoires de la Société géologique de Franc*e 119: 99 pp.

Robertson, A. H., 2012: *Late Palaeozoic–Cenozoic tectonic development of Greece and Albania in the context of alternative reconstructions of Tethys in the Eastern Mediterranean region.* International Geology Review 54 (4): 373–454.

Robertson, A.H.F. & Karamata, S., 1994: *The role of subduction–accretion processes in the tectonic evolution of the Mediterranean Tethys in Serbia*. Tectonophysics 234: 73–94.

Robertson, A. & Shallo, M., 2000: *Mesozoic–Tertiary tectonic evolution of Albania in its regional Eastern Mediterranean context*. Tectonophysics 316: 197–254.

Robertson, A.H.F., Clift, P.D., Degnan, P.J. & Jones, G., 1991: Palaeogeographic and palaeotectonic evolution of the Eastern Mediterranean Neotethys. Palaeogeography, Palaeoclimatology, Palaeoecology 87: 289–343.

Robertson, A.H.F., Trivić, B., Đerić, N. & Bucur, I.I., 2013: *Tectonic development of the Vardar ocean and its margins: evidence from the Republic of Macedonia and Greek Macedonia*. Tectonophysics 595–596: 25–54.

Robin, C., Goričan, Š., Guillocheau, F., Razin, P., Dromart, G. & Mosaffa, H., 2010: *Mesozoic deep-water carbonate deposits from the southern Tethyan passive margin in Iran (Pichakun nappes, Neyriz area): biostratigraphy, facies sedimentology and sequence stratigraphy.* In: Leturmy, P., Robin, C. (Eds.) *Tectonic and Stratigraphic Evolution of Zagros and Makran during the Mesozoic–Cenozoic*. Geological Society London, Special Publication 330: 179–210.

Saccani, E., Bortolotti, V., Marroni, M., Pandolfi, L., Photiades, A. & Principi, G., 2008: *The Jurassic association of backarc basin ophiolites and calc-alkaline volcanics in the Guevgueli Complex (Northern Greece). Implication for the evolution of the Vardar Zone*. Ofioliti 33: 209–227.

Saccani, E., Beccaluva, L., Photiades, A. & Zeda, O., 2011: *Petrogenesis and tectono-magmatic significance of basalts and mantle peridotites from the Albanian-Greek ophiolites and sub-ophiolitic melanges. New constraints for the Triassic-Jurassic evolution of the Neo-Tethys in the Dinaride sector.* Lithos 124: 227–242.

Saccani, E., Dilek, Y., Marroni, M. & Pandolfi, L., 2015: *Continental margin ophiolites of Neotethys: Remnants of Ancient Ocean–Continent Transition Zone (OCTZ) lithosphere and their geochemistry, mantle sources and melt evolution patterns*. Episodes 38: 230–249.

Sandoval Gutierrez, M. I., 2015: *Late Mesozoic to Neogene radiolarian biostratigraphy and palaeoceanography in the Caribbean and East Pacific Region*. PhD Université de Lausanne.

Schefer, S., Egli, D., Missoni, S., Bernoulli, D., Fügenschuh, B., Gawlick, H.-J., Jovanović, D., Krystyn, L., Lein, R., Schmid, S. & Sudar, M., 2010: *Triassic metasediments in the Internal Dinarides (Kopaonik area, southern Serbia): stratigraphy, paleogeography and tectonic significance*. Geologica Carpathica 61: 89–109.

Scherreiks, R., Bosence, D., BouDagher-Fadel, M., Meléndez, G. & Baumgartner, P.O., 2010: *Evolution of the Pelagonian carbonate platform complex and the adjacent oceanic realm in response to plate tectonic forcing (Late Triassic and Jurassic), Evvoia, Greece*. International Journal of Earth Sciences 99: 1317–1334.

Schlagintweit, F., Gawlick, H.-J. & Lein, R., 2005: *Mikropaläontologie und Biostratigraphie der Plassen-Karbonatplattform der Typlokalität (Ober-Jura bis Unter-Kreide, Salzkammergut, Österreich)*. J Alp Geol Mitt Ges Geol Bergbaustud Österreich 47: 11–102.

Schlagintweit, F., Gawlick, H.-J., Missoni, S., Hoxha, L., Lein, R. & Frisch, W., 2008: *The eroded Late Jurassic Kurbnesh carbonate platform in the Mirdita Ophiolite Zone of Albania and its bearing on the Jurassic orogeny of the Neotethys realm*. Swiss Journal of Geosciences 101: 125–138.

Schmid, S.M., Bernoulli, D., Fügenschuh, B., Matenco, L., Schefer, S., Schuster, R., Tischler, M. & Ustaszewski, K. 2008: *The Alpine-Carpathian-Dinaridic orogenic system: correlation and evolution of tectonic units*. Swiss Journal of Geosciences 101: 139–183.

Schmid, S.M., Fügenschuh, B., Kounov, A., Maţenco, L., Nievergelt, P., Oberhänsli, R., Pleuger, J., Schefer, S., Schuster, R., Tomljenović, B., Ustaszewski, K. & van Hinsbergen, D.J.J., 2020: *Tectonic units of the Alpine collision zone between Eastern Alps and western Turkey*. Gondwana Research 78: 308–374.

Šegvić, B., Kukoć, D., Dragičević, I., Vranjković, A., Brčić, V., Goričan, Š., Babajić, E. & Hrvatović, H., 2014: *New record of Middle Jurassic radiolarians and evidence of Neotethyan dynamics documented in a mélange from the Central Dinaridic Ophiolite belt (CDOB, NE Bosnia and Herzegovina)*. Ofioliti 39: 31–41.

Slovenec, D., Šegvić, B., Halamić, J., Goričan, Š. & Zanoni, G., 2020: *An ensialic volcanic arc along the northwestern edge of Palaeotethys – Insights from the Mid-Triassic volcano-sedimentary succession of Ivanščica Mt. (northwestern Croatia)*. Geological Journal 55: 4324–4351.

Spray, J.G., Bebien, J., Rex, D.C. & Roddick, J.C., 1984: *Age constraints on the igneous and metamorphic evolution of the Hellenic-Dinaric ophiolites*. In: Dixon, J.E. & Robertson, A.H.F. (Eds.) *The Geological Evolution of the Eastern Mediterranean*. Geological Society London, Special Publications 17: 619–627.

Stampfli, G. M. & Borel, G. D., 2002: *A plate tectonic model for the Paleozoic and Mesozoic constrained by dynamic plate boundaries and restored synthetic oceanic isochrons*. Earth Planet. Sci. Lett. 196: 17–33.

Stampfli, G.M. & Borel, G.D., 2004: *The TRANSMED transects in space and time: constraints on the paleotectonic evolution of the Mediterranean domain*. In: Cavazza, W., Roure, F., Spakman, W., Stampfli, G.M. & Ziegler, P. (Eds.), *The TRANSMED Atlas: The Mediterranean Region from Crust to Mantle*, Springer, 53–80.

Stampfli, G. M. & Kozur, H. W., 2006: *Europe from Variscan to the Alpine cycles*. In: Gee, D. G., Stephenson, R. A. (Eds.), *European Lithosphere Dynamics*. Geological Society London, Memoirs 32: 57–82.

Stockar, R., Dumitrica, P. & Baumgartner, P.O., 2012: *Early Ladinian radiolarian fauna from the Monte San Giorgio (Southern Alps, Switzerland): systematics, biostratigraphy and paleo(bio)geographic implications*. Rivista Italiana di Paleontologia e Stratigrafia 118 (3): 375–437.

Sudar, M.N., Gawlick, H.-J., Lein, R., Missoni, S., Kovács, S. & Jovanović, D., 2013: *Depositional environment, age and facies of the Middle Triassic Bulog and Rid formations in the Inner Dinarides (Zlatibor Mountain, SW Serbia): evidence for the Anisian break-up of the Neotethys Ocean*. N- Jb. Geol. Paläont. Abh. 269 (3): 291–320.

Tang, T., Kisslinger, K. & Lee, C., 2014: *Silicate deposition during decomposition of cyanobacteria may promote export of picophytoplankton to the deep ocean*. Nature Communications 5: 4143, DOI: 10.1038/ncomms5143.

Tekin, U.K., 1999: *Biostratigraphy and systematics of late Middle to Late Triassic radiolarians from the Taurus Mountains and Ankara region, Turkey*. Geologisch– Paläontologische Mitteilungen Innsbruck, Sonderband 5, 1–297.

Ustaszewski, K., Schmid, S.M., Lugović, B., Schuster, R., Schaltegger, U., Bernoulli, D., Hottinger, L., Kounov, A., Fügenschuh, B. & Schefer, S., 2009. *Late Cretaceous intra-oceanic magmatism in the internal Dinarides (northern Bosnia and Herzegovina): Implications for the collision of the Adriatic and European plates*. Lithos 108: 106–125.

van Gelder, I.E., Matenco, L., Willingshofer, E., Tomljenović, B., Andriessen, P.A.M., Ducea, M.N., Beniest, A. & Gruić, A., 2015: *The tectonic evolution of a critical segment of the Dinarides-Alps connection: Kinematic and geochronological inferences from the Medvednica Mountains, NE Croatia*. Tectonics 34 (9): 1952–1978.

van Unen, M., Matenco, L., Nader, F. H., Darnault, R., Mandic, O. & Demir, V., 2019: *Kinematics of foreland-vergent crustal accretion: Inferences from the Dinarides evolution*. Tectonics 38 (1): 49–76. https://doi.org/10.1029/2018TC005066

Vishnevskaya, V.S., Djerić, N. & Zakariadze, G.S., 2009: *New data on Mesozoic Radiolaria of Serbia and Bosnia, and implications for the age and evolution of oceanic volcanic rocks in the Central and Northern Balkans*. Lithos 108: 72–105.

Vlahović, I., Tišljar, J., Velić, I., & Matičec, D., 2005: *Evolution of the Adriatic Carbonate Platform: Palaeogeography, main events and depositional dynamics*. Palaeogeography, Palaeoclimatology, Palaeoecology 220: 333–360.

Wang, Y., Yang, Q., Matsuoka, A., Kobayashi, K., Nagahashi, T. & Zeng, Q., 2002: *Triassic radiolarians from the Yarlung Zangbo Suture Zone in the Jinlu area, Zetang County, Southern Tibet*. Acta Micropaleontologica Sinica 19 (3): 215–227.

Williford, K.H., Ward, P.D., Garrison, G.H. & Buick, R., 2007: *An extended organic carbon-isotope record across the Triassic-Jurassic boundary in the Queen Charlotte Islands, British Columbia, Canada*. Palaeogeography, Palaeoclimatology, Palaeoecology 244: 290–296.

Yurtsever, T.Ş., Tekin, U.K. & Demirel, İ.H. 2003: *First evidence of the Cenomanian/Turonian boundary event (CTBE) in the Alakırçay Nappe of the Antalya nappes, southwest Turkey*. Cretaceous Research 24: 41–53.

Ziabrev, S.V., Aitchison, J.C., Abrajevitch, A.V., Badengzhu, Davis, A.M. & Luo, H., 2004. *Bainang Terrane, Yarlung–Tsangpo suture, southern Tibet (Xizang, China): a record of intra-Neotethyan subduction–accretion processes preserved on the roof of the world*. J. Geol. Soc. London 161 (3): 523–539.

Ziegler, P.A. & Stampfli, G.M., 2001: *Late Paleozoic – early Mesozoic plate boundary reorganization: collapse of the Variscan orogen and opening of Neotethys*. Natura Bresciana, Ann. Mus. Civ. Sc. Nat., Monografia 25: 17–34.

Živaljević, M., 1989: *Explanations for Geological Map of SR Montenegro, Scale 1: 200,000*. Geological Survey of Montenegro, 62 p. (In Serbo-Croatian, English summary).

FOLIA BIOLOGICA ET GEOLOGICA = Ex RAZPRAVE IV. RAZREDA SAZU
ISSN 1855-7996 · Letnik / Volume 63 · Številka / Number 2 · 2022

ISSN 1855-7996
9 771855 799005

VSEBINA / CONTENTS

RAZPRAVE / ESSAYS